

DATABASE DEVELOPMENT FOR TSUNAMI WARNING SYSTEM IN
MEDITERRANEAN BASIN BY TSUNAMI MODELING

A THESIS SUBMITTED TO
THE GRADUATE SCHOOL OF NATURAL AND APPLIED SCIENCES
OF
MIDDLE EAST TECHNICAL UNIVERSITY

BY

YAPRAK ONAT

IN PARTIAL FULFILLMENT OF THE REQUIREMENTS
FOR
THE DEGREE OF MASTER OF SCIENCE
IN
CIVIL ENGINEERING
JUNE 2011

Approval of the thesis:

**DATABASE DEVELOPMENT FOR TSUNAMI WARNING SYSTEM IN
MEDITERRANEAN BASIN BY TSUNAMI MODELING**

submitted by **YAPRAK ONAT** in partial fulfillment of the requirements for the degree of **Master of Science in Civil Engineering Department, Middle East Technical University** by,

Prof. Dr. Canan Özgen
Dean, Graduate School of **Natural and Applied Sciences** _____

Prof. Dr. Güney Özcebe,
Head of Department, **Civil Engineering** _____

Prof. Dr. Ahmet Cevdet Yalçınar
Supervisor, **Civil Engineering Department, METU** _____

Examining Committee Members:

Prof. Dr. Ayşen Ergin
Civil Engineering, METU _____

Prof. Dr. Ahmet Cevdet Yalçınar
Civil Engineering, METU _____

Dr. Işıkhan Güler
Civil Engineering, METU _____

Assoc. Prof. Dr. Utku Kanoğlu
Engineering Sciences, METU _____

Dr. Bergüzar Öztunalı Özbahçeci
DLH General Directorate _____

Date: _____

I hereby declare that all information in this document has been obtained and presented in accordance with academic rules and ethical conduct. I also declare that, as required by these rules and conduct, I have fully cited and referenced all material and results that are not original to this work.

Name, Last Name: Yaprak ONAT

Signature :

ABSTRACT

DATABASE DEVELOPMENT FOR TSUNAMI WARNING SYSTEM IN MEDITERRANEAN BASIN BY TSUNAMI MODELING

Onat, Yaprak

M.Sc., Department of Civil Engineering

Supervisor: Prof. Dr. Ahmet Cevdet Yalciner

June 2011, 166 pages

Wider awareness, proper preparedness and effective mitigation strategies need better understanding of tsunamis and tsunami hazard assessment. Tsunami assessment study covers the exchange and enhancement of available earthquake and tsunami data, development of bathymetric and topographic data in sufficient resolution, selection of possible or credible tsunami scenarios, selection and application of the valid and verified numerical tools for tsunami generation, propagation, coastal amplification, inundation and visualization. From this point of view, this thesis deals with all these components of tsunami hazards assessment. The database of 38 different seismic sources is generated and applied to Eastern Mediterranean Basin by using numerical code called NAMI DANCE. Furthermore, the simulation results are compared and discussed. In the thesis, the difficulties in defining seismic source parameters, the effect of dip and rake (slip) angle on seismic generated tsunamis are evaluated. Moreover, the performance of the

numerical code, the accuracy of results, the efficiency of the numerical methods in the application to Mediterranean Basin Tsunamis and the comparisons of simulations in nested domains for Bodrum, Kas and Iskenderun are given as case studies. According to the study, north-west and south-west of Turkey may have tsunami risk more than other regions. The maximum wave amplitudes, which may be expected to occur near the shore, are found more than 4 m. However, maximum positive wave amplitude observed in history is approximately 8 m. The arrival time of first wave to hit the coasts vary in a range of 15 to 60 minutes depending on the closeness of the location to the sources' epicenter.

Keywords: Tsunami warning system, Eastern Mediterranean, tsunami modeling, tsunami generation, tsunami propagation, seismic, run up

ÖZ

AKDENİZ HAVZASINDA TSUNAMİ UYARI SİSTEMİ İÇİN TSUNAMİ MODELLEMESİYLE VERİTABANI HAZIRLANMASI

Onat, Yaprak

Yüksek Lisans, İnşaat Mühendisliği Bölümü

Tez Yöneticisi: Prof. Dr. Ahmet Cevdet Yalçınér

Haziran 2011, 166 sayfa

Tsunami afet değerlendirmesi, bu afetin araştırılarak tanınması, olası etkilerinin belirlenmesi ve ona göre gerekli sakinme yöntemlerinin geliştirilmesi ve hazırlıkların yapılması için gerekli aşamaları içerir. Bunun için tsunami uyarı sistemi geliştirilmesi de önemli işlerden biridir. Bu tezde, tsunami uyarı sistemine fayda sağlamak üzere veri tabanı geliştirilmeye çalışılmıştır. Tsunami tehlike değerlendirmesi, eldeki deprem ve tsunami verilerinin toplanıp geliştirilmesini, batimetri ve topografik verilerin uygun çözünürlüklerde geliştirilmesini, olası tsunami kaynaklarının seçimini, onaylanmış bir sayısal araçla tsunami oluşumu, ilerlemesi, dalga yüksekliği ve kıyıdaki sel baskınını görselleştirmesini kapsar. Bu çalışmada 38 farklı sismik kaynaklı tsunamiler Doğu Akdeniz havzasında NAMI DANCE sayısal kodu kullanılarak yaratılıp uygulanmış ve elde edilen sonuçlarla ayrı ayrı tartışılarak sunulmuştur. Sismik kaynaklı tsunami parametrelerinin belirlenmesindeki zorluk, dalma ve kayma açılarının sismik kaynaklı

tsunami oluşumuna etkisi ayrı olarak incelenmiş, bundan başka yazılımın performansı, sonuçların netliği, sayısal metodun Akdeniz havzasına uygulanmasındaki verimliliği, ve Bodrum, İskenderun ve Kaş'ta uygulanan iç içe geçmiş benzetimlerin karşılaştırılması ve tartışması yapılmıştır. Bu sonuçlara göre, Türkiye'nin kuzeybatı ve güneybatı kısımları daha fazla tehlikeye maruz kalabilir. Genel olarak Akdeniz havzasındaki geçmiş tsunamiler ile ilgili veriler incelendiğinde 8 metreye kadar dalga yüksekliği kıyılara vurmuştur. Bu çalışmada kullanılan verileere bağlı yapılan benzetimler, Türkiye'nin, batı ve güney kıyıları için tsunami dalga yüksekliğinin 4 metreyi aşاقısını göstermektedir. İlk dalganın kıyıya vurma süresi sismik kaynağın merkezinin kıyıya yakınlığına göre 15 ile 60 dakika arasında değişmektedir.

Anahtar Kelimeler: Tsunami uyarı sistemi, Doğu Akdeniz, tsunami oluşumu, tsunami modellemesi, tsunami ilerlemesi, sismik, tırmanma

“To my Angel Binnur Akay”

ACKNOWLEDGEMENTS

I would like to thank my advisor Prof. Dr. Ahmet Cevdet Yalçiner who has been supported me since the beginning of my graduate studies. He has been always patient, sincere, love full, fun and calm that makes all the time that I spent with him was amazing. He is like a friend to me and understands me beyond the levels of student advisor relationship. I hope we will continue to work on project in future.

I would like to thank my beloved one Binnur Akay. Since the beginning of my life she is my angel, always protect and love me, believe in me. She sprinkles the sparks and beauties in my life even in the worst dark night. I would never survive without her support. I hope I will continue to make her proud during my whole life and we will never be apart.

I would like to thank Prof. Dr. Ayşen Ergin who inspires me to choose coastal and ocean engineering. Her energy and vision always remember me to keep the enthusiasm that I carry for my career. She saw the light in me and changed the destiny of my academic life. She cares about me and makes me see the specialty that I have. I wish I could represent my country like her and be called Jr. Ayşen.

I would like to thank Prof. Dr. Fevzi Gümrah who always supported me, concerns me and give me strength to not give up during my graduate studies. He is like father to me and gives me a reason to smile. My love for him is beyond the limits of ocean. I wish I could be a wonderful professor like him.

I would like to thank Prof. Dr. Güney Özcebe who encourages me to choose academic career. He trusts me and gives me big responsibilities during my career. I will never forget how he cares me and become a person that has sincere talks.

I would like to thank Dr. Işıkhan Güler who pushes the edge of the envelope of me and gives me the chance to reflect my personality to my work.

I would like to thank Prof. Dr. Cengiz Ertekin who changed my whole life, believed in me and made me pursue my passion in University of Hawaii.

I would like to thank Prof. Turhan Erdogan, Prof. Mustafa Tokyay and Assist. Prof. İ.Özgür Yaman who showed me a peaceful and enjoyable work environment in Materials of Construction Division.

I would like to thank Ezgi Köker who is always with me in my day and night. We shared every moment of our life and make them glorious. We worked, laughed, cried, sit up all night, promenade, chat and did all the things that come to a person's mind and always had fun together. I could never wish a sister better than her. I wish our souls were never fall apart.

I would like to thank Gülseda Karakuş who cares me and always near me whenever I need. She sparks a light with her smile whenever we met. She supports me and makes me believe that everything is going to be all right. She is kind a person that you will never want to be apart and I hope we never will.

I would like to thank Cihan Sadık Yürek who cares about me and be with me in my good and bad days. He was a shoulder that I could rest. I believe we will solve the mysteries and fight for the ethical values that we care all time in the future.

I would like to thank Alt Kat Crew for creating a love full, funny, elegant, amazingly cool working environment. I will never forget my chats and secrets with Ayşe Karancı, who encourages and understands me, deep and funny talks with Koray Kaan Özdemir, who cares me and becomes sincere shoulder, excellent discussions with Aykut Ayça, who protects me like a brother, and Kemal Cihan Şimşek, who creates and environment to have fun of the moment. I hope the distances in countries will not break our bond.

In addition, I would like to thank Pelin Öğünç and Gülistan Özyurt for being so sincere to me and good work partners.

I would like to thank Emir Alimoğlu who gives me a breathe whenever I need. I believe we will have fun, laugh, and make excellent jokes in future.

I would like to thank my friends S. Melek Yılmaztürk, S.Bahadır Keskin, Burhan Alam, Derya Över, Yaprak Servi and Tümay Çelikkol for cuddling me with their sincere feelings and make me have a good time.

I would like to thank Alper Önen, Tuğçe Yıldırım, Meriç S. Apaydın and Gizem Okyay for their company and joyful feelings. I can eat their cat life.

I would like to thank Şevki Öztürk who was an amazing roommate and work partner.

I would like to thank Recep Ejder, Sevda Polat, Cuma Yıldırım and Arif Kayışlı for helping me at work.

I would like to thank Özge Tekin who comes across with me like a star and embraces me with love and support.

I would like to thank PhdComics and Facebook account for understanding me and giving me a joy during my graduate studies. They were there with me during late nights and encouraging me to pursue my relationship with MyThesis Work.

I would like to thank Mustafa Kemal ATATÜRK. I own you my existence. I always follow your way without any attempt to rest and transfer your doctrine to new generations. Moreover, whenever I will surround by the darkness of abysmal ignorance, I will fight with them using the sword of science.

Finally, I would like to thank God for everything.

TABLE OF CONTENTS

ABSTRACT	iv
ÖZ	vi
ACKNOWLEDGEMENTS	ix
TABLE OF CONTENTS	xii
LIST OF FIGURES	xvi
LIST OF TABLES	xxvi
CHAPTERS	
1. INTRODUCTION	2
2. LITERATURE SURVEY	5
2.1 Historical Tsunamis in Mediterranean Basin	5
2.2 Past Attempts of Tsunami Modeling in Eastern Mediterranean Basin	11
2.3 Purpose of the Study.....	12
3. TSUNAMI SOURCE MECHANISMS.....	13
3.1 Non-Seismic Tsunami Source Mechanisms	13
3.1.1 Meteoroid Effect on Tsunami Generation	14
3.1.2 Volcanic Eruption Effect on Tsunami Generation	14
3.1.3 Submarine or Sub Aerial Landslide Effect on Tsunami Generation	15
3.2 Seismic Tsunami Source Mechanisms	15
3.2.1 Rupture Parameters of Earthquake Tsunami Source Mechanisms	16
3.2.2 Seismic Tsunami Sources in Eastern Mediterranean.....	20
3.3 Tsunami Numerical Modeling.....	29
3.3.1 Theoretical Background.....	29
3.3.2 Numerical Background	31
3.2.3 Computational Tool	34

3.4 Bathymetry Processing.....	35
3.5 Tsunami Forecast Points along Eastern Mediterranean Coast of Turkey	36
3.6 Uncertainty in Input Data Analysis	38
3.6.1 Uncertainty in Defining Rupture Parameters	38
3.6.2 Uncertainty on Bathymetry Preparation	39
4. MODEL APPLICATIONS.....	40
4.1 The Effect of Dip and Rake Angle on the Results of Simulations.....	41
4.2 Single Domain Simulations.....	49
4.3 Nested Domain Simulations	52
4.3.1 Nested Domain Simulations for Bodrum.....	52
4.3.2 Nested Domain Simulations for Iskenderun.....	58
4.3.3 Nested Domain Simulations for Kas	63
5. DISCUSSION OF RESULTS	68
5.1 Discussion on Uncertainties in Source Parameters	68
5.1.1 Discussion on the Dip – Rake(Slip) Angle Effect on Seismic Source.....	70
5.1.2 Discussion on Fault Displacement Effect on Tsunami Source	70
5.2 Bathymetry Effect on Tsunami Modeling	70
5.3 Tsunami Risk Analysis in Eastern Mediterranean Basin	71
6. CONCLUSION.....	73
REFERENCES.....	75
APPENDICES	81
A1. Tsunamis on the Turkish coasts from Yolsal and Ersoy (2000)	81
A.2 Earthquake Database of TRANSFER Project for Selected Domain (Magnitude > 6).....	88
A.3 Summary outputs of Single Domain Simulations	93
A.3.1. Simulation of Source s02-Z04	93
A.3.2. Simulation of Source s03-Z10-1	95
A.3.3. Simulation of Source s04-Z10-2	97
A.3.4. Simulation of Source s05-Z10-3.....	99

A.3.5. Simulation of Source s06-Z10-4.....	101
A.3.6. Simulation of Source s07-Z11-1	103
A.3.7. Simulation of Source s08-Z11-2.....	105
A.3.8. Simulation of Source s09-Z11-3.....	107
A.3.9. Simulation of Source s10-Z12-1	109
A.3.10. Simulation of Source s11-Z12-2.....	111
A.3.11. Simulation of Source s12-Z14	113
A.3.12. Simulation of Source s13-Z15-1	115
A.3.13. Simulation of Source s14-Z15-2.....	117
A.3.14. Simulation of Source s15-Z17-1	119
A.3.15. Simulation of Source s16-Z17-2.....	121
A.3.16. Simulation of Source s17-Z17-3	123
A.3.17. Simulation of Source s18-Z22	125
A.3.18. Simulation of Source s19-Z24	127
A.3.19. Simulation of Source s20-Z25	129
A.3.20. Simulation of Source s21-Z13-1	131
A.3.21. Simulation of Source s22-Z13-2	133
A.3.22. Simulation of Source s23-Z13-3	135
A.3.23. Simulation of Source s24-Z26-1	137
A.3.24. Simulation of Source s25-Z26-2	139
A.3.25. Simulation of Source s26-Z28	141
A.3.26. Simulation of Source s27-Z29-1	143
A.3.27. Simulation of Source s28-Z29-2	145
A.3.28. Simulation of Source s29-Z30	147
A.3.29. Simulation of Source s30-Z31-1	149
A.3.30. Simulation of Source s31-Z31-2	151
A.3.31. Simulation of Source s32-Z32	153
A.3.32. Simulation of Source s33-Z38	155

A.3.33. Simulation of Source s34-Z41	157
A.3.34. Simulation of Source s35	159
A.3.35. Simulation of Source s36	161
A.3.36. Simulation of Source s37	163
A.3.37. Simulation of Source s38	165

LIST OF FIGURES

FIGURES

Figure 2.1: The tsunamigenic zones of the Mediterranean Sea	7
Figure 3.1: Focal mechanism of a fault (Rawlinson 2007).....	17
Figure 3.2: Fault types (Rawlinson 2007).....	18
Figure 3.3: Rupture characteristics of seismic generated source mechanisms.	19
Figure 3.5: Map of possible tsunami sources in Eastern Mediterranean Basin	23
Figure 3.6: Sources between s01-365 to s10-Z12-1	27
Figure 3.7: Sources Between s11-Z12-2 to s20-Z25	27
Figure 3.8: Sources between s21-Z13-1 to s31-Z31-2.....	28
Figure 3.9: Sources between s32-Z32 to s38	28
Figure 3.10: Point schematics for the numerical scheme (Imamura et al. 2006).....	33
Figure 3.11: The bathymetric/topographic data of Eastern Mediterranean Basin obtained from GEBCO 30 sec.	36
Figure 3.12: Forecast points along Turkish coasts illustration on Google Earth, 2011..	37
Figure 4.1: Gauge points on regular batymetry(left) and cross section of batymetry(right)	42
Figure 4.2: Source dip 10° – rake 110° (left) and dip 110° - rake 10° (right) on regular batymetry.....	44
Figure 4.3: Maximum positive sea level elevations for Source dip 10° – rake 110° (left) and dip 110° - rake 10° (right) on regular batymetry.....	44
Figure 4.4: Maximum negative sea level elevations for Source dip 10° – rake 110° (left) and dip 110° - rake 10° (right) on regular batymetry.....	44
Figure 4.5: Maximum positive sea level elevations for Source dip 10° – rake 90° (left) and dip 30° - rake 90° (right) on irregular batymetry	46

Figure 4.6: Maximum positive sea level elevations for Source dip 90° – rake 10° (left) and dip 90° - rake 30° (right) on regular bathymetry.....	46
Figure 4.7: The location of tsunami source 01-365 and the distributions of water elevations after t=1hr in the study domain (Eastern Mediterranean) in the duration of simulation (4 hours) for the tsunami source 01-365	50
Figure 4.8: The distributions of maximum(left) and minimum (right) of the water elevations and first wave in the study domain (Eastern Mediterranean) in the duration of simulation (4 hours) for the tsunami source 01-365	50
Figure 4.9: The smaller domains (C and D) of Bodrum	53
Figure 4.10: Selected forecasts points in Bodrum Headland on Google Earth image....	53
Figure 4.11: Maximum positive wave distribution and sea level fluctuations of source s01-365 in C domain on Bodrum	55
Figure 4.12: Maximum positive wave distribution and sea level fluctuations of source s35 with doubled fault displacement in C domain on Bodrum.....	57
Figure 4.13: The smaller domains (C and D) of Iskenderun	59
Figure 4.15: Maximum positive wave distribution and sea level fluctuations of source s33-Z38 with doubled fault displacement in C domain on Iskenderun	62
Figure 4.16: The smaller domains (C and D) of Kas	64
Figure 4.17: Selected forecasts points in Kas headland on Google Earth image.....	65
Figure A.3.1: The location of tsunami source 02-Z04(left) and the distribution wave at t=1hr(right) in the study domain (Eastern Mediterranean) in the duration of simulation (4 hours) for the tsunami source 02-Z04	93
Figure A.3.2: The distributions of maximum positive of the water elevations(left) and negative water elevations(right) in the in the study domain (Eastern Mediterranean) in the duration of simulation (4 hours) for the tsunami source 02-Z04	93
Figure A.3.3: The location of tsunami source 03-Z10-1 (left) and) and the distribution wave at t=1hr(left) in the study domain (Eastern Mediterranean) in the duration of simulation (4 hours) for the tsunami source 03-Z10-1.....	95

Figure A.3.4: The distributions of maximum positive of the water elevations(left) and negative water elevations(right) in the in the study domain (Eastern Mediterranean) in the duration of simulation (4 hours) for the tsunami source 03-Z10-1	95
Figure A.3.5: The location of tsunami source 04-Z10-2 (left) and the distribution wave at t=1hr(right) of the water elevations in the study domain (Eastern Mediterranean) in the duration of simulation (4 hours) for the tsunami source 04-Z10-2	97
Figure A.3.6: The distributions of maximum positive of the water elevations(left) and negative water elevations(right) in the in the study domain (Eastern Mediterranean) in the duration of simulation (4 hours) for the tsunami source 04-Z10-2	97
Figure A.3.7: The location of tsunami source 05-Z10-3 (left) and the distributions wave at t=1hr of the water elevations(right) in the study domain (Eastern Mediterranean) in the duration of simulation (4 hours) for the tsunami source 05-Z10-3	99
Figure A.3.8: The distributions of maximum positive of the water elevations(left) and negative water elevations(right) in the in the study domain (Eastern Mediterranean) in the duration of simulation (4 hours) for the tsunami source 05-Z10-3	99
Figure A.3.9: The location of tsunami source 06-Z10-4 (left) and the distribution wave at t=1hr(right) in the study domain (Eastern Mediterranean) in the duration of simulation (4 hours) for the tsunami source 06-Z10-4	101
Figure A.3.10: The distributions of maximum positive of the water elevations(left) and negative water elevations(right) in the in the study domain (Eastern Mediterranean) in the duration of simulation (4 hours) for the tsunami source 06-Z10-4	101
Figure A.3.11: The location of tsunami source 07-Z11-1 (left) and the distributions of wave at t=1hr(right) of the water elevations in the study domain (Eastern Mediterranean) in the duration of simulation (4 hours) for the tsunami source 07-Z11-1	103
Figure A.3.12: The The distributions of maximum positive of the water elevations(left) and negative water elevations(right) in the in the study domain (Eastern Mediterranean) in the duration of simulation (4 hours) for the tsunami source 07-Z11-1	103

Figure A.3.13: The location of tsunami source 08-Z11-2 (left) and the distributions of wave at t=1hr(right) in the study domain (Eastern Mediterranean) in the duration of simulation (4 hours) for the tsunami source 08-Z11-2.....	105
Figure A.3.14: The distributions of maximum positive of the water elevations(left) and negative water elevations(right) in the in the study domain (Eastern Mediterranean) in the duration of simulation (4 hours) for the tsunami source 08-Z11-2	105
Figure A.3.15: The location of tsunami source 09-Z11-3 (left) and the distributions of wave at t=1hr(right) in the study domain (Eastern Mediterranean) in the duration of simulation (4 hours) for the tsunami source 09-Z11-3.....	107
Figure A.3.16: The distributions of maximum positive of the water elevations(left) and negative water elevations(right) in the in the study domain (Eastern Mediterranean) in the duration of simulation (4 hours) for the tsunami source 09-Z11-3	107
Figure A.3.17: The location of tsunami source 10-Z12-1 (left) and the distributions of wave at t=1hr(right) in the study domain (Eastern Mediterranean) in the duration of simulation (4 hours) for the tsunami source 10-Z12-1.....	109
Figure A.3.18: The distributions maximum positive(left) and negative water elevations(right) in the study domain (Eastern Mediterranean) in the duration of simulation (4 hours) for the tsunami source 10-Z12-1.....	109
Figure A.3.19: The location of tsunami source 11-Z12-2 (left) and the distributions of wave at t=1hr(right) in the study domain (Eastern Mediterranean) in the duration of simulation (4 hours) for the tsunami source 11-Z12-2.....	111
Figure A.3.20: The distributions maximum positive(left) and negative water elevations(right) in the study domain (Eastern Mediterranean) in the duration of simulation (4 hours) for the tsunami source 11-Z12-2.....	111
Figure A.3.24: The distributions maximum positive(left) and negative water elevations(right) in the study domain (Eastern Mediterranean) in the duration of simulation (4 hours) for the tsunami source 13-Z15-1.....	115

Figure A.3.25: The location of tsunami source 14-Z15-2 (left) and the distributions of wave at t=1hr(right) in the study domain (Eastern Mediterranean) in the duration of simulation (4 hours) for the tsunami source 14-Z15-2.....	117
Figure A.3.26: The distributions maximum positive(left) and negative water elevations(right) in the study domain (Eastern Mediterranean) in the duration of simulation (4 hours) for the tsunami source 14-Z15-2.....	117
Figure A.3.27: The location of tsunami source 15-Z17-1 (left) and the distributions of wave at t=1hr(right) in the study domain (Eastern Mediterranean) in the duration of simulation (4 hours) for the tsunami source 15-Z17-1.....	119
Figure A.3.27: The distributions maximum positive(left) and negative water elevations(right) in the study domain (Eastern Mediterranean) in the duration of simulation (4 hours) for the tsunami source 15-Z17-1.....	119
Figure A.3.29: The location of tsunami source 16-Z17-2 (left) and the distribution wave at t=1hr(right) in the study domain (Eastern Mediterranean) in the duration of simulation (4 hours) for the tsunami source 16-Z17-2	121
Figure A.3.30: The distributions of maximum positive of the water elevations(left) and negative water elevations(right) in the in the study domain (Eastern Mediterranean) in the duration of simulation (4 hours) for the tsunami source 16-Z17-2	121
Figure A.3.31: The location of tsunami source 17-Z17-3 (left) and the distribution wave at t=1hr(right) in the study domain (Eastern Mediterranean) in the duration of simulation (4 hours) for the tsunami source 17-Z17-3	123
Figure A.3.32: The distributions of maximum positive of the water elevations(left) and negative water elevations(right) in the in the study domain (Eastern Mediterranean) in the duration of simulation (4 hours) for the tsunami source 17-Z17-3	123
Figure A.3.33: The location of tsunami source 18-Z22 (left) and the distribution wave at t=1hr(right) in the study domain (Eastern Mediterranean) in the duration of simulation (4 hours) for the tsunami source 18-Z22	125

Figure A.3.34: The distributions of maximum positive of the water elevations(left) and negative water elevations(right) in the in the study domain (Eastern Mediterranean) in the duration of simulation (4 hours) for the tsunami source 18-Z22	125
Figure A.3.35: The location of tsunami source 19-Z24 (left) and the distribution wave at t=1hr(right) in the study domain (Eastern Mediterranean) in the duration of simulation (4 hours) for the tsunami source 19-Z24.....	127
Figure A.3.36: The distributions of maximum positive of the water elevations(left) and negative water elevations(right) in the in the study domain (Eastern Mediterranean) in the duration of simulation (4 hours) for the tsunami source 19-Z24	127
Figure A.3.37: The location of tsunami source 20-Z25 (left) and the distribution wave at t=1hr(right) in the study domain (Eastern Mediterranean) in the duration of simulation (4 hours) for the tsunami source 20-Z25	129
Figure A.3.38: The distributions of maximum positive of the water elevations(left) and negative water elevations(right) in the in the study domain (Eastern Mediterranean) in the duration of simulation (4 hours) for the tsunami source 20-Z25	129
Figure A.3.39: The location of tsunami source 21-Z13-1 (left and the distribution wave at t=1hr(right) in the study domain (Eastern Mediterranean) in the duration of simulation (4 hours) for the tsunami source 21-Z13-1	131
Figure A.3.40: The distributions of maximum positive of the water elevations(left) and negative water elevations(right) in the in the study domain (Eastern Mediterranean) in the duration of simulation (4 hours) for the tsunami source 21-Z13-1	131
Figure A.3.41: The location of tsunami source 22-Z13-2 (left and the distribution wave at t=1hr(right) in the study domain (Eastern Mediterranean) in the duration of simulation (4 hours) for the tsunami source 22-Z13-2	133
Figure A.3.42: The distributions of maximum positive of the water elevations(left) and negative water elevations(right) in the in the study domain (Eastern Mediterranean) in the duration of simulation (4 hours) for the tsunami source 22-Z13-2	133

Figure A.3.43: The location of tsunami source 23-Z13-3 (left) and the distribution wave at t=1hr(right) in the study domain (Eastern Mediterranean) in the duration of simulation (4 hours) for the tsunami source 23-Z13-3	135
Figure A.3.44: The distributions of maximum positive of the water elevations(left) and negative water elevations(right) in the in the study domain (Eastern Mediterranean) in the duration of simulation (4 hours) for the tsunami source 23-Z13-3	135
Figure A.3.45: The location of tsunami source 24-Z26-1 (left) and the distribution wave at t=1hr(right) in the study domain (Eastern Mediterranean) in the duration of simulation (4 hours) for the tsunami source 24-Z26-1.....	137
Figure A.3.46: The distributions of maximum positive of the water elevations(left) and negative water elevations(right) in the in the study domain (Eastern Mediterranean) in the duration of simulation (4 hours) for the tsunami source 24-Z26-1	137
Figure A.3.47: The location of tsunami source 25-Z26-2 (left) and the distribution wave at t=1hr(right) in the study domain (Eastern Mediterranean) in the duration of simulation (4 hours) for the tsunami source 25-Z26-2	139
Figure A.3.48: The distributions of maximum positive of the water elevations(left) and negative water elevations(right) in the in the study domain (Eastern Mediterranean) in the duration of simulation (4 hours) for the tsunami source 25-Z26-2	139
Figure A.3.49: The location of tsunami source 26-Z28 (left) and the distribution wave at t=1hr(right) in the study domain (Eastern Mediterranean) in the duration of simulation (4 hours) for the tsunami source 26-Z28	141
Figure A.3.50: The distributions of maximum positive of the water elevations(left) and negative water elevations(right) in the in the study domain (Eastern Mediterranean) in the duration of simulation (4 hours) for the tsunami source 26-Z28	141
Figure A.3.51: The location of tsunami source 27-Z29-1 (left) and the distribution wave at t=1hr(right) in the study domain (Eastern Mediterranean) in the duration of simulation (4 hours) for the tsunami source 27-Z29-1	143

Figure A.3.52: The distributions of maximum positive of the water elevations(left) and negative water elevations(right) in the in the study domain (Eastern Mediterranean) in the duration of simulation (4 hours) for the tsunami source 27-Z29-1	143
Figure A.3.53: The location of tsunami source 28-Z29-2 (left) and the distribution wave at t=1hr(right) in the study domain (Eastern Mediterranean) in the duration of simulation (4 hours) for the tsunami source 28-Z29-2	145
Figure A.3.54: The distributions of maximum positive of the water elevations(left) and negative water elevations(right) in the in the study domain (Eastern Mediterranean) in the duration of simulation (4 hours) for the tsunami source 28-Z29-2	145
Figure A.3.55: The location of tsunami source 29-Z30 (left) and the distribution wave at t=1hr(right) in the study domain (Eastern Mediterranean) in the duration of simulation (4 hours) for the tsunami source 29-Z30	147
Figure A.3.56: The distributions of maximum positive of the water elevations(left) and negative water elevations(right) in the in the study domain (Eastern Mediterranean) in the duration of simulation (4 hours) for the tsunami source 29-Z30	147
Figure A.3.57: The location of tsunami source 30-Z31-1 (left) and the distribution wave at t=1hr(right) in the study domain (Eastern Mediterranean) in the duration of simulation (4 hours) for the tsunami source 30-Z31-1	149
Figure A.3.58: The distributions of maximum positive of the water elevations(left) and negative water elevations(right) in the in the study domain (Eastern Mediterranean) in the duration of simulation (4 hours) for the tsunami source 30-Z31-1	149
Figure A.3.59: The location of tsunami source 31-Z31-2 (left) and the distribution wave at t=1hr(right) in the study domain (Eastern Mediterranean) in the duration of simulation (4 hours) for the tsunami source 31-Z31-2	151
Figure A.3.60: The distributions of maximum positive of the water elevations(left) and negative water elevations(right) in the in the study domain (Eastern Mediterranean) in the duration of simulation (4 hours) for the tsunami source 31-Z31-2	151

Figure A.3.61: The location of tsunami source s32-Z32 (left) and the distribution wave at t=1hr(right) in the study domain (Eastern Mediterranean) in the duration of simulation (4 hours) for the tsunami source s32-Z32	153
Figure A.3.62: The distributions of maximum positive of the water elevations(left) and negative water elevations(right) in the in the study domain (Eastern Mediterranean) in the duration of simulation (4 hours) for the tsunami source s32-Z32.....	153
Figure A.3.63: The location of tsunami source s33-Z38 (left and the distribution wave at t=1hr(right) in the study domain (Eastern Mediterranean) in the duration of simulation (4 hours) for the tsunami source s33-Z38.....	155
Figure A.3.64: The distributions of maximum positive of the water elevations(left) and negative water elevations(right) in the in the study domain (Eastern Mediterranean) in the duration of simulation (4 hours) for the tsunami source s33-Z38.....	155
Figure A.3.65: The location of tsunami source 34-Z41 (left and the distribution wave at t=1hr(right) in the study domain (Eastern Mediterranean) in the duration of simulation (4 hours) for the tsunami source 34-Z41	157
Figure A.3.66: The distributions of maximum positive of the water elevations(left) and negative water elevations(right) in the in the study domain (Eastern Mediterranean) in the duration of simulation (4 hours) for the tsunami source 34-Z41	157
Figure A.3.67: The location of tsunami source s35 (left) and the distribution wave at t=1hr(right) in the study domain (Eastern Mediterranean) in the duration of simulation (4 hours) for the tsunami source s35	159
Figure A.3.68: The distributions of maximum positive of the water elevations(left) and negative water elevations(right) in the in the study domain (Eastern Mediterranean) in the duration of simulation (4 hours) for the tsunami source s35	159
Figure A.3.69: The location of tsunami source s36 (left and the distribution wave at t=1hr(right) in the study domain (Eastern Mediterranean) in the duration of simulation (4 hours) for the tsunami source s36	161

- Figure A.3.70:** The distributions of maximum positive of the water elevations(left) and negative water elevations(right) in the in the study domain (Eastern Mediterranean) in the duration of simulation (4 hours) for the tsunami source s36161
- Figure A.3.71:** The location of tsunami source s37 (left) and the distribution wave at t=1hr(right) in the study domain (Eastern Mediterranean) in the duration of simulation (4 hours) for the tsunami source s37163
- Figure A.3.72:** The distributions of maximum positive of the water elevations(left) and negative water elevations(right) in the in the study domain (Eastern Mediterranean) in the duration of simulation (4 hours) for the tsunami source s37163
- Figure A.3.73:** The location of tsunami source s38 (left) and the distribution wave at t=1hr(right) in the study domain (Eastern Mediterranean) in the duration of simulation (4 hours) for the tsunami source s38165
- Figure A.3.74:** The distributions of maximum positive of the water elevations(left) and negative water elevations(right) in the in the study domain (Eastern Mediterranean) in the duration of simulation (4 hours) for the tsunami source s38165

LIST OF TABLES

TABLES

Table 3.1: Source Parameters taken from TRANSFER project (TRANSFER Work packages, 2009).....	24
Table 3.2: Locations of Forecast Points	37
Table 4.1: Dip and Rake angle ranges for hypothetical source created on regular bathymetry.....	41
Table 4.2: Summary of Results for dip 10° and rake 110° and for dip 110° and rake 10° of hypothetical source on regular bathymetry.....	1
Table 4.3: Dip and Rake angle ranges for s24-Z26-1	45
Table 4.4: Summary of Results for dip 10°and rake 90° and for dip 30°and rake 90° of s24-Z26-1	38
Table 4.5: Summary of Results for dip 90° and rake 10° and for dip 90° and rake 30° of s24-Z26-1	38
Table 4.6: Rupture Parameters of Tsunami Source 01-365	49
Table 4.7: Summary Results of tsunami impact at forecast points for source 01-365....	51
Table 4.8: Boundaries and Grid Sizes of each domain for Bodrum	52
Table 4.9: Summary Results of tsunami impact at forecast points for source 01-365 on Bodrum.....	54
Table 4.11: Boundaries and Grid Sizes of each domain for Iskenderun.....	58
Table 4.12: Summary Results of tsunami impact at forecast points for source 33-Z38 and for source 33-Z38 with double displacement on Iskenderun	49
Table 4.13: Boundaries and Grid Sizes of each domain for Kas	63
Table 4.14: Summary Results of tsunami impact at forecast points for source s38 on Kas	66

Table A.3.1: Rupture Parameters of Tsunami Source 02-Z04	93
Table A.3.2: Summary Results of tsunami impact at forecast points for source 02-Z04	94
Table A.3.3: Rupture Parameters of Tsunami Source 03-Z10-1	95
Table A.3.4: Summary Results of tsunami impact at forecast points for source 03-Z10-1	96
Table A.3.5: Rupture Parameters of Tsunami Source 04-Z10-2	97
Table A.3.6: Summary Results of tsunami impact at forecast points for source 04-Z10-2	98
Table A.3.7: Rupture Parameters of Tsunami Source 05-Z10-3	99
Table A.3.8: Summary Results of tsunami impact at forecast points for source 05-Z10-3	100
Table A.3.9: Rupture Parameters of Tsunami Source 06-Z10-4	101
Table A.3.10: Summary Results of tsunami impact at forecast points for source 06-Z10-4	102
Table A.3.11: Rupture Parameters of Tsunami Source 07-Z11-1	103
Table A.3.12: Summary Results of tsunami impact at forecast points for source 07-Z11-1	104
Table A.3.13: Rupture Parameters of Tsunami Source 08-Z11-2	105
Table A.3.14: Summary Results of tsunami impact at forecast points for source 08-Z11-2	106
Table A.3.15: Rupture Parameters of Tsunami Source 09-Z11-3	107
Table A.3.16: Summary Results of tsunami impact at forecast points for source 09-Z11-3	108
Table A.3.17: Rupture Parameters of Tsunami Source 10-Z12-1	109
Table A.3.18: Summary Results of tsunami impact at forecast points for source 10-Z12-1	110
Table A.3.19: Rupture Parameters of Tsunami Source 11-Z12-2	111
Table A.3.20: Summary Results of tsunami impact at forecast points for source 11-Z12-2	112

Table A.3.21: Rupture Parameters of Tsunami Source 12-Z14	113
Table A.3.22: Summary Results of tsunami impact at forecast points for source 12-Z14	114
Table A.3.23: Rupture Parameters of Tsunami Source 13-Z15-1	115
Table A.3.24: Summary Results of tsunami impact at forecast points for source 13-Z15-1	116
Table A.3.25: Rupture Parameters of Tsunami Source 14-Z15-2	117
Table A.3.26: Summary Results of tsunami impact at forecast points for source 14-Z15-2	118
Table A.3.27: Rupture Parameters of Tsunami Source 15-Z17-1	119
Table A.3.28: Summary Results of tsunami impact at forecast points for source 15-Z17-1	120
Table A.3.29: Rupture Parameters of Tsunami Source 16-Z17-2	121
Table A.3.30: Summary Results of tsunami impact at forecast points for source 16-Z17-2	122
Table A.3.31: Rupture Parameters of Tsunami Source 17-Z17-3	123
Table A.3.32: Summary Results of tsunami impact at forecast points for source 17-Z17-3	124
Table A.3.33: Rupture Parameters of Tsunami Source 18-Z22	125
Table A.3.34: Summary Results of tsunami impact at forecast points for source 18-Z22	126
Table A.3.35: Rupture Parameters of Tsunami Source 19-Z24	127
Table A.3.36: Summary Results of tsunami impact at forecast points for source 19-Z24	128
Table A.3.37: Rupture Parameters of Tsunami Source 20-Z25	129
Table A.3.38: Summary Results of tsunami impact at forecast points for source 20-Z25	130
Table A.3.39: Rupture Parameters of Tsunami Source 21-Z13-1	131

Table A.3.40: Summary Results of tsunami impact at forecast points for source 21-Z13-1	132
Table A.3.41: Rupture Parameters of Tsunami Source 22-Z13-2	133
Table A.3.42: Summary Results of tsunami impact at forecast points for source 22-Z13-2	134
Table A.3.43: Rupture Parameters of Tsunami Source 23-Z13-3	135
Table A.3.44: Summary Results of tsunami impact at forecast points for source 23-Z13-3	136
Table A.3.45: Rupture Parameters of Tsunami Source 24-Z26-1	137
Table A.3.46: Summary Results of tsunami impact at forecast points for source 24-Z26-1	138
Table A.3.47: Rupture Parameters of Tsunami Source 25-Z26-2	139
Table A.3.48: Summary Results of tsunami impact at forecast points for source 25-Z26-2	140
Table A.3.49: Rupture Parameters of Tsunami Source 26-Z28	141
Table A.3.50: Summary Results of tsunami impact at forecast points for source 26-Z28	142
Table A.3.51: Rupture Parameters of Tsunami Source 27-Z29-1	143
Table A.3.52: Summary Results of tsunami impact at forecast points for source 27-Z29-1	144
Table A.3.53: Rupture Parameters of Tsunami Source 28-Z29-2	145
Table A.3.54: Summary Results of tsunami impact at forecast points for source 28-Z29-2	146
Table A.3.55: Rupture Parameters of Tsunami Source 29-Z30	147
Table A.3.56: Summary Results of tsunami impact at forecast points for source 29-Z30	148
Table A.3.57: Rupture Parameters of Tsunami Source 30-Z31-1	149
Table A.3.58: Summary Results of tsunami impact at forecast points for source 30-Z31-1	150

Table A.3.59: Rupture Parameters of Tsunami Source 31-Z31-2	151
Table A.3.60: Summary Results of tsunami impact at forecast points for source 31-Z31-2.....	152
Table A.3.61: Rupture Parameters of Tsunami Source s32-Z32	153
Table A.3.62: Summary Results of tsunami impact at forecast points for source s32-Z32	154
Table A.3.63: Rupture Parameters of Tsunami Source s33-Z38	155
Table A.3.64: Summary Results of tsunami impact at forecast points for source s33-Z38	156
Table A.3.65: Rupture Parameters of Tsunami Source 34-Z41	157
Table A.3.66: Summary Results of tsunami impact at forecast points for source 34-Z41	158
Table A.3.67: Rupture Parameters of Tsunami Source s35	159
Table A.3.68: Summary Results of tsunami impact at forecast points for source s35..	160
Table A.3.69: Rupture Parameters of Tsunami Source s36	161
Table A.3.70: Summary Results of tsunami impact at forecast points for source s36..	162
Table A.3.71: Rupture Parameters of Tsunami Source s37	163
Table A.3.72: Summary Results of tsunami impact at forecast points for source s37..	164
Table A.3.73: Rupture Parameters of Tsunami Source s38	165
Table A.3.74: Summary Results of tsunami impact at forecast points for source s38..	166

CHAPTER 1

INTRODUCTION

Tsunami is the one of the most devastating marine hazards in nature. A massive earthquake has hit the northeast of Japan triggering a tsunami that has caused extensive damage in March 11, 2011. Tohoku earthquake, which was recorded 9.0 magnitude in richer scale, with ensuing giant tsunami, which hits the coasts up to 10 m waves and caused fatalities about 26,000 people and damage loss of approximately more than 300 billion US dollars even though the tsunami warning alarm was given after the rupture. The flooding reached 5 km to inland and the risk of damage raised by the Fukushima nuclear power plant increased the excitement during the disaster (Wikipedia 2011).

That horrifying example also indicated that the societal preparedness should also be made against attack of that kind of disaster. This event also raised the importance of a question in countries minds about their own precautions about tsunami. Nevertheless, the tsunami occurrence in Mediterranean Basin is lower than Pacific Ocean, a development of a tsunami warning center is needed to decrease the lost before this catastrophic event takes place. The disaster management plan can be done by understanding the parameters that affect tsunami generation, its propagation, estimated effect on neighborhood coasts, developing a tsunami warning strategy and tsunami risk management plan. These parts are all subtitles of development of tsunami warning system.

Throughout the years in history, scientists and researchers work collectively to understand tsunami generation and parameters that may take a role in its properties.

Although there are researches to enlighten the occurrence and propagation, this catastrophic event has still sustaining its mystery due to being born in Deep Ocean. A careful study on historical data should be performed to solve this mystery. By doing this, the ranges of the parameters that are important for tsunami effect on coasts are categorized and estimated. Thus, a catalog can be created to understand the possibility of occurrence and magnitude ranges and probable tsunami effect on coasts. Reliable tsunami databases are great importance of risk evaluation, hazard assessment and public awareness.

Wider awareness, proper preparedness and effective mitigation strategies for tsunamis need collaborative work among different scientific and engineering disciplines with exchange and enhancement of existing data, development and utilization of available computational tools. In order to satisfy this, to Kandilli Observatory and Earthquake Research Institute (KOERI) is taken responsibility of establishing and operating tsunami-warning system in Turkey. According to the duty assigned to Middle East Technical University to develop software to support tsunami-warning system. This study is aimed to develop the database of tsunamis to benefit in order to pursuing the progress of risk assessment of tsunamis in Eastern Mediterranean Basin.

Tsunami assessment study covers the exchange and enhancement of available earthquake and tsunami data, development of bathymetric and topographic data in sufficient resolution, selection of possible or credible tsunami scenarios, selection and application of the valid and verified numerical tools for tsunami generation, propagation, coastal amplification, inundation and visualization. From this point of view, this thesis deals with all these parts for preparing a tsunami assessment.

The literature survey is given in Chapter 2 to look at historical data analysis and catalog studies done by researches and modeling attempts. Chapter 3 focuses on methodology of tsunami parameters, its theoretical background, creating a detailed bathymetric data and selection of record locations and the uncertainty of the model. The scenarios created on

Chapter 3 are applied to a numerical tool called NAMI DANCE in Chapter 4. The discussions of results are given in Chapter 5. Finally, Chapter 6 concludes the thesis.

CHAPTER 2

LITERATURE SURVEY

The Mediterranean Basin is under attack of tsunamis over 3500 years due to the activity of earthquakes, submarine landslides and volcanic eruptions. Therefore, the countries that share the boundaries in that region should be ready when that kind of a disaster takes place. This can be achieved by developing a Mediterranean tsunami warning system with the contribution of scientific investigation groups of neighborhood countries. With detailed searches and studies, the creation of a tsunami warning system can be done by composing a reliable tsunami database as regards to past records, performing tsunami wave simulations and preparing risk assessment.

To compile a trustable and detailed database, the historical and geological tsunami records, developed tsunami databases, and tsunami model studies in Mediterranean region are reviewed and summarized in the following.

2.1 Historical Tsunamis in Mediterranean Basin

There are numerous investigations on historical tsunami events and cataloging by several researchers.

Tinti et al. (2001) pointed out the importance of preparing a tsunami catalogues by connecting fundamental mean of computing the tsunami potential of a given region and determining the degree of tsunami hazard and risk to which a given segment of coast is exposed. In addition, the use of catalogues can also provide an important contribution of

a scientific nature, such as, for example the identification of the tsunami sources and the related tsunamigenic mechanism, and the determination of the tsunami offshore and near shore propagation. Thus, preparedness of the society to the risk of tsunami will gradually increase the development.

The style of seismic deformation along the Cyprus and Hellenic arcs exhibits the characteristics and structural complexities associated with strike-slip, thrust and normal faulting because of convergence between the Aegean, Anatolia, Eurasia and Eastern Mediterranean lithosphere. Existing observations and inferred seismological results indicate that there are younger tectonic, slope failure features within the lower part of the continental slope that are tsunamis-prone locations along the neighboring coastlines of the Mediterranean Sea (Yolsal et al. 2007).

Dawson et al. (2004) stated that in any study of tsunami hazard for a given coastal region, it is very important to have as long a time series of known tsunami as possible. To reveal all the past records, scientific documents, newspapers, historic archives and witnesses to events are not enough to obtain historical data. Firstly, due to the lack of equipment in past, the records are depending on the observations of the person that write that event. Generally, past witnesses can be misjudging the event by confusing storm surge with tsunami. The achievers may add their own personal understanding that makes the records subjective. Secondly, the past data set may be evanished during centuries and that make the data set incomplete. It is very hard to find original reports. The vitality of the reports can be proofed by cross-referencing with other source of references. Another approach Dawson et al. (2004) explaining the partial solution to overcome this problem in recent years as, recognizing that tsunami frequently deposits sediment in the coastal zone. It was realized that a potential existed to identify tsunami that had taken place in prehistory and thereby increase our knowledge of tsunami frequency for given areas over long periods. Thus, the tsunami records can be achieved.

Tsunamis in the Eastern Mediterranean were investigated by Cita and Rimoldi (1997), Guidoboni et al. (1994), Tinti and Maramai (1996), Minoura et al. (2000), Altinok et al. (2001), Dawson et al. (2004), Antonopoulos (1990), Maramai and Gasparini (1991), Stiros (2001), Altinok et al. (2005), Altinok and Ersoy (2000), Papadopoulos and Chalkis (1984), Papadopoulos and Fokaefs (2005), Papadopoulos (2003), Ambraseys and Melville (1987), and Hamouda (2010) using paleotsunami researches and examining historical archives. The tsunamic zone of the Mediterranean Sea is given in Figure 2.1 (Papadopoulos and Fokaefs 2005).

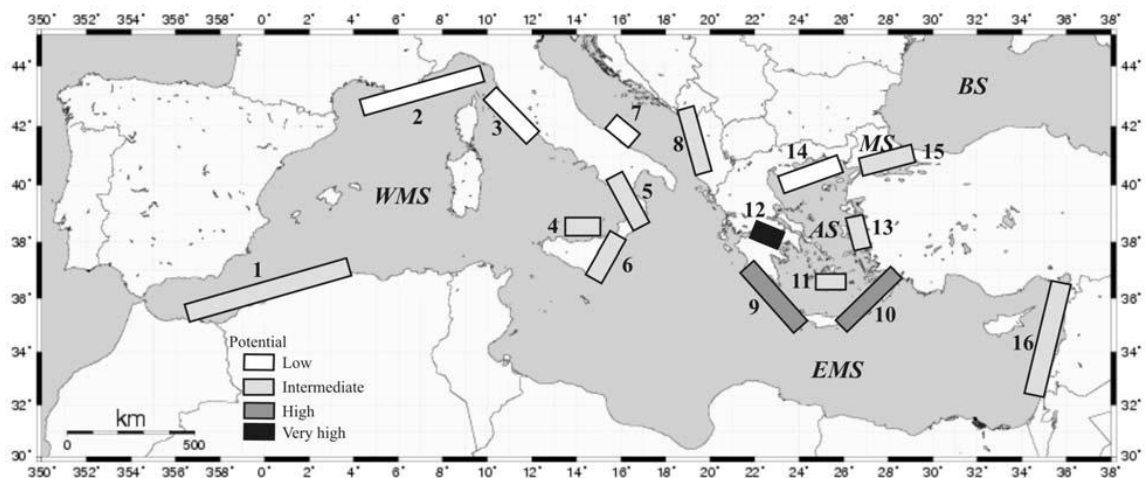


Figure 2.1: The tsunamigenic zones of the Mediterranean Sea.

(WMS = West Mediterranean Sea, EMS = East Mediterranean Sea, AS = Aegean Sea, MS = Marmara Sea, BS = Black Sea, 1 = Alboran Sea, 2 = Liguria and Cote d' Azur, 3 = Tuscany, 4 = Calabria, 5 = Aeolian islands, 6 = Messina straits, 7 = Gargano promontory, 8 = South-East Adriatic Sea, 9 = West Hellenic arc, 10 = East Hellenic arc, 11 = Cyclades, 12 = Corinth Gulf, 13 = East Aegean Sea, 14 = North Aegean Sea, 15 = Marmara Sea, 16 = Levantine Sea (the tsunami potential of each one zone is classified in a relative scale according to the frequency of occurrence and intensity of tsunamis Papadopoulos and Fokaefs (2005)).

According to Dominey-Howes (2002), from 1628 BC to 1996 AD: 2 tsunamis were reported for the period 1628 BC to 550 BC; 14 tsunamis were reported for the time period 550 BC to AD 300; 29 tsunamis were reported for the time period AD 300 to AD 1550; 37 tsunamis are reported for the time period AD 1550 to AD 1845; and finally, 77 tsunamis were reported for the time period AD 1845 to the present. Thus, 71.8% of all recorded tsunamis occurred during the last 12.3% of the time covered by the catalogue. This analysis seems to indicate a quasi-exponential increase in tsunami frequency with time.

To make a close look to the probability of occurrence of tsunamis in local regions in Mediterranean Basin, Fokaefs and Papadopoulos (2005) revealed that based on their investigated historical data, the average tsunami recurrence in the Cyprus-Levantine Sea region is roughly estimated to be around 30 years, 120 years and 375 years for moderate, strong and very strong events, respectively. For a Poissonian (random) process the probabilities of observing at least one moderate, strong or very strong tsunami are 0.28, 0.01, 0.003 and within 1 year, 0.81, 0.34 and 0.13 within 50 years and 0.96, 0.56 and 0.24 within 100 years, respectively. The tsunami potential in the Cyprus- Levantine Sea area is low relative to other Mediterranean tsunamigenic regions. However, the destructiveness of some historical events indicates the need to evaluate tsunami hazard by all available means. In addition, remote tsunamigenic sources, such as those of 1303 and 1481 in the eastern Hellenic arc, are able to threaten the coasts of the Cyprus-Levantine region and, therefore, such regional tsunamis should be taken into account in the evaluation of the tsunami risk of the region.

Moreover, Papadopoulos et al. (2007) reconstituted the datasets and come out with the statistics of the mean recurrence of strong tsunamis is likely equal to about 142 years. This statistical analysis shows the vital importance of tsunami risk mapping.

Historical documents, seismicity and modeling studies showed a clear necessity of understanding and preparedness of the Tsunami hazard in Turkey. Therefore, it was not

a surprise that Turkey was ready to join and contribute to the initiative of a Tsunami Warning System in the Northeastern Atlantic, the Mediterranean and connected seas region (ICG/NEAMTWS), and Kandilli Observatory and Earthquake Research Institute (KOERI), as a pioneer of Earth Sciences in Turkey, was ready to lead related national institutions for the establishment of a National Tsunami Warning System. ICG/NEAMTWS is responsible for the implementation of a Tsunami warning system controlled by the Intergovernmental Oceanographic Commission of UNESCO (IOC-UNESCO) (Ozel et al. 2011).

Turkish coasts have been mentioned previously in the tsunami catalogues and databases compiled by earlier researches: Galanopoulos (1960), Ambraseys (1962), Antonopoulos (1979), and Papadopoulos and Chalkis (1984). On the other hand Soysal et al. (1981), compiled the first Turkish catalogue of tsunamis. Recently, Altinok and Ersoy (2000) compiled historical documents in the Eastern Mediterranean. It includes the list of them with date, region, cause, relevancy, approximate epicenter and magnitude of tsunamigenic earthquakes and other triggering mechanisms. The figure of list is given in Figure 2.2 together with the information on observation and estimated epicenter coordinates of the earthquakes of the historical tsunamis are shown in Appendix A1.

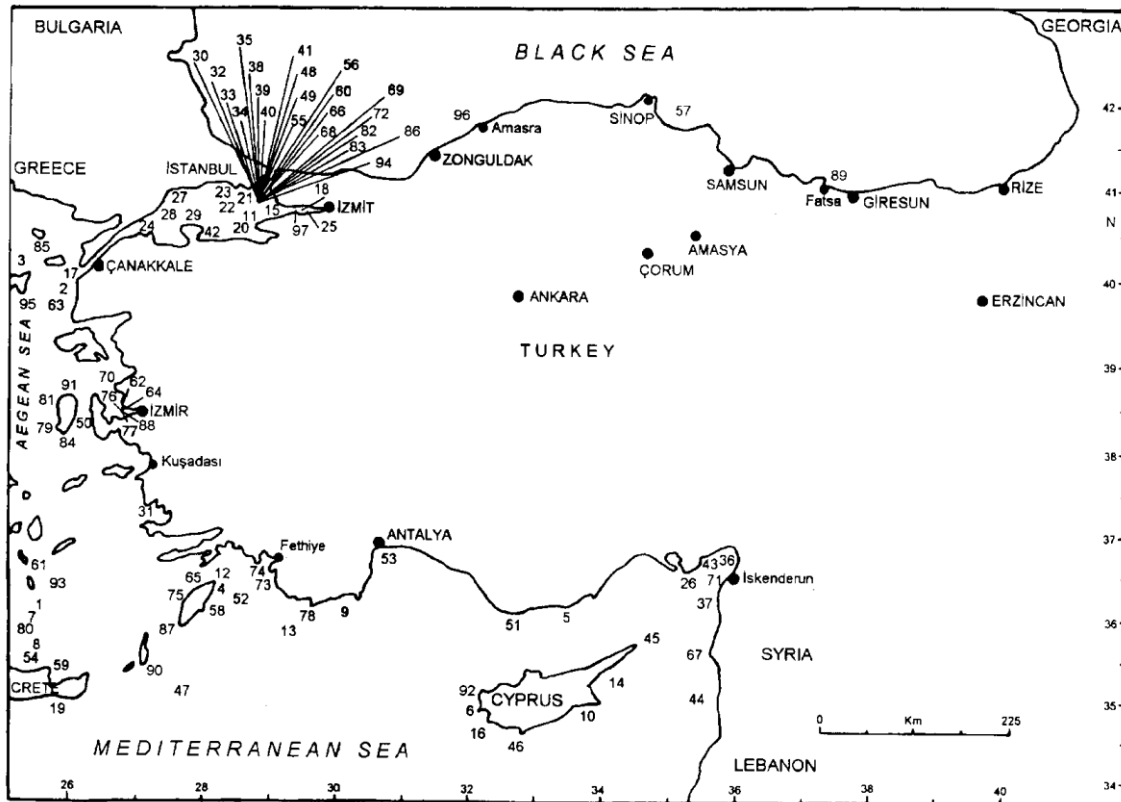


Figure 2.2: Locations of tsunamis which have occurred in Turkey and adjacent areas between 1410 B.C. and 1999 A.D.

Numbers indicate the chronological order in the Appendix A1 (Altinok and Ersoy 2000).

The EU projects GITEC and GITEC-TWO (Genesis and Impact of Tsunamis on the European Coasts) and TRANSFER (Tsunami Risk and Strategies for the European Region) have added important contributions in establishing and developing unified criteria for tsunami parameterization, standards for the quality of the data, the data format and the database general architecture. The current version of the database contains 138 events, most of which have affected the Turkish coasts seriously during the last 3500 years. The reliability index of 76 events was definite, so that they could be

used for assessment of the risk along the Turkish coastal region and for implementation of prevention policies (Altinok et al. 2011).

2.2 Past Attempts of Tsunami Modeling in Eastern Mediterranean Basin

Researchers who obtained and examined the databases offered, realizes the maximum probability of earthquake in a specific region. To investigate the impact of these tsunamis on desired shoreline, they synthetically generate tsunami simulations with possible source parameters. Creating worst-case scenario in region, the maximum run up and flooding on shore can be acquired. This is a logical aspect of risk assessment.

Hamouda (2010) divided region into four seismogenic areas and took into account a seismic fault capable of generating an earthquake with magnitude equal or larger than the highest magnitude registered in that region in historical times.

Yolsal et al. (2007) took maximum displacement of 8m, which is agreement with historical reports. A maximum displacement of 5 m does not adequately explain the lack (or the excess) of tsunami wave heights at most of the northern Africa coastal plains, including Alexandria and Gaza. 11 May 1222 and 8 August 1303 are the tsunamis that are modeled.

Zaytsev et al. (2008) simulated two possible sources. These sources are the ones that are taken from TRANSFER report. These tsunamis are modeled in this thesis too.

Ozel et al. (2011) hypothetically created a tsunami Rhodes and southwest of Turkey.

Salamon et al. (2007) made a landslide generated tsunami simulation. When the studies of researches are examined, there is few modeling attempts are applied in Eastern Mediterranean Basin.

TRANSFER Project covered detailed tsunami modeling studies for the Mediterranean region covering the model improvements and verification efforts (TRANSFER Work packages, 2009).

2.3 Purpose of the Study

A detailed investigation of tsunami records are product of a very detailed study of Altinok et al. (2011). That database combines the studies performed by various groups and creates a reliable source of information. Only 38 sources accepted from TRANSFER project are studied in this thesis considering their possible effects in Eastern Mediterranean (except Marmara and Black sea). These sources create the important tsunami records for Turkish coasts. It is also known that there are uncertainties in estimation of the tsunami source parameters because of the limited data available. The source parameters used or proposed recently may be upgraded when new findings are achieved.

The reliability of the tsunamigenic parameters can also be tested by comparing the effect of run up and inundation computations with past records using modeling tools. This study focuses on i) the effect of tsunamigenic parameters and their reliable range on the coastal amplifications, ii) the bathymetric effect using nested domains, iii) developing the main tsunami parameters' database for the selected tsunami sources by simulations .

The selected tsunami sources are simulated to understand the risk level of selected sensitive coastal locations and visualize the possible effects for the authorities to help them better decision-making and preparedness. This is one of the efficient procedures for tsunami hazard assessments. Moreover, a management plan and future mitigation strategies can be developed. This thesis is planned to be primary source for enhancing a tsunami warning system on Turkish coasts.

CHAPTER 3

TSUNAMI SOURCE MECHANISMS

Tsunamis are series of long waves with depth to wavelength ratio are smaller than one and have large wave periods. Therefore, they are shallow water waves even they are generated in open sea. They travel at high speeds at Deep Ocean and reach thousands of kilometers even in hours. For example, when the ocean is (6100 m) deep, unnoticed tsunami travel about (890 km/hr), the speed of a jet airplane. And they can move from one side of the Pacific Ocean to the other side in less than one day. Their energy is pretty much saved while they are approaching to the shoreline thus, a devastating huge wave wall wash ashore. Because they do not break and dissipate their energy, they show a different wave behavior than storm waves. Therefore, the tsunami generation, propagation and coastal amplification should be carefully studied to understand its near shore effects.

Tsunamis are triggered from an external force that disturbs the stationary position of sea body. Water particles move horizontally by that point-generated source and energy is transferred. The external forces that generate tsunamis can be classified as non-seismic and seismic source mechanisms.

3.1 Non-Seismic Tsunami Source Mechanisms

Non-seismic tsunami source mechanisms can be congregate under three sub-source generation mechanisms. Meteoroidal effect, volcanic eruption and submarine or sub aerial landslides into water bring into existence of tsunamis.

3.1.1 Meteoroid Effect on Tsunami Generation

An extraterrestrial effect on ocean causes mega tsunamis. The documented tsunami deposits from an impact are the Cretaceous Period Tertiary (K/T) deposits from the 170 km diameter Chixculub crater. Based on the size of the rocks that it moved, K/T impact event on the Yucatan peninsula produced a wave that was 50 to 100 meters high at the present location of the Brazos River in Texas (Bourgeois 1988).

The risk observed from this kind of tsunamis is very rare compared to other generation mechanisms. The researchers have not reached an evidence of impact-generated tsunamis in Mediterranean Basin.

3.1.2 Volcanic Eruption Effect on Tsunami Generation

Volcanic explosion or a volcano's slope failure can create disturbances in sea body by forming sudden displacement of water. A massive eruption of Krakatau on August 26, 1883 occurred in Indonesia. After the eruption 2/3 part of the island was drag down. The tsunami waves generated by eruption had wave height reached approximately 40 m and killed more than 36,000 people in coastal towns along Sunda Strait on Java and Sumatra Islands. Tsunami waves were recorded or observed throughout the Indian Ocean, the Pacific Ocean, the American West Coast, South America, and even as far away as the English Channel (Pararas-Carayannis 2001).

Another example of one of the largest volcanic eruption caused tsunami recorded in the history was occurred in Santorin. The final collapse of volcano Santorin was in 1490 B.C. The tsunami produced at the volcano had an estimated +35 to -15 meter initial amplitude and a crest length of about 15 km. By the time, it reached the coastlines of Crete it would have, depending on the shape of the seafloor near the coast and other factors, had variable wave heights ranging from negligible to 26 meters (Bruins et al. 2008).

3.1.3 Submarine or Sub Aerial Landslide Effect on Tsunami Generation

Submarine or subaerial landslides due to ice falls, rockfalls or underwater (submarine) landslides cause the displacement of water with sediment to create a tsunami. Gravitational force is the main activator of these kinds of impacts.

Underwater landslides generally occur some tens of kilometers near the shore on the sloping bottom. The wave is usually steep and shorter in length comparing to other tsunamis. Since the distance from the shore is not so far, it directly propagates towards nearest coastline without any significant dispersion (Insel 2009).

One of the world's largest submarine slides with a total volume of 5,600 km³ occurs on the continental slope west of Norway called Storegga Slide. The slide occurred at a time when the sea level in the southern North Sea stood about 17 m higher than the present level. The highest run up is in Shetland and on the Faeroe Islands more than 15–20 m at the head of small fjords. The run-up estimates from deposits along the outer coast of Norway show run-up of 9–13 m near the slide area, decreasing away from the slide. These large waves extending over such a vast area indicate that most of the volume of the slide was involved in the generation of the tsunami (Bondevik et al. 2004).

Submarine landslide caused by Izmit earthquake in 17th August 1999, occupies tsunami produced flooding over the shore. The disaster took close to 20,000 lives and left more than 10,000 people homeless. In Değirmendere town (south of Izmit bay) the triangular shape (220 m along the shore and 80 m perpendicular to shore) of coastal alluvial headland slid and depth of 15 m in average in the slide location (Yalciner et al. 2002).

3.2 Seismic Tsunami Source Mechanisms

The most common type of tsunami formation is seismic generated source mechanism. The earth is constantly moving on large tectonic plates. When these tectonic plates move past each other, collide or slide under one another, an earthquake results. The

earthquake fault types are normal, reverse and strike slip faults. According to the parameters, those geologists define, the type of the fault is determined. Normal faults occur mainly by a block of the fault move downward relative to other fault and the crust is being extended. Whereas, reverse faults is the movement of a block of fault above relative to other fault and the crust is being subducted. A strike slip fault is the slide of the blocks of faults pass to each other. These faults are identified as either right-lateral or left lateral depending on whether the displacement of the far block is to the right or the left when viewed from either side. Commonly normal faults generate higher magnitude tsunamis.

The formation of seismic generated tsunami is depending on not only fault types and focal mechanism but also magnitude of an earthquake. It should be noted that not all earthquakes produces tsunamis. Generally, underwater earthquakes are triggering the formation of tsunami. The earthquake produces a fluctuation in the mean sea level, which transfer the energy obtained from rupture to the shore as large water column. However, on the history, earthquakes occurred in land also caused tsunami in the near shore. On December 26/27, 1939, during the Erzincan Earthquake (MS=8.0), in Fatsa the sea receded 50 m and after a while the sea returned 20 m inland from the coast (Parejas et al. 1942). In this thesis, submarine earthquake generated source mechanisms are focused.

3.2.1 Rupture Parameters of Earthquake Tsunami Source Mechanisms

“The fault plane is characterized by \vec{n} , its normal vector, and its direction of motion is given by \vec{d} , the slip vector in the fault plane. The slip vector indicates the direction in which the hanging wall (upper side) moves with respect to the footwall (lower side). The slip vector always lies in the fault plane, and is therefore perpendicular to \vec{n} . A coordinate system is useful for studying faults. The x_1 axis is in the strike direction of the fault, x_3 is vertical, and x_2 is perpendicular to x_1 and x_3 (Figure 3.1). δ represents the dip angle, θ the strike of the fault, and λ the rake (slip) angle of the fault, then the vectors

\hat{n} and \hat{d} can be described in terms of the geographic coordinate system" (Rawlinson 2007).

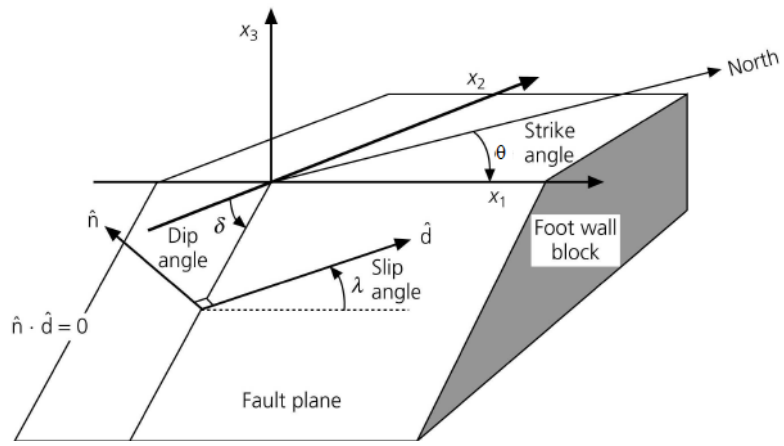


Figure 3.1: Focal mechanism of a fault (Rawlinson 2007)

Although the slip angle can vary between 0 to 2π , several basic fault geometries can be defined as in Figure 3.2.

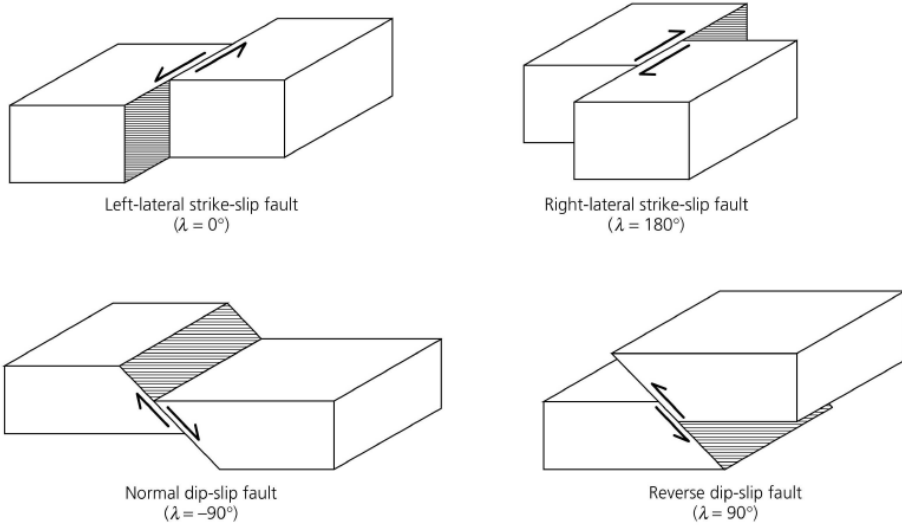


Figure 3.2: Fault types (Rawlinson 2007)

The fault type does not give any evidence of its estimated fault dimensions (Konstantinou et al. 2005).

If a fault is constrained to a rectangular shape, then the distance along strike is the fault length, and the dimension in the dip direction is the fault width. In reality, a fault may be a complicated surface, and an earthquake generated by movement along this surface may ultimately be composed of several sub-events at different places. Complicated seismic events of this type can be treated as a superposition of simpler events, however, so it is useful to understand how seismic waves can be generated by a simple fault with a rectangular geometry (Rawlinson 2007).

There are eight parameters described a rupture generated source mechanism (Figure 3.3):

- The dip angle (δ)
- Strike angle, the direction of the fault axis from North (Clockwise) (Θ)
- The rake (slip) angle (λ)

- Length of the fault (**L**)
- The width of the fault (**W**)
- Epicenter coordinates
- Vertical displacement of the fault (**D**)
- Focal depth (**H**)

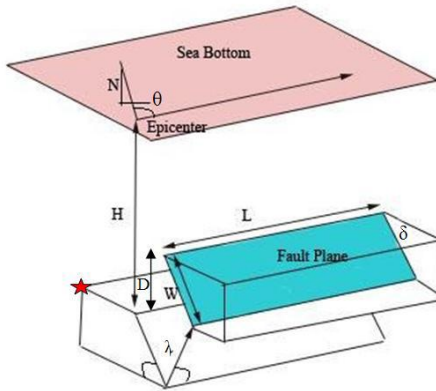


Figure 3.3: Rupture characteristics of seismic generated source mechanisms.

The red star indicates the epicenter of rupture in code NAMI DANCE (NAMI DANCE Manual 2010).

“The use of surface ruptures as primary data for fault dimension estimation exhibit two important problems. First, field observations of ground breakage may not always express the manifestation of the seismogenic fault reaching the surface of the Earth, but rather secondary ground deformation phenomena (like superficial cracks, liquefaction, landslides, etc.). Second, surface rupture lengths usually fail to estimate the actual length of the seismogenic fault by a factor that is inversely proportional to the magnitude of the earthquake” (Wells and Coppersmith 1994).

To evaluate a risk analysis when an earthquake happens, these eight parameters are needed to explain the rupture characteristics of a seismic generated source mechanism. Thus, inputting the parameters needed, the impact of tsunami on the desired shoreline can be forecasted in a short time. However, when an earthquake occurs, only focal depth, epicenter coordinates and magnitude of an earthquake is known. The other parameter may be estimated considering the characteristics of historical data. Geologist estimates the actual values of parameters later.

This study deals with the tsunami simulations due to seismic sources in Eastern Mediterranean.

3.2.2 Seismic Tsunami Sources in Eastern Mediterranean

Mediterranean region consist of Hellenic arc, Cyprus arc, Levantine Basin, Dead Sea Fault, South Anatolian Fault and North Anatolian Fault.

The dominating Hellenic arc controls the trench system while creating active subduction zone beneath the South Aegean Sea (Le Pichon and Angelier 1979). According Mantovani et al. (2000) and Royden (1993) on Hellenic Trench a pattern of the seismic energy release, which is correlated with the total amount of deformation, is non-homogeneous. Generally, the high seismic conductivity in the subducting lithosphere is generated towards the Mediterranean Sea, whereas the other component of low seismic conductivity is generated towards the direction of the Central and North Aegean Sea, which is in the back-arc domain. The dynamic interaction between the Mediterranean and the Aegean lithospheric plates results in the generation of shallow earthquakes in the broad Aegean Sea area and of intermediate focal depth earthquakes in the South Aegean Sea.

There is a complexity in Eastern Mediterranean fault zones. “The African plate subducts underneath Eurasia along the Hellenic Arc at a rate of about 1 cm/year, while the Aegean Sea represents an extensional basin with opening rates in the order of 3.5-4

cm/year” (McClusky et al. 2000). The analysis of oceanic spreading, fault systems, and earthquake slip vectors; the relative plate motions along the North Anatolian fault zone (2.5 cm/a westward) and across the South Aegean Trench (4–5 cm/a southwestward) cause diffuse deformation in the Aegean plate, behind the South Aegean Arc (Dewey and Sengor 1979, Barka and Reilinger 1997, and Altinok et al. 2005). This also reveals that the Aegean Region is rapidly moving and seismically active part of the Alpine-Himalayan Mountain Belt. “The Africa plate and the Anatolia micro plate collides at Cyprian Arc. Moreover, the Mediterranean Ridge, found southwest of the Hellenic trench, represents a structure whose nature is still highly debated” (Le Pichon et al. 2002). Finally, the North-Anatolian Fault is a dextral system of faults forming the broad boundary between the Eurasian plate and the Anatolian block. “The Hellenic Arc is bounded at its northwestern and eastern ends by two major transform faults, known as the Cephalonia (right lateral) and the Rhodes (left lateral) transform faults. The subduction is accompanied by a prominent shallow seismicity with low-angle thrust faults along the Hellenic arc, normal faulting in the back-arc Aegean area, and intermediate depth seismicity forming a well-defined Benioff zone in the southern Aegean” (Tinti et al 2005). The schema of fault movements in Eastern Mediterranean Basin can be seen in Figure 3.4.

As it can be understood from the geological research, there is a high seismic activity in Mediterranean Basin. Due to these seismic activities, the occurrence of earthquakes is highly expected. The advances in the field of seismic instrumentation and the installation of regional and local seismic networks made possible the recording earthquakes including their aftershock sequences. This permits the estimation of fault dimensions, i.e. length, down dip width and epicenter locations (Konstantinou et al. 2005).

However, since the earthquakes generated under the sea are the cause of tsunami it is very hard to obtain the fault parameters soon after rupture occurs. Therefore, geologists and engineers make some estimation of rupture parameters with regard to tsunami

database. The ranges of parameters are also studied in this thesis. The effect of dip and rake angle distribution is emphasized in Chapter 4.

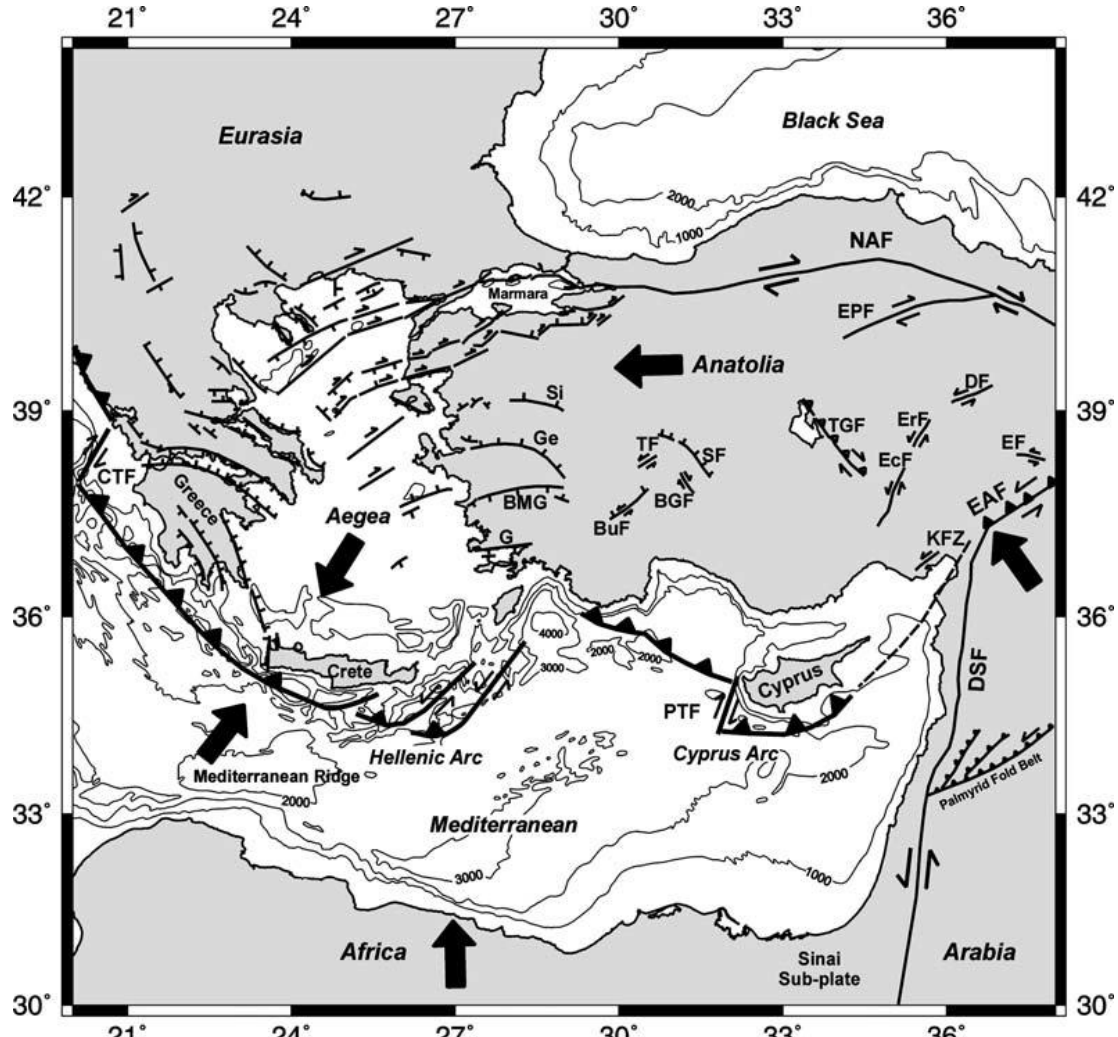


Figure 3.4 Summary sketch map of the faulting and bathymetry in the Eastern Mediterranean Sea region(Yolsal et al. 2007).

NAF, North Anatolian Fault; EAF, East Anatolian Fault; DSF, Dead Sea Fault; EPF, Ezinepazari Fault; PTF, Paphos Transform Fault; CTF, Cephalonia Transform Fault; G, Gokova; BMG, Buyuk Menderes Graben; Ge, Gediz Graben; Si, Simav Graben; BuF, Burdur Fault; BGF, Beysehir Golu Fault; TF, Tatarli Fault; SF, Sultandag Fault; TGF, Tuz Golu Fault; EcF, Ecemis Fault; ErF, Erciyes Fault; DF, Deliler Fault; EF, Elbistan Fault; KFZ, Karatas–Osmaniye Fault Zone. Large black arrows show relative motions of plates with respect to Eurasia. Bathymetric contours are shown at 1000 m interval, and are from GEBCO 30 sec.

The sources from TRANSFER project are given in Figure 3.5. These sources are the product of a careful study of databases. The database of TRANSFER project with earthquakes magnitude equal and greater than 6 in richer scale is given in appendix A2. These sources are grouped by 38 zones and most effective ones are selected. These 38 sources in TRANSFER project are given in Table 3.1 and Figure 3.5, 3.6 and 3.7. The parameters given in Table 3.1 are earthquake epicenter coordinates (in degrees), dip angle, rake angle, strike angle, focal depth, maximum positive and negative wave amplitudes at source, length and width of fault and fault displacement, respectively.

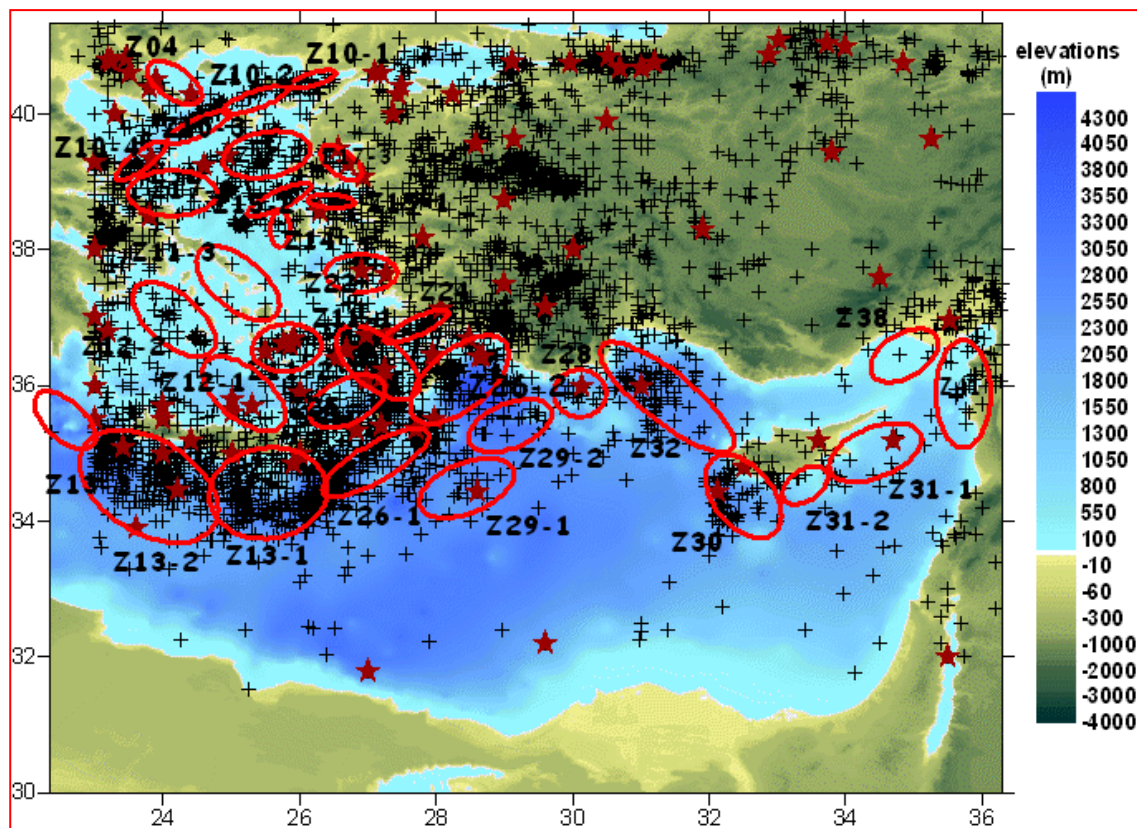


Figure 3.5: Map of possible tsunami sources in Eastern Mediterranean Basin

Table 3.1: Source Parameters taken from TRANSFER project (TRANSFER Work packages, 2009)

Name	Type	Epicenter	Dip (°)	Rake (°)	Strike (°)	Depth (km)	Max (+) amp (m)	Max (-) amp (m)	L (km)	W (km)	D (m)
s01-365	Not Defined	23.45E 35.3N	30	90	315	25	8.1	-0.9	100	90	20
s02-Z04	NOT defined	23.78E 40.83N	45	45	140	10	1.2	-0.2	91.4	12	6
s03-Z10-1	Strike-slip	26.40E 40.40N	45	45	245	10	2.1	-0.4	68.3	15	8
s04-Z10-2	Strike-slip	25.95E 40.15N	45	45	235	10	2.1	-0.4	82.9	15	8
s05-Z10-3	Strike-slip	25.15E 39.75N	45	45	235	10	2.1	-0.4	83.4	15	8
s06-Z10-4	Strike-slip	24.50E 39.20N	45	45	200	10	2.1	-0.4	70.4	15	8
s07-Z11-1	NOT defined	27.68E 36.10N	45	45	330	40	1.0	-0.1	121.8	40	6
s08-Z11-2	NOT defined	25.32E 36.48N	45	45	60	30	0.9	-0.1	82.6	40	6
s09-Z11-3	NOT defined	24.60E 38.00N	45	45	150	30	1.1	-0.2	146.7	30	6
s10-Z12-1	NOT defined	25.76E 35.39N	45	45	330	40	0.9	-0.1	143	30	6
s11-Z12-2	NOT defined	24.70E 36.45N	45	45	330	40	0.9	-0.1	146.5	30	6
s12-Z14	Normal	25.70E 37.97N	45	45	5	20	1.3	-0.2	65.3	30	6
s13-Z15-1	Normal	26.20E 38.69N	45	45	85	15	1.1	-0.2	52.3	15	6
s14-Z15-2	Normal	25.25E 38.53N	45	45	60	15	1.1	-0.2	93.9	15	6
s15-Z17-1	Strike-slip and normal faults	23.70E 39.02N	45	45	120	10	1.9	-0.3	96.9	30	6

Table 3.1. Continued

Name	Type	Epicenter	Dip (°)	Rake (°)	Strike (°)	Depth (km)	Max (+) amp (m)	Max (-) amp (m)	L (km)	W (km)	D(m)
s16-Z17-2	Strike-slip and normal faults	25.00E 39.40N	45	45	80	10	1.4	-0.2	88	15	6
s17-Z17-3	Strike-slip and normal faults	27.12E 38.91N	45	45	330	10	1.3	-0.1	103.7	15	6
s18-Z22	Normal	26.36E 37.64N	45	45	95	20	1.4	-0.2	95.4	30	6
s19-Z24	Strike slip and normal faults	28.18E 37.09N	45	45	240	40	0.3	-0.1	94.6	10	6
s20-Z25	Normal	26.17E 35.69N	45	45	60	40	1.2	-0.2	111.4	50	6
s21-Z13-1	NOT defined	26.41E 34.21N	10	110	240	50	1.3	-0.7	154.8	60	6
s22-Z13-2	NOT defined	24.80E 34.32N	10	110	280	50	1.3	-0.8	191.8	60	6
s23-Z13-3	NOT defined	22.99E 35.13N	10	110	310	50	1.1	-0.7	109.6	60	6
s24-Z26-1	Normal and left-lateral Strike slip fault	27.88E 35.33N	10	110	240	50	1.3	-0.7	169.2	60	6
s25-Z26-2	normal and left-lateral strike slip fault	29.00E 36.66N	10	110	210	50	1.3	-0.8	173.6	60	6
s26-Z28	Strike-slip	29.77E 35.69N	45	45	60	40	0.9	-0.1	72.14	40	6
s27-Z29-1	Strike-slip + cascade	27.78E 34.20N	45	45	60	40	1.1	-0.2	136	40	6

Table 3.1. Continued

Name	Type	Epicenter	Dip (°)	Rake (°)	Strike (°)	Depth (km)	Max (+) amp (m)	Max (-) amp (m)	L (km)	W (km)	D(m)
s28-Z29-2	Strike-slip + cascade	28.48E 35.16N	45	45	60	40	1	-0.2	121.6	40	6
s29-Z30	Strike-slip + cascade	32.98E 33.83N	45	45	330	40	1.1	-0.2	149.3	40	6
s30-Z31-1	NOT defined	33.79E 34.68N	45	45	60	40	1.1	-0.2	137	40	6
s31-Z31-2	NOT defined	33.09E 34.33N	45	45	60	40	0.9	-0.1	72.5	40	6
s32-Z32	Strike slip+ cascading	32.10E 35.40N	45	45	305	20	1.6	-0.2	156	40	6
s33-Z38	left-lateral strike slip fault	34.41E 36.13N	45	45	45	40	1	-0.1	106	40	6
s34-Z41	left-lateral strike slip fault and normal	35.70E 35.07N	45	45	5	40	1.1	-0.1	175.5	40	6
s35	NOT defined	28.46E 34.45N	27	99	294	7.5	1.8	-0.2	126	63	3.65
s36	NOT defined	28.43E 36.07N	47	262	184	7.5	0.2	-1.5	184	50	2.9
s37	NOT defined	28.39E 35.82N	25	90	303	7.5	1.3	-0.3	91	45	2.7
s38	NOT defined	28.4E 35.5N	20	90	55	7.5	2.4	-0.7	190	90	5

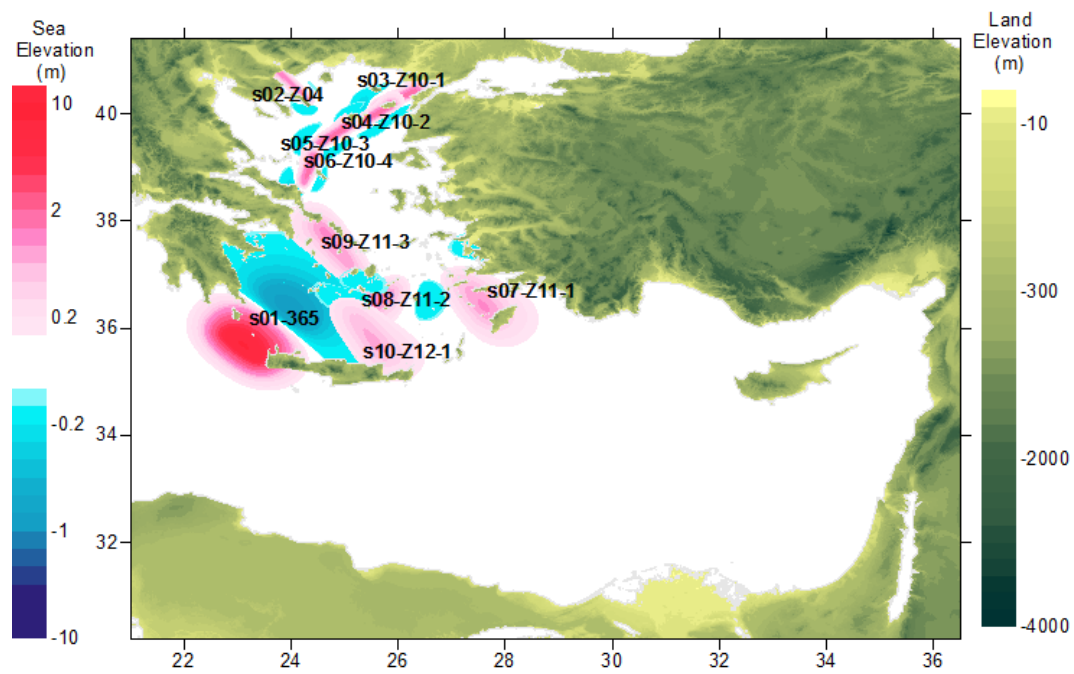


Figure 3.6: Sources between s01-365 to s10-Z12-1

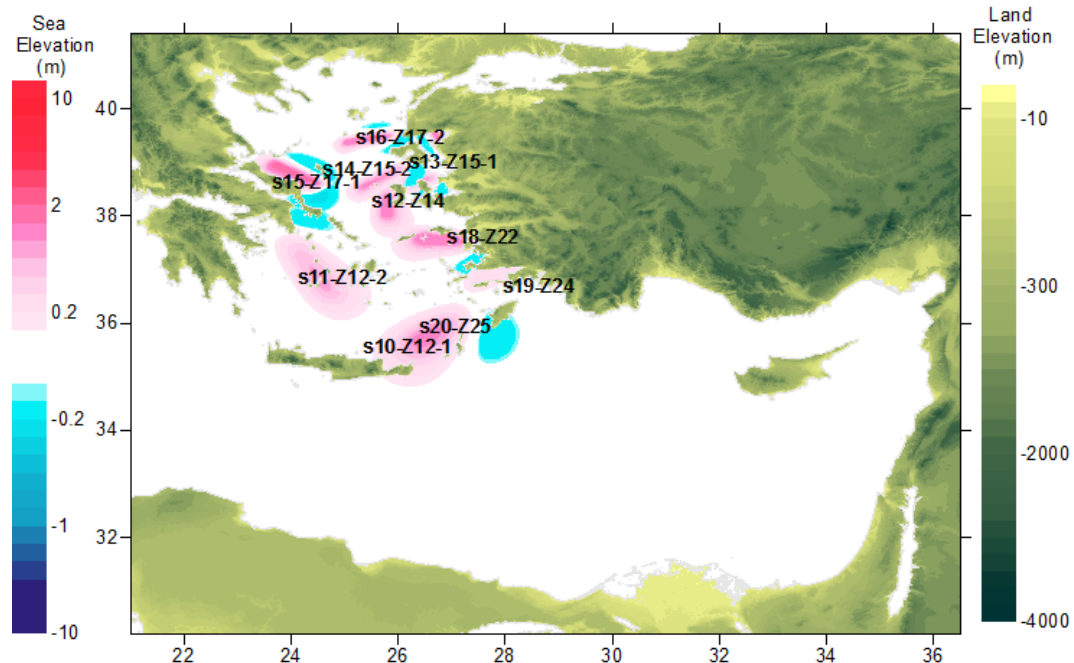
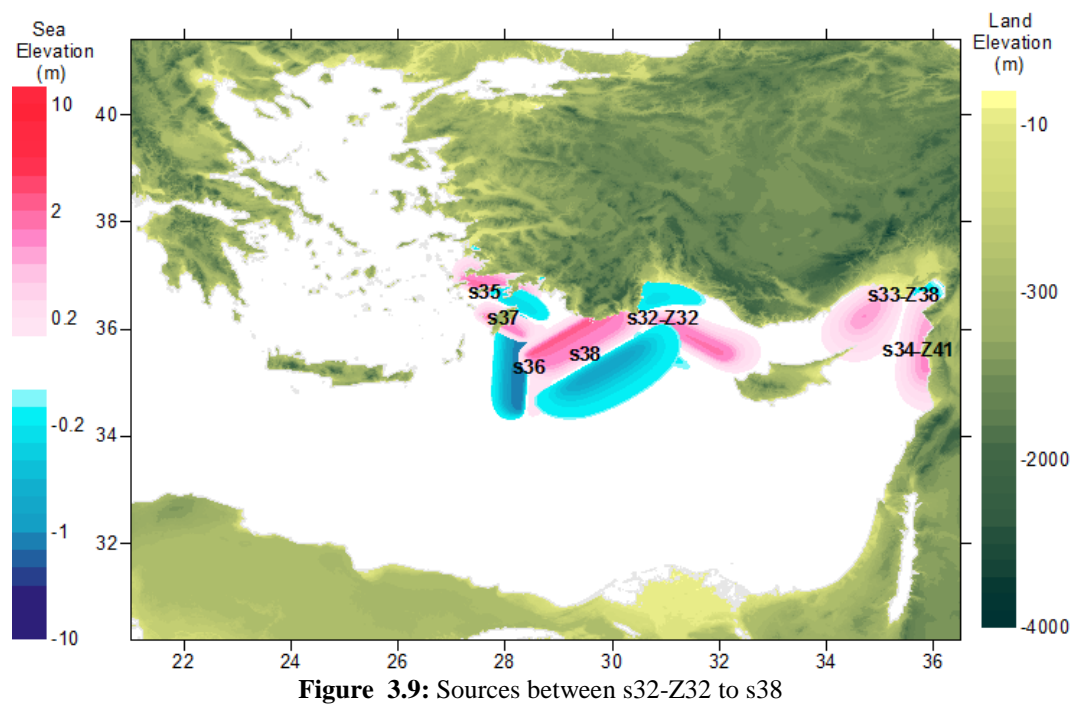
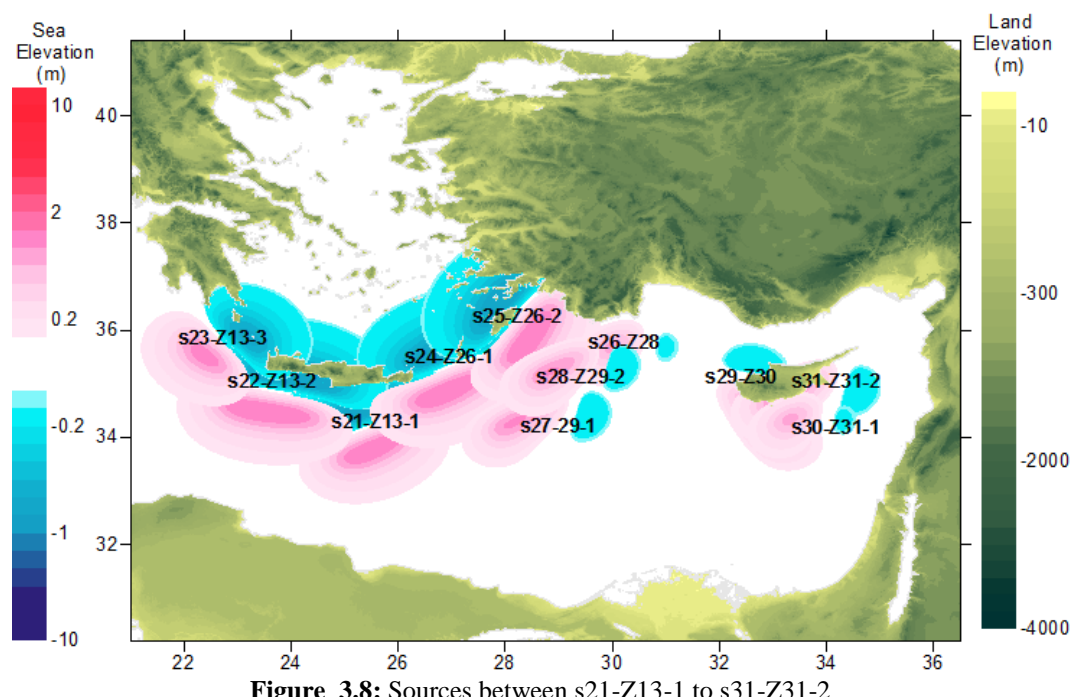


Figure 3.7: Sources Between s11-Z12-2 to s20-Z25



3.3 Tsunami Numerical Modeling

Tsunami as a long wave travel faster than short waves but there is an upper limit. For gravity-induced waves of small amplitude, the maximum speed is:

Where g represents the acceleration due to gravity (about 9.8 m/sec^2 at sea level) and h is the local water depth measured from at the floor of the ocean up to the free surface.

This criterion is especially pertinent for tsunamis, which have very long wavelengths. Tsunami waves move with a high speed at ocean and it is barely noticeable. When the wave approaches shoreline the depth decreases, in front of the wave slows down. However, wave energy does not break and converts the length to the wave height. Moreover, when the following second wave compresses the front wave, since fluids are incompressible, it reflects the horizontal force vertically up. Then huge volume of water hits the shore. A wave that was barely noticeable in open sea can become very large and destructive in near shore. For that reason, the mathematical and numerical background of the wave should be carefully studied to understand tsunami propagation. In the theoretical part, the equations affect the tsunami propagation in open sea and near shore are examined. In the numerical background part, the solution of these equations using a finite difference numerical method is examined.

3.3.1 Theoretical Background

Tsunami propagation can be described by shallow water wave equation. Linear form of shallow water wave theory can be used at open sea. In the theory, there is relatively small effects of non-linear processes, dispersion and friction in the open ocean, as well as the Coriolis effect. The numerical code that was used in this thesis can solve nonlinear wave equation in Cartesian or spherical coordinate systems taking into account dispersion, friction and Coriolis effect. However, the effect of these terms becomes

important when tsunami wave approaches to the shoreline. When water depth decreases less than 50 m the linear form of shallow water wave equations can take its place with nonlinear form of shallow water equations. Shallow water theory is emphasized since it creates the major impact on shore. The vertical motion of water particles has no effect on the pressure distribution. It is a good approximation that the pressure is hydrostatic. In this thesis, Coriolis effect is neglected because tsunami travel distance remains insignificant in relations to the earth's complete rotation time. The governing equations in tsunami numerical modeling are non-linear form of shallow water equations with friction term. The formulas are solved in Cartesian coordinate system. Based upon these approximations and neglecting the vertical acceleration, the equations of mass conservation and momentum in the three dimensional problem Imamura et.al (2006) are given:

$$\frac{\partial \eta}{\partial t} + \frac{\partial M}{\partial x} + \frac{\partial N}{\partial y} = 0 \quad \dots \dots \dots \text{(Eq.2)}$$

$$\frac{\partial M}{\partial t} + \frac{\partial}{\partial x} \left(\frac{M^2}{D} \right) + \frac{\partial}{\partial y} \left(\frac{MN}{D} \right) + gD \frac{\partial \eta}{\partial x} + \frac{g\eta^2}{D^{7/3}} M \sqrt{M^2 + N^2} = 0 \quad \dots \dots \dots \text{(Eq.3)}$$

$$\frac{\partial N}{\partial t} + \frac{\partial}{\partial x} \left(\frac{MN}{D} \right) + \frac{\partial}{\partial y} \left(\frac{N^2}{D} \right) + gD \frac{\partial \eta}{\partial y} + \frac{g\eta^2}{D^{7/3}} N \sqrt{M^2 + N^2} = 0 \quad \dots \dots \dots \text{(Eq.4)}$$

$$M = \int_{-h}^{\eta} u dz = u(h + \eta) = uD \dots \dots \dots \text{(Eq.5)}$$

$$N = \int_{-h}^{\eta} v dz = v(h + \eta) = vD \dots \dots \dots \text{(Eq.6)}$$

where, x and y are horizontal axes, z the vertical axis, t time, h the still water depth, η the vertical displacement of water surface above the still water surface, u , v and w are water particle velocities in x , y and z directions, respectively, g the gravitational acceleration, D is the total water depth given by $h+\eta$, M and N are the discharge fluxes in the x and y directions which are given. The last terms correspond to bottom friction. It is generally expressed as τ_x and τ_y in the x and y directions,

$$\frac{\tau_x}{\rho} = \frac{1}{2g} \frac{f}{D^2} M \sqrt{M^2 + N^2} \dots \dots \dots \text{(Eq.7)}$$

$$\frac{\tau_y}{\rho} = \frac{1}{2g} \frac{f}{D^2} N \sqrt{M^2 + N^2} \dots \dots \dots \text{(Eq.8)}$$

In Eq.7 and Eq.8, ρ is fluid density and f is the friction coefficient. It is preferred to use Manning's roughness coefficient n , which is 0.018 for smooth earth (Chow 1959) and expressed in Eq.9.

$$n = \sqrt{\frac{f D^{1/3}}{2g}} \dots \dots \dots \text{(Eq.9)}$$

A horizontal eddy viscosity that is assumed constant in space, the shear stress on a surface wave is neglected. The equation of momentum in the z direction with the dynamic conditions at a surface yields the hydrostatic pressure (p). The dynamic and kinetic boundary conditions at surface and bottom are given as follows:

$$p=0 \quad \text{at } z=\eta \dots \dots \dots \text{(Eq.10)}$$

$$w = \frac{\partial \eta}{\partial t} + u \frac{\partial \eta}{\partial x} + v \frac{\partial \eta}{\partial y} \quad \text{at } z=\eta \dots \dots \dots \text{(Eq.11)}$$

$$w = -u \frac{\partial h}{\partial x} - v \frac{\partial h}{\partial y} \quad \text{at } z=\eta \dots \dots \dots \text{(Eq.12)}$$

3.3.2 Numerical Background

The finite difference method is used to solve Eq.2, Eq.3 and Eq.4 numerically. The finite difference method based upon the Taylor expansion series is shown in Eq.13 (Imamura et al. 2006).

$$\eta(x, t + \Delta t) = \eta(x, t) + \Delta t \frac{\partial \eta(x, t)}{\partial t} + \frac{\Delta t^2}{2} \frac{\partial^2 \eta(x, t)}{\partial t^2} + \frac{\Delta t^3}{3!} \frac{\partial^3 \eta(x, t)}{\partial t^3} + \dots \dots \dots \text{(Eq.13)}$$

where Δt is the grid interval. The staggered leapfrog scheme is used by applying central difference method (Eq.14) with the staggered numerical points for water level and discharges. $O(\Delta t)$ is truncation error.

$$\frac{\partial \eta(x,t)}{\partial t} = \frac{\eta(x,t+\frac{1}{2}\Delta t) - \eta(x,t-\frac{1}{2}\Delta t)}{\Delta t} + O(\Delta t^2) \dots \text{(Eq.14)}$$

Imamura and Goto (1988) investigated the truncation errors in three kinds of typical scheme for long wave's simulations and showed that in term of numerical accuracy the staggered leapfrog scheme is the best among them. Eq.2 and Eq.3 are simplified to one-dimensional form in order to show the application to Eq. 13 and 14 and given in below.

$$\frac{1}{\Delta t} (\eta_i^{n+1} - \eta_i^n) + \frac{1}{\Delta x} \left(M_{i+1/2}^{n+1/2} - M_{i-1/2}^{n+1/2} \right) + O(\Delta x^2) = 0 \dots \text{(Eq.15)}$$

$$\frac{1}{\Delta t} \left(M_{i+1/2}^{n+1/2} - M_{i-1/2}^{n-1/2} \right) + g \frac{(D_{i+1}^n + D_i^n)}{2} \frac{1}{\Delta x} (\eta_{i+1}^n - \eta_i^n) + O(\Delta x^2) = 0 \dots \text{(Eq.16)}$$

Where Δx and Δt are the grid size in x direction and in time t and $D_i^n = \eta_i^n + h_i$. The point schematics for the numerical scheme are illustrated in Figure 3.9 (Imamura et al. 2006).

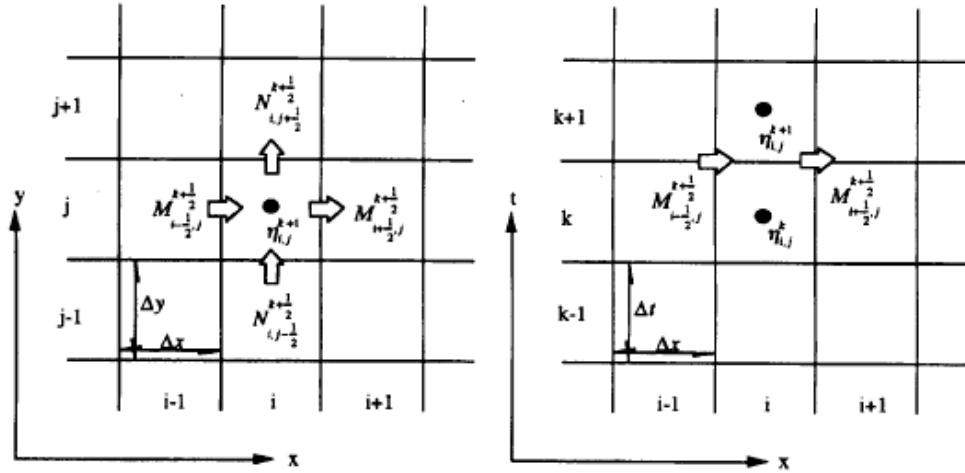


Figure 3.10: Point schematics for the numerical scheme (Imamura et al. 2006)

The difference should be taken in the direction of the flow. This is the reason why this scheme is called the upwind difference. Although the leapfrog scheme has the truncation error of the order of Δx^2 , as long as the convection term concerns, its order become large as Δx .

In numerical simulations, a numerical result is unexpectedly diverged depending on grid size and time step, which is caused by instability in numerical simulations. A stable numerical scheme is one for which errors from any sources (round-off, truncation and so on) are not permitted to grow in the sequence of numerical procedures as the calculation proceeds from one marching step to the next. The finite method provides stable results as long as it satisfies Eq. 17.

$$C \text{ (celerity)} < \Delta x / \Delta t \dots \dots \dots \text{(Eq.17)}$$

In designing numerical computations for long waves, it is recommended to set an open sea boundary. For the continuation of computation at the boundary of a region of

different grid length and for stability of numerical computation, Eq.18 should be satisfied.

$$\Delta x / \Delta t \geq \sqrt{2gh_{max}} \dots \dots \dots \text{(Eq.18)}$$

Where Δx and Δt are the temporal and spatial grid lengths, respectively and the ratio defines numerical speed, and h_{max} is the maximum still water depth in a computation region. The numerical speed must be equal and greater than actual speed. In the leapfrog scheme, grid points are alternatively located for velocity and water level. The wave profile deforms, depending upon the spatial grid length and the travel distance. The smaller the grid length and the shorter the travel distance is, the truer the solution becomes. In order to eliminate this kind of numerical decay in wave height, the grid length should be carefully determined (Hamouda 2009).

3.2.3 Computational Tool

NAMI DANCE used for simulation and efficient visualization of tsunamis, understanding and investigation of tsunami generation and propagation mechanisms. NAMI DANCE simulates, animates and visualizes generation, propagation, coastal amplification and inundation of tsunami given arbitrary shaped bathymetry under the input wave and current conditions. NAMI DANCE is developed in collaboration with Ocean Engineering Research Center, Middle East Technical University, Turkey and Institute of Applied Physics, Russian Academy of Science, Russia especially for tsunami modeling. NAMI DANCE has been, tested and verified parallel to TUNAMI-N2 in the international workshops (NAMI DANCE Manual 2010).

“NAMI DANCE is developed by using C++ programming language by following leap frog scheme numerical solution procedures for faster simulation and better visualizations. The model creates the initial wave from different sources and generates the sea state at specific time intervals of tsunami during simulation. NAMI DANCE also

computes the distributions of current velocities and their directions at selected time intervals, relative damage levels according to drag and impact forces, and it also prepares 3D plots of sea state at selected time intervals from different camera and light positions, and animates the tsunami propagation from source to target for visualization” (Zaytsev st. al. (2008)). NAMI DANCE is used for modeling of tsunamis in several oceans and seas (Yalciner et al. 2007).

The accuracy and the success of the models need higher accuracy of bathymetry. The bathymetry processing for simulations is given in the following.

3.4 Bathymetry Processing

Developing a bathymetric data is the basic step of tsunami modeling because tsunami propagation is affected by ocean bottom thus plays a great role in determining the wave height distributions in coastlines. It is necessary to note that high-resolution bathymetry maps are a crucial component in tsunami wave simulations, and this aspect is rather poorly developed in the Eastern Mediterranean (Yolsal et al. 2007).

The bathymetric and topographic data in digital form for Eastern Mediterranean region is developed (Figure 3.10). The coordinates of existing shoreline are obtained from the Google Earth image. Since the direct field measurements are necessary for the near shore bathymetry and land topography, and since this kind of instrumental accurate data is not available, the bathymetry topography database for tsunami modeling is developed from the best available data source, which is called GEBCO 30 sec. The bound coordinates are selected $21^{\circ} - 36.5^{\circ}$ E longitudes and $30.2^{\circ} - 41.4^{\circ}$ N latitudes.

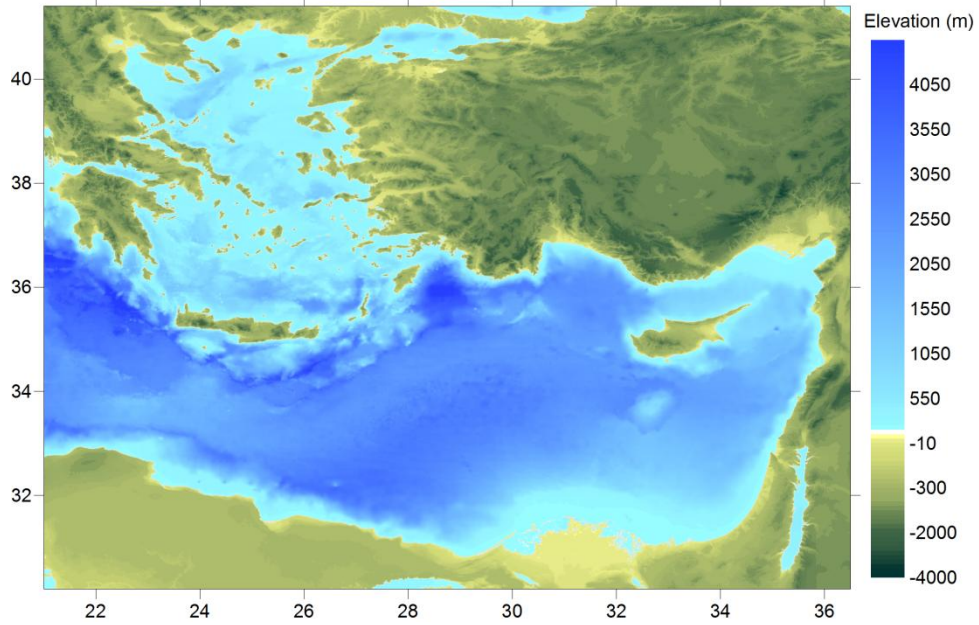


Figure 3.11: The bathymetric/topographic data of Eastern Mediterranean Basin obtained from GEBCO 30 sec.

3.5 Tsunami Forecast Points along Eastern Mediterranean Coast of Turkey

28 locations are selected whether the region has touristic, industrial and geopolitical importance along the Turkish coasts. The coordinates of the points satisfies the sea depth less than 10 m to better examine tsunami effect. The forecast points' locations Gokceada, Mentes, Bodrum, Aksaz, Girne, Gazimagusa, Tasucu, Erdemli, Canakkale, Aliaga, TCDD Alsancak Port, Cesme, Kusadasi, Didim, Marmaris, Fethiye, Kas, Finike, Kemer, Antalya Bay, Alanya, Karatas, Anamur, Iskenderun Bay, Arsuz, Samandag are illustrated in Figure 3.11 and given in Table 3.2.



Figure 3.12: Forecast points along Turkish coasts illustration on Google Earth, 2011.

Table 3.2: Locations of Forecast Points

Name of gauge pt.	Depth of gauge pt.(m)	Longitude	Latitude	Name of gauge pt.	Depth of gauge pt.(m)	Longitude	Latitude
Gokceada	0.4	25.9006	40.2379	Bodrum	6.7	27.4242	37.0228
Mentes	7.4	26.7374	38.4340	Marmaris	1.9	28.3271	36.8107
Bodrum	8.4	27.4171	37.0193	Fethiye	11.7	28.9502	36.7235
Aksaz	4.7	28.4313	36.8453	Fethiye Bay	4.2	29.0546	36.6537
Girne	1.1	33.3276	35.3493	Kas	10.8	29.6436	36.1965
Gazimagusa	7.1	33.9468	35.1367	Finike	5.3	30.1554	36.3000
Tasucu	3.5	33.8327	36.2664	Kemer	0.0	30.5728	36.6052
Erdemli	2.9	34.2629	36.5700	Antalya Bay	10.8	30.6123	36.8362
Canakkale	2.5	26.3772	40.1043	Alanya	10.0	31.9911	36.5243
Aliaga	3.9	26.9423	38.8421	Karatas	2.1	35.3872	36.5604
Alsancak P.	6.8	27.1387	38.4464	Anamur	7.2	32.8582	36.0565
Cesme	10.0	26.2879	38.3288	Iskenderun B.	2.5	36.1898	36.6046
Kusadasi	3.5	27.2588	37.8668	Arsuz	3.2	35.8965	36.4272
Didim	3.7	27.2615	37.3329	Samandag	7.9	35.9564	36.0549

3.6 Uncertainty in Input Data Analysis

Data selection and preparation are important parts of tsunami modeling. Since it is the basic step for creating inundation maps and visualization of potential tsunamis, it should be carefully studied at the first place. However, it is not possible to model a real life problem in to a mathematical environment perfectly. There are always errors come from the unforeseen factors that affect the nature of the problem. This is also the case when tsunami modeling is the purpose. Although statistical analyses are made using historical data, the time factor and frequency are still an enigma. In addition to this, uncertainty on defining rupture parameters and bathymetry preparation is faced in this study. The engineering judgments are made and explained to overcome these disadvantages.

The main uncertainties in tsunami modeling are:

- i) uncertainty in defining rupture parameters
- ii) the resolution of the bathymetry and topographic data

3.6.1 Uncertainty in Defining Rupture Parameters

Since the seismic activity occurring under the sea generally generates tsunami, it is not possible to identify all the rupture parameters correctly. The engineers and geologists are simulating hypothetical tsunami models to get similar results that past tsunamis act on coasts. Thus, they can give a range for defining parameters.

In this thesis, the effect of dip-slip angle is focused and the hypothetical seismic sources are created to observe the effects of these angles on tsunami modeling for Eastern Mediterranean Basin. The worst-case scenario ranges are obtained. Moreover, the influence of fault displacement is practiced.

In this study, the rupture parameters are taken from TRANSFER project. It is clear that these parameters have uncertainties which may be identified in the near future.

3.6.2 Uncertainty on Bathymetry Preparation

Bathymetry preparation has an influence on tsunami modeling. GEBCO 30 sec data is taken and converted to bathymetry / topography data used in this study. However, it is observed that the resolution of 30 sec arc length size is not sufficient to produce fine grid data for the nearshore regions in smaller domains. Bays and headlands cannot be perfectly extrapolated by grid node editor. Thus, gauge points located on sea may be seen on land if the grid size is large. A solution is that, the smaller grid size fits more perfectly on base map. However, this increase time of simulation. Moreover, the accuracy of the bathymetry data in smaller domains depends on the accuracy of the main domain. The nested domains, which is developed by main domain by choosing a small grid length, carries the quality of the main domain data. To enhance the small domain accuracy, satellite image is taken as base map, and a digitization along to coast is a solution to increase the reliability.

CHAPTER 4

MODEL APPLICATIONS

The tsunami simulations can model tsunami generation, propagation, coastal amplification and inundation and the simulation results can be visualized. The accurate and reliable applications in tsunami simulation need tsunami model, which was validated and verified with high resolution reliable tsunamigenic data (tsunami source parameters) and accurate bathymetric - topographic data.

In the first stage of simulations, NAMI DANCE software is used in a single domain bounded by the Easting coordinates of 21°E and 30.2°N and northing coordinates of 36.5°E and 41.4°N in the Eastern Mediterranean. The study domain is gridded by the 3103 grid nodes in easting direction and 2767 grid nodes in northing direction. The grid size is 900 m in both directions. The boundaries of the single domain simulations are given in Chapter 3.

Chapter 3 provided data of the initial conditions of tsunami sources for the computational model to be used in understanding the propagation of tsunamis in the open sea and their coastal amplifications at shallower regions of Turkish coasts.

Each tsunami source is simulated and the distributions of maximum positive amplitudes and maximum negative amplitudes of the water elevations throughout the study domain in the duration of simulations (4 hours) are computed and presented in the following sections.

Chapter 4.1 focuses on the effect of dip and slip angle ranges while determining source parameters. Chapter 4.2 gives the inundation model for forecast points using sources

defined by historical tsunami data. Chapter 4.3 is the detailed study of tsunami simulation on nested domains for Bodrum, Iskenderun and Kas.

4.1 The Effect of Dip and Rake Angle on the Results of Simulations

As mentioned in Chapter 3, source determination is very difficult process since some of the parameters are uncertain. The effect of the dip and rake (slip) angle is examined in this section. Firstly, the effect of angles on regular bathymetry is examined. The study domain is gridded by the 960 grid nodes in easting direction and 988 grid nodes in northing direction. A hypothetical source with strike 360° , length 440 km, width 80 km, focal depth 10 m and fault displacement 10 m is created by changing dip and rake angle given in Table 4.1. This table shows that wave height is higher when the rake angle is chosen higher than the dip angle. The maximum and minimum waves correspond to these angle ranges are given in Table 4.2.

Table 4.1: Dip and Rake angle ranges for hypothetical source created on regular bathymetry

Dip($^\circ$)	10	110
Rake (Slip) ($^\circ$)	110	10
Max (+) amp(m)	3.7	0.4
Max (-) amp(m)	-2.1	-1.4

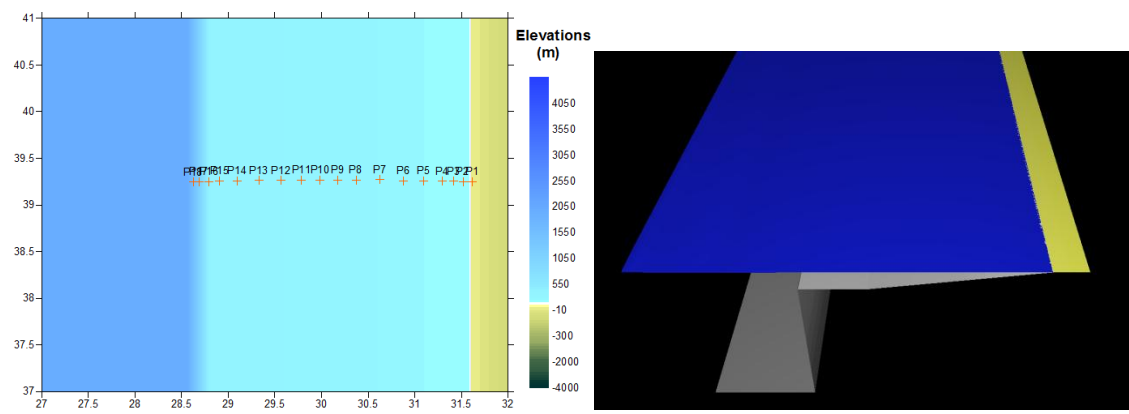


Figure 4.1: Gauge points on regular bathymetry(left) and cross section of bathymetry(right)

The gauge points on regular bathymetry and the sources are given in Figure 4.1 and 4.2. The maximum and minimum sea level distributions are given in Figure 4.3 and 4.4.

Table 4.2: Summary of Results for dip 10° and rake 110° and for dip 110° and rake 10° of hypothetical source on regular bathymetry

Name of gauge pt.	Depth of gauge pt.(m)	XCoord(°)	YCoord(°)	Dip 10° and Rake 110°				Dip 110° and Rake 10°			
				Arrival time of initial wave (min)	Arrival time of max.wave (min)	Max (+) amp.(m)	Max (-) amp.(m)	Arrival time of initial wave (min)	Arrival time of max.wave (min)	Max (+) amp.(m)	Max (-) amp.(m)
P1	-1.3	31.6160	39.2480	0	0	0.0	0.0	0	0	0.0	0.0
P2	8.7	31.5180	39.2480	0	142	4.1	-1.4	86	144	0.5	-0.5
P3	18.6	31.4161	39.2525	0	130	5.0	-2.0	70	132	0.5	-0.4
P4	30.6	31.2986	39.2525	0	120	4.3	-2.2	55	121	0.4	-0.4
P5	50.4	31.0987	39.2570	0	107	4.0	-2.1	32	107	0.4	-0.3
P6	72.3	30.8793	39.2570	0	95	3.8	-2.0	19	94	0.4	-0.3
P7	97.8	30.6246	39.2704	0	83	3.6	-1.9	0	81	0.3	-0.3
P8	123.4	30.3699	39.2659	35	72	3.4	-1.8	0	70	0.3	-0.3
P9	142.6	30.1779	39.2659	24	65	3.3	-1.8	0	63	0.3	-0.3
P10	161.9	29.9859	39.2659	14	58	3.2	-1.8	0	55	0.3	-0.3
P11	181.8	29.7861	39.2659	4	51	3.1	-1.7	0	49	0.3	-0.3
P12	200.0	29.5666	39.2615	0	44	3.0	-1.7	0	41	0.3	-0.3
P13	200.0	29.3276	39.2615	0	36	3.0	-1.7	0	34	0.3	-0.3
P14	200.0	29.0964	39.2570	0	29	3.0	-1.7	0	26	0.3	-0.3
P15	200.0	28.9083	39.2570	0	23	3.0	-1.7	0	20	0.3	-0.3
P16	380.0	28.7947	39.2480	0	19	3.0	-1.7	0	17	0.3	-0.2
P17	1136.0	28.6850	39.2480	0	17	2.5	-1.5	0	15	0.3	-0.2
P18	1604.0	28.6223	39.2436	0	22	2.4	-1.4	0	14	0.3	-0.2

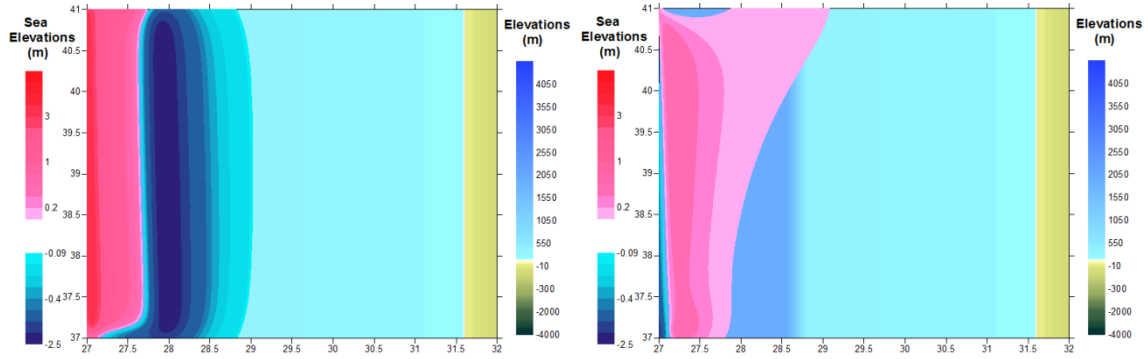


Figure 4.2: Source dip 10° – rake 110° (left) and dip 110° - rake 10° (right) on regular batymetry

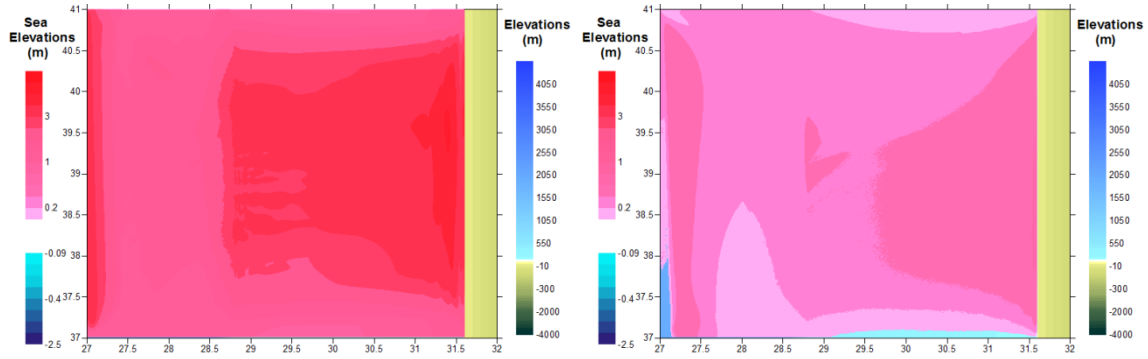


Figure 4.3: Maximum positive sea level elevations for Source dip 10° – rake 110° (left) and dip 110° - rake 10° (right) on regular batymetry

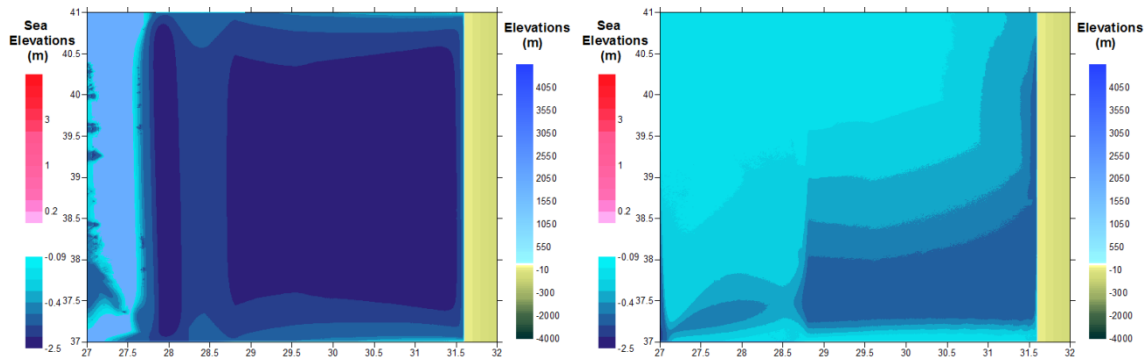


Figure 4.4: Maximum negative sea level elevations for Source dip 10° – rake 110° (left) and dip 110° - rake 10° (right) on regular batymetry

In addition, dip and rake angle change on maximum positive and negative wave height distribution, is not affected by bathymetry type whether it is regular or irregular. The source s24-Z26-1 is chosen from Table 3.1 for 450 m grid bathymetric data in the same region given in Chapter 3. Besides dip and rake angle all the parameters are taken from Table 3.1. Strike angle is 240°, focal depth is 50 km, length of fault is 169.2 km, width of fault is 60 km and fault displacement of the fault is 6 m. The angle ranges are given in Table 4.3 for irregular bathymetry.

Table 4.3: Dip and Rake angle ranges for s24-Z26-1

Dip(°)	10	10	30	45	90	90
Rake (Slip) (°)	110	90	90	45	10	30
Max (+) amp(m)	1.3	1.0	1.2	0.9	0.2	0.4
Max (-) amp(m)	-0.7	-0.6	-0.2	-0.1	-0.2	-0.4

As it can be seen from Table 4.3 the lower dip and higher rake angle give higher amplification at selected locations. The maximum and minimum waves correspond to these angle ranges are given in Table 4.4 and 4.5. These tables clearly show that the dip angle range does not affect the arrival time of initial wave and maximum wave. On the other hand, rake angle changes the position of source so; the areas affected by tsunami are changed. Decreasing rake angle gives small values of wave height. To create a worst-case scenario, rake angle should be increased to a proportional range and dip angle should be decreased. If there is not sufficient information, about these angles dip and rake angles can be chosen as 10° and 110°, respectively for Eastern Mediterranean Basin. The maximum positive sea level changes are given in Figure 4.5 and 4.6.

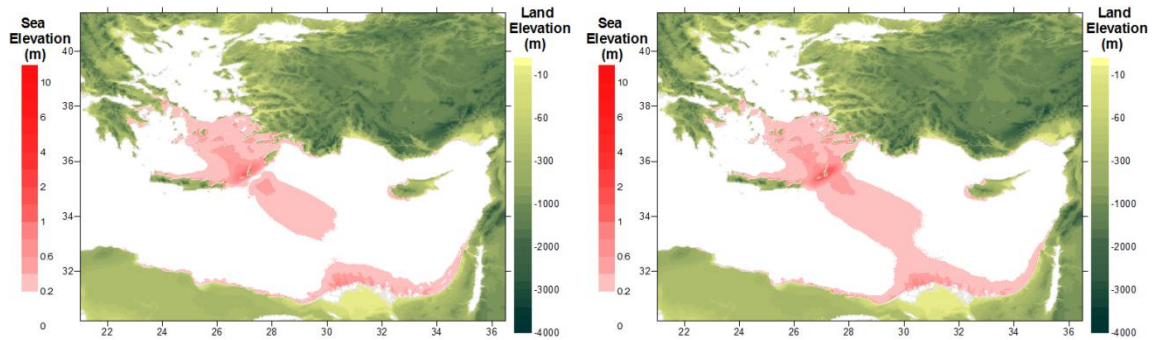


Figure 4.5: Maximum positive sea level elevations for Source dip 10° – rake 90° (left) and dip 30° - rake 90° (right) on irregular batymetry

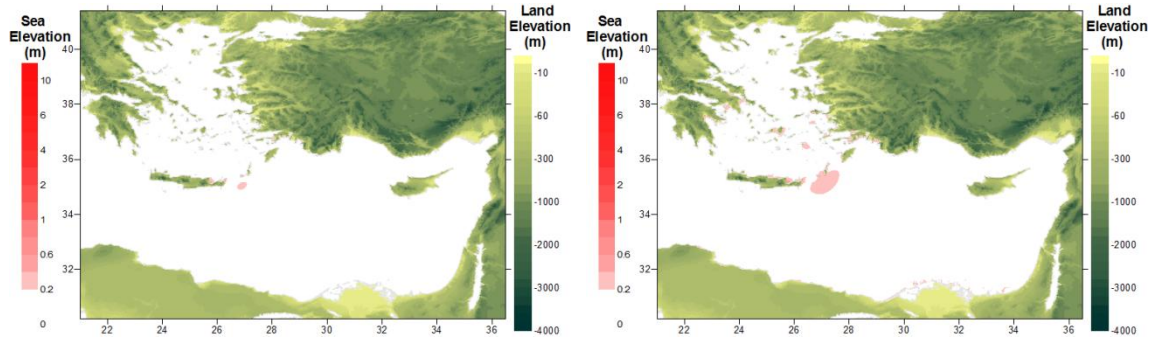


Figure 4.6: Maximum positive sea level elevations for Source dip 90° – rake 10° (left) and dip 90° - rake 30° (right) on regular batymetry

Table 4.4: Summary of Results for dip 10°and rake 90° and for dip 30°and rake 90° of s24-Z26-1

Name of gauge pt.	Depth of gauge pt.(m)	Longitude (E)	Latitude (N)	Dip 10° and Rake 90°				Dip 30° and Rake 90°			
				Arrival time of initial wave (min)	Arrival time of max.wave (min)	Max (+) amp.(m)	Max (-) amp.(m)	Arrival time of initial wave (min)	Arrival time of max.wave (min)	Max (+) amp.(m)	Max (-) amp.(m)
Canakkale	3.2	26.1821	40.0009	173	180	0.1	0.0	175	188	0.1	-0.1
Ayvalik	1.6	26.7322	39.2415	165	167	0.1	0.0	169	170	0.1	-0.1
Cesme	3.7	26.8194	38.1456	72	199	0.2	-0.1	76	85	0.2	-0.2
Kusadasi	9.3	27.2279	37.8541	83	174	0.2	-0.3	86	104	0.2	-0.3
Didim	3.7	27.5357	37.1871	74	236	0.6	-0.5	77	239	0.6	-0.6
Bodrum	7.4	27.4276	37.0287	14	77	1.7	-1.8	31	78	1.8	-2.1
Mugla	0.5	28.0402	36.8929	32	52	0.6	-0.4	42	233	0.6	-0.4
Datca	5.7	27.6951	36.7258	0	100	0.6	-0.7	10	171	0.8	-0.8
Marmaris	6.4	28.3110	36.8119	20	121	0.8	-0.8	30	230	0.6	-0.7
Dalaman	2.5	28.6209	36.7789	17	127	0.5	-0.3	28	101	0.5	-0.4
Gocek	6.6	28.9381	36.7510	0	0	0.0	0.0	0	0	0.0	0.0
Fethiye	6.6	28.9381	36.7510	0	0	0.0	0.0	0	0	0.0	0.0

Table 4.5: Summary of Results for dip 90° and rake 10° and for dip 90° and rake 30° of s24-Z26-1

Name of gauge pt.	Depth of gauge pt.(m)	Longitude	Latitude	Dip 90° and Rake 10°				Dip 90° and Rake 30°			
				Arrival time of initial wave (min)	Arrival time of max.wave (min)	Max (+) amp.(m)	Max (-) amp.(m)	Arrival time of initial wave (min)	Arrival time of max.wave (min)	Max (+) amp.(m)	Max (-) amp.(m)
Canakkale	3.2	26.1821	40.0009	0	0	0.0	0.0	0	0	0.0	0.0
Ayvalik	1.6	26.7322	39.2415	0	0	0.0	0.0	0	0	0.0	0.0
Cesme	3.7	26.8194	38.1456	0	0	0.0	0.0	74	118	0.1	-0.1
Kusadasi	9.3	27.2279	37.8541	0	0	0.0	0.0	86	145	0.1	-0.1
Didim	3.7	27.5357	37.1871	0	0	0.0	0.0	78	144	0.2	-0.2
Bodrum	7.4	27.4276	37.0287	0	66	0.3	-0.3	32	91	0.4	-0.5
Mugla	0.5	28.0402	36.8929	0	38	0.1	-0.2	43	115	0.2	-0.2
Datca	5.7	27.6951	36.7258	0	66	0.2	-0.2	0	82	0.2	-0.2
Marmaris	6.4	28.3110	36.8119	20	36	0.3	-0.4	28	112	0.3	-0.4
Dalaman	2.5	28.6209	36.7789	17	82	0.2	-0.3	25	80	0.3	-0.3
Gocek	6.6	28.9381	36.7510	0	0	0.0	0.0	0	0	0.0	0.0
Fethiye	6.6	28.9381	36.7510	0	0	0.0	0.0	0	0	0.0	0.0

4.2 Single Domain Simulations

This section focuses on time needed for the first tsunami signals to reach the remote coasts. Indeed deeper attention should be paid to the long-term features of the tsunami propagation for each scenario in order to evaluate the expected total duration of the phenomena, the characteristic periods, and the relative amplitude of the wave packets and the role of edge waves.

During each simulation, the water surface fluctuations are computed and stored at selected locations along Turkish coastal area. The grid length is chosen as 900 m. The location where the maximum positive and maximum negative amplitudes, the coordinates of the location and its depth, the arrival time of first wave and maximum wave to this location are selected and tabulated. The output of first scenario is given as an example in Table 4.6 and 4.7 and Figure 4.7 and 4.8. The maximum positive and negative wave amplitude indicated in summary sheet is recorded at source location. The rest of the 37 scenarios are given in Appendix A3.

Table 4.6: Rupture Parameters of Tsunami Source 01-365

Rupture Parameters			
Epicenter of fault axis	23.45E 35.3N	Dip angle (deg.)	30
Length of fault (km)	100	Slip angle (deg.)	90
Strike angle (deg. CW)	315	Fdisplacement (m)	20
Width of fault (km)	90	Maximum (+)ve amp. (m)	8.1
Focal depth (km)	25	Maximum (-)ve amp. (m)	-0.9

It can be seen from the summary results given in Appendix A3 that the tsunami sources s01-365, s03-Z10-1, s04-Z10-2, s05-Z10-3, s06-Z10-4, s15-Z17-1, s35 and s38 cause more effect on Eastern Mediterranean region comparing the effects of the other sources.

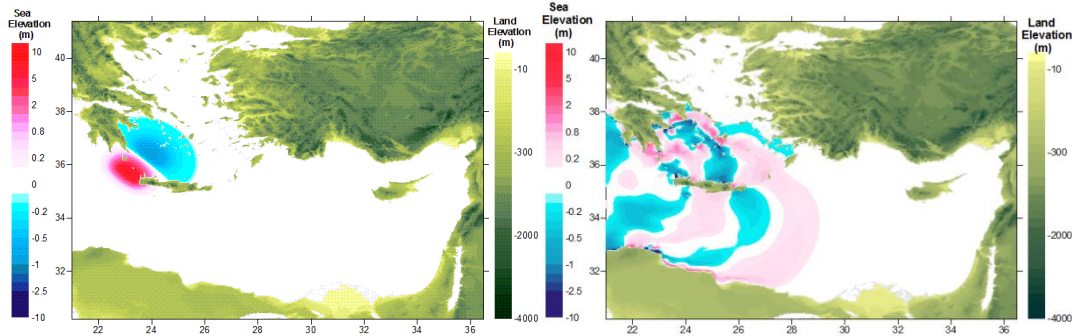


Figure 4.7: The location of tsunami source 01-365 and the distributions of water elevations after $t=1\text{hr}$ in the study domain (Eastern Mediterranean) in the duration of simulation (4 hours) for the tsunami source 01-365

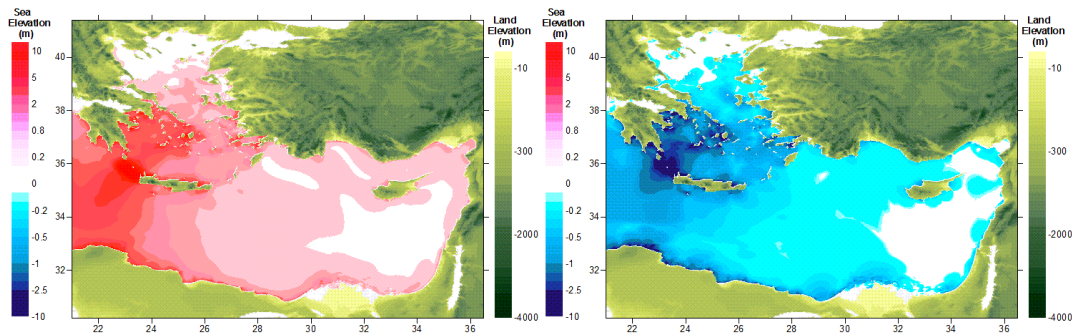


Figure 4.8: The distributions of maximum(left) and minimum (right) of the water elevations and first wave in the study domain (Eastern Mediterranean) in the duration of simulation (4 hours) for the tsunami source 01-365

Table 4.7: Summary Results of tsunami impact at forecast points for source 01-365

Name of gauge pt.	Depth of gauge pt.(m)	Longitude	Latitude	Arrival time of initial wave (min)	Arrival time of max.wave (min)	Maximum (+)ve amp.(m)	Maximum (-)ve amp.(m)
Gokceada	0.4	25.9006	40.2379	67	235	0.1	-0.1
Mentes	7.4	26.7374	38.4340	78	226	0.2	-0.1
Bodrum	8.4	27.4171	37.0193	16	175	3.0	-3.3
Aksaz	4.7	28.4313	36.8453	23	228	2.0	-2.1
Girne	1.1	33.3276	35.3493	48	148	0.2	-0.2
Gazimagusa	7.1	33.9468	35.1367	66	208	0.5	-0.5
Tasucu	3.5	33.8327	36.2664	73	146	0.3	-0.3
Erdemli	2.9	34.2629	36.5700	83	189	0.5	-0.3
Canakkale	2.5	26.3772	40.1043	102	219	0.3	-0.1
Aliaga	3.9	26.9423	38.8421	63	172	0.3	-0.2
AlsancakP.	6.8	27.1387	38.4464	121	234	0.3	-0.2
Cesme	10.0	26.2879	38.3288	31	201	0.5	-0.7
Kusadasi	3.5	27.2588	37.8668	34	144	1.3	-1.2
Didim	3.7	27.2615	37.3329	36	173	0.6	-0.4
Bodrum	6.7	27.4242	37.0228	17	175	3.5	-3.5
Marmaris	1.9	28.3271	36.8107	21	151	1.1	-1.0
Fethiye	11.7	28.9502	36.7235	19	240	0.6	-0.6
Fethiye Bay	4.2	29.0546	36.6537	17	199	1.0	-1.2
Kas	10.8	29.6436	36.1965	16	234	0.5	-0.8
Finike	5.3	30.1554	36.3000	23	121	1.3	-1.7
Kemer	0.0	30.5728	36.6052	103	132	0.5	0.0
Antalya B.	10.8	30.6123	36.8362	35	134	0.6	-0.7
Alanya	10	31.9911	36.5243	36	135	0.5	-0.2
Karatas	2.1	35.3872	36.5604	116	186	0.5	-0.1
Anamur	7.2	32.8582	36.0565	45	143	0.4	-0.4
IskenderunB	2.5	36.1898	36.6046	141	240	0.6	-0.1
Arsuz	3.2	35.8965	36.4272	114	216	0.4	-0.1
Samandag	7.9	35.9564	36.0549	91	200	0.5	-0.3

4.3 Nested Domain Simulations

Bodrum, Iskenderun and Kas region in high resolution are also considered as selected sources for nested simulations. The nested domains are B, C and D. B domain is same for all regions and is chosen as Mediterranean Basin bathymetry used in single domain simulations. The boundaries and grid size of each domain are given. The time histories of near shore water surface fluctuations at several coastal locations in domains are plotted for each simulation (source).

4.3.1 Nested Domain Simulations for Bodrum

Two sources are simulated for Bodrum to observe the impacts on coasts for worst case scenarios. These sources are s01-365 and s35. These sources give the maximum amplitude in single domain simulations. Boundaries and grid sizes of each domain are given in Table 4.8. The smaller domains are shown in Figure 4.9. The forecasts points in Bodrum headland are illustrated on Figure 4.10.

The output summary table for source s01-365 is given in Table 4.9 and maximum positive amplitude of source and sea level fluctuations can be seen from Figure 4.11.

Table 4.8: Boundaries and Grid Sizes of each domain for Bodrum

Domain	Longitude (W)	Longitude(E)	Latitude (S)	Latitude (N)	Grid Size (m)
B	21.00	30.20	36.50	41.40	900
C	27.20	27.56	36.94	37.20	300
D	27.36	27.48	36.98	37.04	100

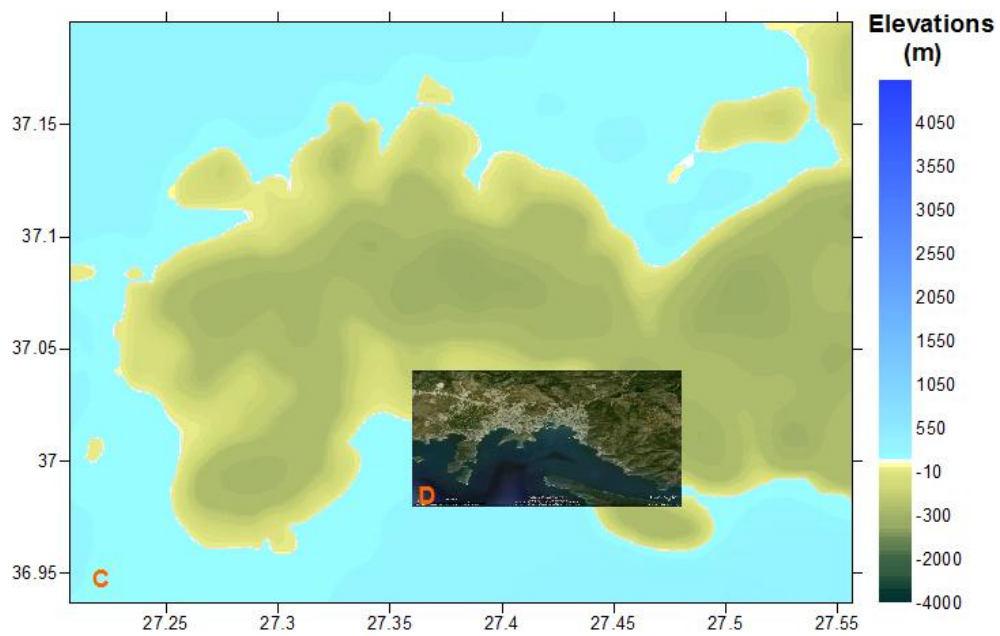


Figure 4.9: The smaller domains (C and D) of Bodrum

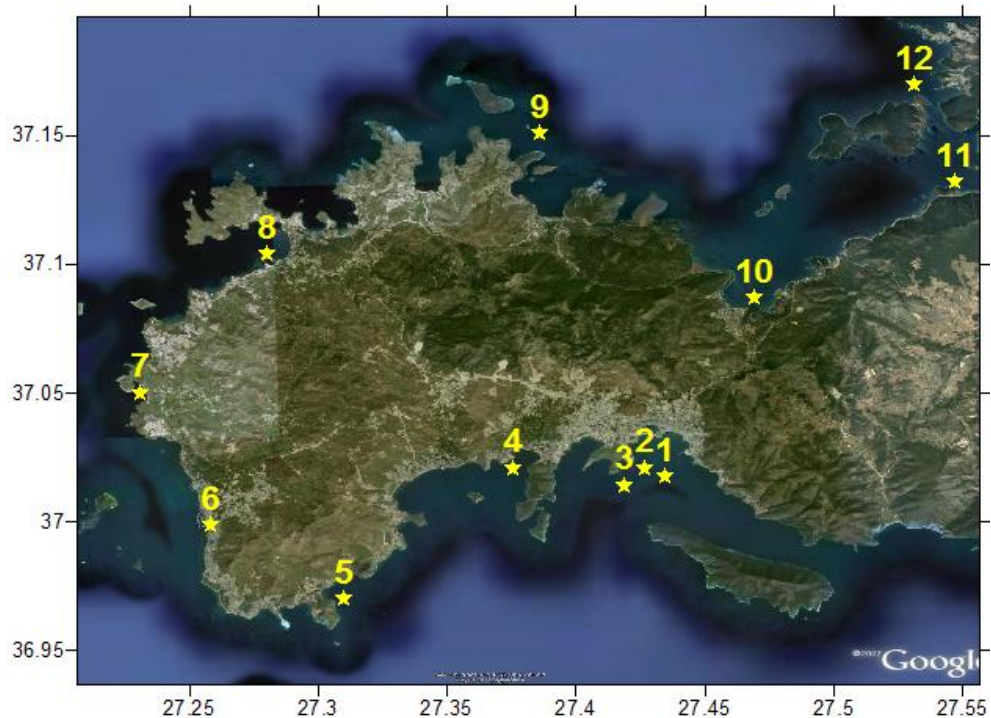


Figure 4.10: Selected forecasts points in Bodrum Headland on Google Earth image

For the selected source is s35, to examine the effect of fault displacement on source parameters, the fault displacement of source s35 is doubled and a new simulation results are compared with old one. Output summary table is given in Table 4.10. The source s35 with doubled fault displacement ($U = 7.3$ m) is worst-case scenario for Bodrum so, maximum positive amplitude of source and sea level fluctuations can be seen from Figure 4.12.

As it can be seen, the maximum positive wave height that can be expected on Bodrum is more than 4 m. The increase in fault displacement increases the effect of seismic source.

Table 4.9: Summary Results of tsunami impact at forecast points for source 01-365 on Bodrum

Name of gauge pt.	Depth of gauge pt.(m)	Longitude	Latitude	Arrival time of initial wave (min)	Arrival time of max.wave (min)	Max (+) amp.(m)	Max (-) amp.(m)
1	10.0	27.4342	37.0176	2	18	3.3	-3.4
2	10.0	27.4263	37.0210	2	18	3.2	-3.1
3	0.1	27.4184	37.0142	2	18	2.8	-2.8
4	4.0	27.3756	37.0209	3	22	3.6	-2.7
5	2.9	27.3100	36.9702	2	17	2.5	-2.5
6	0.3	27.2579	36.9989	3	49	3.3	-0.5
7	8.9	27.2307	37.0502	2	19	2.0	-2.6
8	3.4	27.2798	37.1039	4	39	2.2	-2.6
9	1.5	27.3858	37.1510	7	44	1.1	-1.2
10	1.4	27.4689	37.0869	8	43	2.1	-1.4
11	3.4	27.5466	37.1319	9	44	3.3	-3.4
12	9.5	27.5308	37.1697	7	80	1.8	-2.0

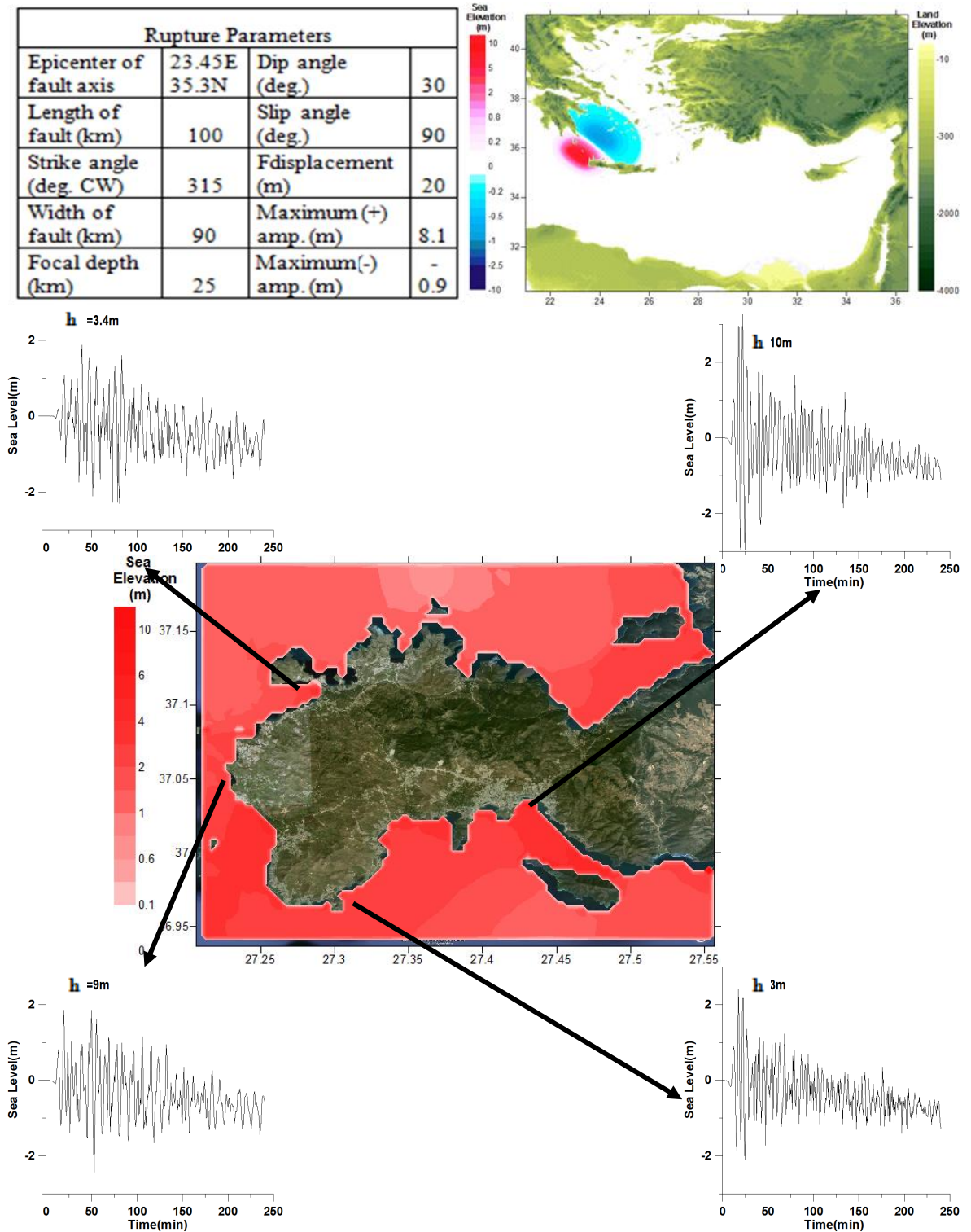


Figure 4.11: Maximum positive wave distribution and sea level fluctuations of source s01-365 in C domain on Bodrum

Table 4.10: Summary Results of tsunami impact at forecast points for source 35 on Bodrum

Name of gauge pt.	Depth of gauge pt.(m)	Longitude	Latitude	source 35				source 35 with double fault displacement			
				Arrival time of initial wave (min)	Arrival time of max.wave (min)	Max (+) amp.(m)	Max (-) amp.(m)	Arrival time of initial wave (min)	Arrival time of max.wave (min)	Max (+) amp.(m)	Max (-) amp.(m)
1	10.0	27.4342	37.0176	0	45	1.6	-1.8	0	110	2.5	-2.7
2	10.0	27.4263	37.0210	0	9	1.6	-1.7	0	111	2.4	-2.5
3	0.1	27.4184	37.0142	0	8	1.6	-1.5	0	76	2.1	-2.3
4	4.0	27.3756	37.0209	0	79	2.2	-1.8	0	214	2.6	-1.9
5	2.9	27.3100	36.9702	0	3	1.9	-1.9	0	107	1.6	-2.0
6	0.3	27.2579	36.9989	0	2	1.2	-0.4	0	198	2.1	-0.4
7	8.9	27.2307	37.0502	0	216	1.0	-0.8	0	95	1.0	-0.9
8	3.4	27.2798	37.1039	3	6	1.0	-0.8	4	209	1.3	-1.2
9	1.5	27.3858	37.1510	1	8	0.8	-0.5	2	236	0.5	-0.4
10	1.4	27.4689	37.0869	2	111	0.7	-0.7	2	187	0.9	-0.8
11	3.4	27.5466	37.1319	4	107	1.1	-0.9	5	183	1.2	-1.3
12	9.5	27.5308	37.1697	0	5	0.8	-0.8	0	236	0.7	-0.6

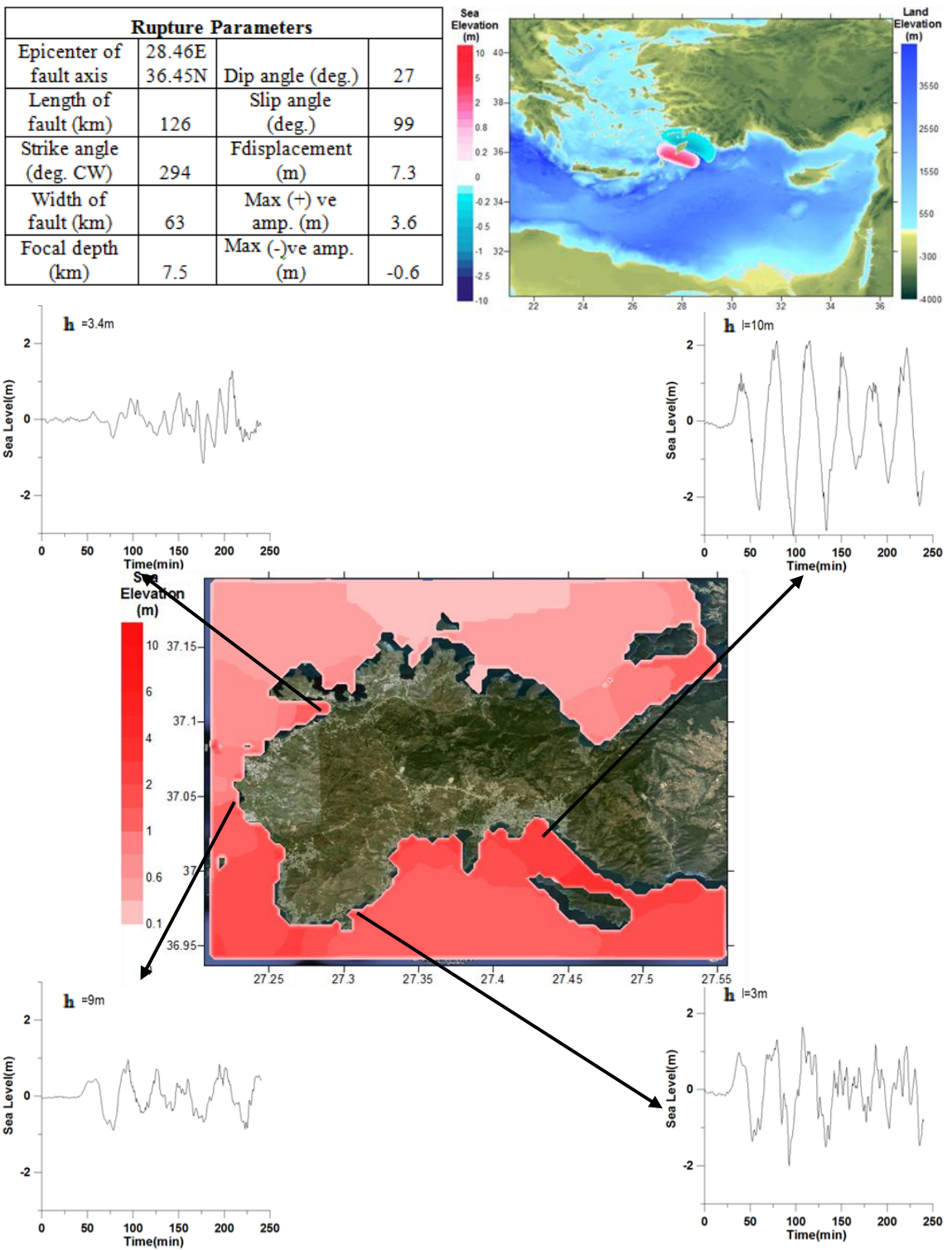


Figure 4.12: Maximum positive wave distribution and sea level fluctuations of source s35 with doubled fault displacement in C domain on Bodrum

4.3.2 Nested Domain Simulations for Iskenderun

Boundaries and grid sizes of each domain are given in Table 4.11. The smaller domains are shown in Figure 4.13. The forecasts points in Iskenderun Bay are illustrated on Figure 4.14. The selected source is s33-Z38. These sources give the maximum amplitude in single domain simulations. Moreover, to examine the effect of fault displacement on source parameters, the fault displacement of source s33-Z38 is doubled and new simulation results are compared with previous ones. The distributions of computed maximum positive and minimum negative tsunami amplitudes in Iskenderun region according to the selected tsunami source is shown in Figure 4.15.

Table 4.11: Boundaries and Grid Sizes of each domain for Iskenderun

Domain	Longitude (W)	Longitude(E)	Latitude (S)	Latitude (N)	Grid Size (m)
B	21.00	30.20	36.50	41.40	900
C	33.81	36.36	35.75	37.11	300
D	35.47	36.31	36.11	37.02	100

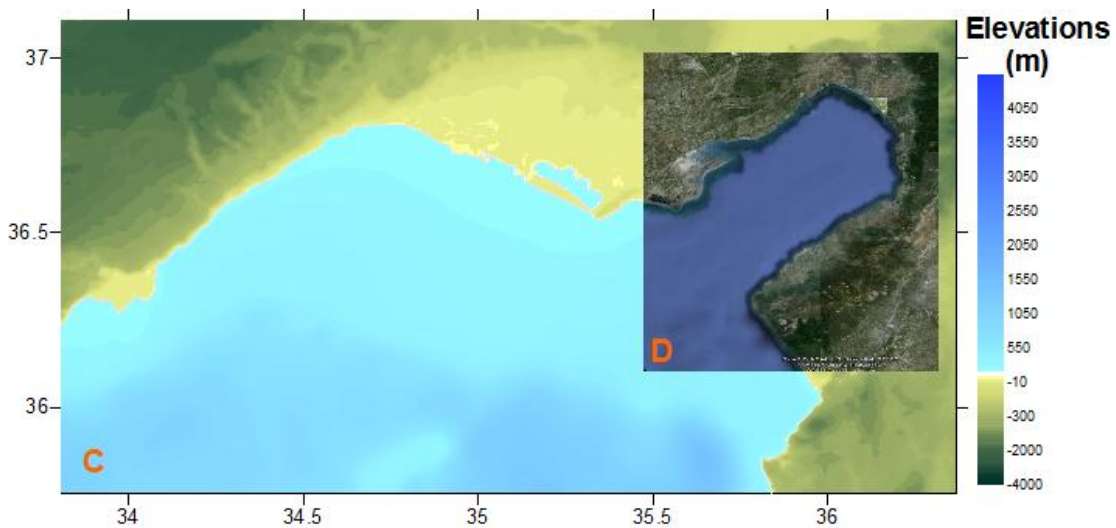


Figure 4.13: The smaller domains (C and D) of Iskenderun



Figure 4.14: Selected forecasts points in Iskenderun Bay on Google Earth image

The output summary table is given in Table 4.12. The source s33-Z38 with doubled fault displacement ($U = 12$ m) is worst-case scenario for Iskenderun so, the maximum positive amplitude of source and the sea level fluctuations can be seen from Figure 4.15.

As it can be seen, the maximum positive wave height that can be expected on Iskenderun is more than 2 m.

Table 4.12: Summary Results of tsunami impact at forecast points for source 33-Z38 and for source 33-Z38 with double displacement on Iskenderun

				source 33-Z38				source 33-Z38 with double fault displacement			
Name of gauge pt.	Depth of gauge pt.(m)	Longitude	Latitude	Arrival time of initial wave (min)	Arrival time of max.wave (min)	Max (+) amp.(m)	Max (-) amp.(m)	Arrival time of initial wave (min)	Arrival time of max.wave (min)	Max (+) amp.(m)	Max (-) amp.(m)
1	3.7	35.8152	36.3584	0	199	0.5	-0.5	0	200	1.0	-0.9
2	1.2	35.8871	36.4187	12	207	0.6	-0.5	12	207	1.0	-1.1
3	7.9	36.1797	36.5962	19	120	0.4	-0.8	18	121	0.8	-1.5
4	7.9	36.2092	36.661	17	119	0.5	-0.9	17	122	0.9	-1.5
5	7.5	36.1645	36.8211	0	97	0.6	-1.1	0	97	1.2	-1.9
6	3.0	36.0069	36.9281	0	95	0.6	-0.9	0	93	1.1	-1.7
7	2.9	35.7725	36.7635	0	232	0.5	-0.6	0	70	0.8	-1.2

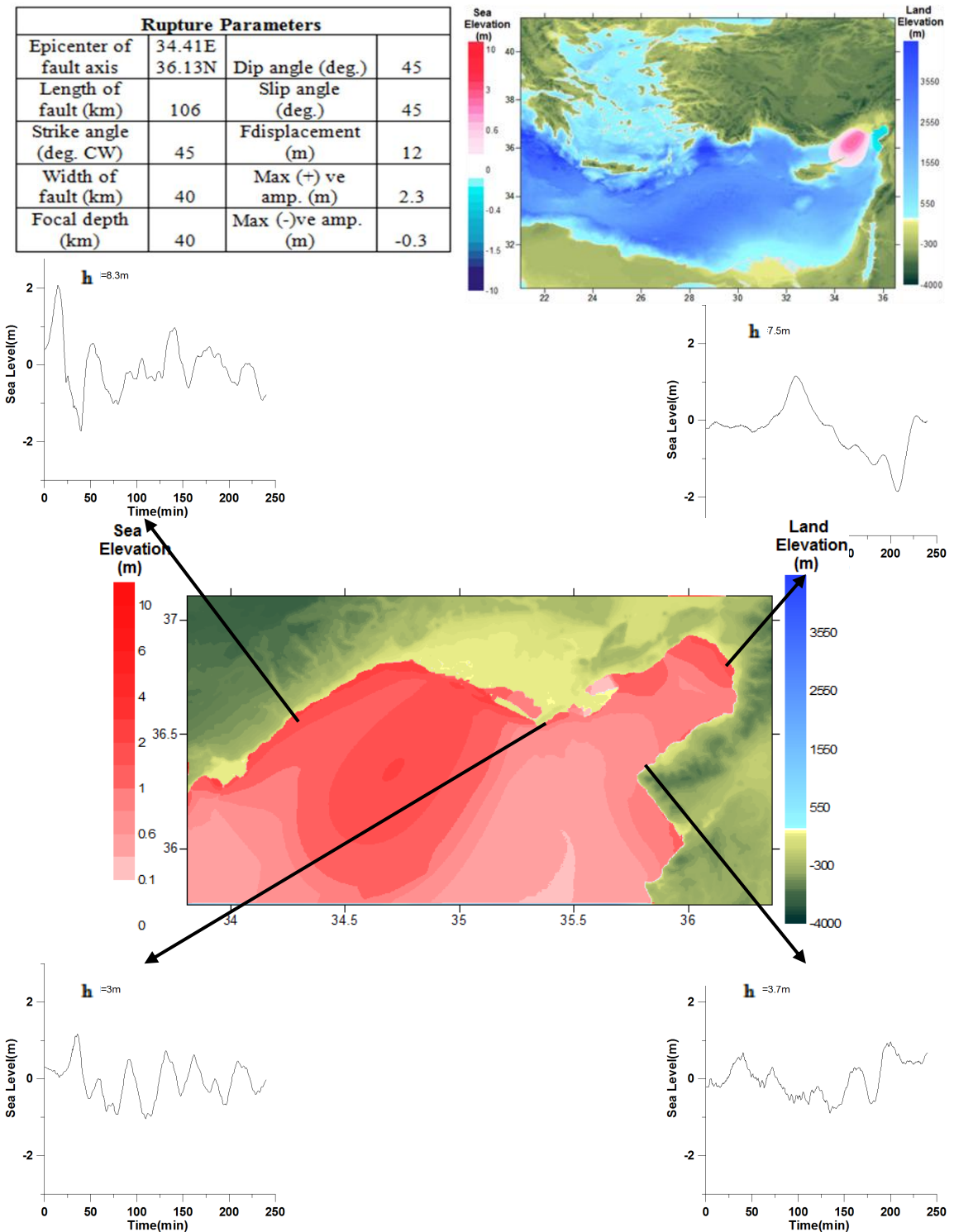


Figure 4.15: Maximum positive wave distribution and sea level fluctuations of source s33-Z38 with doubled fault displacement in C domain on Iskenderun

4.3.3 Nested Domain Simulations for Kas

Boundaries and grid sizes of each domain are given in Table 4.13. The smaller domains are shown in Figure 4.16.

Table 4.13: Boundaries and Grid Sizes of each domain for Kas

Domain	Longitude (W)	Longitude(E)	Latitude (S)	Latitude (N)	Grid Size (m)
B	21.00	30.20	36.50	41.40	450
C	29.07	29.95	36.10	36.40	135
D	29.58	29.65	36.18	36.22	45

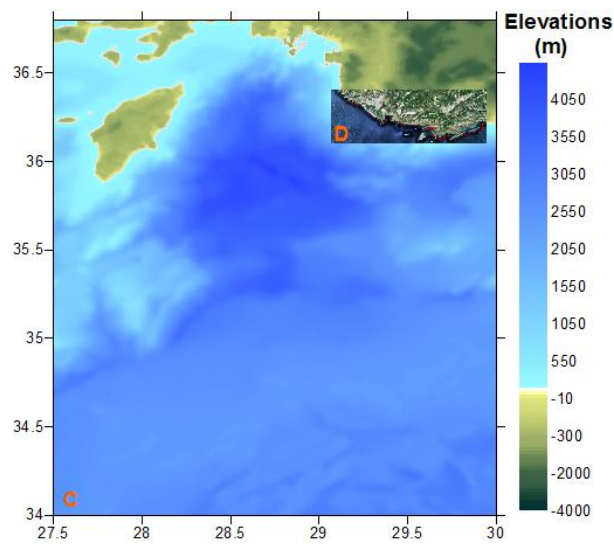


Figure 4.16: The smaller domains (C and D) of Kas

The forecasts points in Kas headland are illustrated on Figure 4.17. The selected source is s38. These sources give the maximum amplitude in single domain simulations. The output summary is given in Table 4.14.

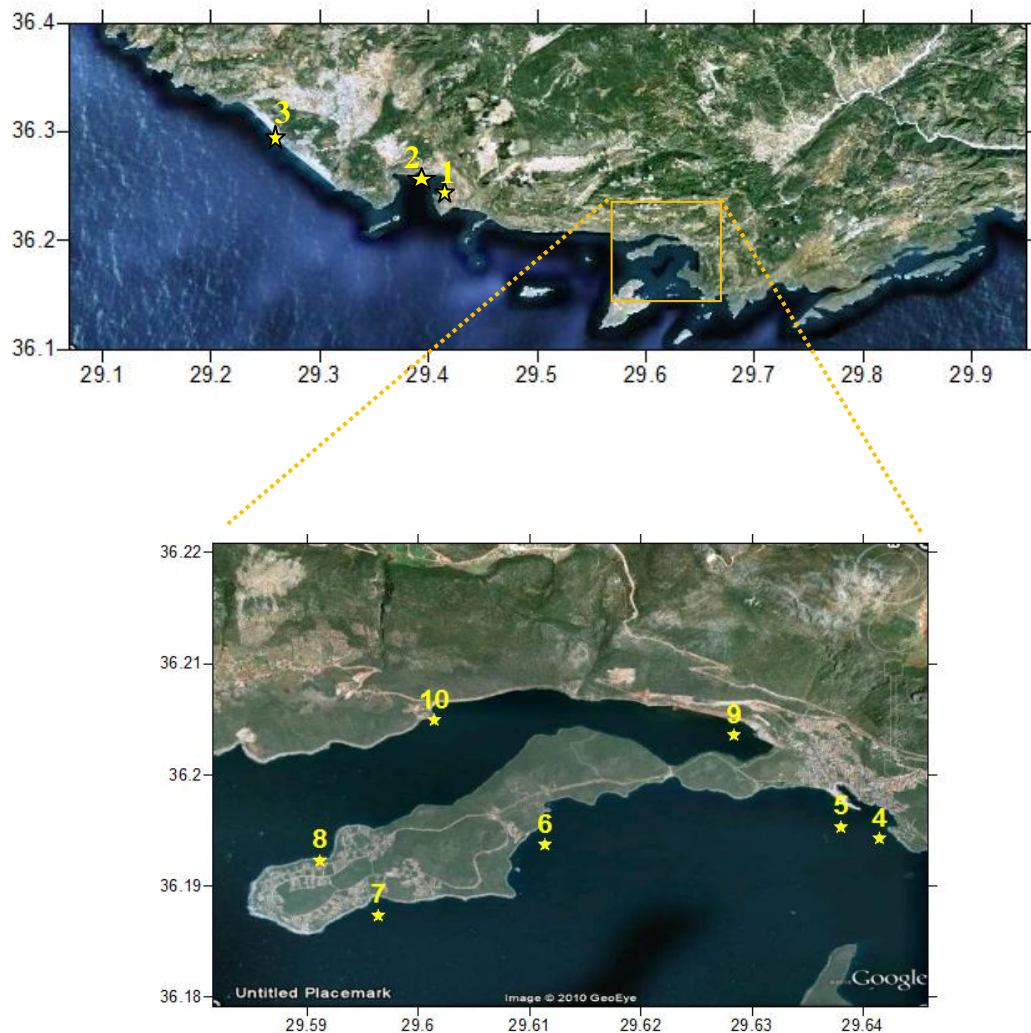


Figure 4.17: Selected forecasts points in Kas headland on Google Earth image

The distributions of computed maximum positive and minimum negative tsunami amplitudes in Kas region according to the selected tsunami source is shown in the Figure 4.18.

Table 4.14: Summary Results of tsunami impact at forecast points for source s38 on Kas

Name of gauge pt.	Depth of gauge pt.(m)	Longitude	Latitude	Arrival time of initial wave (min)	Arrival time of max.wave (min)	Maximum (+)amp.(m)	Maximum (-) amp.(m)
1	9.8	29.4097	36.2543	1	24	6.5	-5.5
2	3.7	29.3964	36.2602	1	23	4.5	-3.7
3	11.8	29.2588	36.2897	0	20	4.4	-5.2
4	5.8	29.6414	36.1942	1	14	1.4	-0.5
5	5.5	29.6379	36.1953	1	13	1.4	-0.4
6	10.8	29.6113	36.1937	0	2	1.7	-0.4
7	4.6	29.5964	36.1874	1	2	3.3	-2.0
8	2.2	29.5911	36.1923	2	27	1.9	-1.1
9	7.0	29.6283	36.2036	12	37	1.1	0.0
10	3.1	29.6014	36.2049	5	13	1.8	-1.0

As it can be seen, the maximum positive wave height that can be expected on Kas is more than 5 m.

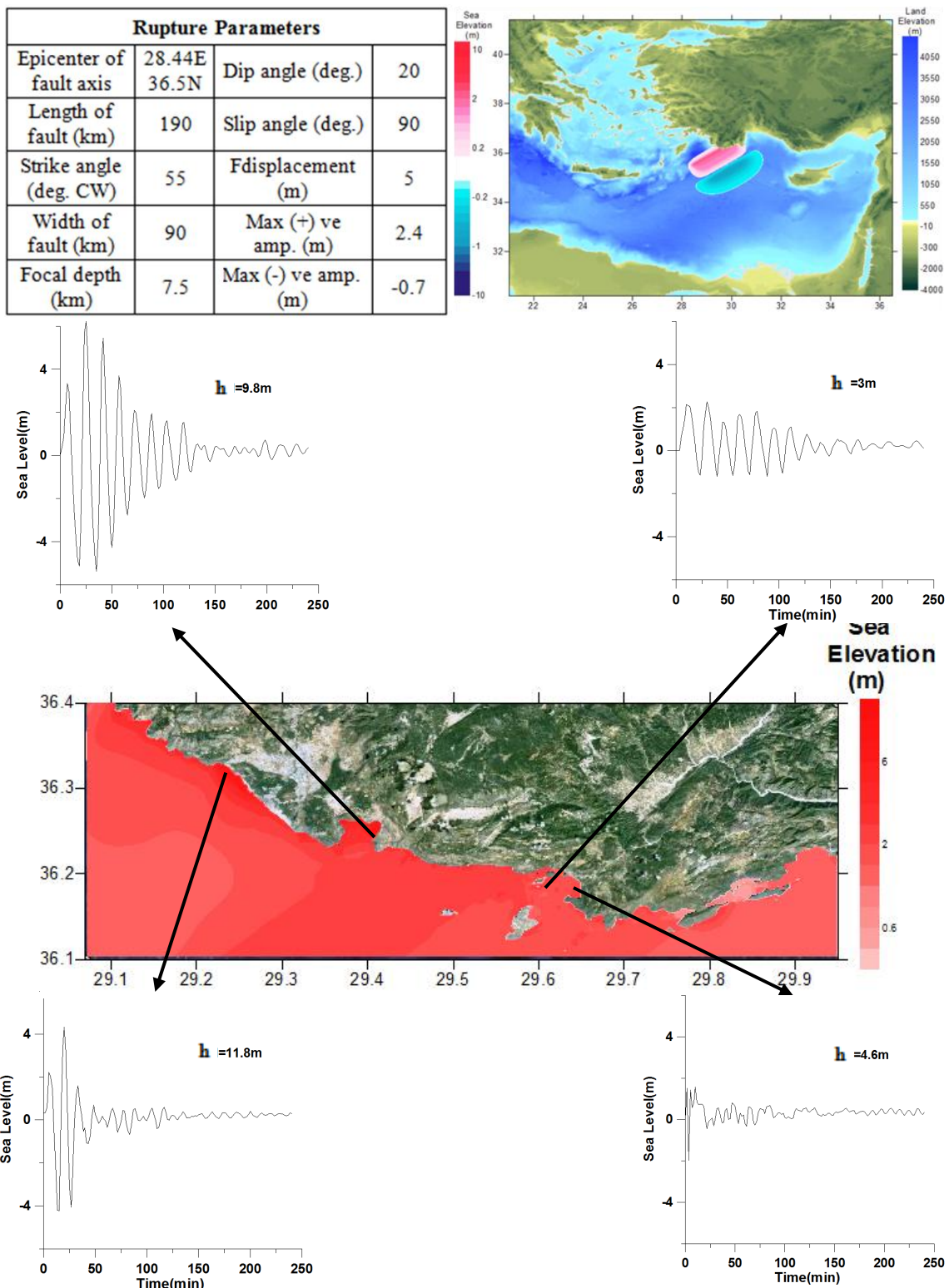


Figure 4.18: Maximum (+) wave distribution and sea level fluctuations of source s38 in C domain on Kas

CHAPTER 5

DISCUSSION OF RESULTS

Preparing a database for a tsunami assessment of a region is a detailed and complex work. The necessary technical activities are needed to perform such as literature review, obtaining of available data, conversion, comparison, processing of data, and development of database for the computational tools, computing and generating processed data by using necessary tools for different input conditions and data sets. Since there is limited data than there are uncertainties in tsunami source parameters, the difficulties on determining input parameters and the discussion of the results obtained from this thesis are explained below.

5.1 Discussion on Uncertainties in Source Parameters

Different types of sources generated tsunamis are observed during centuries in Mediterranean Basin. Tsunamis generated by non-seismic sources are rare but also rather unknown comparing to the seismic sources. It is important to consider the possible submarine landslide areas using available results of the investigations and scientific publications. There is some information about the landslide possibilities offshore Nile delta in the literature. There must be many more unstable bodies under the sea and those should be identified.

There are also uncertainties in estimation of tsunami source parameters. It is difficult to determine these parameters correctly. However, there are geophysical methods using the seismic-tectonic instrumental data covering more than a century period only. December

26, 2004 event is one of the major examples of these kinds of uncertainties. Until the event, there were not any detailed investigations and warnings on the large-scale magnitude earthquake generation and tsunami occurrence capability of Sunda Arc. The event showed much higher near field and ocean wide impact of tsunami than expected in Indian Ocean. It is also proved that the tsunami had to be considered as one of the major marine hazards (cyclones, storm surges etc.) in Indian Ocean. Japan event is another recent example and a lesson that the rupture parameters of worst-case scenarios may be under estimated.

Some examples of landslide generated tsunamis (November 18, 1929 Grand Bank tsunami, 1979 Nice tsunami, 1998 Papua New Guinea tsunami etc.) also showed that the submarine landslides at the alluvial deposited near shore or offshore marine areas can be triggered by the earthquakes and or other internal mechanisms in the marine environment and cause unexpected size of tsunamis. Considering these uncertainties, the conservative approaches in determining the tsunami generation mechanisms and or interpreting the results may be necessary.

The seismic source mechanisms also maintaining its uncertainty in defining rupture parameter. Since the generation of the earthquake is under Deep Ocean and the first parameters that are immediately determined are epicenter locations, magnitudes and focal depths. Length, width, dip, rake and strike angles and fault displacement can be obtained by analyzing the aftershocks, which takes time. Therefore, an investigation of tsunami effect by mathematical modeling of historical data and paleotsunami studies are needed to reduce the uncertainty on rupture parameters. 38 different seismic source parameters, which based on different reports and publications are used to prepare a tsunami database for Eastern Mediterranean Basin along Turkish Coasts.

Although the output parameters used in this study can be regarded as one of the best available data, the effects of uncertainties in some rupture parameters on the computational results must be investigated and discussed.

5.1.1 Discussion on the Dip – Rake(Slip) Angle Effect on Seismic Source

In general, there is not exact estimation of dip and rake angles. It is better to test their effect on tsunami by using their extreme combinations. The simulation in regular bathymetry using show that decreasing dip angle and increasing rake angle extenuates the maximum positive and negative wave amplitude on source. So, other tests are made on irregular bathymetry created for Eastern Mediterranean Basin for selected forecast points using s24-Z26-1 seismic source with the extreme combinations. These simulations also show that lower dip angle and higher rake angle creates higher waves at source. Moreover, 10° dip angle and 110° rake angle can be chosen if there is not sufficient information about these rupture parameters that affect Aegean and Mediterranean coasts along Turkey.

5.1.2 Discussion on Fault Displacement Effect on Tsunami Source

The influences of fault displacement on seismic source mechanism are tested on nested simulations for Bodrum and Iskenderun. The sources of (s35 for Bodrum and s33-Z38 for Iskenderun) with doubled fault displacements are modeled. The influence of the parameter is observed by comparing the maximum positive and negative wave amplitude along selected forecast points. It can be said that increasing fault displacement increases the impression of tsunami wave amplitude on gauge points.

5.2 Bathymetry Effect on Tsunami Modeling

Decreasing the grid size gives more accurate bathymetry data that matches with real life. Although smaller grid size simulations weaken the effect of uncertainty, it increases the simulation run time. The bathymetry data is based on one of the best available data and limited to the accuracy of the data. Bathymetry data created from GEBCO 30 sec is enhanced by local data based on measurements and is verified by Google Earth, 2011. The accuracy of extrapolation along bathymetry data to create a digital elevation map is based on grid size. For the cases, where immediate results of simulations are needed, it

is advisable to choose grid size large enough. Since the domain studied is 900 m grid size that can be advisable to use for extrapolation due to giving accurate results in hours.

The near shore high-resolution bathymetry and topography in selected specific regions can be used for results that are more accurate. Especially for regions where the shoreline is irregular due to many bays and headlands, smaller grid size is advisable to choose in nested simulations.

5.3 Tsunami Risk Analysis in Eastern Mediterranean Basin

The tsunami analyses include information about the historical tsunamis. The strong earthquakes may cause tsunamis effecting Turkey; brief history, capabilities and the details are examined and tsunami numerical models are applied using NAMI DANCE. 38 different tsunami sources are simulated and their coastal amplifications along Turkey are compared.

The sources defined in thesis can be considered as possible tsunami sources that may be created in Eastern Mediterranean Basin in the future. It may be said that the effect of future tsunamis will be close to the influence of these sources. It can be seen that the tsunami sources of s01-365, s03-Z10-1, s04-Z10-2, s05-Z10-3, s06-Z10-4, s15-Z17-1, s35 and s38 cause more effect on Eastern Mediterranean region comparing the effects of the other sources. It can be said that north-west and south-west of Turkey carries tsunami risk more than other regions. The maximum positive wave amplitude observed in history is approximately 8 m. However, the results of s01-365 event is unique impact along coast and the general maximum wave amplitudes hit the coasts are more than 4 m and about 6 m at some localities. It can be said that Eastern Mediterranean coasts of Turkey should be ready against the tsunami with 4-6 m height. The impact of these waves may be more destructive than storm waves with same magnitude. It is because tsunami waves conserve their energy and face with little energy loss while they are approaching to the shore. Thus, tsunami demolishes everything in front of it and cause

inundations. That characteristic of tsunami develops a need for taking precautions to estimated scenarios. It should also be kept in mind that there is always a possibility to have a destructive tsunami due to high seismic activity in Eastern Mediterranean Basin.

The tsunami propagation maps, time histories of water level fluctuations at selected locations near Turkey, the arrival time distributions of the first wave and maximum wave, the distributions of maximum positive and negative amplitudes are given. The geomorphology affects tsunami propagation and its impact on coasts. The arrival time of first wave to hit the coasts vary in a range of 15 to 60 minutes depending on the closeness of the location to the sources' epicenter. Since Mediterranean Basin is a close basin, tsunami travels along the coasts quickly. The tsunami alert should be made immediately due to the short arrival time of waves. The alert must be kept until the tsunami energy dissipates in the basin, which takes about 6 hours or more.

Bodrum, Iskenderun and Kas are examined by using nested domains with higher resolutions. The results of the simulations are given. Sources s01-365 and s35 for Bodrum, s33-Z38 for Iskenderun and s38 for Kas can be considered as worst-case scenarios for selected domains. According to these nested simulations, approximately 4 m for Bodrum, 2 m for Iskenderun and 5 m for Kas can be experienced as maximum wave amplitude in future. The possible expected tsunami influence on selected forecast coasts can be simulated in considering the future needs.

When the results of nested domain are compared with results of single domain, there is a slight difference of results, which is around 10%. It can be understood from this comparison that in case of immediate results are needed single domain simulations are fast and accurate enough to obtain desired information. On the other hand, nested domain simulations provide detailed study of a specific location according to the desired needs.

CHAPTER 6

CONCLUSION

The results of any tsunami numerical modeling, even if it is valid, tested and verified, are highly dependent on the input data especially the source parameters, bathymetric and topographic conditions of the far and near field regions of the study area, and the types and distributions of the coastal defense structures, land structures and land use plans. In this study, one of the internationally recognized tsunami numerical model called NAMIDANCE is used for modeling one of the best available data for the tsunami sources and bathymetric/topographic data. The results of the tsunami numerical computations will highly be affected by any changes in the bathymetry and land topography. Therefore, in the design stage of the coastal structures and land use plans, the computations of the critical tsunami parameters should be reviewed by taking these morphological changes and structural distributions into consideration.

The tsunami sources used in this study reports only seismic sources. The rupture parameters are estimated according to available scientific publications. The rupture parameters may vary and new estimations can be available at later stages. Then if the rupture parameters are modified, new simulations may be necessary for re-evaluation of the simulation results. Furthermore, new selected forecast points can be added in the need of tsunami effect investigation for desired location. Nested simulations should widely applied for selected locations in future considerations.

This study provides a database for tsunami warning system built in Eastern Mediterranean Basin. Non-seismic generated sources should also be added to this

database. Thus, the database will provide of simulations tsunamis generated by both seismic and non-seismic sources. In addition to that, a database of Marmara Sea and Black Sea should be prepared and added to the database to obtain a full dataset of tsunamis of Turkish coasts.

For a future consideration, a user-friendly computer code can be developed using this database. Therefore, when a possible tsunami effect is needed to be known in a specific region, the code envisages the arrival time and maximum wave amplitudes from the respected scenario. Thus, a coastal structure can be designed according to that information. Furthermore, when an earthquake occurs, user can obtain the arrival time of initial and maximum wave to the selected point by entering the coordinates of epicenter. In this way, tsunami-warning can be issued and the zone may be evacuated before the tsunami waves hit the coasts.

In conclusion, tsunami-warning system not only includes a preparation of tsunami dataset, but also should be combined with increasing public awareness and developing mitigation strategies. Properly issued tsunami warning if coupled with proper disaster management system can save lives. This thesis attempted to establish suitable information for preliminary evaluation of the general characteristics on propagation and coastal amplification of Eastern Mediterranean tsunamis. This provides an implementation of early warning system by creating a risk evaluation map for Turkish coasts.

As a suggestion for future efforts, a detailed tsunami database and a computer model converting this database for decision support systems should be developed and operated in real time.

As for conclusion, considering the uncertainties in the source parameters, the values used in this thesis should be re-evaluated and re-estimated when new data or information is obtained. Those will reduce uncertainties.

REFERENCES

- Altinok, Y., Alpar, B., Ozer, N., and Aykurt, H. (2011). "Revision of the tsunami catalogue affecting Turkish coasts and surrounding regions." Natural Hazards and Earth System Sciences **11**: 237-291.
- Altinok, Y., Alpar, B., Ozer, N., and Gazioglu, C. (2005). "1881 and 1949 earthquakes at the Chios-Cesme Strait (Aegean Sea)" Natural Hazards and Earth System Sciences **5**: 717-725.
- Altinok, Y., and Ersoy, S. (2000). "Tsunamis Observed on and Near the Turkish Coast." Natural Hazards **21**: 185-205.
- Altinok, Y., Ersoy S., Yalciner, A.C., Alpar B. and Kuran U. (2001). Historical Tsunamis in the Sea of Marmara. Seattle. **4**: 527-535.
- Ambraseys, N. N. (1962). "Data for the investigation of the seismic seawaves in the Eastern Mediterranean." Bull.Seismic Society Am. **52**: 895-913.
- Ambraseys, N. N., and Melville, C.P. (1987). An Analysis of The Eastern Mediterranean Earthquake of 20 May 1202. Historical Seismograms and Earthquakes. W. H. K. Lee. San Francisco.
- Antonopoulos, J. (1979). "Catalogue of tsunamis in the Eastern Mediterranean from antiquity to present times." Annualy Geophys **32**: 113-130.
- Antonopoulos, J. (1990). "Data for Investigating Tsunami Activity in The Mediterranean Sea." Science of Tsunami Hazards **8-1**: 39-53.
- Barka, A. and Reilinger, R. (1997). "Active tectonics of the Eastern Mediterranean region: deduced from GPS, neotectonic and seismicity data." Annali di Geofisica **40**: 587-609.
- Bondevik, S., Løvholt, F., Harbitz, C., Mangerud, J., Dawson, A., and Svendsen, J.I. (2004). "The Storegga Slide tsunami—comparing field observations with numerical simulations" Marine and Petroleum Geology **22-1**: 195-208.
- Bourgeois, J. (1988). "A tsunami deposit at the Cretaceous-Tertiary boundary in Texas." Science **241**: 567-570.

- Bruins, M., Synolakis, Benjamini, Keller, Kisch, Klugel and Van der Plicht (2008). "Geoarchaeological tsunami deposits at Palaikastro (Crete) and the Late Minoan IA eruption of Santorini." Journal of Archaeological Science **35**: 191-212.
- Chow, V. T. (1959). Open Channel Hydraulics. New York.
- Cita, M. B., Rimoldi, B. (1997). "Geological and Geophysical Evidence for a Holocene Tsunami Deposit in the Eastern Mediterranean Deep-Sea Record." Journal of Geodynamics **24**: 293-304.
- Dawson, A. G., Lockett, P., Shi, S. (2004). "Tsunami Hazards in Europe." Environment International **30**: 577-585.
- Dewey, J. F. and Sengor, A. M. C (1979). "Aegean and surrounding regions: complex multiplate and continuum tectonics in a convergent zone." Bull. Geol.Soc. America **90**: 84-92.
- Dominey-Howes, D. (2002). "Documentary and Geological Records of Tsunamis in the Aegean Sea Region of Greece and their Potential Value to Risk Assessment and Disaster Management." Natural Hazards **25**: 195-224.
- Fokaefs, A., and Papadopoulos, G.A. (2005). "Tsunami hazard in the Eastern Mediterranean: Strong Earthquakes and Tsunamis in Cyprus and the Levantine Sea." Natural Hazards. doi: **10.1007/s11069-006-9011-3**
- Galanopoulos, A. G. (1960). "Tsunamis observed on the coasts of Greece from antiquity to present time." Annual Geophys **13**: 369-386.
- Guidoboni, E., Comastri, A., and Traina, G. (1994). Catalogue of Ancient Earthquakes in the Mediterranean Area up to the 10th Century.
- Hamouda, A. Z. (2009). "A Reanalysis of the AD 365 Tsunami Impact along the Egyptian Mediterranean Coast." Acta Geophysica **58-4**: 687-704.
- Hamouda, A. Z. (2010). "Worst scenarios of tsunami effects along the Mediterranean coast of Egypt." Marine Geophys **31**: 197-214.
- Imamura, F., and Goto, C. (1988). "Truncation error in numerical tsunami simulation by finite difference method." Coastal Engineering Japan **31**: 245-263.
- Imamura, F., Yalciner, A.C. and Ozyurt, G. (2006). Tsunami Modelling Manual.

Insel, I. (2009). The Effects of The Material Density and Dimensions of the Landslide on The Generated Tsunamis. Master of Science, Middle East Technical University.

Konstantinou, K. I., Papadopoulos, G.A. and Fokaefs, A. and K. Orphanogiannakib (2005). "Empirical relationships between aftershock area dimensions and magnitude for earthquakes in the Mediterranean Sea region." Tectonophysics **403**: 95-115.

Le Pichon, X., and J. Angelier (1979). "The Hellenic Arc and trench system: A key to the neotectonic evolution of the eastern Mediterranean area." Tectonophysics **60**: 1-42.

Le Pichon, X., Lallemand, S.J., Chamot-Rooke, N., Lemeur, D. and Pascal, G. (2002). "The Mediterranean Ridge Backstop and the Hellenic Nappes." Marine Geology **186 No1-2**: 111-125.

Mantovani, E., D. Albarello, D. Babbucci, C. Tamburelli, and M. Viti (2000). Genetic mechanism of back-arc opening: Insights from the Mediterranean deformation pattern. Problems in Geophysics for the New Millennium, Proceedings Erice 1999. G. E. E. Boschi, and A. Morelli. Roma, Italy, Istituto Nazionale di Geofisica: 151-178.

Maramai, A., Gasparini, C. (1991). "A Proposal for a New Catalog on Tsunamis in The Mediterranean Area." Science of Tsunami Hazards **9-1**: 39-47.

McClusky, S., Balassanian, S., Barka, A., Demir, C., Ergintav, S., Georgiev, I., Gurkan, O., Hamburger, M., Hurst, K., Kahle, H., Kastens, K., Kekelidze, G., King, R., Kotzev, V., Lenk, O., Mahmoud, S., Mishin, A., Nadariya, M., Ouzounis, A., Paradissis, D., Peter, Y., Prilepin, M., Reilinger, R., Sanli, I., Seeger, H., Tealeb, A., Toksöz, M.N. and Veis, G. (2000). "Global Positioning System Constraints on Plate Kinematics and Dynamics in the Eastern Mediterranean and Caucasus." Journal of Geophysical Research **105-B3**: 5695-5720.

- Minoura, K., Imamura, Kuran,U., Nakamura, T., Papadopoulos, G., Takahashi, T., Yalciner, A.C. (2000). "Discovery of Minoan Tsunami Deposits." Journal of Geology **28**: 59-62.
- NAMI DANCE Manual (2010). Developed by Zaytsev, C., Yalciner, Pelinovsky, Kurkin. Tsunami Simulation/Visualization Code NAMI DANCE versions 4.9. <http://www.namidance.ce.metu.edu.tr> (Reviewed on June 15, 2011)
- Ozel, N., Ocal, N., Yalciner, A.C., Kalafat, D., and Erdik, M. (2011). "Tsunami hazard in the Eastern Mediterranean and its connected seas: Toward a Tsunami warning center in Turkey." Soil Dynamics and Earthquake Engineering **31**: 598-610.
- Papadopoulos, G. A. (2003). "Tsunami Hazard in the Eastern Mediterranean: Strong Earthquakes and Tsunamis in the Corinth Gulf, Central Greece." Natural Hazards **29**: 437-464.
- Papadopoulos, G. A. and Chalkis., B. J (1984). "Tsunamis observed in Greece and the surrounding area from antiquity to the present times." Marine Geology **56**: 309-317.
- Papadopoulos, G. A., and Fokaefs, A. (2005). "Strong Tsunamis in The Mediterranean Sea: A Re-Evaluation." ISET Journal of Earthquake Technology **42-4**: 159-170.
- Papadopoulos, G. A., Daskalaki, E., Fokaefs, A., and Giraleas, N. (2007). "Tsunami hazards in the Eastern Mediterranean: Strong earthquakes and tsunamis in the East Hellenic Arc and Trench system." Natural Hazards and Earth System Sciences **7**: 57-64.
- Pararas-Carayannis, G. (2001) [Web Site] "The Great Explosion of the Krakatau Volcano ("Krakatoa") of August 26, 1883, in Indonesia" <http://www.drgeorgepc.com/Volcano1883Krakatoa.html> (Reviewed on May 30, 2011)
- Parejas, I., Akyol, M. and Altinli, E. (1942). "Le tremblement de terre d'Erzincan du 27 Décembre 1939 (secteur occidental)." I.U. Jeoloji Enstitusu Nesriyati **10**: 187-222.

- Rawlinson, N. (2007) [Powerpoint Slides] Lecture 11: Earthquake source mechanisms and radiation patterns I. <http://rses.anu.edu.au/~nick/teachdoc/lecture11.pdf> (Reviewed on May 16, 2011)
- Royden, L. H. (1993). "Evolution of retreating subduction boundaries formed during continental collision." *Tectonics* **12**: 629-638.
- Salamon, A., Rockwell, T., Ward, S.N., Guidoboni, E. and Comastri, A. (2007). "Tsunami Hazard Evaluation of the Eastern Mediterranean: Historical Analysis and Selected Modeling." *Bulletin of the Seismological Society of America* **97**: 705-724.
- Soysal, H., Sipahioglu, S., Kolcak, D., and Altinok, Y. (1981). *Turkiye ve Cevresinin Tarihsel Deprem Katalogu (MO 2100–MS 1900)*. Istanbul, TUBITAK, TBAG **Proje No. 341**.
- Stiros, S. C. (2001). "The AD 365 Crete earthquake and possible seismic clustering during the fourth to sixth centuries AD in the Eastern Mediterranean: a review of historical and archaeological data." *Journal of Structural Geology* **23**: 545-562.
- Tinti, S., Armigliato, A., Pagnoni, G., and Zaniboni, F. (2005). "Scenarios of Giant Tsunamis of Tectonic Origin in the Mediterranean." *ISET Journal of Earthquake Technology* **42-4**: 171-188.
- Tinti, S., Maramai, A. (1996). "Catalogue of Tsunamis Generated in Italy and in Côte d' Azur, France: A Step Towards a Unified Catalogue of Tsunamis in Europe." *Annali di Geofisica* **39**: 1253-1299.
- Tinti, S., Maramai, A., Graziani, L. (2001). "A new version of the European tsunami catalogue: updating and revision." *Natural Hazards and Earth System Sciences* **1**: 255-262.
- TRANSFER Work packages (2009) <http://www.transferproject.eu/> Reviewed on 05/27/2011
- Wells, D. L. and Coppersmith., K.J. (1994). "New empirical relationships among magnitude, rupture length, rupture width, rupture area, surface displacement." *Bull. Seismol. Soc. Am* **84**: 974-1002.

Wikipedia, 2011 [Web Site] "2011 Tohoku Earthquake and Tsunami"
http://en.wikipedia.org/wiki/2011_T%C5%8Dhoku_earthquake_and_tsunami

(Reviewed on May 30, 2011)

Yalciner, A. C., Alpar, B. , Altinok, Y. , Ozbay, I. , Imamura, F. (2002). "Tsunamis in the Sea of Marmara, Historical Documents for the Past, Models for the Future." Marine Geology **190**: 445-463.

Yalciner, A. C., Synolakis, C. E, Gonzales, M., Kanoglu, U., (2007) "Joint Workshop on Improvements of Tsunami Models, Inundation Map and Test Sites of EU TRANSFER Project", June 11-14, Fethiye, Turkey

Yolsal, S., Taymaz, T. and Yalciner, A.C. (2007). "Understanding Tsunamis, Potential Source Regions and Tsunami-Rrone Mechanisms in the Eastern Mediterranean." Geological Society **291**: 201-230.

Zaytsev, A., Karakus, H., Yalciner, A.C., Chernov, A., Pelinovsky, E., Kurkin, A., Ozer, C., Dilmen, D.I., Insel, I and Ozyurt, G. (2008). Tsunamis in Eastern Mediteranean, Histories, Possibilities and Realities. COPEDEC VII. Dubai.

Paper No:Z-01.

APPENDICES

A1. Tsunamis on the Turkish coasts from Yolsal and Ersøy (2000)

- i*: Tsunami intensity (according to the Modified Sieberg Scale, after Ambraseys, 1962);
H: Maximum wave height (m);
D: The distance that the water penetrated inland (m);
NTI: No tsunami information;
(No): Reference number in the reference section;
/: Separates two alternative dates or periods;
-: Joins the beginning and end of a chronological period;
Rel: Reliability (according to Modified Iida, 1984 Scale, after Soloviev, 1990; Tinti and Maramai, 1996).

Table A.1: List of Tsunamis (Yolsal and Ersøy 2000)

No.	Date	Place	References	Remarks	Rel
1	1410 ± 100 B.C.	North east of Crete	6, 8, 35, 43, 45	1600–1500 B.C. (46), <i>i</i> = 6? (6), The tsunami was generated by the Minoan eruption of the Santorini Volcano (35)	3
2	1300	Çanakkale Region (Dardanelles), Troy	5, 6, 8, 35, 46	<i>i</i> = 6? (6, 35)	2
3	330	North east of Limnos Isl.	6, 8, 35, 43, 45		1
4	222	Rhodes, Cyprus, Corinth	5, 6, 8, 10, 43, 45	227 (35)	1
5	140	Acre, Tyr-Syria	10, 45	138 B.C., <i>i</i> = 4 (6). Silifke Region was affected by tsunami (45)	3
6	26	Paphos-Cyprus	6, 8, 45	<i>i</i> = 3 (6), NTI (45)	2

Table A1. Continued

TSUNAMIS OBSERVED ON AND NEAR THE TURKISH COAST

No.	Date	Place	References	Remarks	Rel
7	46 A.D.	North east of Crete, Santorini Isl.	6, 8, 35, 43, 45	South coasts of Crete (6). Eruption of Santorini Volcano (35)	1
8	53/62/66	Cnossos-Crete, Leben	6, 8, 14, 35, 43, 45	62, South coasts of Crete (6, 8), 62, midday (45), 66 (35, 43), <i>i</i> = 3 (6, 35)	4
9	68	Demre, Patara-Lycia	14		2
10	76-78	Larnaca, Paphos, Salamis-Cyprus	5, 6, 8, 10, 45, 46	77-78 (10)	2
11	120/128	Kapudag Peninsula (Cyzicus), Iznik, Izmit	14, 45	120, NTI (45)	2
12	142	Fethiye Gulf, Rhodes, Kos, Seriphos, Syme Isls.	6, 8, 46	148 (35, 37), Rhodes, <i>i</i> = 4, Kos, Seriphos, Syme, <i>i</i> = 3 (6, 35, 37)	2
13	261-262	South coasts of Anatolia	6, 8, 14, 45, 46	262 (6, 8, 14, 45), West Anatolia (45), <i>i</i> = 4? (6)	3
14	293-306	Salamis-Cyprus	14		1
15	325	Izmit Gulf	46		1
16	342	Paphos	6, 8, 45, 46		2
		Famagusta-Cyprus			
17	344	Çanakkale Region, Thracian coasts	6, 8, 46	Dardanelles, <i>i</i> = 4, Thracian coasts, <i>i</i> = 3 (6)	3
18	358.08.24	Izmit Gulf, Iznik, Istanbul	9, 10, 45, 46	NTI (9)	3
19	365.07.21	East Mediterranean, Crete, Greece, Adriatic coasts, Alexandria, West Anatolia	5, 6, 8, 14, 16, 35, 37, 43, 45	Methone, Epidaurus, Crete, <i>i</i> = 4, Adriatic coasts, Alexandria, Sicily, <i>i</i> = 3+ (6). Methone, <i>D</i> = 2000 m, Epidaurus, Crete, <i>i</i> = 4, Alexandria, Albania, Sicily, <i>i</i> = 4 (35), Crete, <i>i</i> = 6, Epidaurus, <i>i</i> = 4+, Methone, <i>i</i> = 4, Alexandria, <i>i</i> = 3+ (37)	4
20	368.10.11	Iznik and its surrounding	14, 45	NTI (45)	2
21	407.04.01	Istanbul	14	408.07.05, NTI (45)	0
22	447.11.08	Marmara Sea, Istanbul, Izmit Gulf, Marmara Isls., Marmara and Çanakkale coasts	6, 8, 14, 35, 37, 45, 46	447.11. (6, 8, 46), 447.01.26 night (14), 447.12.08, NTI (45), Marmara coasts, <i>i</i> = 4- (6), <i>i</i> = 4 (35), Istanbul, <i>i</i> = 3 (6, 35, 37), Erdek	3

Table A1. Continued

No.	Date	Place	References	Remarks	Rel
				Gulf, $i = 4$, Marmara Isls., $i = 4-$ (37)	
23	450.01.26	Marmara Sea, Istanbul	6, 8, 45, 46	450.01. (6, 8), NTI (45), $i = 3$ (6)	2
24	477/480.09 24/25/26	Gelibolu, Çanakkale, Istanbul, Izmit, Bozcaada	14		2
25	488.09.26	Izmit Gulf	45, 46	NTI (45)	2
26	524/525	South coasts of Anatolia, Anazarba-Adana	45, 46	524 (45)	3
27	529 winter	Thracian coasts of Marmara	46		1
28	542 winter	West coasts of Thracia, Bandırma Gulf	6, 8, 46	Edremit Gulf (6, 8), $i = 4$ (6)	2
29	543.09.06	Kapıdag Peninsula, Erdek, Bandırma	5, 10, 14, 35, 43, 45, 46	Edremit Gulf (46)	3
30	553.08.15	Istanbul, Izmit Gulf	45, 46	NTI (45), $D = 3000$ m (46)	2
31	554.08.15	South west coasts of Anatolia, Kos Isl., Mandalya Gulf	5, 6, 8, 10, 14, 35, 37, 43, 45, 46	554-558 (14), 554 (10, 43, 45), $i = 4-$ (6), $i = 4$ (35), Mandalya Gulf, $i = 4+$, Kos, $i = 4-$ (35)	4
32	555.08.15/16	Istanbul, Izmit Gulf	9, 10, 43, 46		4
33	557.12.14	Istanbul, Izmit Gulf	10, 45, 46	558.12.14 (5), night, NTI (45), $D = 5000$ m (46)	2
34	715	Istanbul, Izmit Gulf	45, 46	NTI (45)	1
35	740.10.26	Marmara Sea, Istanbul, Izmit, İznik Lake	5, 6, 8, 14, 16, 35, 37, 45, 46	Early afternoon (14), 08.00 a.m., NTI (45), $i = 3$ (6, 35), $i = 4-$ (37)	3
36	803.12.19	İskenderun Gulf	6, 8, 41, 46	803, NTI (41), $i = 3$ (6)	2
37	859.11.	Syrian coasts, Near Samandag	6, 8, 41, 45	859.04.08, NTI (45), 859, NTI (41), $i = 3$ (6)	2
38	975.10.26	Istanbul, Thracian coasts of Marmara	6, 8, 46	986.10.26 (45), $i = 3$ (6)	3
39	989	Istanbul, Marmara coasts	9, 10, 46		3
40	990	Istanbul, Marmara coasts	46		1
41	1039.02.02	Istanbul, Marmara coasts	6, 8, 35, 46	1039.01. (6, 8, 46)	0
42	1064.09.23	İznik, Bandırma, Mürefte, Istanbul	10, 45, 46		3

Table A1. Continued

No.	Date	Place	References	Remarks	Rel
43	1114.08.10	Ceyhan, Antakya, Maraş	24, 41, 45	1114.11.20, NTI (41)	3
44	1157.07.15	Hama-Homs, Chaizar Region	45		1
45	1202.05.22	Cyprus, Syrian coasts, Egypt	6, 8, 24, 45	1201.06.02, Cyprus (41) 1202.05.20 (24, 45), NTI (45) Syrian coasts, $i = 5$, Cyprus, $i = 4$, Egypt, $i = 3$ (6)	4
46	1222.05	Paphos, Limasol-Cyprus	5, 6, 8, 10, 45, 46	1222.12.25 (5, 10), $i = 4$ (6)	3
47	1304.08.08	East Mediterranean, Rhodes, Crete, Peloponnesus	35, 37, 45	1303.08.08 (6, 8), NTI (45), 1304.08. (37) Egyptian coasts, $i = 5$ –, Syrian coasts, $i = 4$, Crete, $i = 4$? (6). East Mediterranean, $i = 4$, Rhodes, $i = 3$, Crete, $i = 4$, Peloponnesus, $i = 3$ (35), Crete (Herakleion), $i = 4+$ (37)	4
48	1332.02.12	Marmara Sea, Istanbul	6, 8, 45, 46	NTI (45), $i = 3+$ (6)	2
49	1344.10.14	Marmara Sea, Istanbul, Thracian coasts, Gelibolu	5, 6, 8, 16, 35, 37, 45, 46	$i = 4$, $D = 2000$ m (6, 35), NTI (45), $i = 4+$ (37)	3
50	1389.03.20	Izmir, Chios and Lesvos Isls.	5, 6, 8, 35, 37, 43, 45, 46	Chios, $i = 3$ (6, 35), Chios, $i = 4$ (37)	4
51	1403.11.16	South coasts of Anatolia, Syrian coasts	6, 8, 46	1402 (10, 16, 45), 1408.12.30, Latakia (41), $i = 3$ (6)	2
52	1481.05.03	Rhodes, South west coasts of Anatolia, Crete	5, 6, 8, 10, 35, 37, 43, 45, 46	1481.10.03 (10, 43, 45), Rhodes, $i = 3$, $H = 1.8$ m, $D = 60$ m (6, 35), Rhodes, $i = 4$ (37)	3
53	1489	South coast of Anatolia, Antalya	6, 8, 46	$i = 3$ (6)	2
54	1494.07.01	Herakleion-Crete	6, 8, 35, 37, 45	Evening (35, 45), NTI (45), $i = 2+$ (6), $i = 2$ (35), $i = 3+$ (37)	3
55	1509.09.10	Istanbul, Marmara coasts	5, 6, 7, 8, 10, 16, 32, 35, 37, 43, 45, 46	1509.09.14 (5, 6, 8, 16, 35, 37, 43, 45, 46), $i = 3$ (6, 35), $i = 3+$ (37), $H \geq 6.0$ m (32)	4
56	1577.07.17	Istanbul	7		1
57	1598	Amasya, Çorum	7, 10, 12, 30, 39, 45	NTI (10, 12, 39, 45), On the coasts of the Black Sea,	4

Table A1. Continued

No.	Date	Place	References	Remarks	Rel
58	1609.04.	Rhodes, East Mediterranean	7	Over 10 000 people drowned by a sea wave	4
59	1612.12.08	North of Crete	5, 6, 8, 35, 37, 45	$i = 5$ —(6), $i = 5$ (35), $i = 4+$ (37), NTI (45)	2
60	1646.04.05	Istanbul	5, 6, 8, 16, 37, 45	1641.04.05 (46), $i = 3$ (6), $i = 4$ —(37), NTI (45)	3
61	1650.09.29	Santorini Patmos, Sikinos Isls., Northern Crete	5, 6, 8, 35, 37	1650.10.09 (6, 8), 1650.10.29 (35, 37), Santorini, $i = 6$, West Patmos, $H = 30$ m, East Patmos, $H = 27$ m, Ios, $H = 18$ m, Sikinos, $i = 5$, Kos, Crete, $i = 4$ —(6), East Santorini, $i = 4$, $H = 19$ m, $D = 200$ m, Patmos, $i = 6$, $H = 30$ m, Ios, $i = 6$, $H = 18$ m, Sikinos, $i = 5$ $D = 100$ m, Herakleion, $i = 4$ (35), Santorini, $i = 5+$, Ios, $i = 5$, Sikinos, $i = 4+$, Herakleion, $i = 4$, Patmos, $i = 4+$, Kea, $i = 4$ (37)	4
62	1667.11.30	Izmir Gulf	6, 7, 8, 45, 46	1667.11., NTI (7, 45) 1668.07.10 (9, 10, 35, 46), $i = 2$ (6, 35)	2
63	1672.02.14	Bozcaada, Kos Isl.	7, 8, 35, 43, 45	1672.04. (43, 45), 1672 Cyclades, Santorini (8), Kos (35)	2
64	1688.07.10	Izmir Gulf	6, 7, 8, 37, 45	11.00 a.m. (45), 11.45 a.m. (7), $i = 3$ (37)	3
65	1741.01.31	Rhodes	7	The sea retreated and then flooded the coast 12 times	4
66	1751.08.15	Istanbul	7		0
67	1752.07.21	Syrian coasts	6, 8, 10, 45	$i = 3?$ (6)	4
68	1754.09.02	Izmit Gulf, Istanbul	7, 45	09.45 p.m., NTI (45)	1
69	1766.05.22	Istanbul, Marmara Sea	6, 7, 8, 35, 43, 45, 46	05.30 a.m. (35, 45), $i = 2$ (6, 35)	4
70	1772.11.24	Chios Isl., Foça	7	07.45 a.m.	2
71	1822.08.13	Antakya, Iskenderun, Kilis	21, 45	Evening	4
72	1829.05.23	Istanbul, Gelibolu	6, 8, 21, 45, 46	$i = 2$ (6)	4
73	1851.02.28	Fethiye, Kaya- Mugla, Rhodes	6, 8, 21, 35, 37, 43, 45	$i = 3$, $H = 0.6$ m (6, 35), $i = 3$ (37)	4
74	1851.04.03	Fethiye Gulf	6, 8, 35, 46	$i = 3$, $H = 1.8$ m (6, 35)	3

Table A1. Continued

No.	Date	Place	References	Remarks	Rel
75	1851.05.23	Rhodes, Dodecanese, Chalki	6, 8, 35, 46	$i = 2$ (6, 35)	3
76	1852.05.12	Izmir	6, 8, 21, 35, 46	$i = 3$ (6, 35)	3
77	1852.09.08	Izmir	6, 8, 21, 35, 46	$i = 3$ (6, 35)	3
78	1855.02.13	Fethiye Gulf	6, 8, 10, 24, 35, 46	1855.02.09/10/13 (10, 24), 1855.03.02 NTI (45), Chios (46), $i = 3$ (6, 35)	4
79	1856.11.13	Chios Isl.	6, 8, 21, 35, 37, 43, 46	Rhodes (45), 1856.12.13 (46), $i = 3+$ (6), $i = 3$ (35)	3
80	1866.01.31	Santorini Isl.	37, 45	NTI (45), Santorini, $i = 4$, Kythera, $i = 3$, Chios, $i = 3-$ (37)	2
81	1866.02.02	Chios Isl.	6, 8, 10, 21, 45, 46	NTI (45), $i = 3$ (6)	3
82	1878.04.19	Izmit, Istanbul, Marmara Sea	5, 6, 8, 21, 45, 46	09.00 a.m., NTI (45), $i = 3$ (6)	3
83	1878.05.10	Izmit, Istanbul, Bursa	9, 10, 45, 46	08.00 a.m., most probably aftershock of 1878.04.19 Earthquake, NTI (45), South coasts of Anatolia (46), 40 people killed by tsunami (9, 10)	2
84	1886.08.27	Southern Peloponnesus, Pylos, Izmir	6, 8, 21, 35, 37, 45	1886.11.27, 08.05 a.m., NTI (45), 21.32 p.m., $i = 2$ (35), Pylos, $i = 3$, Izmir, $i = 2$ (6)	4
85	1893.02.09	Northern Aegean Sea, Samothrace Isl., Thracian coasts, Alexandroupolis	5, 6, 8, 10, 21, 35, 37, 45	1893.01.29 (5, 45), 1893.01.28 (10) 18.00 p.m. (35, 45), Samothrace, $i = 3+$ (6, 37), $i = 3$ (35), $H = 0.9$ m (6, 35), $D = 30$ m (35), Alexandroupolis, $i = 3$ (6, 35, 37), $H = 0.9$ m (35), $D = 40$ m (6, 35), Thracian coasts, $i = 3$ (6)	4
86	1894.07.10	Istanbul	6, 8, 21, 24, 32, 33, 35, 37, 45	NTI (45), $i = 3$ (6, 35, 37), $H \leq 6.0$ m (32)	4
87	1926.06.26	Rhodes, South west of Turkey, Archangelo, Fethiye, Karpathos, Herakleion	50	The epicenter is located east of Rhodes and near the Turkish coast. Felt in Sicily, Italy, Switz, Syria, Palestine, Egypt	2

Table A1. Continued

No.	Date	Place	References	Remarks	Rel
88	1928.03.31	Izmir	6, 8, 21, 35	00 29 47 (35), $i = 2$ (6, 35)	4
89	1939.12.26– 27	Fatsa-Black Sea	13, 24, 29, 38, 42	25 57 16 (13), $i = 4$ (24)	4
90	1948.02.09	Karpathos- Dodecanese	6, 8, 28, 35, 36, 37	12 58 13 (35), $i = 4$ (6, 35, 36, 37), $D = 900$ m (6, 35, 36)	4
91	1949.07.23	East Aegean Sea, North Chios Isl.	36	15 03 30, $i = 2$, $H = 0.7$ m or $H = 2$ m	4
92	1953.09.10	South coasts of Turkey	28	35.00N-32.00E	1
93	1956.07.09	Greek Archipelago. Amorgos, Astypalaea Isls.	6, 8, 28, 35, 36	03 11 40 (35, 36), Amorgos, $i = 6$ (35, 36), $H = 30$ m (6), $H = 20$ –25 m, $D = 80$ –100 m (35, 36), $H = 30$ m (6), Astypalaea, $i = 6$ (35, 36), $H = 20$ m (6, 35, 36), $D = 400$ m (35, 36), Pholegandros, $i = 5$ (35), $H = 10$ m (6, 35), $D = 8$ m (35), Patmos, $H = 4$ m, Kalimnos, $H = 3.6$ m, Crete, $H = 3$ m, Tinos, $H = 3$ m (6), $i = 5$ – 3, $H = \text{up to } 5$ m, $D = \text{up to}$ 700 m (35)	4
94	1963.09.18	Eastern Marmara, Yalova, Karamürsel, Kılıç, Armutlu, Mudanya, Gemlik Gulf	24, 31	16 58 14.8, $H = 1$ m	4
95	1968.02.19	North Aegean Sea	8, 28, 35, 36	22 45 42 (35), 22 57 47 (36), $i = 2$, $H = 1.2$ m (35)	4
96	1968.09.03	Amasra-Black Sea	1, 22, 24, 25, 42, 49	08 19 51.6 (1), $H = 3$ m (42), $i = 3+$	4
97	1999.08.17	Izmit Gulf	4, 51	00 01 47.8 $i = 3$	4

A.2 Earthquake Database of TRANSFER Project for Selected Domain (Magnitude ≥ 6)

Table A.2: Earthquake Database of TRANSFER Project

Id	Latitude	Longitude	Locality	Strike	Dip	Rake	Mag.	Depth
3760	39.4	25	Aegean Sea	311	90	20	7.29	0
7922	36.5	28.6	Aegean Sea	58	85	19	7.2	1
3742	40	27.4	Aegean Sea	60	90	180	7.18	0
3747	36.7	25.8	Aegean Sea	65	45	-90	7.18	0
7324	36.5	28.6	Aegean Region	303.92	58.122	-175.36	7.18	0
12018	40.26	24.33	Aegean Sea	72	64	-167	7.1	0
14369	40.26	24.33	Aegean Sea	72	64	-167	7.1	0
3764	39.18	29.49	Aegean Sea	308	35	-90	7.07	0
4194	39.2	29.5	Greece	280	30	-90	7.07	10
4773	38.6	22.4	Turkey	359.649	28.458	150.32	7.07	0
5684	35.5	27	E.Medi Greece	190	62	-90	7.07	40
3709	37.9	30.4	Aegean Sea	222	42	-107	6.96	0
4688	39.3	22.6	Turkey	46.573	38.37	-80.748	6.96	0
4689	39.3	22.6	Turkey	50.854	36.596	-83.261	6.96	0
4690	39.3	22.6	Turkey	15.897	39.702	-104.26	6.96	0
3708	40.1	26.8	Aegean Sea	68	55	-145	6.85	0
3712	39.1	27.4	Aegean Sea	270	45	-90	6.85	0
3739	36.8	22	Aegean Sea	200	45	-80	6.85	0
3752	40.1	28	Aegean Sea	100	40	-90	6.85	0
4693	36.4	28.6	Turkey	233.386	14.379	125.70	6.85	0
4694	36.4	28.6	Turkey	114.26	29.088	27.921	6.85	0
7655	34.49	32.12	Cyprus	40	64	162	6.8	85
9583	34.49	32.12	Cyprus	40	64	162	6.8	85

Table A.2. Continued

Id	Latitude	Longitude	Locality	Strike	Dip	Rake	Mag.	Depth
52757	39.39	25.09	AEGEAN SEA	219.649	73.014	171.32	6.78	15
3738	39.7	26.8	Aegean Sea	262	41	-70	6.75	0
3756	39.2	24.6	Aegean Sea	313	43	-56	6.75	0
53794	40.18	24.73	AEGEAN SEA	229	81	-174	6.72	10
5625	35.75	25	Turkey	270.331	68.985	111.82	6.7	80
7467	32.9	29.8		215.419	72.236	22.162	6.7	0
3743	39.3	22.2	Aegean Sea	300	45	-70	6.65	0
3745	37.6	27.25	Aegean Sea	55	51	-137	6.65	0
63948	34.56	32.13	CYPRUS	48	77	170	6.62	33
40496	38.57	31.27	TURKEY	106.322	44.643	-50.745	6.6	10
40798	36.29	23.24	S. GREECE	189.401	52.317	29.051	6.6	30
3716	36.8	23.2	Aegean Sea	340	45	-90	6.55	0
3741	38.7	26.7	Aegean Sea	262	41	-108	6.55	0
3749	39.4	22.7	Aegean Sea	58	41	-128	6.55	0
4677	32.2	29.6	Turkey	314.886	58.609	35.559	6.55	0
5494	39.5	33.8	Central Turkey	298	87	149.95	6.55	0
3718	38.2	27.4	Aegean Sea	90	45	-90	6.46	0
3727	36.7	27.4	Aegean Sea	60	45	-90	6.46	0
3731	39.1	27	Aegean Sea	262	41	-70	6.46	0
3740	37.2	23.2	Aegean Sea	300	45	-90	6.46	0
3753	39.4	24	Aegean Sea	135	85	15	6.46	0
3763	38.59	28.45	Aegean Sea	281	34	-90	6.46	0
4051	34.4	24.5	Greece	268.159	75.323	-163.4	6.46	0
4679	39.9	30.4	Turkey	283.631	34.235	-171.82	6.46	0
4680	39.9	30.4	Turkey	136.358	7.456	15.721	6.46	0
5046	39.4	22.7	Aegean Sea	58	41	-128	6.46	0
5628	35	23.5	E.Medi Greece	153	90	-180	6.46	100
5636	38	22.5	E.Medi Greece	280	40	-90	6.46	100
5674	33.75	28.5	E.Medi Greece	220	45	90	6.46	80
7443	34.7	24.7		319.953	79.987	-163.74	6.46	0
64791	36.38	22.07	S. Greece	297.864	19.645	89.34	6.41	24
1807	38.38	22.26		136	76	78	6.38	55
40492	35.79	26.62	CRETE	17.604	34.666	-163.09	6.38	88

Table A.2 Continued

Id	Latitude	Longitude	Locality	Strike	Dip	Rake	Mag.	Depth
3713	39.9	23.2	Aegean Sea	315	45	-45	6.36	0
4663	34.4	24.5	Turkey	127	25.158	51.172	6.36	0
4664	34.4	24.5	Turkey	162.428	19.242	81.622	6.36	0
4706	34.9	27.4	Turkey	56.475	67.215	-168.2	6.36	0
4707	34.9	27.4	Turkey	54.197	69.92	175.64	6.36	0
4708	34.9	27.4	Turkey	294.483	30.53	25.788	6.36	0
4712	36.4	27.3	Turkey	12.561	76.574	172.10	6.36	0
4713	36.4	27.3	Turkey	7.746	22.392	-154.2	6.36	0
5056	39.23	22.76	Aegean Sea	58	41	-128	6.36	0
62663	40.14	21.68	GREECE	72.84	43.78	-83.05	6.36	13
12024	40.3	27.5	Aegean Sea	256	64	-145	6.3	0
12934	38.38	22.26	S.Aegean Sea	136	76	78	6.3	55
13003	36.45	22.16	S. Aegean Sea	123	72	84	6.3	33
52330	38.22	22.93	GREECE	284.57	37.091	-63.68	6.3	33
68419	39.06	24.24	AEGEAN SEA	147.628	76.148	-0.879	6.3	10
52809	40	24.32	AEGEAN SEA	240.641	57.389	-175.9	6.29	10
1882	36.6	28.3		89	62	90	6.27	72
1885	37.8	22.9		241	52	57.395	6.27	100
1903	38.6	22.4		136	76	78.654	6.27	78
3717	36.78	22.25	Aegean Sea	335	45	-90	6.27	0
3721	38	23	Aegean Sea	264	42	-80	6.27	0
4717	37	28.5	Turkey	8.471	39.764	-2.766	6.27	0
53150	33.73	22.97	MEDI. SEA	219.251	33.535	92.726	6.25	10
62764	38.4	22.27	GREECE	264.781	43.061	-102.6	6.25	14
5626	35.5	27	Turkey	325	70	90	6.23	130
52342	38.21	23.29	GREECE	257.542	41.643	-59.55	6.21	29
7771	38.1	30.175	Dinar (SW TR.)	135	40	-105	6.2	8
7773	38.09	30.15	Dinar (SW TR.)	312	56	-84	6.2	10
7775	38.06	30.13	Dinar (SW TR.)	136	43	-87	6.2	4
11947	36.53	35.33	Adana	50	85	10	6.2	32
12944	36.1	29.2	S. Aegean Sea	100	74	82	6.2	7
3710	38.2	23.5	Aegean Sea	100	45	-90	6.18	0
3722	39.41	29.45	Aegean Sea	300	45	-90	6.18	0

Table A.2. Continued

Id	Latitude	Longitude	Locality	Strike	Dip	Rake	Mag.	Depth
3735	39.38	28.1	Aegean Sea	90	40	-104	6.18	0
3744	39.3	23.1	Aegean Sea	58	41	-128	6.18	0
3765	38.43	22.66	Aegean Sea	75	67	-94	6.18	0
3766	37.65	29.72	Aegean Sea	64	50	-75	6.18	0
4060	38	21	Greece	120.055	69.534	73.124	6.18	0
4668	34.9	32.2	Turkey	150.263	23.227	-33.927	6.18	0
4669	34.9	32.2	Turkey	25.75	63.67	171.151	6.18	0
4670	34.9	32.2	Turkey	144.718	66.547	12.595	6.18	0
4691	39.2	22.8	Turkey	195.332	65.406	170.18	6.18	0
4696	36.2	28.9	Turkey	193.076	24.072	2.645	6.18	0
4724	35.3	24.5	Turkey	239.093	41.566	-20.168	6.18	0
10061	35.1	23.6	Hellenic sub.z.	309	18	89	6.18	40
10191	35.2	22.7	Hellenic sub. z.	108	90	90	6.18	33
40759	35.8	29.7	E.MEDI.	215.643	40.118	-12.67	6.16	30
7658	34.49	32.12	Cyprus	48	77	170	6.14	23
5088	35.14	23.54	Crete	112	74	98	6.11	36
3711	39.1	21.4	Aegean Sea	200	56	-40	6.1	0
3730	38.3	23.8	Aegean Sea	290	45	-70	6.1	0
3732	39.7	22.4	Aegean Sea	58	41	-128	6.1	0
3746	39.96	30.11	Aegean Sea	264	50	-135	6.1	0
3762	39.18	28.37	Aegean Sea	90	40	-104	6.1	0
7853	37.7	28.89	Aegean Sea	276	69	-131	6.1	4
10255	35.1	26.6	Hellenic sub. z.	172	38	-106	6.1	20
12026	40	24	Aegean Sea	50	64	-167	6.1	0
12935	37.7	22	S. Aegean Sea	226	58	-161	6.1	28
13001	36.07	27.46	S. Aegean Sea	9	53	-114	6.1	12
14272	35.1	26.6	Hellenic sub. z.	172	38	-106	6.1	20
14273	35.1	26.6	Hellenic sub.z.	172	38	-106	6.1	20
51989	39.27	23.04	AEGEAN SEA	57.727	41.288	-127.54	6.1	14
9584	34.49	32.12	Cyprus	125	12	-73	6.09	25
5084	34.92	24.27	Crete	63	76	157	6.05	24
40497	38.63	30.9	TURKEY	24.407	41.728	-90.733	6.05	10
61763	35.58	24.72	CRETE	176.902	62.761	22.14	6.05	77

Table A.2. Continued

Id	Latitude	Longitude	Locality	Strike	Dip	Rake	Mag.	Depth
3704	38.7	26.9	Aegean Sea	262	41	108	6.02	0
3714	39.08	30.14	Aegean Sea	308	35	-90	6.02	0
3715	37.9	29.6	Aegean Sea	64	50	-75	6.02	0
3723	39.6	23.2	Aegean Sea	310	45	-70	6.02	0
3733	37.2	28.2	Aegean Sea	65	45	-90	6.02	0
3737	38.9	29.26	Aegean Sea	308	35	-90	6.02	0
3761	40.08	27.5	Aegean Sea	60	40	68	6.02	0
4025	35.2	23.8	Aegean Sea	283	38	97	6.02	18
5057	39.23	22.59	Aegean Sea	58	41	-128	6.02	0
65402	36.88	35.31	TURKEY	320.532	75.467	170.638	6.01	33
7796	38.02	26.97	Aegean Sea	146	76	13	6	6
7930	35.4	27.9	Aegean Sea	314	25	119	6	27
12943	36.6	26.9	S. Aegean Sea	57	46	-72	6	7
52331	38.12	23.14	GREECE	264.459	34.286	-51.351	6	33

A.3 Summary outputs of Single Domain Simulations

A.3.1. Simulation of Source s02-Z04

Table A.3.1: Rupture Parameters of Tsunami Source 02-Z04

Rupture Parameters			
Epicenter of fault axis	23.78E 40.83N	Dip angle (deg.)	40
Length of fault (km)	91	Slip angle (deg.)	45
Strike angle (deg. CW)	140	Fdisplacement (m)	6
Width of fault (km)	12	Maximum (+)ve amp. (m)	1.2
Focal depth (km)	10	Minimum (-)ve amp. (m)	-0.2

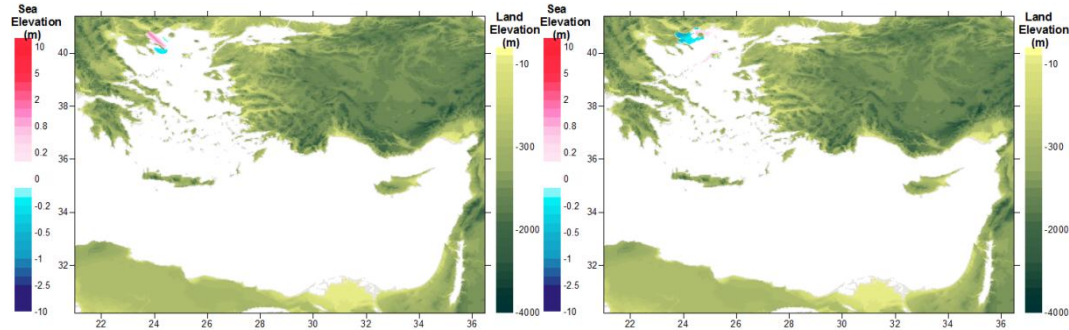


Figure A.3.1: The location of tsunami source 02-Z04(left) and the distribution wave at t=1hr(right) in the study domain (Eastern Mediterranean) in the duration of simulation (4 hours) for the tsunami source 02-Z04

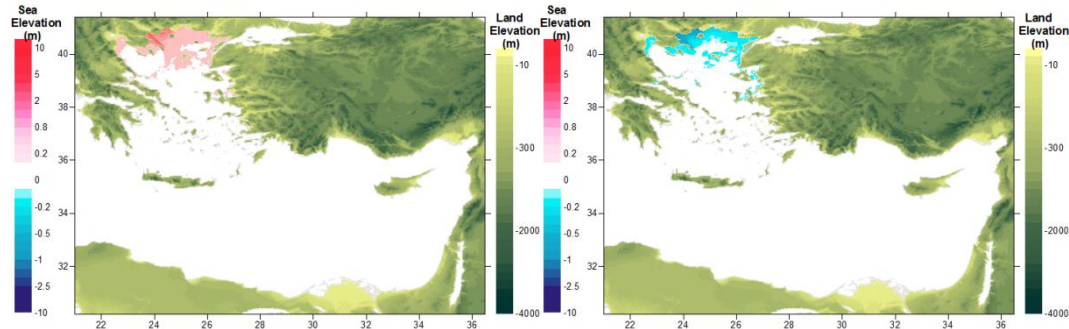


Figure A.3.2: The distributions of maximum positive of the water elevations(left) and negative water elevations(right) in the in the study domain (Eastern Mediterranean) in the duration of simulation (4 hours) for the tsunami source 02-Z04

Table A.3.2: Summary Results of tsunami impact at forecast points for source 02-Z04

Name of gauge pt.	Depth of gauge pt.(m)	Longitude	Latitude	Arrival time of initial wave (min)	Arrival time of max.wave (min)	Maximum (+)ve amp.(m)	Maximum (-)ve amp.(m)
Gokceada	0.4	25.9006	40.2379	7	71	0.1	-0.1
Mentes	7.4	26.7374	38.434	101	192	0.1	0.0
Bodrum	8.4	27.4171	37.0193	182	211	0.0	0.0
Aksaz	4.7	28.4313	36.8453	224	224	0.0	0.0
Girne	1.1	33.3276	35.3493	0	0	0.0	0.0
Gazimagusa	7.1	33.9468	35.1367	0	0	0.0	0.0
Tasucu	3.5	33.8327	36.2664	0	0	0.	0.0
Erdemli	2.9	34.2629	36.57	0	0	0.0	0.0
Canakkale	2.5	26.3772	40.1043	47	113	0.1	-0.1
Aliaga	3.9	26.9423	38.8421	87	149	0.1	-0.1
Alsancak P.	6.8	27.1387	38.4464	146	227	0.1	0.0
Cesme	10	26.2879	38.3288	84	148	0.1	-0.1
Kusadasi	3.5	27.2588	37.8668	102	157	0.1	-0.1
Didim	3.7	27.2615	37.3329	140	203	0.0	0.0
Bodrum	6.7	27.4242	37.0228	177	212	0.0	0.0
Marmaris	1.9	28.3271	36.8107	202	202	0.0	0.0
Fethiye	11.7	28.9502	36.7235	236	236	0.0	0.0
Fethiye Bay	4.2	29.0546	36.6537	225	225	0.0	0.0
Kas	10.8	29.6436	36.1965	222	222	0.0	0.0
Finike	5.3	30.1554	36.3	235	235	0.0	0.0
Kemer	0	30.5728	36.6052	0	0	0.0	0.0
Antalya B.	10.8	30.6123	36.8362	0	0	0.0	0.0
Alanya	10	31.9911	36.5243	0	0	0.0	0.0
Karatas	2.1	35.3872	36.5604	0	0	0.0	0.0
Anamur	7.2	32.8582	36.0565	0	0	0.0	0.0
Iskenderun B.	2.5	36.1898	36.6046	0	0	0.0	0.0
Arsuz	3.2	35.8965	36.4272	0	0	0.0	0.0
Samandag	7.9	35.9564	36.0549	0	0	0.0	0.0

A.3.2. Simulation of Source s03-Z10-1

Table A.3.3: Rupture Parameters of Tsunami Source 03-Z10-1

Rupture Parameters			
Epicenter of fault axis	26.4E 40.4N	Dip angle (deg.)	45
Length of fault (km)	91	Slip angle (deg.)	45
Strike angle (deg. CW)	245	Fdisplacement (m)	8
Width of fault (km)	15	Maximum (+)ve amp. (m)	1.8
Focal depth (km)	10	Minimum (-)ve amp. (m)	-0.3

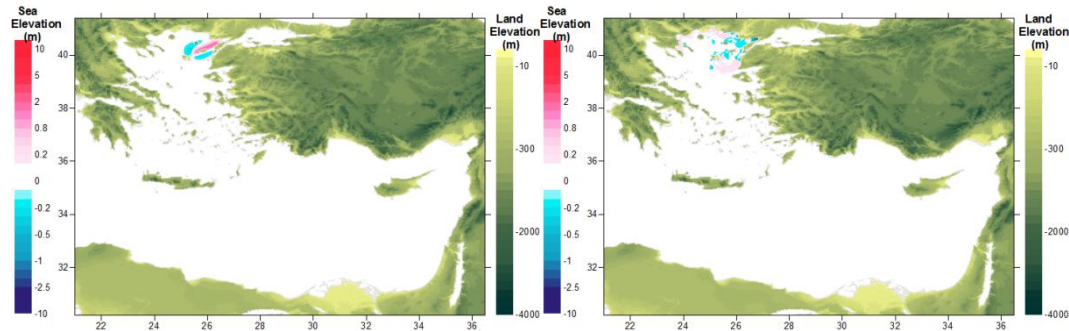


Figure A.3.3: The location of tsunami source 03-Z10-1 (left) and the distribution wave at t=1hr(left) in the study domain (Eastern Mediterranean) in the duration of simulation (4 hours) for the tsunami source 03-Z10-1

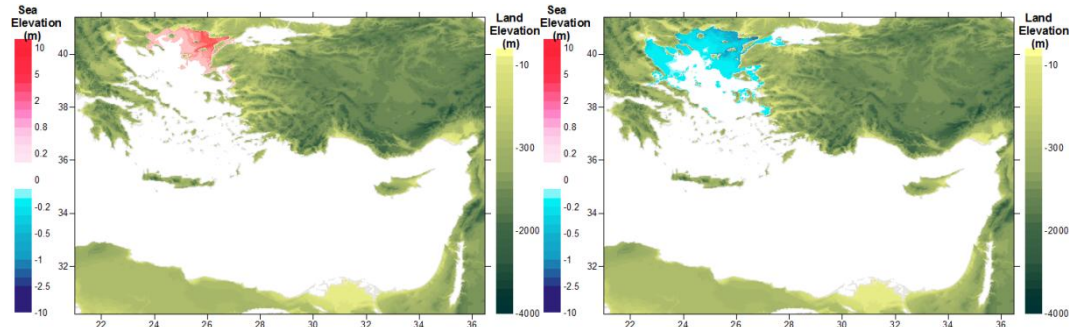


Figure A.3.4: The distributions of maximum positive of the water elevations(left) and negative water elevations(right) in the in the study domain (Eastern Mediterranean) in the duration of simulation (4 hours) for the tsunami source 03-Z10-1

Table A.3.4: Summary Results of tsunami impact at forecast points for source 03-Z10-1

Name of gauge pt.	Depth of gauge pt.(m)	Longitude	Latitude	Arrival time of initial wave (min)	Arrival time of max.wave (min)	Maximum (+)ve amp.(m)	Maximum (-)ve amp.(m)
Gokceada	0.4	25.9006	40.2379	0	0	1.7	-0.5
Mentes	7.4	26.7374	38.434	62	176	0.2	-0.2
Bodrum	8.4	27.4171	37.0193	133	208	0.0	0.0
Aksaz	4.7	28.4313	36.8453	206	206	0.0	0.0
Girne	1.1	33.3276	35.3493	0	0	0.0	0.0
Gazimagusa	7.1	33.9468	35.1367	0	0	0.0	0.0
Tasucu	3.5	33.8327	36.2664	0	0	0.0	0.0
Erdemli	2.9	34.2629	36.57	0	0	0.0	0.0
Canakkale	2.5	26.3772	40.1043	0	35	0.7	-0.6
Aliaga	3.9	26.9423	38.8421	46	141	0.2	-0.2
Alsancak P.	6.8	27.1387	38.4464	109	199	0.2	-0.1
Cesme	10	26.2879	38.3288	46	129	0.1	-0.2
Kusadasi	3.5	27.2588	37.8668	71	172	0.2	-0.2
Didim	3.7	27.2615	37.3329	111	206	0.1	0.0
Bodrum	6.7	27.4242	37.0228	133	210	0.0	0.0
Marmaris	1.9	28.3271	36.8107	201	201	0.0	0.0
Fethiye	11.7	28.9502	36.7235	219	219	0.0	0.0
Fethiye Bay	4.2	29.0546	36.6537	220	220	0.0	0.0
Kas	10.8	29.6436	36.1965	217	217	0.0	0.0
Finike	5.3	30.1554	36.3	227	227	0.0	0.0
Kemer	0	30.5728	36.6052	0	0	0.0	0.0
Antalya B.	10.8	30.6123	36.8362	0	0	0.0	0.0
Alanya	10	31.9911	36.5243	0	0	0.0	0.0
Karatas	2.1	35.3872	36.5604	0	0	0.0	0.0
Anamur	7.2	32.8582	36.0565	0	0	0.0	0.0
Iskenderun B.	2.5	36.1898	36.6046	0	0	0.0	0.0
Arsuz	3.2	35.8965	36.4272	0	0	0.0	0.0
Samandag	7.9	35.9564	36.0549	0	0	0.0	0.0

A.3.3. Simulation of Source s04-Z10-2

Table A.3.5: Rupture Parameters of Tsunami Source 04-Z10-2

Rupture Parameters			
Epicenter of fault axis	25.95E 40.15N	Dip angle (deg.)	45
Length of fault (km)	83	Slip angle (deg.)	45
Strike angle (deg. CW)	235	Fdisplacement (m)	8
Width of fault (km)	15	Maximum (+)ve amp. (m)	1.8
Focal depth (km)	10	Minimum (-)ve amp. (m)	-0.3

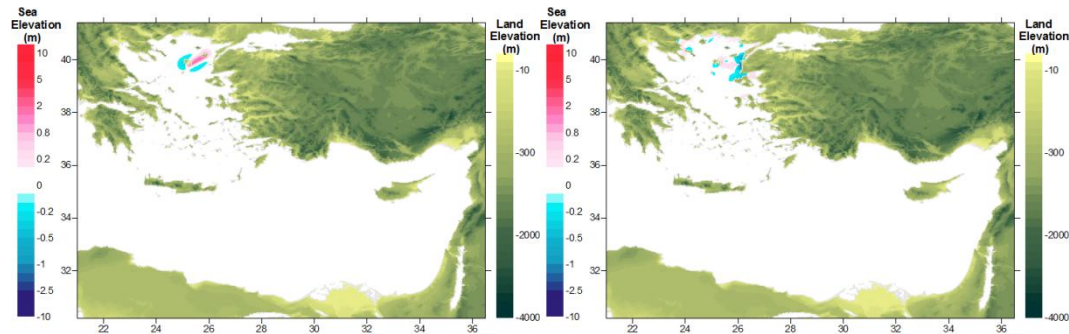


Figure A.3.5: The location of tsunami source 04-Z10-2 (left) and the distribution wave at t=1hr(right) of the water elevations in the study domain (Eastern Mediterranean) in the duration of simulation (4 hours) for the tsunami source 04-Z10-2

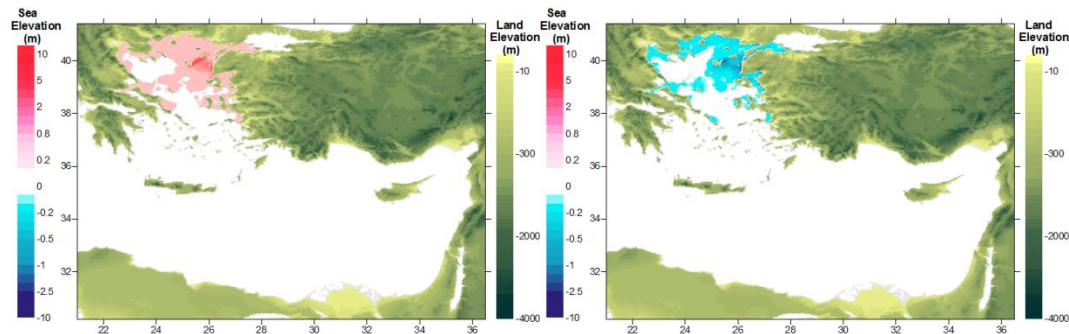


Figure A.3.6: The distributions of maximum positive of the water elevations(left) and negative water elevations(right) in the in the study domain (Eastern Mediterranean) in the duration of simulation (4 hours) for the tsunami source 04-Z10-2

Table A.3.6: Summary Results of tsunami impact at forecast points for source 04-Z10-2

Name of gauge pt.	Depth of gauge pt.(m)	Longitude	Latitude	Arrival time of initial wave (min)	Arrival time of max.wave (min)	Maximum (+)ve amp.(m)	Maximum (-)ve amp.(m)
Gokceada	0.4	25.9006	40.2379	0	0	1.0	-0.4
Mentes	7.4	26.7374	38.434	60	111	0.1	0.1
Bodrum	8.4	27.4171	37.0193	120	157	0.0	0.0
Aksaz	4.7	28.4313	36.8453	178	178	0.0	0.0
Girne	1.1	33.3276	35.3493	0	0	0.0	0.0
Gazimagusa	7.1	33.9468	35.1367	0	0	0.0	0.0
Tasucu	3.5	33.8327	36.2664	0	0	0.0	0.0
Erdemli	2.9	34.2629	36.57	0	0	0.0	0.0
Canakkale	2.5	26.3772	40.1043	4	115	0.7	-0.9
Aliaga	3.9	26.9423	38.8421	45	183	0.3	-0.2
Alsancak P.	6.8	27.1387	38.4464	103	161	0.2	-0.2
Cesme	10	26.2879	38.3288	43	89	0.1	-0.1
Kusadasi	3.5	27.2588	37.8668	61	130	0.2	-0.2
Didim	3.7	27.2615	37.3329	99	160	0.1	0.0
Bodrum	6.7	27.4242	37.0228	120	197	0.0	0.0
Marmaris	1.9	28.3271	36.8107	174	174	0.0	0.0
Fethiye	11.7	28.9502	36.7235	191	191	0.0	0.0
Fethiye B.	4.2	29.0546	36.6537	191	191	0.0	0.0
Kas	10.8	29.6436	36.1965	186	186	0.0	0.0
Finike	5.3	30.1554	36.3	197	197	0.0	0.0
Kemer	0	30.5728	36.6052	0	0	0.0	0.0
Antalya B.	10.8	30.6123	36.8362	215	215	0.0	0.0
Alanya	10	31.9911	36.5243	222	222	0.0	0.0
Karatas	2.1	35.3872	36.5604	0	0	0.0	0.0
Anamur	7.2	32.8582	36.0565	0	0	0.0	0.0
Iskenderun B.	2.5	36.1898	36.6046	0	0	0.0	0.0
Arsuz	3.2	35.8965	36.4272	0	0	0.0	0.0
Samandag	7.9	35.9564	36.0549	0	0	0.0	0.0

A.3.4. Simulation of Source s05-Z10-3

Table A.3.7: Rupture Parameters of Tsunami Source 05-Z10-3

Rupture Parameters			
Epicenter of fault axis	25.15E 39.75N	Dip angle (deg.)	45
Length of fault (km)	83.4	Slip angle (deg.)	45
Strike angle (deg. CW)	235	Fdisplacement (m)	8
Width of fault (km)	15	Maximum (+)ve amp. (m)	1.8
Focal depth (km)	10	Minimum (-)ve amp. (m)	-0.3

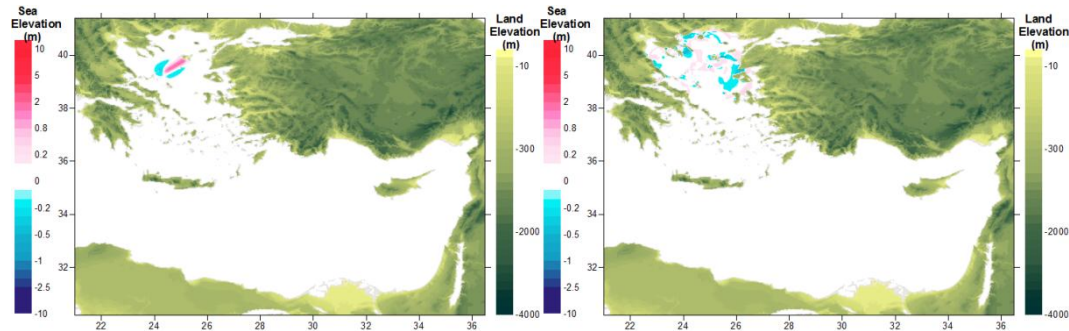


Figure A.3.7: The location of tsunami source 05-Z10-3 (left) and the distributions wave at t=1hr of the water elevations(right) in the study domain (Eastern Mediterranean) in the duration of simulation (4 hours) for the tsunami source 05-Z10-3

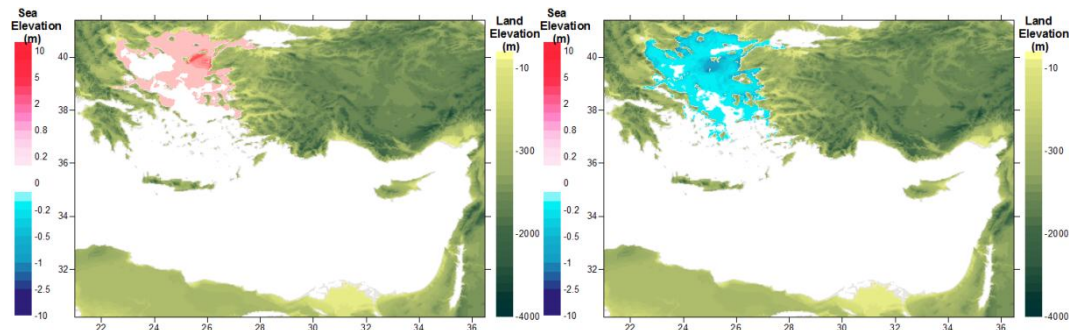


Figure A.3.8: The distributions of maximum positive of the water elevations(left) and negative water elevations(right) in the in the study domain (Eastern Mediterranean) in the duration of simulation (4 hours) for the tsunami source 05-Z10-3

Table A.3.8: Summary Results of tsunami impact at forecast points for source 05-Z10-3

Name of gauge pt.	Depth of gauge pt.(m)	Longitude	Latitude	Arrival time of initial wave (min)	Arrival time of max.wave (min)	Maximum (+)ve amp.(m)	Maximum (-)ve amp.(m)
Gokceada	0.4	25.9006	40.2379	0	35	0.1	-0.2
Mentes	7.4	26.7374	38.434	75	95	0.4	-0.4
Bodrum	8.4	27.4171	37.0193	130	223	0.1	-0.1
Aksaz	4.7	28.4313	36.8453	156	203	0.0	0.0
Girne	1.1	33.3276	35.3493	207	207	0.0	0.0
Gazimagusa	7.1	33.9468	35.1367	0	0	0.0	0.0
Tasucu	3.5	33.8327	36.2664	236	236	0.0	0.0
Erdemli	2.9	34.2629	36.57	0	0	0.0	0.0
Canakkale	2.5	26.3772	40.1043	41	153	0.5	-0.5
Aliaga	3.9	26.9423	38.8421	61	83	0.3	-0.3
Alsancak P.	6.8	27.1387	38.4464	115	198	0.3	-0.4
Cesme	10	26.2879	38.3288	57	117	0.6	-0.5
Kusadasi	3.5	27.2588	37.8668	66	231	0.3	-0.3
Didim	3.7	27.2615	37.3329	100	136	0.1	-0.1
Bodrum	6.7	27.4242	37.0228	125	223	0.1	-0.1
Marmaris	1.9	28.3271	36.8107	152	152	0.0	0.0
Fethiye	11.7	28.9502	36.7235	163	211	0.0	0.0
Fethiye Bay	4.2	29.0546	36.6537	165	218	0.0	0.0
Kas	10.8	29.6436	36.1965	162	162	0.0	0.0
Finike	5.3	30.1554	36.3	173	173	0.0	0.0
Kemer	0	30.5728	36.6052	0	0	0.0	0.0
Antalya B.	10.8	30.6123	36.8362	190	190	0.0	0.0
Alanya	10	31.9911	36.5243	193	193	0.0	0.0
Karatas	2.1	35.3872	36.5604	0	0	0.0	0.0
Anamur	7.2	32.8582	36.0565	204	204	0.0	0.0
Iskenderun B.	2.5	36.1898	36.6046	0	0	0.00	0.00
Arsuz	3.2	35.8965	36.4272	0	0	0.00	0.00
Samandag	7.9	35.9564	36.0549	0	0	0.00	0.00

A.3.5. Simulation of Source s06-Z10-4

Table A.3.9: Rupture Parameters of Tsunami Source 06-Z10-4

Rupture Parameters			
Epicenter of fault axis	24.5E 39.2N	Dip angle (deg.)	45
Length of fault (km)	70.4	Slip angle (deg.)	45
Strike angle (deg. CW)	200	Fdisplacement (m)	8
Width of fault (km)	15	Maximum (+)ve amp. (m)	1.8
Focal depth (km)	10	Minimum (-)ve amp. (m)	-0.3

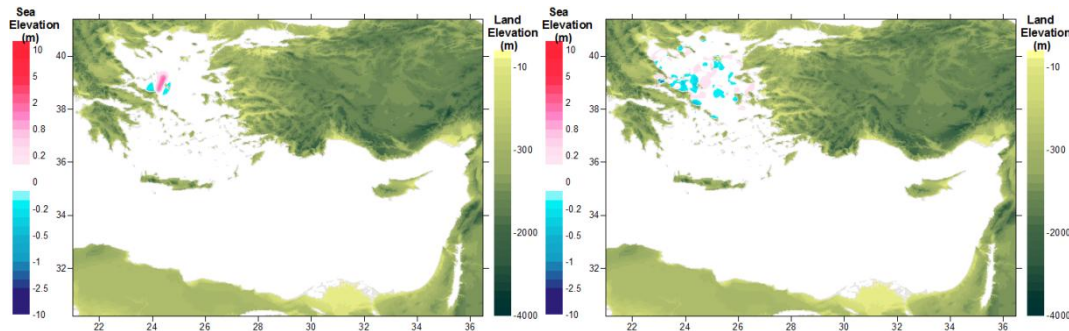


Figure A.3.9: The location of tsunami source 06-Z10-4 (left) and the distribution wave at t=1hr(right) in the study domain (Eastern Mediterranean) in the duration of simulation (4 hours) for the tsunami source 06-Z10-4

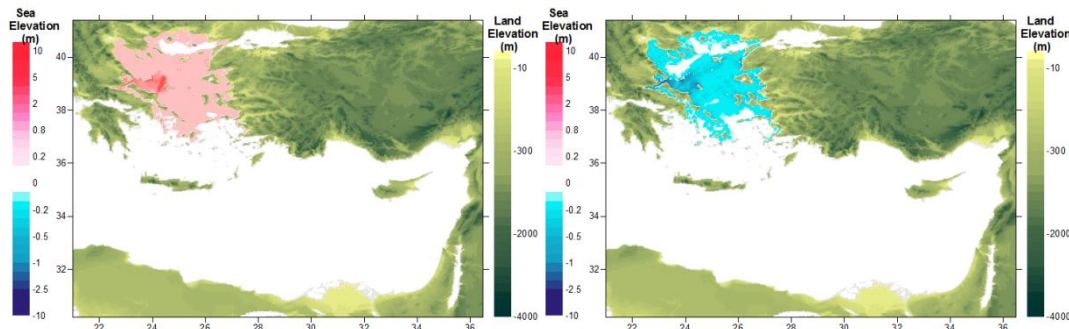


Figure A.3.10: The distributions of maximum positive of the water elevations(left) and negative water elevations(right) in the in the study domain (Eastern Mediterranean) in the duration of simulation (4 hours) for the tsunami source 06-Z10-4

Table A.3.10: Summary Results of tsunami impact at forecast points for source 06-Z10-4

Name of gauge pt.	Depth of gauge pt.(m)	Longitude	Latitude	Arrival time of initial wave (min)	Arrival time of max.wave (min)	Maximum (+)ve amp.(m)	Maximum (-)ve amp.(m)
Gokceada	0,4	25,9006	40,2379	28	86	0,1	-0,1
Mentes	7,4	26,7374	38,434	77	165	0,4	-0,4
Bodrum	8,4	27,4171	37,0193	112	166	0,1	-0,1
Aksaz	4,7	28,4313	36,8453	138	239	0,0	0,0
Girne	1,1	33,3276	35,3493	190	190	0,0	0,0
Gazimagusa	7,1	33,9468	35,1367	223	223	0,0	0,0
Tasucu	3,5	33,8327	36,2664	218	218	0,0	0,0
Erdemli	2,9	34,2629	36,57	232	232	0,0	0,0
Canakkale	2,5	26,3772	40,1043	76	215	0,4	-0,4
Aliaga	3,9	26,9423	38,8421	64	85	0,3	-0,2
Alsancak P.	6,8	27,1387	38,4464	118	147	0,2	-0,3
Cesme	10	26,2879	38,3288	48	114	0,4	-0,4
Kusadasi	3,5	27,2588	37,8668	54	218	0,3	-0,4
Didim	3,7	27,2615	37,3329	88	115	0,1	-0,1
Bodrum	6,7	27,4242	37,0228	112	167	0,1	-0,1
Marmaris	1,9	28,3271	36,8107	134	134	0,0	0,0
Fethiye	11,7	28,9502	36,7235	146	199	0,0	0,0
Fethiye Bay	4,2	29,0546	36,6537	148	239	0,0	0,0
Kas	10,8	29,6436	36,1965	146	146	0,0	0,0
Finike	5,3	30,1554	36,3	156	156	0,0	0,0
Kemer	0	30,5728	36,6052	0	0	0,0	0,0
Antalya B.	10,8	30,6123	36,8362	172	172	0,0	0,0
Alanya	10	31,9911	36,5243	176	176	0,0	0,0
Karatas	2,1	35,3872	36,5604	0	0	0,0	0,0
Anamur	7,2	32,8582	36,0565	186	186	0,0	0,0
Iskenderun B.	2,5	36,1898	36,6046	0	0	0,0	0,0
Arsuz	3,2	35,8965	36,4272	0	0	0,0	0,0
Samandag	7,9	35,9564	36,0549	0	0	0,0	0,0

A.3.6. Simulation of Source s07-Z11-1

Table A.3.11: Rupture Parameters of Tsunami Source 07-Z11-1

Rupture Parameters			
Epicenter of fault axis	27.68E 36.1N	Dip angle (deg.)	45
Length of fault (km)	122	Slip angle (deg.)	45
Strike angle (deg. CW)	330	Fdisplacement (m)	6
Width of fault (km)	40	Maximum (+)ve amp. (m)	1
Focal depth (km)	40	Minimum (-)ve amp. (m)	-0.1

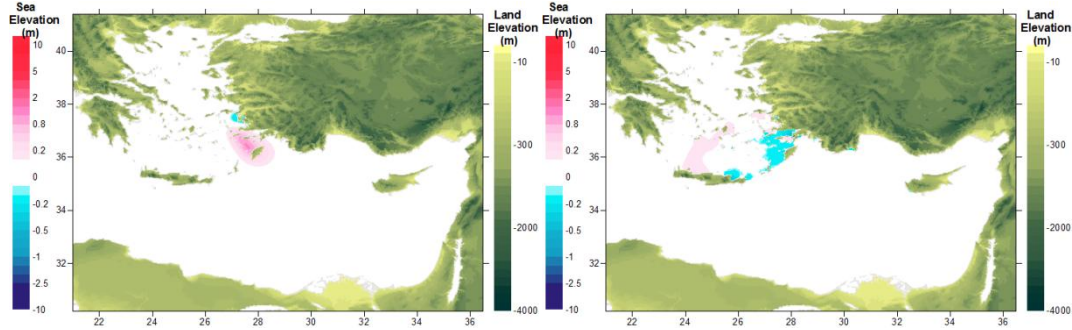


Figure A.3.11: The location of tsunami source 07-Z11-1 (left) and the distributions of wave at $t=1\text{hr}$ (right) of the water elevations in the study domain (Eastern Mediterranean) in the duration of simulation (4 hours) for the tsunami source 07-Z11-1

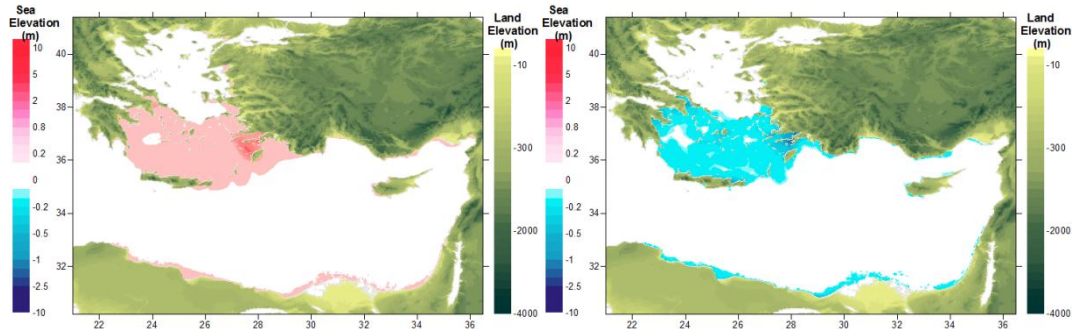


Figure A.3.12: The The distributions of maximum positive of the water elevations(left) and negative water elevations(right) in the in the study domain (Eastern Mediterranean) in the duration of simulation (4 hours) for the tsunami source 07-Z11-1

Table A.3.12: Summary Results of tsunami impact at forecast points for source 07-Z11-1

Name of gauge pt.	Depth of gauge pt.(m)	Longitude	Lattitude	Arrival time of initial wave (min)	Arrival time of max.wave (min)	Maximum (+)ve amp.(m)	Maximum (-)ve amp.(m)
Gokceada	0,4	25,9006	40,2379	87	212	0,0	0,0
Mentes	7,4	26,7374	38,434	0	167	0,1	0,0
Bodrum	8,4	27,4171	37,0193	0	14	0,7	-0,7
Aksaz	4,7	28,4313	36,8453	3	197	0,8	-0,7
Girne	1,1	33,3276	35,3493	49	157	0,1	-0,1
Gazimagusa	7,1	33,9468	35,1367	77	111	0,1	-0,1
Tasucu	3,5	33,8327	36,2664	73	172	0,2	-0,1
Erdemli	2,9	34,2629	36,57	82	180	0,1	-0,1
Canakkale	2,5	26,3772	40,1043	105	197	0,1	-0,1
Aliaga	3,9	26,9423	38,8421	0	149	0,1	-0,1
Alsancak P.	6,8	27,1387	38,4464	0	214	0,1	0,0
Cesme	10	26,2879	38,3288	0	148	0,1	-0,1
Kusadasi	3,5	27,2588	37,8668	0	185	0,2	-0,3
Didim	3,7	27,2615	37,3329	0	233	0,2	-0,2
Bodrum	6,7	27,4242	37,0228	0	14	0,7	-0,7
Marmaris	1,9	28,3271	36,8107	0	146	0,3	-0,5
Fethiye	11,7	28,9502	36,7235	5	18	0,3	-0,3
Fethiye Bay	4,2	29,0546	36,6537	4	122	0,4	-0,5
Kas	10,8	29,6436	36,1965	10	35	0,6	-0,6
Finike	5,3	30,1554	36,3	18	75	0,6	-0,7
Kemer	0	30,5728	36,6052	0	0	0,0	0,0
Antalya B.	10,8	30,6123	36,8362	31	63	0,1	-0,1
Alanya	10	31,9911	36,5243	32	64	0,1	-0,1
Karatas	2,1	35,3872	36,5604	116	221	0,2	-0,1
Anamur	7,2	32,8582	36,0565	45	149	0,1	-0,1
Iskenderun B.	2,5	36,1898	36,6046	142	169	0,1	0,0
Arsuz	3,2	35,8965	36,4272	116	219	0,1	0,0
Samandag	7,9	35,9564	36,0549	97	107	0,1	0,0

A.3.7. Simulation of Source s08-Z11-2

Table A.3.13: Rupture Parameters of Tsunami Source 08-Z11-2

Rupture Parameters			
Epicenter of fault axis	25.32E 36.48N	Dip angle (deg.)	45
Length of fault (km)	82.6	Slip angle (deg.)	45
Strike angle (deg. CW)	60	Fdisplacement (m)	6
Width of fault (km)	40	Maximum (+)ve amp. (m)	1.2
Focal depth (km)	30	Minimum (-)ve amp. (m)	-0.2

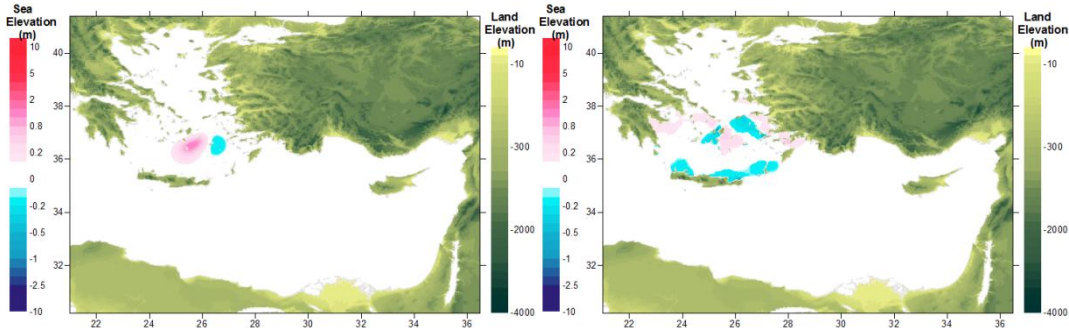


Figure A.3.13: The location of tsunami source 08-Z11-2 (left) and the distributions of wave at t=1hr(right) in the study domain (Eastern Mediterranean) in the duration of simulation (4 hours) for the tsunami source 08-Z11-2

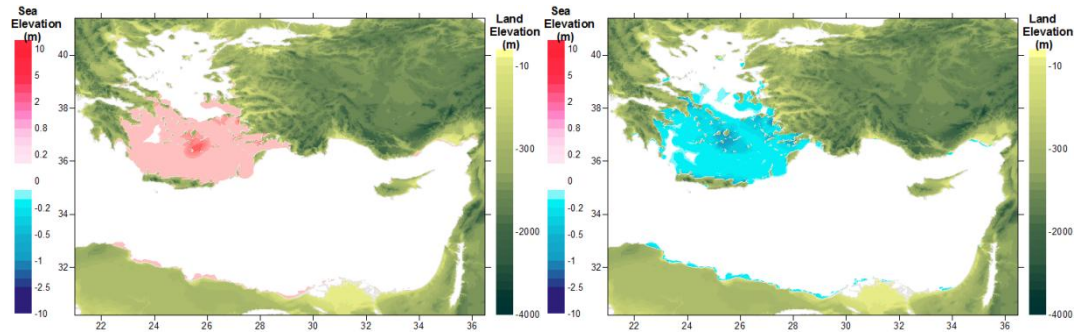


Figure A.3.14: The distributions of maximum positive of the water elevations(left) and negative water elevations(right) in the in the study domain (Eastern Mediterranean) in the duration of simulation (4 hours) for the tsunami source 08-Z11-2

Table A.3.14: Summary Results of tsunami impact at forecast points for source 08-Z11-2

Name of gauge pt.	Depth of gauge pt.(m)	Longitude	Lattitude	Arrival time of initial wave (min)	Arrival time of max.wave (min)	Maximum (+)ve amp.(m)	Maximum (-)ve amp.(m)
Gokceada	0,4	25,9006	40,2379	110	184	0,0	0,0
Mentes	7,4	26,7374	38,434	0	181	0,1	0,0
Bodrum	8,4	27,4171	37,0193	0	216	0,5	-0,4
Aksaz	4,7	28,4313	36,8453	25	112	0,5	-0,6
Girne	1,1	33,3276	35,3493	81	110	0,1	0,0
Gazimagusa	7,1	33,9468	35,1367	105	167	0,1	0,0
Tasucu	3,5	33,8327	36,2664	102	208	0,2	-0,1
Erdemli	2,9	34,2629	36,57	113	143	0,1	0,0
Canakkale	2,5	26,3772	40,1043	120	172	0,1	-0,1
Aliaga	3,9	26,9423	38,8421	58	126	0,1	-0,1
Alsancak P.	6,8	27,1387	38,4464	11	235	0,1	0,0
Cesme	10	26,2879	38,3288	0	131	0,1	-0,2
Kusadasi	3,5	27,2588	37,8668	0	84	0,3	-0,3
Didim	3,7	27,2615	37,3329	0	239	0,3	-0,3
Bodrum	6,7	27,4242	37,0228	0	216	0,6	-0,4
Marmaris	1,9	28,3271	36,8107	21	67	0,3	-0,3
Fethiye	11,7	28,9502	36,7235	32	73	0,2	-0,2
Fethiye Bay	4,2	29,0546	36,6537	31	121	0,2	-0,2
Kas	10,8	29,6436	36,1965	31	139	0,1	-0,1
Finike	5,3	30,1554	36,3	40	178	0,1	-0,2
Kemer	0	30,5728	36,6052	0	0	0,0	0,0
Antalya B.	10,8	30,6123	36,8362	57	89	0,1	-0,1
Alanya	10	31,9911	36,5243	60	89	0,1	0,0
Karatas	2,1	35,3872	36,5604	150	180	0,1	-0,1
Anamur	7,2	32,8582	36,0565	74	103	0,1	-0,1
Iskenderun B.	2,5	36,1898	36,6046	177	201	0,1	0,0
Arsuz	3,2	35,8965	36,4272	150	177	0,1	0,0
Samandag	7,9	35,9564	36,0549	128	157	0,1	0,0

A.3.8. Simulation of Source s09-Z11-3

Table A.3.15: Rupture Parameters of Tsunami Source 09-Z11-3

Rupture Parameters			
Epicenter of fault axis	24.6E 38N	Dip angle (deg.)	45
Length of fault (km)	146.7	Slip angle (deg.)	45
Strike angle (deg. CW)	150	Fdisplacement (m)	6
Focal depth (km)	30	Maximum (+)ve amp. (m)	1.1
Width of fault (km)	30	Minimum (-)ve amp. (m)	-0.2

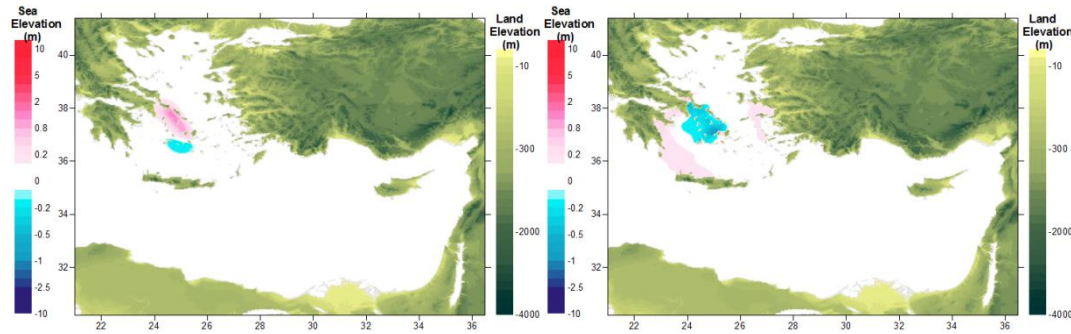


Figure A.3.15: The location of tsunami source 09-Z11-3 (left) and the distributions of wave at t=1hr(right) in the study domain (Eastern Mediterranean) in the duration of simulation (4 hours) for the tsunami source 09-Z11-3

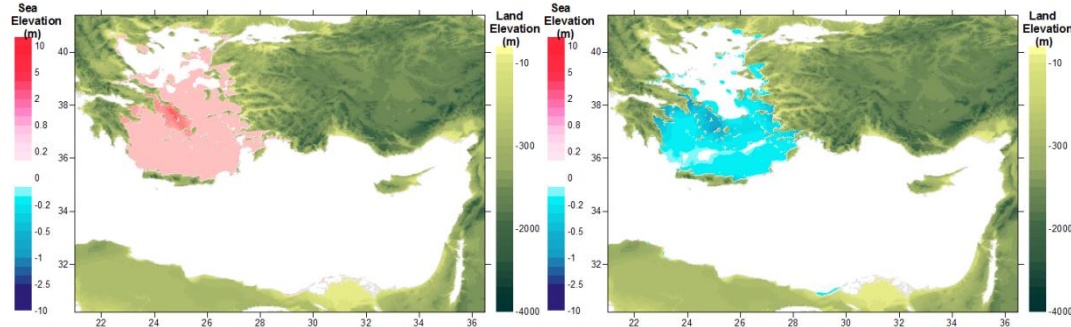


Figure A.3.16: The distributions of maximum positive of the water elevations(left) and negative water elevations(right) in the in the study domain (Eastern Mediterranean) in the duration of simulation (4 hours) for the tsunami source 09-Z11-3

Table A.3.16: Summary Results of tsunami impact at forecast points for source 09-Z11-3

Name of gauge pt.	Depth of gauge pt.(m)	Longitude	Latitude	Arrival time of initial wave (min)	Arrival time of max.wave (min)	Maximum (+)ve amp.(m)	Maximum (-)ve amp.(m)
Gokceada	0,4	25,9006	40,2379	75	125	0,1	0,0
Mentes	7,4	26,7374	38,434	68	118	0,2	-0,2
Bodrum	8,4	27,4171	37,0193	0	132	0,2	-0,3
Aksaz	4,7	28,4313	36,8453	31	204	0,2	-0,2
Girne	1,1	33,3276	35,3493	84	167	0,0	0,0
Gazimagusa	7,1	33,9468	35,1367	131	224	0,0	0,0
Tasucu	3,5	33,8327	36,2664	112	175	0,0	0,0
Erdemli	2,9	34,2629	36,57	125	199	0,0	0,0
Canakkale	2,5	26,3772	40,1043	109	125	0,1	-0,1
Aliaga	3,9	26,9423	38,8421	52	103	0,2	-0,1
Alsancak P.	6,8	27,1387	38,4464	122	155	0,2	-0,3
Cesme	10	26,2879	38,3288	7	196	0,4	-0,2
Kusadasi	3,5	27,2588	37,8668	18	76	0,4	-0,5
Didim	3,7	27,2615	37,3329	0	97	0,2	-0,3
Bodrum	6,7	27,4242	37,0228	0	133	0,2	-0,3
Marmaris	1,9	28,3271	36,8107	27	198	0,1	-0,1
Fethiye	11,7	28,9502	36,7235	35	203	0,1	-0,1
Fethiye Bay	4,2	29,0546	36,6537	40	205	0,1	-0,1
Kas	10,8	29,6436	36,1965	33	128	0,0	0,0
Finike	5,3	30,1554	36,3	50	132	0,0	0,0
Kemer	0	30,5728	36,6052	0	0	0,0	0,0
Antalya B.	10,8	30,6123	36,8362	67	146	0,0	0,0
Alanya	10	31,9911	36,5243	70	147	0,0	0,0
Karatas	2,1	35,3872	36,5604	163	234	0,1	0,0
Anamur	7,2	32,8582	36,0565	87	158	0,0	0,0
Iskenderun B.	2,5	36,1898	36,6046	191	0	0,0	0,0
Arsuz	3,2	35,8965	36,4272	162	232	0,0	0,0
Samandag	7,9	35,9564	36,0549	140	224	0,1	0,0

A.3.9. Simulation of Source s10-Z12-1

Table A.3.17: Rupture Parameters of Tsunami Source 10-Z12-1

Rupture Parameters			
Epicenter of fault axis	25.7E 35.39N	Dip angle (deg.)	45
Length of fault (km)	143	Slip angle (deg.)	45
Strike angle (deg. CW)	330	Fdisplacement (m)	6
Focal depth (km)	40	Maximum (+)ve amp. (m)	0.9
Width of fault (km)	30	Minimum (-)ve amp. (m)	-0.1

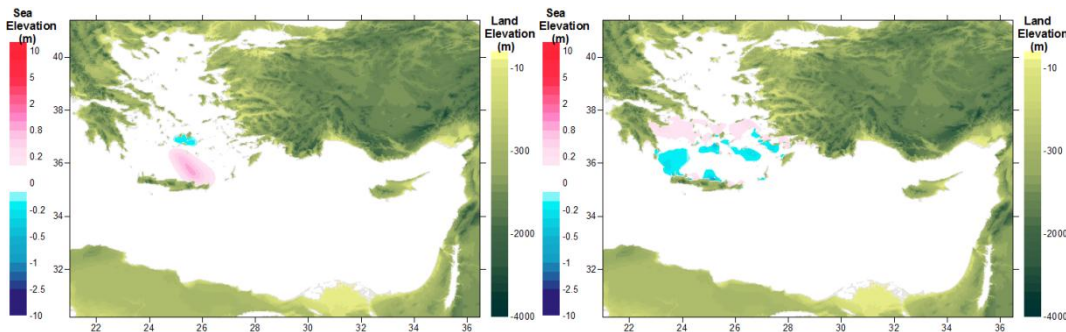


Figure A.3.17: The location of tsunami source 10-Z12-1 (left) and the distributions of wave at t=1hr(right) in the study domain (Eastern Mediterranean) in the duration of simulation (4 hours) for the tsunami source 10-Z12-1

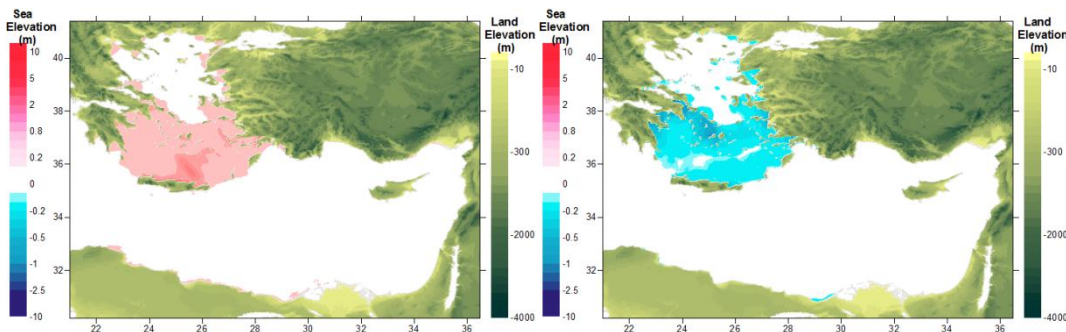


Figure A.3.18: The distributions maximum positive(left) and negative water elevations(right) in the study domain (Eastern Mediterranean) in the duration of simulation (4 hours) for the tsunami source 10-Z12-1

Table A.3.18: Summary Results of tsunami impact at forecast points for source 10-Z12-1

Name of gauge pt.	Depth of gauge pt.(m)	Longitude	Latitude	Arrival time of initial wave (min)	Arrival time of max.wave (min)	Maximum (+)ve amp.(m)	Maximum (-)ve amp.(m)
Gokceada	0,4	25,9006	40,2379	106	192	0,1	0,0
Mentes	7,4	26,7374	38,434	84	173	0,1	-0,1
Bodrum	8,4	27,4171	37,0193	18	183	0,9	-0,7
Aksaz	4,7	28,4313	36,8453	43	205	0,6	-0,6
Girne	1,1	33,3276	35,3493	73	193	0,0	0,0
Gazimagusa	7,1	33,9468	35,1367	96	154	0,0	0,0
Tasucu	3,5	33,8327	36,2664	98	193	0,1	-0,1
Erdemli	2,9	34,2629	36,57	108	200	0,1	-0,1
Canakkale	2,5	26,3772	40,1043	119	201	0,1	-0,2
Aliaga	3,9	26,9423	38,8421	69	159	0,2	-0,1
Alsancak P.	6,8	27,1387	38,4464	131	215	0,2	-0,1
Cesme	10	26,2879	38,3288	29	145	0,2	-0,2
Kusadasi	3,5	27,2588	37,8668	30	106	0,3	-0,4
Didim	3,7	27,2615	37,3329	21	205	0,3	-0,3
Bodrum	6,7	27,4242	37,0228	19	183	1,1	-0,9
Marmaris	1,9	28,3271	36,8107	42	189	0,4	-0,3
Fethiye	11,7	28,9502	36,7235	39	208	0,2	-0,2
Fethiye Bay	4,2	29,0546	36,6537	37	203	0,2	-0,2
Kas	10,8	29,6436	36,1965	37	237	0,1	-0,1
Finike	5,3	30,1554	36,3	44	237	0,2	-0,2
Kemer	0	30,5728	36,6052	0	0	0,0	0,0
Antalya B.	10,8	30,6123	36,8362	57	78	0,0	-0,1
Alanya	10	31,9911	36,5243	59	226	0,1	0,0
Karatas	2,1	35,3872	36,5604	144	163	0,1	-0,1
Anamur	7,2	32,8582	36,0565	69	184	0,1	0,0
Iskenderun B.	2,5	36,1898	36,6046	169	195	0,1	0,0
Arsuz	3,2	35,8965	36,4272	143	167	0,1	0,0
Samandag	7,9	35,9564	36,0549	121	147	0,1	0,0

A.3.10. Simulation of Source s11-Z12-2

Table A.3.19: Rupture Parameters of Tsunami Source 11-Z12-2

Rupture Parameters			
Epicenter of fault axis	24.7E 36.45N	Dip angle (deg.)	45
Length of fault (km)	146.5	Slip angle (deg.)	45
Strike angle (deg. CW)	330	Fdisplacement (m)	6
Focal depth (km)	40	Maximum (+)ve amp. (m)	0.9
Width of fault (km)	30	Minimum (-)ve amp. (m)	-0.1

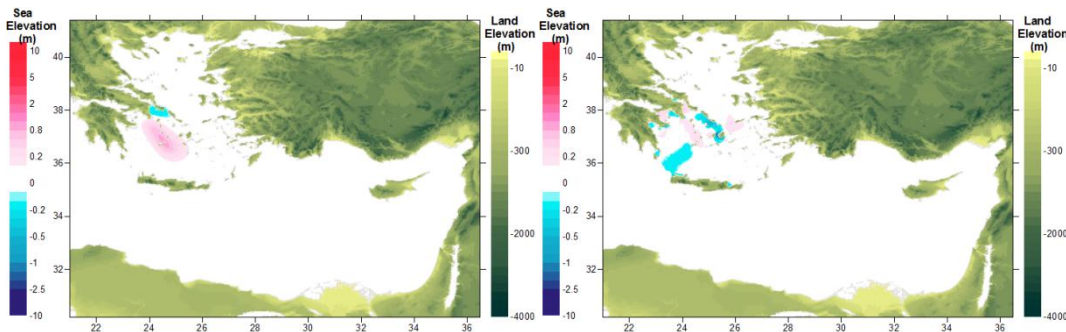


Figure A.3.19: The location of tsunami source 11-Z12-2 (left) and the distributions of wave at t=1hr(right) in the study domain (Eastern Mediterranean) in the duration of simulation (4 hours) for the tsunami source 11-Z12-2

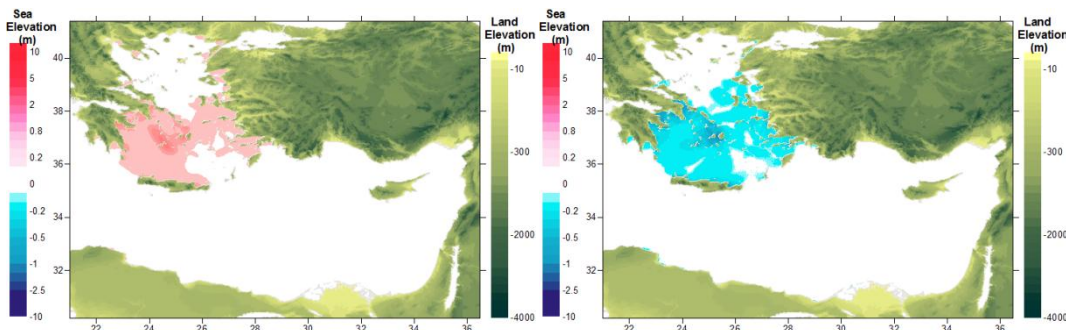


Figure A.3.20: The distributions maximum positive(left) and negative water elevations(right) in the study domain (Eastern Mediterranean) in the duration of simulation (4 hours) for the tsunami source 11-Z12-2

Table A.3.20: Summary Results of tsunami impact at forecast points for source 11-Z12-2

Name of gauge pt.	Depth of gauge pt.(m)	Longitude	Latitude	Arrival time of initial wave (min)	Arrival time of max.wave (min)	Maximum (+)ve amp.(m)	Maximum (-)ve amp.(m)
Gokceada	0,4	25,9006	40,2379	66	160	0,1	0,0
Mentes	7,4	26,7374	38,434	68	201	0,1	0,0
Bodrum	8,4	27,4171	37,0193	49	213	0,4	-0,3
Aksaz	4,7	28,4313	36,8453	65	173	0,2	-0,2
Girne	1,1	33,3276	35,3493	101	216	0,0	0,0
Gazimagusa	7,1	33,9468	35,1367	128	170	0,0	0,0
Tasucu	3,5	33,8327	36,2664	127	220	0,0	0,0
Erdemli	2,9	34,2629	36,57	138	233	0,0	0,0
Canakkale	2,5	26,3772	40,1043	94	239	0,2	-0,1
Aliaga	3,9	26,9423	38,8421	52	131	0,2	-0,2
Alsancak P.	6,8	27,1387	38,4464	111	231	0,2	-0,1
Cesme	10	26,2879	38,3288	25	126	0,1	-0,2
Kusadasi	3,5	27,2588	37,8668	31	101	0,4	-0,4
Didim	3,7	27,2615	37,3329	65	121	0,2	-0,3
Bodrum	6,7	27,4242	37,0228	49	213	0,4	-0,3
Marmaris	1,9	28,3271	36,8107	62	171	0,2	-0,1
Fethiye	11,7	28,9502	36,7235	64	173	0,1	-0,1
Fethiye Bay	4,2	29,0546	36,6537	63	174	0,1	-0,1
Kas	10,8	29,6436	36,1965	61	173	0,0	0,0
Finike	5,3	30,1554	36,3	70	236	0,0	-0,1
Kemer	0	30,5728	36,6052	0	0	0,0	0,0
Antalya B.	10,8	30,6123	36,8362	84	192	0,0	0,0
Alanya	10	31,9911	36,5243	88	98	0,0	0,0
Karatas	2,1	35,3872	36,5604	174	192	0,1	0,0
Anamur	7,2	32,8582	36,0565	97	108	0,0	0,0
Iskenderun B.	2,5	36,1898	36,6046	200	232	0,1	0,0
Arsuz	3,2	35,8965	36,4272	173	216	0,0	0,0
Samandag	7,9	35,9564	36,0549	152	167	0,0	0,0

A.3.11. Simulation of Source s12-Z14

Table A.3.21: Rupture Parameters of Tsunami Source 12-Z14

Rupture Parameters			
Epicenter of fault axis	25.7E 37.97N	Dip angle (deg.)	45
Length of fault (km)	65.3	Slip angle (deg.)	45
Strike angle (deg. CW)	5	Fdisplacement (m)	6
Focal depth (km)	20	Maximum (+)ve amp. (m)	1.3
Width of fault (km)	30	Minimum (-)ve amp. (m)	-0.2

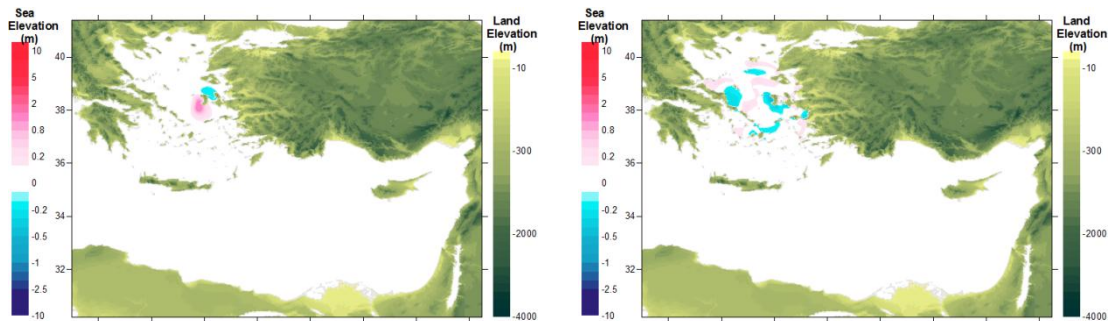


Figure A.3.21: The location of tsunami source 12-Z14 (left) and the distributions of wave at t=1hr(right) in the study domain (Eastern Mediterranean) in the duration of simulation (4 hours) for the tsunami source 12-Z14

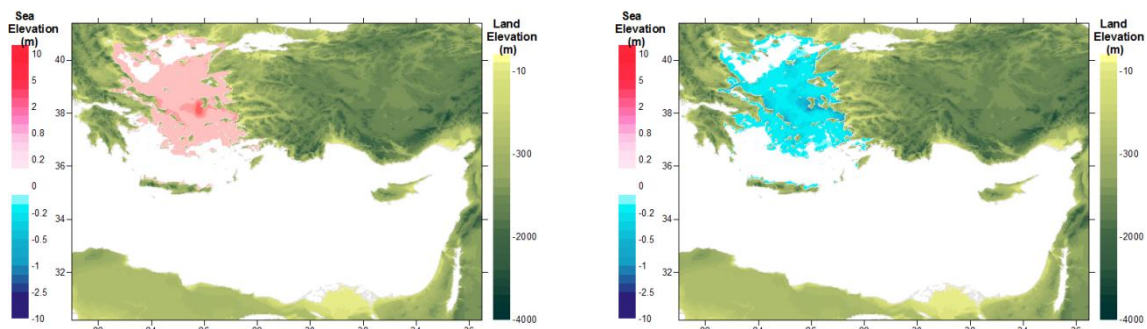


Figure A.3.22: The distributions maximum positive(left) and negative water elevations(right) in the study domain (Eastern Mediterranean) in the duration of simulation (4 hours) for the tsunami source 12-Z14

Table A.3.22: Summary Results of tsunami impact at forecast points for source 12-Z14

Name of gauge pt.	Depth of gauge pt.(m)	Longitude	Latitude	Arrival time of initial wave (min)	Arrival time of max.wave (min)	Maximum (+)ve amp.(m)	Maximum (-)ve amp.(m)
Gokceada	0,4	25,9006	40,2379	37	122	0,1	-0,1
Mentes	7,4	26,7374	38,434	0	128	0,3	-0,3
Bodrum	8,4	27,4171	37,0193	59	219	0,2	-0,2
Aksaz	4,7	28,4313	36,8453	86	171	0,1	-0,1
Girne	1,1	33,3276	35,3493	136	136	0,0	0,0
Gazimagusa	7,1	33,9468	35,1367	167	167	0,0	0,0
Tasucu	3,5	33,8327	36,2664	163	240	0,0	0,0
Erdemli	2,9	34,2629	36,57	175	188	0,0	0,0
Canakkale	2,5	26,3772	40,1043	49	199	0,3	-0,4
Aliaga	3,9	26,9423	38,8421	0	233	0,4	-0,3
Alsancak P.	6,8	27,1387	38,4464	0	163	0,4	-0,4
Cesme	10	26,2879	38,3288	0	147	0,7	-0,7
Kusadasi	3,5	27,2588	37,8668	17	40	0,7	-0,7
Didim	3,7	27,2615	37,3329	50	232	0,2	-0,3
Bodrum	6,7	27,4242	37,0228	59	150	0,2	-0,2
Marmaris	1,9	28,3271	36,8107	82	150	0,0	-0,1
Fethiye	11,7	28,9502	36,7235	94	170	0,0	0,0
Fethiye Bay	4,2	29,0546	36,6537	95	176	0,0	0,0
Kas	10,8	29,6436	36,1965	94	166	0,0	0,0
Finike	5,3	30,1554	36,3	104	238	0,0	0,0
Kemer	0	30,5728	36,6052	0	0	0,0	0,0
Antalya B.	10,8	30,6123	36,8362	119	201	0,0	0,0
Alanya	10	31,9911	36,5243	123	203	0,0	0,0
Karatas	2,1	35,3872	36,5604	211	215	0,0	0,0
Anamur	7,2	32,8582	36,0565	132	132	0,0	0,0
Iskenderun B.	2,5	36,1898	36,6046	239	240	0,0	0,0
Arsuz	3,2	35,8965	36,4272	211	214	0,0	0,0
Samandag	7,9	35,9564	36,0549	190	203	0,0	0,0

A.3.12. Simulation of Source s13-Z15-1

Table A.3.23: Rupture Parameters of Tsunami Source 13-Z15-1

Rupture Parameters			
Epicenter of fault axis	26.2E 38.69N	Dip angle (deg.)	45
Length of fault (km)	52.3	Slip angle (deg.)	45
Strike angle (deg. CW)	85	Fdisplacement (m)	6
Focal depth (km)	15	Maximum (+)ve amp. (m)	1.0
Width of fault (km)	15	Minimum (-)ve amp. (m)	-0.1

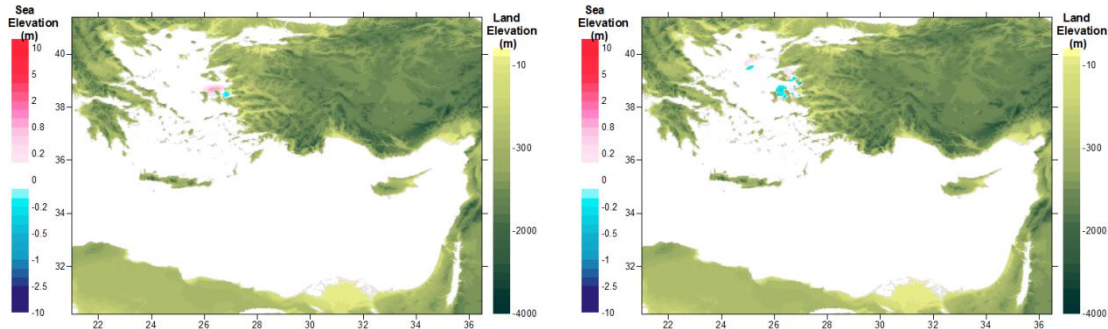


Figure A.3.23: The location of tsunami source 13-Z15-1 (left) and the distributions of wave at t=1hr(right) in the study domain (Eastern Mediterranean) in the duration of simulation (4 hours) for the tsunami source 13-Z15-1

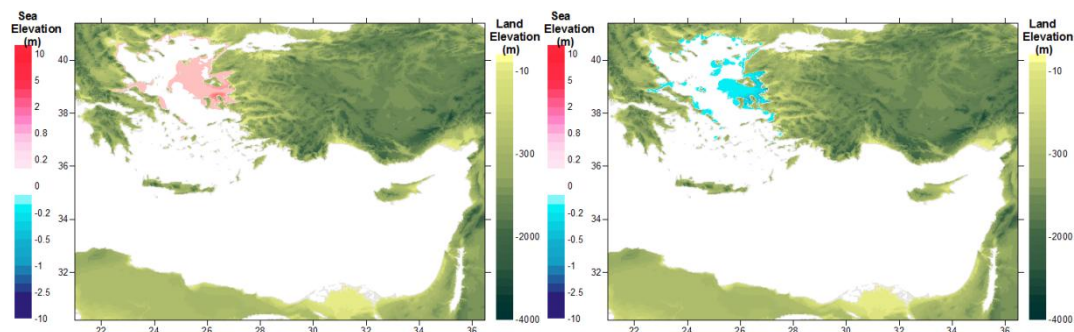


Figure A.3.24: The distributions maximum positive(left) and negative water elevations(right) in the study domain (Eastern Mediterranean) in the duration of simulation (4 hours) for the tsunami source 13-Z15-1

Table A.3.24: Summary Results of tsunami impact at forecast points for source 13-Z15-1

Name of gauge pt.	Depth of gauge pt.(m)	Longitude	Latitude	Arrival time of initial wave (min)	Arrival time of max.wave (min)	Maximum (+)ve amp.(m)	Maximum (-)ve amp.(m)
Gokceada	0,4	25,9006	40,2379	37	122	0,1	-0,1
Mentes	7,4	26,7374	38,434	0	128	0,3	-0,3
Bodrum	8,4	27,4171	37,0193	59	219	0,2	-0,2
Aksaz	4,7	28,4313	36,8453	86	171	0,1	-0,1
Girne	1,1	33,3276	35,3493	136	136	0,0	0,0
Gazimagusa	7,1	33,9468	35,1367	167	167	0,0	0,0
Tasucu	3,5	33,8327	36,2664	163	240	0,0	0,0
Erdemli	2,9	34,2629	36,57	175	188	0,0	0,0
Canakkale	2,5	26,3772	40,1043	49	199	0,3	-0,4
Aliaga	3,9	26,9423	38,8421	0	233	0,4	-0,3
Alsancak P.	6,8	27,1387	38,4464	0	163	0,4	-0,4
Cesme	10	26,2879	38,3288	0	147	0,7	-0,7
Kusadasi	3,5	27,2588	37,8668	17	40	0,7	-0,7
Didim	3,7	27,2615	37,3329	50	232	0,2	-0,3
Bodrum	6,7	27,4242	37,0228	59	150	0,2	-0,2
Marmaris	1,9	28,3271	36,8107	82	150	0,0	-0,1
Fethiye	11,7	28,9502	36,7235	94	170	0,0	0,0
Fethiye Bay	4,2	29,0546	36,6537	95	176	0,0	0,0
Kas	10,8	29,6436	36,1965	94	166	0,0	0,0
Finike	5,3	30,1554	36,3	104	238	0,0	0,0
Kemer	0	30,5728	36,6052	0	0	0,0	0,0
Antalya B.	10,8	30,6123	36,8362	119	201	0,0	0,0
Alanya	10	31,9911	36,5243	123	203	0,0	0,0
Karatas	2,1	35,3872	36,5604	211	215	0,0	0,0
Anamur	7,2	32,8582	36,0565	132	132	0,0	0,0
Iskenderun B.	2,5	36,1898	36,6046	239	240	0,0	0,0
Arsuz	3,2	35,8965	36,4272	211	214	0,0	0,0
Samandag	7,9	35,9564	36,0549	190	203	0,0	0,0

A.3.13. Simulation of Source s14-Z15-2

Table A.3.25: Rupture Parameters of Tsunami Source 14-Z15-2

Rupture Parameters			
Epicenter of fault axis	25.25E 38.53N	Dip angle (deg.)	45
Length of fault (km)	94	Slip angle (deg.)	45
Strike angle (deg. CW)	60	Fdisplacement (m)	6
Focal depth (km)	15	Maximum (+)ve amp. (m)	1.0
Width of fault (km)	15	Minimum (-)ve amp. (m)	-0.2

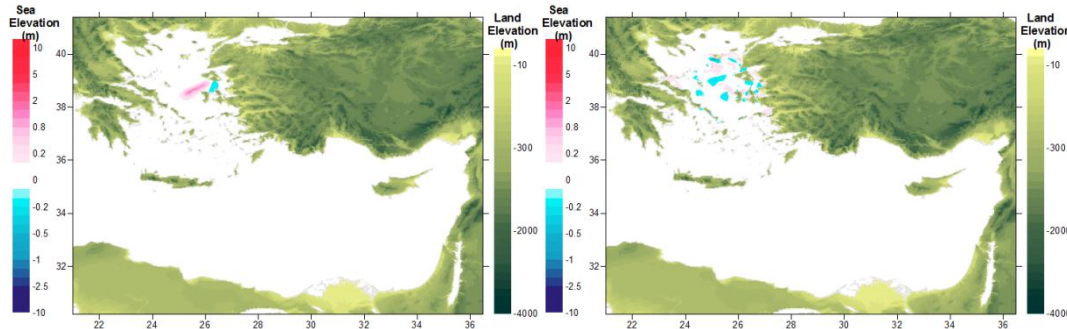


Figure A.3.25: The location of tsunami source 14-Z15-2 (left) and the distributions of wave at $t=1\text{hr}$ (right) in the study domain (Eastern Mediterranean) in the duration of simulation (4 hours) for the tsunami source 14-Z15-2

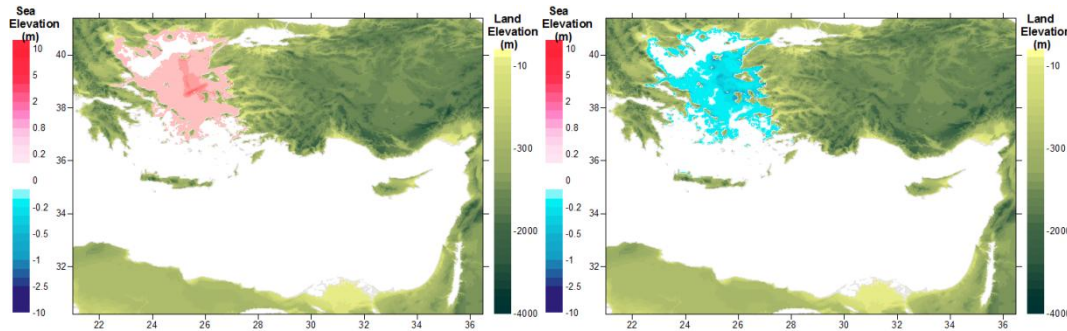


Figure A.3.26: The distributions maximum positive(left) and negative water elevations(right) in the study domain (Eastern Mediterranean) in the duration of simulation (4 hours) for the tsunami source 14-Z15-2

Table A.3.26: Summary Results of tsunami impact at forecast points for source 14-Z15-2

Name of gauge pt.	Depth of gauge pt.(m)	Longitude	Latitude	Arrival time of initial wave (min)	Arrival time of max.wave (min)	Maximum (+)ve amp.(m)	Maximum (-)ve amp.(m)
Gokceada	0,4	25,9006	40,2379	55	171	0,1	-0,1
Mentes	7,4	26,7374	38,434	0	108	0,3	-0,3
Bodrum	8,4	27,4171	37,0193	86	141	0,1	-0,1
Aksaz	4,7	28,4313	36,8453	112	217	0,1	-0,1
Girne	1,1	33,3276	35,3493	162	162	0,0	0,0
Gazimagusa	7,1	33,9468	35,1367	193	193	0,0	0,0
Tasucu	3,5	33,8327	36,2664	189	189	0,0	0,0
Erdemli	2,9	34,2629	36,57	202	202	0,0	0,0
Canakkale	2,5	26,3772	40,1043	7	101	0,3	-0,4
Aliaga	3,9	26,9423	38,8421	0	116	0,5	-0,5
Alsancak P.	6,8	27,1387	38,4464	45	103	0,3	-0,4
Cesme	10	26,2879	38,3288	0	89	0,4	-0,5
Kusadasi	3,5	27,2588	37,8668	32	66	0,3	-0,3
Didim	3,7	27,2615	37,3329	78	91	0,1	-0,1
Bodrum	6,7	27,4242	37,0228	87	142	0,1	-0,2
Marmaris	1,9	28,3271	36,8107	109	215	0,0	0,0
Fethiye	11,7	28,9502	36,7235	118	171	0,0	0,0
Fethiye Bay	4,2	29,0546	36,6537	116	171	0,0	0,0
Kas	10,8	29,6436	36,1965	117	117	0,0	0,0
Finike	5,3	30,1554	36,3	127	207	0,0	0,0
Kemer	0	30,5728	36,6052	0	0	0,0	0,0
Antalya B.	10,8	30,6123	36,8362	144	144	0,0	0,0
Alanya	10	31,9911	36,5243	148	148	0,0	0,0
Karatas	2,1	35,3872	36,5604	238	240	0,0	0,0
Anamur	7,2	32,8582	36,0565	158	158	0,0	0,0
Iskenderun B.	2,5	36,1898	36,6046	0	0	0,0	0,0
Arsuz	3,2	35,8965	36,4272	238	238	0,0	0,0
Samandag	7,9	35,9564	36,0549	216	216	0,0	0,0

A.3.14. Simulation of Source s15-Z17-1

Table A.3.27: Rupture Parameters of Tsunami Source 15-Z17-1

Rupture Parameters			
Epicenter of fault axis	23.7E 39.02N	Dip angle (deg.)	45
Length of fault (km)	97	Slip angle (deg.)	45
Strike angle (deg. CW)	120	Fdisplacement (m)	6
Focal depth (km)	10	Maximum (+)ve amp. (m)	2.0
Width of fault (km)	30	Minimum (-)ve amp. (m)	-0.3

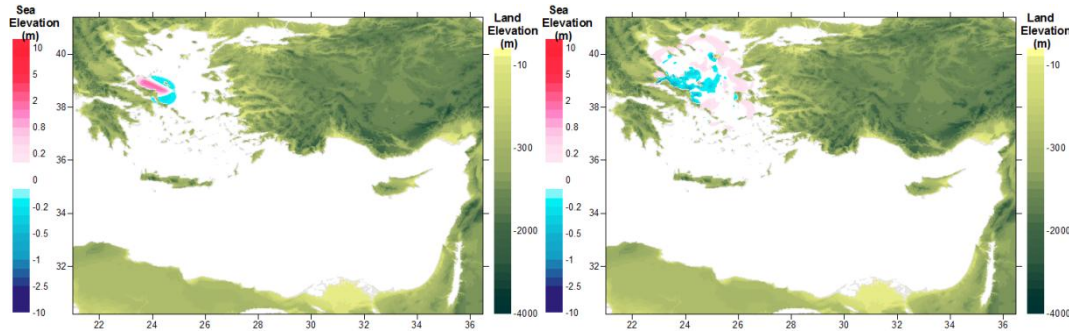


Figure A.3.27: The location of tsunami source 15-Z17-1 (left) and the distributions of wave at t=1hr(right) in the study domain (Eastern Mediterranean) in the duration of simulation (4 hours) for the tsunami source 15-Z17-1

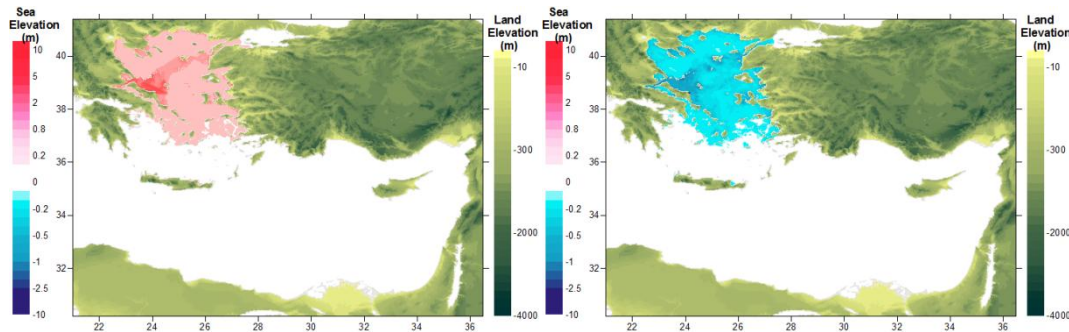


Figure A.3.27: The distributions maximum positive(left) and negative water elevations(right) in the study domain (Eastern Mediterranean) in the duration of simulation (4 hours) for the tsunami source 15-Z17-1

Table A.3.28: Summary Results of tsunami impact at forecast points for source 15-Z17-1

Name of gauge pt.	Depth of gauge pt.(m)	Longitude	Latitude	Arrival time of initial wave (min)	Arrival time of max.wave (min)	Maximum (+)ve amp.(m)	Maximum (-)ve amp.(m)
Gokceada	0,4	25,9006	40,2379	43	237	0,2	-0,1
Mentes	7,4	26,7374	38,434	0	109	0,4	-0,3
Bodrum	8,4	27,4171	37,0193	87	227	0,2	-0,2
Aksaz	4,7	28,4313	36,8453	111	235	0,0	0,0
Girne	1,1	33,3276	35,3493	185	185	0,0	0,0
Gazimagusa	7,1	33,9468	35,1367	215	215	0,0	0,0
Tasucu	3,5	33,8327	36,2664	212	212	0,0	0,0
Erdemli	2,9	34,2629	36,57	225	225	0,0	0,0
Canakkale	2,5	26,3772	40,1043	67	123	0,6	-0,8
Aliaga	3,9	26,9423	38,8421	0	101	0,5	-0,6
Alsancak P.	6,8	27,1387	38,4464	32	157	0,5	-0,4
Cesme	10	26,2879	38,3288	0	171	0,6	-0,7
Kusadasi	3,5	27,2588	37,8668	25	188	0,6	-0,6
Didim	3,7	27,2615	37,3329	68	144	0,1	-0,2
Bodrum	6,7	27,4242	37,0228	86	228	0,3	-0,3
Marmaris	1,9	28,3271	36,8107	107	226	0,0	0,0
Fethiye	11,7	28,9502	36,7235	121	225	0,0	0,0
Fethiye Bay	4,2	29,0546	36,6537	126	224	0,0	0,0
Kas	10,8	29,6436	36,1965	120	182	0,0	0,0
Finike	5,3	30,1554	36,3	131	219	0,0	0,0
Kemer	0	30,5728	36,6052	0	0	0,0	0,0
Antalya B.	10,8	30,6123	36,8362	167	167	0,0	0,0
Alanya	10	31,9911	36,5243	171	171	0,0	0,0
Karatas	2,1	35,3872	36,5604	0	0	0,0	0,0
Anamur	7,2	32,8582	36,0565	181	181	0,0	0,0
Iskenderun B.	2,5	36,1898	36,6046	0	0	0,0	0,0
Arsuz	3,2	35,8965	36,4272	0	0	0,0	0,0
Samandag	7,9	35,9564	36,0549	238	238	0,0	0,0

A.3.15. Simulation of Source s16-Z17-2

Table A.3.29: Rupture Parameters of Tsunami Source 16-Z17-2

Rupture Parameters			
Epicenter of fault axis	25E 39.4N	Dip angle (deg.)	45
Length of fault (km)	88	Slip angle (deg.)	45
Strike angle (deg. CW)	80	Fdisplacement (m)	6
Focal depth (km)	10	Maximum (+)ve amp. (m)	1.4
Width of fault (km)	15	Minimum (-)ve amp. (m)	-0.2

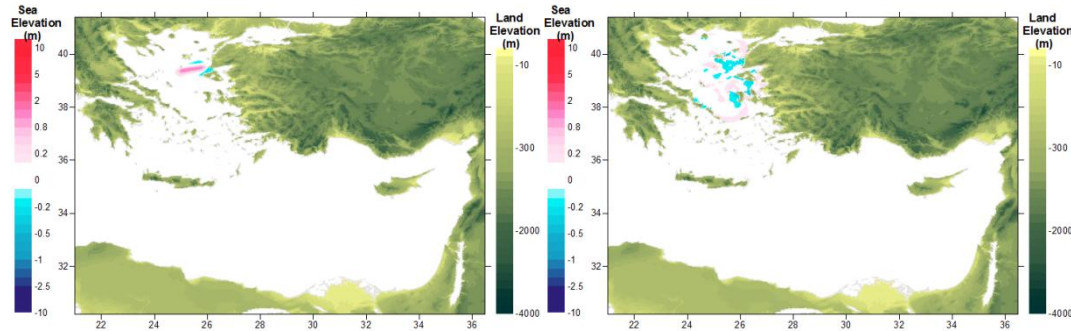


Figure A.3.29: The location of tsunami source 16-Z17-2 (left) and the distribution wave at t=1hr(right) in the study domain (Eastern Mediterranean) in the duration of simulation (4 hours) for the tsunami source 16-Z17-2

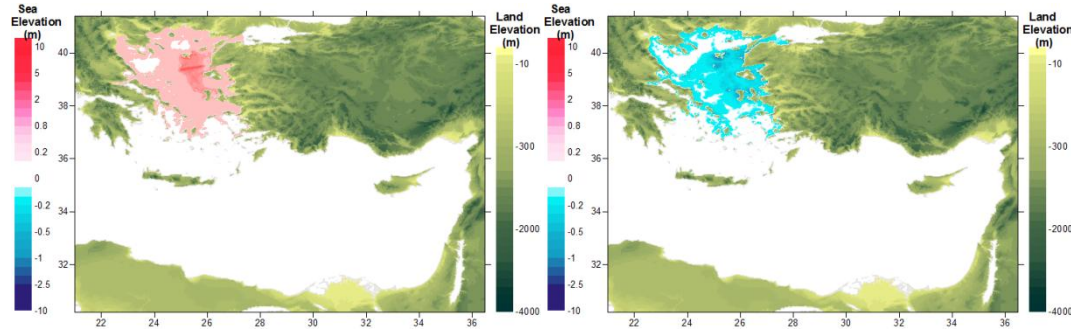


Figure A.3.30: The distributions of maximum positive of the water elevations(left) and negative water elevations(right) in the in the study domain (Eastern Mediterranean) in the duration of simulation (4 hours) for the tsunami source 16-Z17-2

Table A.3.30: Summary Results of tsunami impact at forecast points for source 16-Z17-2

Name of gauge pt.	Depth of gauge pt.(m)	Longitude	Lattitude	Arrival time of initial wave (min)	Arrival time of max.wave (min)	Maximum (+)ve amp.(m)	Maximum (-)ve amp.(m)
Gokceada	0,4	25,9006	40,2379	0	52	0,2	-0,2
Mentes	7,4	26,7374	38,434	49	236	0,3	-0,4
Bodrum	8,4	27,4171	37,0193	117	203	0,1	-0,2
Aksaz	4,7	28,4313	36,8453	144	144	0,0	0,0
Girne	1,1	33,3276	35,3493	193	193	0,0	0,0
Gazimagusa	7,1	33,9468	35,1367	232	232	0,0	0,0
Tasucu	3,5	33,8327	36,2664	221	221	0,0	0,0
Erdemli	2,9	34,2629	36,57	233	233	0,0	0,0
Canakkale	2,5	26,3772	40,1043	0	144	0,5	-0,6
Aliaga	3,9	26,9423	38,8421	33	146	0,4	-0,3
Alsancak P.	6,8	27,1387	38,4464	92	128	0,3	-0,4
Cesme	10	26,2879	38,3288	36	99	0,5	-0,6
Kusadasi	3,5	27,2588	37,8668	65	164	0,3	-0,4
Didim	3,7	27,2615	37,3329	101	124	0,1	-0,1
Bodrum	6,7	27,4242	37,0228	117	204	0,2	-0,2
Marmaris	1,9	28,3271	36,8107	140	209	0,0	0,0
Fethiye	11,7	28,9502	36,7235	149	198	0,0	0,0
Fethiye Bay	4,2	29,0546	36,6537	148	199	0,0	0,0
Kas	10,8	29,6436	36,1965	148	148	0,0	0,0
Finike	5,3	30,1554	36,3	158	206	0,0	0,0
Kemer	0	30,5728	36,6052	0	0	0,0	0,0
Antalya B.	10,8	30,6123	36,8362	176	176	0,0	0,0
Alanya	10	31,9911	36,5243	182	182	0,0	0,0
Karatas	2,1	35,3872	36,5604	0	0	0,0	0,0
Anamur	7,2	32,8582	36,0565	189	189	0,0	0,0
Iskenderun B.	2,5	36,1898	36,6046	0	0	0,0	0,0
Arsuz	3,2	35,8965	36,4272	0	0	0,0	0,0
Samandag	7,9	35,9564	36,0549	0	0	0,0	0,0

A.3.16. Simulation of Source s17-Z17-3

Table A.3.31: Rupture Parameters of Tsunami Source 17-Z17-3

Rupture Parameters			
Epicenter of fault axis	27.12E 38.91N	Dip angle (deg.)	45
Length of fault (km)	103.7	Slip angle (deg.)	45
Strike angle (deg. CW)	330	Fdisplacement (m)	6
Focal depth (km)	10	Maximum (+)ve amp. (m)	1.3
Width of fault (km)	15	Minimum (-)ve amp. (m)	-0.1

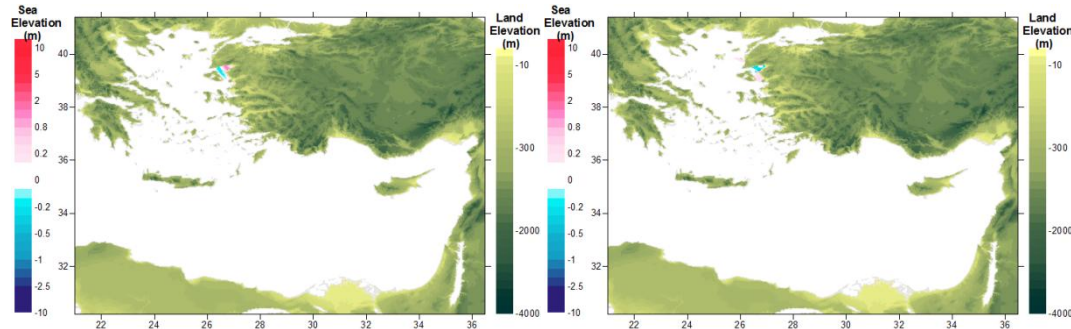


Figure A.3.31: The location of tsunami source 17-Z17-3 (left) and the distribution wave at t=1hr(right) in the study domain (Eastern Mediterranean) in the duration of simulation (4 hours) for the tsunami source 17-Z17-3

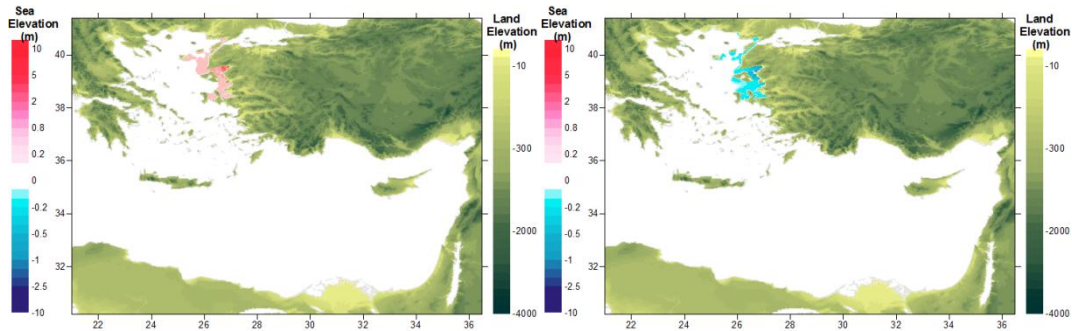


Figure A.3.32: The distributions of maximum positive of the water elevations(left) and negative water elevations(right) in the in the study domain (Eastern Mediterranean) in the duration of simulation (4 hours) for the tsunami source 17-Z17-3

Table A.3.32: Summary Results of tsunami impact at forecast points for source 17-Z17-3

Name of gauge pt.	Depth of gauge pt.(m)	Longitude	Latitude	Arrival time of initial wave (min)	Arrival time of max.wave (min)	Maximum (+)ve amp.(m)	Maximum (-)ve amp.(m)
Gokceada	0,4	25,9006	40,2379	0	107	0,0	0,0
Mentes	7,4	26,7374	38,434	32	125	0,2	-0,2
Bodrum	8,4	27,4171	37,0193	152	213	0,0	0,0
Aksaz	4,7	28,4313	36,8453	227	227	0,0	0,0
Girne	1,1	33,3276	35,3493	0	0	0,0	0,0
Gazimagusa	7,1	33,9468	35,1367	0	0	0,0	0,0
Tasucu	3,5	33,8327	36,2664	0	0	0,0	0,0
Erdemli	2,9	34,2629	36,57	0	0	0,0	0,0
Canakkale	2,5	26,3772	40,1043	0	106	0,1	-0,1
Aliaga	3,9	26,9423	38,8421	0	179	0,2	-0,3
Alsancak P.	6,8	27,1387	38,4464	74	165	0,3	-0,4
Cesme	10	26,2879	38,3288	36	224	0,2	-0,2
Kusadasi	3,5	27,2588	37,8668	91	153	0,1	-0,1
Didim	3,7	27,2615	37,3329	131	205	0,0	0,0
Bodrum	6,7	27,4242	37,0228	152	212	0,0	0,0
Marmaris	1,9	28,3271	36,8107	223	223	0,0	0,0
Fethiye	11,7	28,9502	36,7235	239	239	0,0	0,0
Fethiye Bay	4,2	29,0546	36,6537	0	0	0,0	0,0
Kas	10,8	29,6436	36,1965	238	238	0,0	0,0
Finike	5,3	30,1554	36,3	0	0	0,0	0,0
Kemer	0	30,5728	36,6052	0	0	0,0	0,0
Antalya B.	10,8	30,6123	36,8362	0	0	0,0	0,0
Alanya	10	31,9911	36,5243	0	0	0,0	0,0
Karatas	2,1	35,3872	36,5604	0	0	0,0	0,0
Anamur	7,2	32,8582	36,0565	0	0	0,0	0,0
Iskenderun B.	2,5	36,1898	36,6046	0	0	0,0	0,0
Arsuz	3,2	35,8965	36,4272	0	0	0,0	0,0
Samandag	7,9	35,9564	36,0549	0	0	0,0	0,0

A.3.17. Simulation of Source s18-Z22

Table A.3.33: Rupture Parameters of Tsunami Source 18-Z22

Rupture Parameters			
Epicenter of fault axis	26.36E 37.64N	Dip angle (deg.)	45
Length of fault (km)	103.7	Slip angle (deg.)	45
Strike angle (deg. CW)	95	Fdisplacement (m)	6
Focal depth (km)	20	Maximum (+)ve amp. (m)	1.4
Width of fault (km)	30	Minimum (-)ve amp. (m)	-0.2

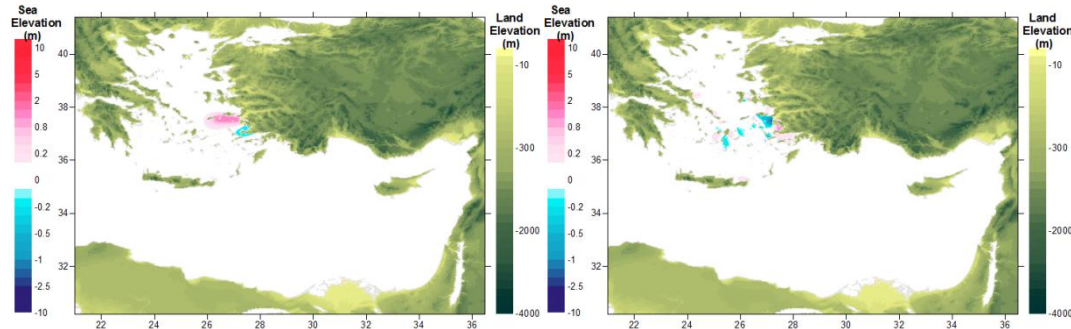


Figure A.3.33: The location of tsunami source 18-Z22 (left) and the distribution wave at t=1hr(right) in the study domain (Eastern Mediterranean) in the duration of simulation (4 hours) for the tsunami source 18-Z22

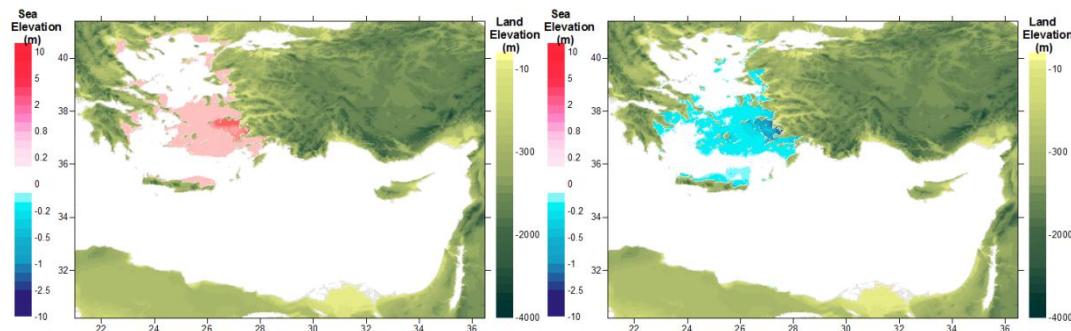


Figure A.3.34: The distributions of maximum positive of the water elevations(left) and negative water elevations(right) in the in the study domain (Eastern Mediterranean) in the duration of simulation (4 hours) for the tsunami source 18-Z22

Table A.3.34: Summary Results of tsunami impact at forecast points for source 18-Z22

Name of gauge pt.	Depth of gauge pt.(m)	Longitude	Latitude	Arrival time of initial wave (min)	Arrival time of max.wave (min)	Maximum (+)ve amp.(m)	Maximum (-)ve amp.(m)
Gokceada	0,4	25,9006	40,2379	100	162	0,1	0,0
Mentes	7,4	26,7374	38,434	0	123	0,1	-0,2
Bodrum	8,4	27,4171	37,0193	0	216	0,5	-0,6
Aksaz	4,7	28,4313	36,8453	0	152	0,2	-0,2
Girne	1,1	33,3276	35,3493	116	227	0,0	0,0
Gazimagusa	7,1	33,9468	35,1367	144	188	0,0	0,0
Tasucu	3,5	33,8327	36,2664	140	228	0,1	0,0
Erdemli	2,9	34,2629	36,57	151	238	0,0	0,0
Canakkale	2,5	26,3772	40,1043	125	158	0,1	-0,1
Aliaga	3,9	26,9423	38,8421	51	107	0,1	-0,1
Alsancak P.	6,8	27,1387	38,4464	0	162	0,2	-0,3
Cesme	10	26,2879	38,3288	0	86	0,3	-0,3
Kusadasi	3,5	27,2588	37,8668	0	50	0,6	-0,5
Didim	3,7	27,2615	37,3329	0	47	0,8	-0,8
Bodrum	6,7	27,4242	37,0228	0	216	0,6	-0,7
Marmaris	1,9	28,3271	36,8107	0	167	0,1	-0,1
Fethiye	11,7	28,9502	36,7235	21	163	0,1	-0,1
Fethiye Bay	4,2	29,0546	36,6537	18	162	0,1	-0,1
Kas	10,8	29,6436	36,1965	26	158	0,0	0,0
Finike	5,3	30,1554	36,3	55	162	0,1	-0,1
Kemer	0	30,5728	36,6052	0	0	0,0	0,0
Antalya B.	10,8	30,6123	36,8362	73	107	0,0	0,0
Alanya	10	31,9911	36,5243	98	106	0,0	0,0
Karatas	2,1	35,3872	36,5604	187	206	0,1	0,0
Anamur	7,2	32,8582	36,0565	88	212	0,0	0,0
Iskenderun B.	2,5	36,1898	36,6046	214	227	0,0	0,0
Arsuz	3,2	35,8965	36,4272	187	201	0,0	0,0
Samandag	7,9	35,9564	36,0549	166	179	0,0	0,0

A.3.18. Simulation of Source s19-Z24

Table A.3.35: Rupture Parameters of Tsunami Source 19-Z24

Rupture Parameters			
Epicenter of fault axis	28.18E 37.09N	Dip angle (deg.)	45
Lenth of fault (km)	103.7	Slip angle (deg.)	45
Strike angle (deg. CW)	240	Fdisplacement (m)	6
Focal depth (km)	40	Maximum (+)ve amp. (m)	0.3
Width of fault (km)	10	Minimum (-)ve amp. (m)	-0.1

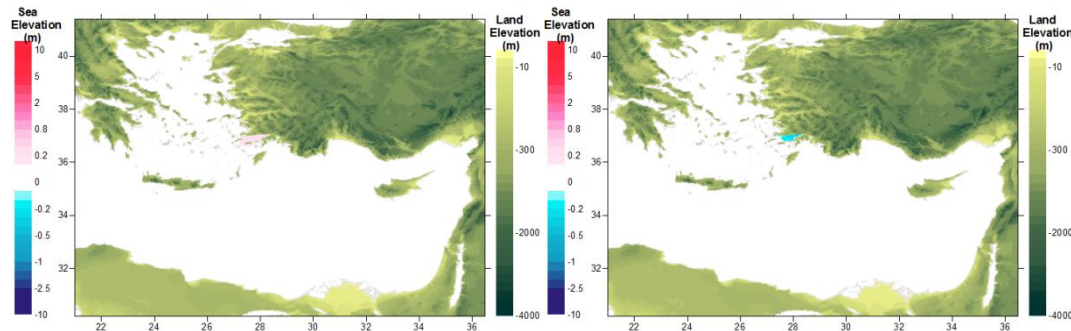


Figure A.3.35: The location of tsunami source 19-Z24 (left) and the distribution wave at t=1hr(right) in the study domain (Eastern Mediterranean) in the duration of simulation (4 hours) for the tsunami source 19-Z24

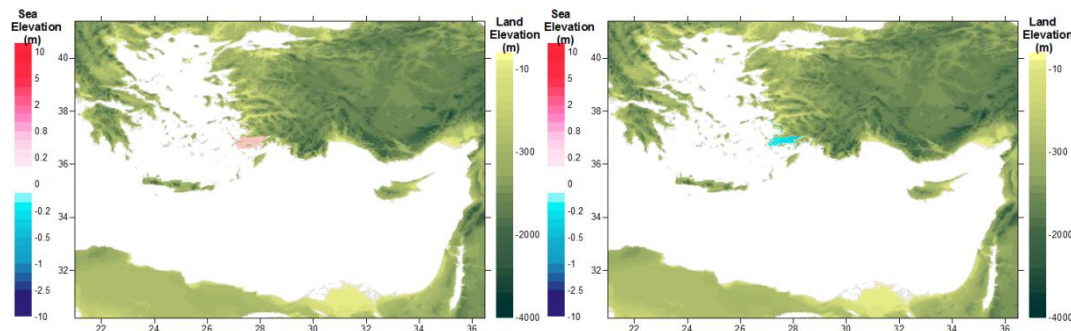


Figure A.3.36: The distributions of maximum positive of the water elevations(left) and negative water elevations(right) in the in the study domain (Eastern Mediterranean) in the duration of simulation (4 hours) for the tsunami source 19-Z24

Table A.3.36: Summary Results of tsunami impact at forecast points for source 19-Z24

Name of gauge pt.	Depth of gauge pt.(m)	Longitude	Latitude	Arrival time of initial wave (min)	Arrival time of max.wave (min)	Maximum (+)ve amp.(m)	Maximum (-)ve amp.(m)
Gokceada	0,4	25,9006	40,2379	190	190	0,0	0,0
Mentes	7,4	26,7374	38,434	123	215	0,0	0,0
Bodrum	8,4	27,4171	37,0193	0	11	0,3	-0,3
Aksaz	4,7	28,4313	36,8453	0	69	0,2	-0,1
Girne	1,1	33,3276	35,3493	82	82	0,0	0,0
Gazimagusa	7,1	33,9468	35,1367	115	115	0,0	0,0
Tasucu	3,5	33,8327	36,2664	109	109	0,0	0,0
Erdemli	2,9	34,2629	36,57	123	123	0,0	0,0
Canakkale	2,5	26,3772	40,1043	163	204	0,0	0,0
Aliaga	3,9	26,9423	38,8421	104	157	0,0	0,0
Alsancak P.	6,8	27,1387	38,4464	172	237	0,0	0,0
Cesme	10	26,2879	38,3288	50	145	0,0	0,0
Kusadasi	3,5	27,2588	37,8668	44	114	0,1	-0,1
Didim	3,7	27,2615	37,3329	0	232	0,1	-0,1
Bodrum	6,7	27,4242	37,0228	0	15	0,3	-0,3
Marmaris	1,9	28,3271	36,8107	0	57	0,1	-0,1
Fethiye	11,7	28,9502	36,7235	14	40	0,0	0,0
Fethiye Bay	4,2	29,0546	36,6537	13	204	0,0	0,0
Kas	10,8	29,6436	36,1965	18	64	0,0	0,0
Finike	5,3	30,1554	36,3	27	233	0,1	-0,1
Kemer	0	30,5728	36,6052	0	0	0,0	0,0
Antalya B.	10,8	30,6123	36,8362	64	64	0,0	0,0
Alanya	10	31,9911	36,5243	68	68	0,0	0,0
Karatas	2,1	35,3872	36,5604	161	161	0,0	0,0
Anamur	7,2	32,8582	36,0565	79	79	0,0	0,0
Iskenderun B.	2,5	36,1898	36,6046	0	0	0,0	0,0
Arsuz	3,2	35,8965	36,4272	160	160	0,0	0,0
Samandag	7,9	35,9564	36,0549	137	137	0,0	0,0

A.3.19. Simulation of Source s20-Z25

Table A.3.37: Rupture Parameters of Tsunami Source 20-Z25

Rupture Parameters			
Epicenter of fault axis	26.17E 35.69N	Dip angle (deg.)	45
Length of fault (km)	111.4	Slip angle (deg.)	45
Strike angle (deg. CW)	60	Fdisplacement (m)	6
Focal depth (km)	40	Maximum (+)ve amp. (m)	1.2
Width of fault (km)	50	Minimum (-)ve amp. (m)	-0.2

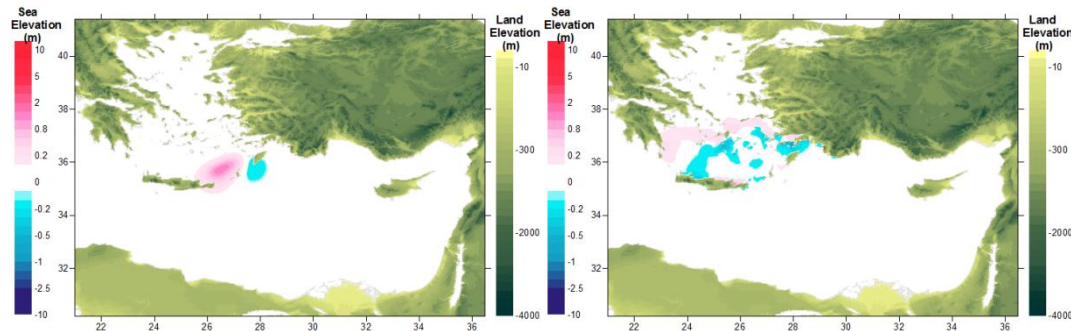


Figure A.3.37: The location of tsunami source 20-Z25 (left) and the distribution wave at $t=1\text{hr}$ (right) in the study domain (Eastern Mediterranean) in the duration of simulation (4 hours) for the tsunami source 20-Z25

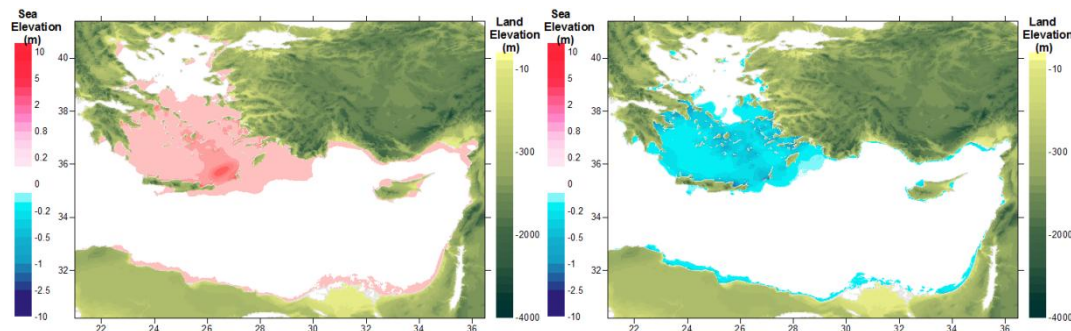


Figure A.3.38: The distributions of maximum positive of the water elevations(left) and negative water elevations(right) in the in the study domain (Eastern Mediterranean) in the duration of simulation (4 hours) for the tsunami source 20-Z25

Table A.3.38: Summary Results of tsunami impact at forecast points for source 20-Z25

Name of gauge pt.	Depth of gauge pt.(m)	Longitude	Latitude	Arrival time of initial wave (min)	Arrival time of max.wave (min)	Maximum (+)ve amp.(m)	Maximum (-)ve amp.(m)
Gokceada	0,4	25,9006	40,2379	131	203	0,1	0,0
Mentes	7,4	26,7374	38,434	105	155	0,1	-0,1
Bodrum	8,4	27,4171	37,0193	0	160	0,9	-1,0
Aksaz	4,7	28,4313	36,8453	0	128	0,9	-0,9
Girne	1,1	33,3276	35,3493	46	83	0,1	-0,1
Gazimagusa	7,1	33,9468	35,1367	73	142	0,1	-0,1
Tasucu	3,5	33,8327	36,2664	70	178	0,3	-0,2
Erdemli	2,9	34,2629	36,57	80	113	0,1	-0,1
Canakkale	2,5	26,3772	40,1043	145	197	0,2	-0,1
Aliaga	3,9	26,9423	38,8421	88	147	0,1	-0,1
Alsancak P.	6,8	27,1387	38,4464	154	211	0,2	0,0
Cesme	10	26,2879	38,3288	29	207	0,2	-0,2
Kusadasi	3,5	27,2588	37,8668	0	176	0,4	-0,6
Didim	3,7	27,2615	37,3329	0	228	0,5	-0,4
Bodrum	6,7	27,4242	37,0228	0	159	0,9	-1,2
Marmaris	1,9	28,3271	36,8107	0	42	0,4	-0,5
Fethiye	11,7	28,9502	36,7235	0	48	0,4	-0,4
Fethiye Bay	4,2	29,0546	36,6537	0	222	0,3	-0,5
Kas	10,8	29,6436	36,1965	0	48	0,4	-0,4
Finike	5,3	30,1554	36,3	14	84	0,4	-0,4
Kemer	0	30,5728	36,6052	0	0	0,0	0,0
Antalya B.	10,8	30,6123	36,8362	27	223	0,1	-0,1
Alanya	10	31,9911	36,5243	30	71	0,1	-0,1
Karatas	2,1	35,3872	36,5604	115	155	0,2	-0,2
Anamur	7,2	32,8582	36,0565	41	82	0,1	-0,1
Iskenderun B.	2,5	36,1898	36,6046	141	179	0,1	0,0
Arsuz	3,2	35,8965	36,4272	115	229	0,2	-0,1
Samandag	7,9	35,9564	36,0549	95	132	0,2	-0,1

A.3.20. Simulation of Source s21-Z13-1

Table A.3.39: Rupture Parameters of Tsunami Source 21-Z13-1

Rupture Parameters			
Epicenter of fault axis	26.41E 34.21N	Dip angle (deg.)	10
Length of fault (km)	154.8	Slip angle (deg.)	110
Strike angle (deg. CW)	240	Fdisplacement (m)	6
Focal depth (km)	50	Maximum (+)ve amp. (m)	1.2
Width of fault (km)	60	Minimum (-)ve amp. (m)	-0.7

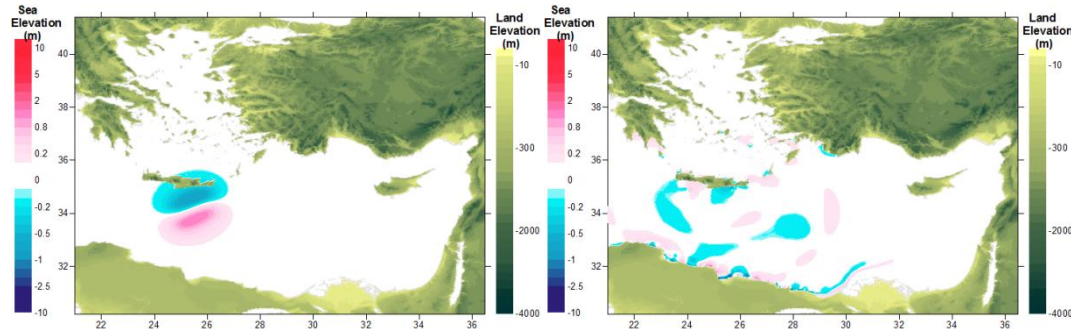


Figure A.3.39: The location of tsunami source 21-Z13-1 (left) and the distribution wave at $t=1\text{hr}$ (right) in the study domain (Eastern Mediterranean) in the duration of simulation (4 hours) for the tsunami source 21-Z13-1

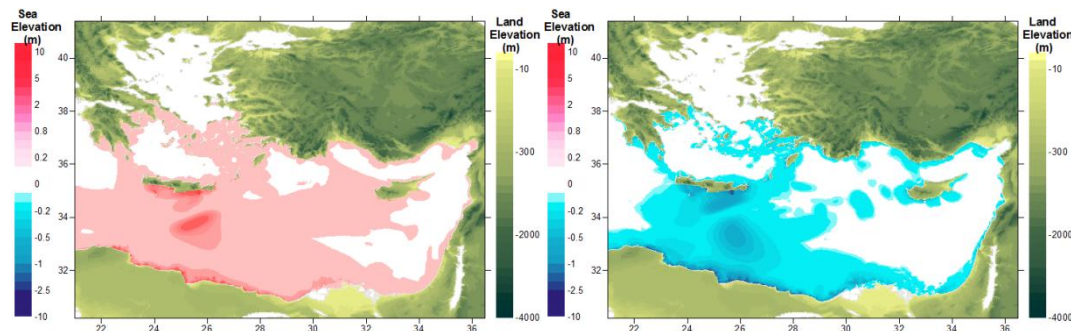


Figure A.3.40: The distributions of maximum positive of the water elevations(left) and negative water elevations(right) in the in the study domain (Eastern Mediterranean) in the duration of simulation (4 hours) for the tsunami source 21-Z13-1

Table A.3.40: Summary Results of tsunami impact at forecast points for source 21-Z13-1

Name of gauge pt.	Depth of gauge pt.(m)	Longitude	Latitude	Arrival time of initial wave (min)	Arrival time of max.wave (min)	Maximum (+)ve amp.(m)	Maximum (-)ve amp.(m)
Gokceada	0,4	25,9006	40,2379	161	239	0,0	0,0
Mentes	7,4	26,7374	38,434	142	239	0,1	0,0
Bodrum	8,4	27,4171	37,0193	25	182	0,7	-0,8
Aksaz	4,7	28,4313	36,8453	26	208	0,8	-0,9
Girne	1,1	33,3276	35,3493	60	194	0,1	-0,1
Gazimagusa	7,1	33,9468	35,1367	86	191	0,2	-0,2
Tasucu	3,5	33,8327	36,2664	86	225	0,2	-0,2
Erdemli	2,9	34,2629	36,57	104	234	0,2	-0,2
Canakkale	2,5	26,3772	40,1043	180	237	0,1	-0,1
Aliaga	3,9	26,9423	38,8421	124	213	0,1	0,0
Alsancak P.	6,8	27,1387	38,4464	188	0	0,0	-0,1
Cesme	10	26,2879	38,3288	73	195	0,1	-0,1
Kusadasi	3,5	27,2588	37,8668	73	141	0,1	-0,1
Didim	3,7	27,2615	37,3329	53	179	0,2	-0,2
Bodrum	6,7	27,4242	37,0228	25	183	0,9	-0,9
Marmaris	1,9	28,3271	36,8107	24	174	0,5	-0,5
Fethiye	11,7	28,9502	36,7235	22	203	0,4	-0,6
Fethiye Bay	4,2	29,0546	36,6537	21	101	0,4	-0,4
Kas	10,8	29,6436	36,1965	21	146	0,7	-0,6
Finike	5,3	30,1554	36,3	29	111	0,7	-0,9
Kemer	0	30,5728	36,6052	150	152	0,4	0,0
Antalya B.	10,8	30,6123	36,8362	43	122	0,3	-0,4
Alanya	10	31,9911	36,5243	45	96	0,2	-0,2
Karatas	2,1	35,3872	36,5604	135	145	0,2	-0,2
Anamur	7,2	32,8582	36,0565	56	159	0,3	-0,2
Iskenderun B.	2,5	36,1898	36,6046	158	202	0,2	-0,2
Arsuz	3,2	35,8965	36,4272	133	232	0,2	-0,1
Samandag	7,9	35,9564	36,0549	111	150	0,1	-0,2

A.3.21. Simulation of Source s22-Z13-2

Table A.3.41: Rupture Parameters of Tsunami Source 22-Z13-2

Rupture Parameters			
Epicenter of fault axis	24.8E 34.32N	Dip angle (deg.)	10
Length of fault (km)	192	Slip angle (deg.)	110
Strike angle (deg. CW)	280	Fdisplacement (m)	6
Focal depth (km)	50	Maximum (+)ve amp. (m)	1.3
Width of fault (km)	60	Minimum (-)ve amp. (m)	-0.8

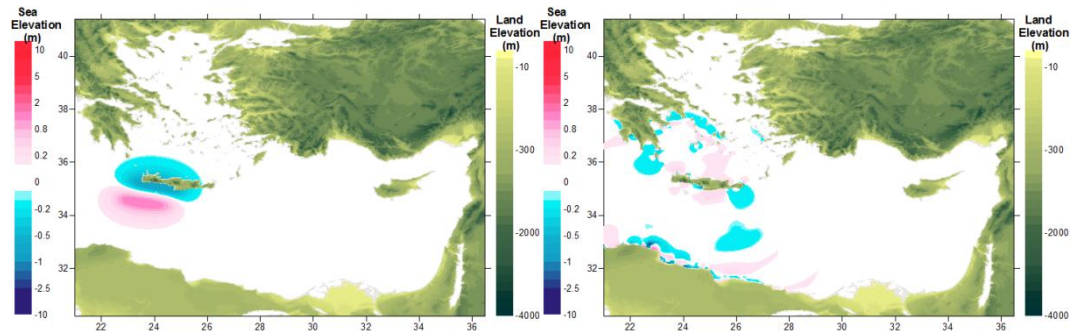


Figure A.3.41: The location of tsunami source 22-Z13-2 (left) and the distribution wave at t=1hr(right) in the study domain (Eastern Mediterranean) in the duration of simulation (4 hours) for the tsunami source 22-Z13-2

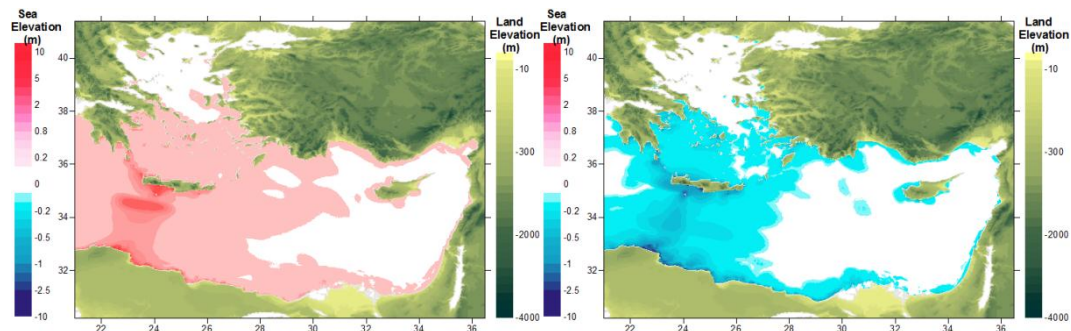


Figure A.3.42: The distributions of maximum positive of the water elevations(left) and negative water elevations(right) in the in the study domain (Eastern Mediterranean) in the duration of simulation (4 hours) for the tsunami source 22-Z13-2

Table A.3.42: Summary Results of tsunami impact at forecast points for source 22-Z13-2

Name of gauge pt.	Depth of gauge pt.(m)	Longitude	Latitude	Arrival time of initial wave (min)	Arrival time of max.wave (min)	Maximum (+)ve amp.(m)	Maximum (-)ve amp.(m)
Gokceada	0.4	25.9006	40.2379	153	0	0.0	0.0
Mentes	7.4	26.7374	38.434	129	239	0.1	-0.1
Bodrum	8.4	27.4171	37.0193	32	214	0.4	-0.6
Aksaz	4.7	28.4313	36.8453	37	239	0.9	-0.8
Girne	1.1	33.3276	35.3493	68	235	0.1	-0.1
Gazimagusa	7.1	33.9468	35.1367	93	203	0.1	-0.2
Tasucu	3.5	33.8327	36.2664	94	240	0.2	-0.2
Erdemli	2.9	34.2629	36.57	105	194	0.2	-0.2
Canakkale	2.5	26.3772	40.1043	166	239	0.1	-0.1
Aliaga	3.9	26.9423	38.8421	117	207	0.2	-0.1
Alsancak P.	6.8	27.1387	38.4464	177	0	0.0	-0.2
Cesme	10	26.2879	38.3288	64	214	0.2	-0.1
Kusadasi	3.5	27.2588	37.8668	64	159	0.4	-0.2
Didim	3.7	27.2615	37.3329	55	180	0.2	-0.2
Bodrum	6.7	27.4242	37.0228	33	215	0.5	-0.6
Marmaris	1.9	28.3271	36.8107	35	125	0.6	-0.8
Fethiye	11.7	28.9502	36.7235	34	127	0.5	-0.4
Fethiye Bay	4.2	29.0546	36.6537	33	176	0.7	-0.5
Kas	10.8	29.6436	36.1965	31	111	0.4	-0.5
Finike	5.3	30.1554	36.3	39	151	0.7	-1.1
Kemer	0	30.5728	36.6052	189	191	0.4	0.0
Antalya B.	10.8	30.6123	36.8362	53	190	0.3	-0.3
Alanya	10	31.9911	36.5243	54	140	0.2	-0.2
Karatas	2.1	35.3872	36.5604	140	170	0.2	-0.2
Anamur	7.2	32.8582	36.0565	64	227	0.2	-0.2
Iskenderun B.	2.5	36.1898	36.6046	166	214	0.1	0.0
Arsuz	3.2	35.8965	36.4272	139	167	0.1	-0.1
Samandag	7.9	35.9564	36.0549	117	146	0.1	-0.1

A.3.22. Simulation of Source s23-Z13-3

Table A.3.43: Rupture Parameters of Tsunami Source 23-Z13-3

Rupture Parameters			
Epicenter of fault axis	22.99E 35.13N	Dip angle (deg.)	10
Length of fault (km)	109.6	Slip angle (deg.)	110
Strike angle (deg. CW)	310	Fdisplacement (m)	6
Focal depth (km)	50	Maximum (+)ve amp. (m)	1.1
Width of fault (km)	60	Minimum (-)ve amp. (m)	-0.6

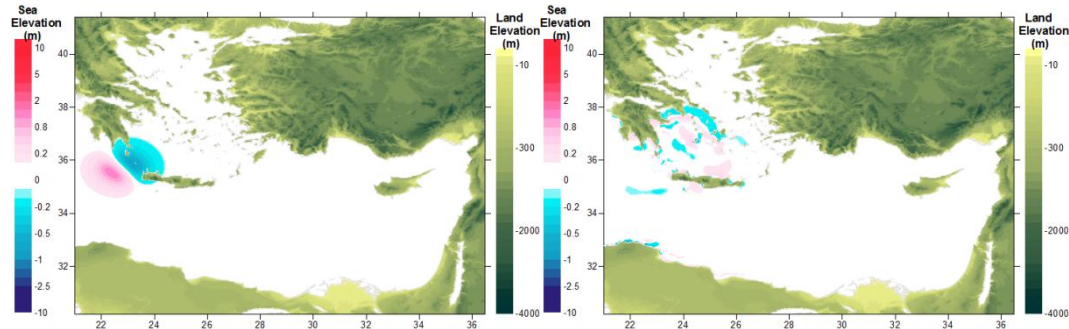


Figure A.3.43: The location of tsunami source 23-Z13-3 (left) and the distribution wave at $t=1\text{hr}$ (right) in the study domain (Eastern Mediterranean) in the duration of simulation (4 hours) for the tsunami source 23-Z13-3

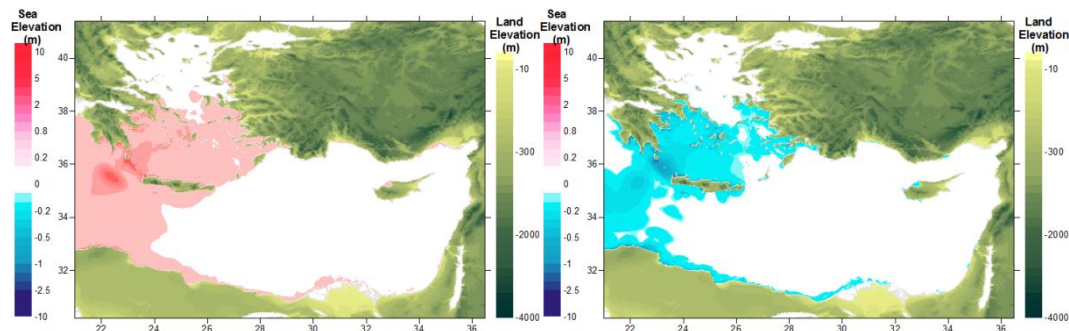


Figure A.3.44: The distributions of maximum positive of the water elevations(left) and negative water elevations(right) in the in the study domain (Eastern Mediterranean) in the duration of simulation (4 hours) for the tsunami source 23-Z13-3

Table A.3.44: Summary Results of tsunami impact at forecast points for source 23-Z13-3

Name of gauge pt.	Depth of gauge pt.(m)	Longitude	Latitude	Arrival time of initial wave (min)	Arrival time of max.wave (min)	Maximum (+)ve amp.(m)	Maximum (-)ve amp.(m)
Gokceada	0.4	25.9006	40.2379	148	0	0.0	0.0
Mentes	7.4	26.7374	38.434	134	238	0.1	-0.1
Bodrum	8.4	27.4171	37.0193	55	176	0.3	-0.2
Aksaz	4.7	28.4313	36.8453	65	167	0.5	-0.6
Girne	1.1	33.3276	35.3493	95	157	0.1	0.0
Gazimagusa	7.1	33.9468	35.1367	129	212	0.1	-0.1
Tasucu	3.5	33.8327	36.2664	122	183	0.1	-0.1
Erdemli	2.9	34.2629	36.57	134	192	0.1	-0.1
Canakkale	2.5	26.3772	40.1043	167	238	0.1	-0.1
Aliaga	3.9	26.9423	38.8421	116	205	0.1	-0.1
Alsancak P.	6.8	27.1387	38.4464	181	0	0.0	-0.1
Cesme	10	26.2879	38.3288	81	212	0.3	-0.1
Kusadasi	3.5	27.2588	37.8668	83	168	0.4	-0.3
Didim	3.7	27.2615	37.3329	77	204	0.2	-0.1
Bodrum	6.7	27.4242	37.0228	56	177	0.4	-0.3
Marmaris	1.9	28.3271	36.8107	62	121	0.3	-0.2
Fethiye	11.7	28.9502	36.7235	62	126	0.2	-0.2
Fethiye Bay	4.2	29.0546	36.6537	61	172	0.2	-0.2
Kas	10.8	29.6436	36.1965	58	203	0.1	-0.2
Finike	5.3	30.1554	36.3	66	120	0.3	-0.2
Kemer	0	30.5728	36.6052	0	0	0.0	0.0
Antalya B.	10.8	30.6123	36.8362	80	132	0.1	-0.1
Alanya	10	31.9911	36.5243	83	133	0.1	-0.1
Karatas	2.1	35.3872	36.5604	177	234	0.1	0.0
Anamur	7.2	32.8582	36.0565	91	153	0.1	-0.1
Iskenderun B.	2.5	36.1898	36.6046	201	211	0.1	0.0
Arsuz	3.2	35.8965	36.4272	176	218	0.1	0.0
Samandag	7.9	35.9564	36.0549	146	202	0.1	0.0

A.3.23. Simulation of Source s24-Z26-1

Table A.3.45: Rupture Parameters of Tsunami Source 24-Z26-1

Rupture Parameters			
Epicenter of fault axis	27.88E 35.33N	Dip angle (deg.)	10
Length of fault (km)	169.2	Slip angle (deg.)	110
Strike angle (deg. CW)	240	Fdisplacement (m)	6
Focal depth (km)	50	Maximum (+)ve amp. (m)	1.3
Width of fault (km)	60	Minimum (-)ve amp. (m)	-0.7

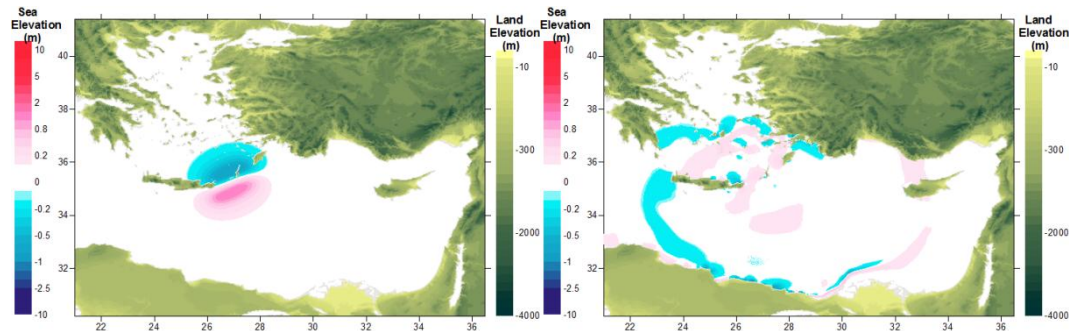


Figure A.3.45: The location of tsunami source 24-Z26-1 (left) and the distribution wave at t=1hr(right) in the study domain (Eastern Mediterranean) in the duration of simulation (4 hours) for the tsunami source 24-Z26-1

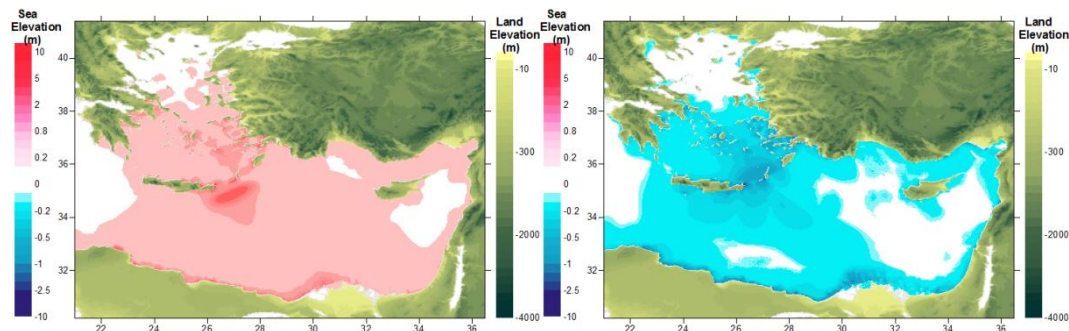


Figure A.3.46: The distributions of maximum positive of the water elevations(left) and negative water elevations(right) in the in the study domain (Eastern Mediterranean) in the duration of simulation (4 hours) for the tsunami source 24-Z26-1

Table A.3.46: Summary Results of tsunami impact at forecast points for source 24-Z26-1

Name of gauge pt.	Depth of gauge pt.(m)	Longitude	Latitude	Arrival time of initial wave (min)	Arrival time of max.wave (min)	Maximum (+)ve amp.(m)	Maximum (-)ve amp.(m)
Gokceada	0.4	25.9006	40.2379	125	233	0.0	-0.1
Mentes	7.4	26.7374	38.434	98	239	0.1	-0.1
Bodrum	8.4	27.4171	37.0193	0	93	1.8	-1.5
Aksaz	4.7	28.4313	36.8453	0	150	1.6	-1.7
Girne	1.1	33.3276	35.3493	52	141	0.2	-0.2
Gazimagusa	7.1	33.9468	35.1367	71	165	0.2	-0.2
Tasucu	3.5	33.8327	36.2664	76	161	0.5	-0.6
Erdemli	2.9	34.2629	36.57	85	240	0.2	-0.3
Canakkale	2.5	26.3772	40.1043	140	233	0.1	-0.1
Aliaga	3.9	26.9423	38.8421	79	238	0.1	-0.1
Alsancak P.	6.8	27.1387	38.4464	148	0	0.0	-0.2
Cesme	10	26.2879	38.3288	28	186	0.3	-0.2
Kusadasi	3.5	27.2588	37.8668	0	129	0.4	-0.3
Didim	3.7	27.2615	37.3329	0	238	0.5	-0.6
Bodrum	6.7	27.4242	37.0228	0	93	2.2	-1.8
Marmaris	1.9	28.3271	36.8107	0	136	0.9	-1.2
Fethiye	11.7	28.9502	36.7235	0	79	0.9	-0.9
Fethiye Bay	4.2	29.0546	36.6537	0	84	0.9	-0.5
Kas	10.8	29.6436	36.1965	0	78	1.0	-0.7
Finike	5.3	30.1554	36.3	17	206	0.8	-1.1
Kemer	0	30.5728	36.6052	108	208	0.5	0.0
Antalya B.	10.8	30.6123	36.8362	31	110	0.2	-0.2
Alanya	10	31.9911	36.5243	34	50	0.2	-0.2
Karatas	2.1	35.3872	36.5604	118	199	0.4	-0.4
Anamur	7.2	32.8582	36.0565	48	60	0.2	-0.2
Iskenderun B.	2.5	36.1898	36.6046	142	159	0.2	-0.1
Arsuz	3.2	35.8965	36.4272	117	133	0.2	-0.3
Samandag	7.9	35.9564	36.0549	96	114	0.2	-0.2

A.3.24. Simulation of Source s25-Z26-2

Table A.3.47: Rupture Parameters of Tsunami Source 25-Z26-2

Rupture Parameters			
Epicenter of fault axis	29E 36.66N	Dip angle (deg.)	10
Length of fault (km)	173.6	Slip angle (deg.)	110
Strike angle (deg. CW)	210	Fdisplacement (m)	6
Focal depth (km)	50	Maximum (+)ve amp. (m)	1.3
Width of fault (km)	60	Minimum (-)ve amp. (m)	-0.7

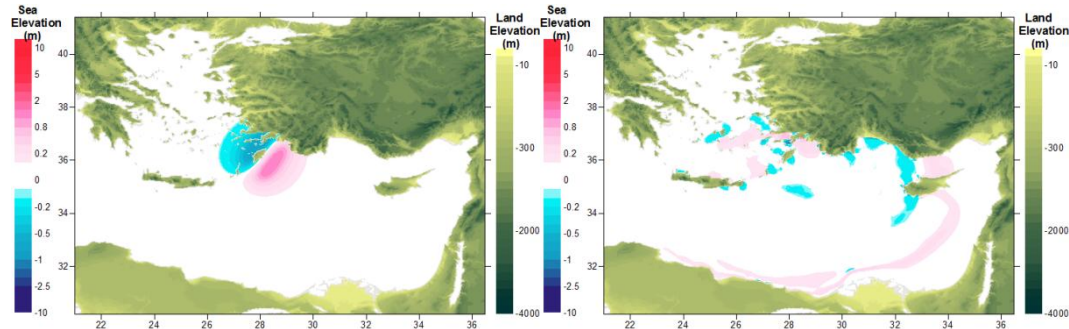


Figure A.3.47: The location of tsunami source 25-Z26-2 (left) and the distribution wave at t=1hr(right) in the study domain (Eastern Mediterranean) in the duration of simulation (4 hours) for the tsunami source 25-Z26-2

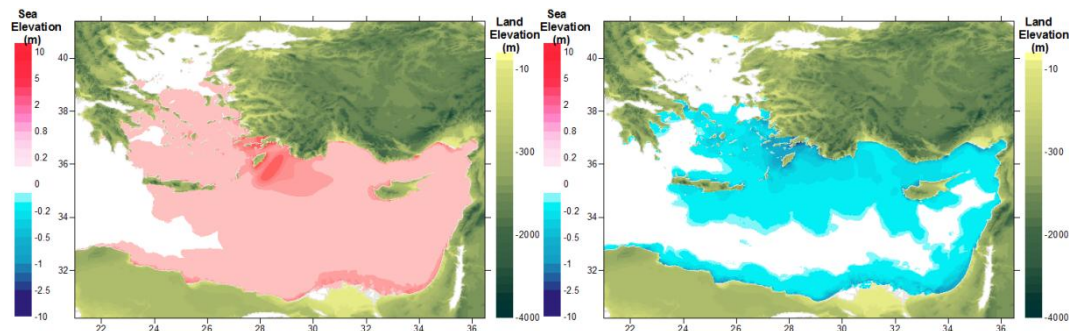


Figure A.3.48: The distributions of maximum positive of the water elevations(left) and negative water elevations(right) in the in the study domain (Eastern Mediterranean) in the duration of simulation (4 hours) for the tsunami source 25-Z26-2

Table A.3.48: Summary Results of tsunami impact at forecast points for source 25-Z26-2

Name of gauge pt.	Depth of gauge pt.(m)	Longitude	Latitude	Arrival time of initial wave (min)	Arrival time of max.wave (min)	Maximum (+)ve amp.(m)	Maximum (-)ve amp.(m)
Gokceada	0.4	25.9006	40.2379	118	0	0.0	-0.1
Mentes	7.4	26.7374	38.434	0	238	0.1	-0.1
Bodrum	8.4	27.4171	37.0193	0	91	1.8	-1.4
Aksaz	4.7	28.4313	36.8453	0	60	4.2	-4.7
Girne	1.1	33.3276	35.3493	31	53	0.4	-0.4
Gazimagusa	7.1	33.9468	35.1367	59	187	0.3	-0.4
Tasucu	3.5	33.8327	36.2664	55	147	1.0	-0.8
Erdemli	2.9	34.2629	36.57	65	154	0.5	-0.5
Canakkale	2.5	26.3772	40.1043	129	227	0.1	-0.1
Aliaga	3.9	26.9423	38.8421	64	239	0.1	-0.1
Alsancak P.	6.8	27.1387	38.4464	0	238	0.0	-0.1
Cesme	10	26.2879	38.3288	0	181	0.2	-0.1
Kusadasi	3.5	27.2588	37.8668	0	219	0.5	-0.4
Didim	3.7	27.2615	37.3329	0	131	0.3	-0.5
Bodrum	6.7	27.4242	37.0228	0	91	2.0	-1.5
Marmaris	1.9	28.3271	36.8107	0	17	2.7	-1.9
Fethiye	11.7	28.9502	36.7235	0	12	0.9	-1.4
Fethiye Bay	4.2	29.0546	36.6537	0	66	0.9	-0.9
Kas	10.8	29.6436	36.1965	0	64	2.6	-1.9
Finike	5.3	30.1554	36.3	0	94	1.0	-1.4
Kemer	0	30.5728	36.6052	0	34	0.6	0.0
Antalya B.	10.8	30.6123	36.8362	9	36	0.5	-0.4
Alanya	10	31.9911	36.5243	15	39	0.4	-0.3
Karatas	2.1	35.3872	36.5604	100	125	0.6	-0.8
Anamur	7.2	32.8582	36.0565	27	50	0.5	-0.5
Iskenderun B.	2.5	36.1898	36.6046	126	149	0.4	-0.3
Arsuz	3.2	35.8965	36.4272	100	201	0.4	-0.4
Samandag	7.9	35.9564	36.0549	81	104	0.5	-0.3

A.3.25. Simulation of Source s26-Z28

Table A.3.49: Rupture Parameters of Tsunami Source 26-Z28

Rupture Parameters			
Epicenter of fault axis	29.77E 35.69N	Dip angle (deg.)	45
Length of fault (km)	72.14	Slip angle (deg.)	45
Strike angle (deg. CW)	60	Fdisplacement (m)	6
Focal depth (km)	40	Maximum (+)ve amp. (m)	0.9
Width of fault (km)	40	Minimum (-)ve amp. (m)	-0.1

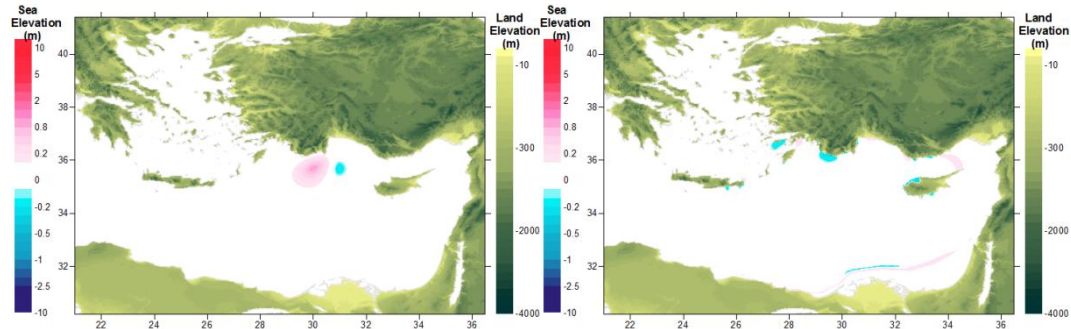


Figure A.3.49: The location of tsunami source 26-Z28 (left) and the distribution wave at t=1hr(right) in the study domain (Eastern Mediterranean) in the duration of simulation (4 hours) for the tsunami source 26-Z28

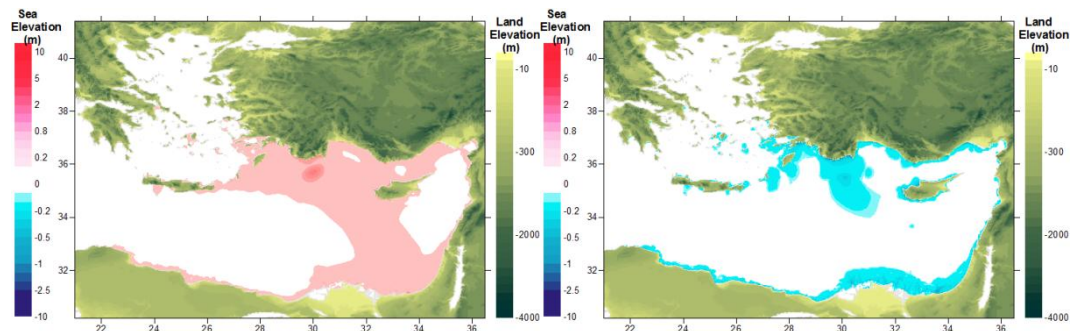


Figure A.3.50: The distributions of maximum positive of the water elevations(left) and negative water elevations(right) in the in the study domain (Eastern Mediterranean) in the duration of simulation (4 hours) for the tsunami source 26-Z28

Table A.3.50: Summary Results of tsunami impact at forecast points for source 26-Z28

Name of gauge pt.	Depth of gauge pt.(m)	Longitude	Latitude	Arrival time of initial wave (min)	Arrival time of max.wave (min)	Maximum (+)ve amp.(m)	Maximum (-)ve amp.(m)
Gokceada	0.4	25.9006	40.2379	207	207	0.0	0.0
Mentes	7.4	26.7374	38.434	183	183	0.0	0.0
Bodrum	8.4	27.4171	37.0193	56	105	0.4	-0.3
Aksaz	4.7	28.4313	36.8453	17	70	1.4	-1.6
Girne	1.1	33.3276	35.3493	16	38	0.2	-0.2
Gazimagusa	7.1	33.9468	35.1367	49	143	0.2	-0.2
Tasucu	3.5	33.8327	36.2664	39	132	0.3	-0.3
Erdemli	2.9	34.2629	36.57	49	79	0.3	-0.3
Canakkale	2.5	26.3772	40.1043	221	231	0.0	0.0
Aliaga	3.9	26.9423	38.8421	166	181	0.0	0.0
Alsancak P.	6.8	27.1387	38.4464	230	230	0.0	0.0
Cesme	10	26.2879	38.3288	119	195	0.0	0.0
Kusadasi	3.5	27.2588	37.8668	116	216	0.1	-0.1
Didim	3.7	27.2615	37.3329	92	100	0.0	-0.1
Bodrum	6.7	27.4242	37.0228	56	104	0.4	-0.4
Marmaris	1.9	28.3271	36.8107	15	30	0.6	-0.9
Fethiye	11.7	28.9502	36.7235	0	71	0.5	-0.6
Fethiye Bay	4.2	29.0546	36.6537	0	69	0.4	-0.4
Kas	10.8	29.6436	36.1965	1	29	1.5	-1.3
Finike	5.3	30.1554	36.3	0	35	1.7	-1.7
Kemer	0	30.5728	36.6052	0	107	0.4	0.0
Antalya B.	10.8	30.6123	36.8362	0	23	0.3	-0.3
Alanya	10	31.9911	36.5243	0	23	0.3	-0.2
Karatas	2.1	35.3872	36.5604	84	202	0.3	-0.3
Anamur	7.2	32.8582	36.0565	12	34	0.3	-0.3
Iskenderun B.	2.5	36.1898	36.6046	110	135	0.1	-0.1
Arsuz	3.2	35.8965	36.4272	84	199	0.2	-0.2
Samandag	7.9	35.9564	36.0549	65	91	0.2	-0.1

A.3.26. Simulation of Source s27-Z29-1

Table A.3.51: Rupture Parameters of Tsunami Source 27-Z29-1

Rupture Parameters			
Epicenter of fault axis	27.78E 34.2N	Dip angle (deg.)	45
Length of fault (km)	136	Slip angle (deg.)	45
Strike angle (deg. CW)	60	Fdisplacement (m)	6
Focal depth (km)	40	Maximum (+)ve amp. (m)	1.0
Width of fault (km)	40	Minimum (-)ve amp. (m)	-0.1

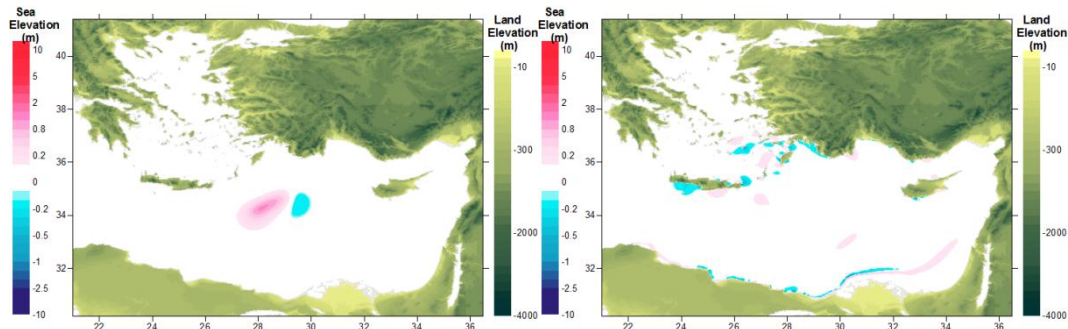


Figure A.3.51: The location of tsunami source 27-Z29-1 (left) and the distribution wave at t=1hr(right) in the study domain (Eastern Mediterranean) in the duration of simulation (4 hours) for the tsunami source 27-Z29-1

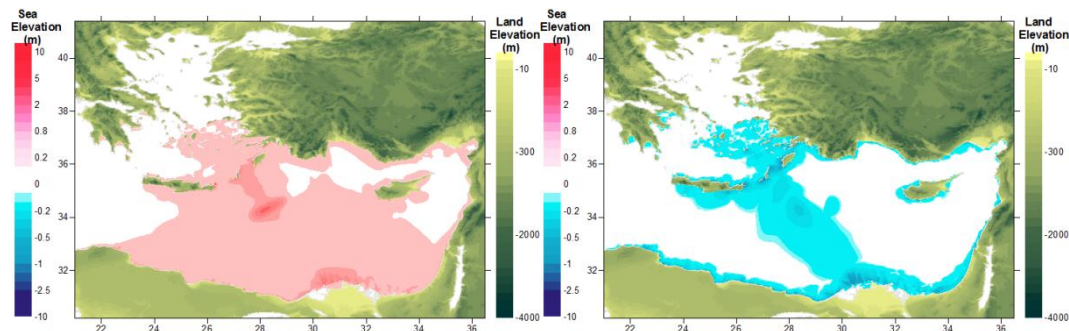


Figure A.3.52: The distributions of maximum positive of the water elevations(left) and negative water elevations(right) in the in the study domain (Eastern Mediterranean) in the duration of simulation (4 hours) for the tsunami source 27-Z29-1

Table A.3.52: Summary Results of tsunami impact at forecast points for source 27-Z29-1

Name of gauge pt.	Depth of gauge pt.(m)	Longitude	Latitude	Arrival time of initial wave (min)	Arrival time of max.wave (min)	Maximum (+)ve amp.(m)	Maximum (-)ve amp.(m)
Gokceada	0.4	25.9006	40.2379	195	195	0.0	0.0
Mentes	7.4	26.7374	38.434	172	220	0.0	0.0
Bodrum	8.4	27.4171	37.0193	38	238	0.7	-0.7
Aksaz	4.7	28.4313	36.8453	12	73	0.9	-0.9
Girne	1.1	33.3276	35.3493	28	53	0.1	-0.1
Gazimagusa	7.1	33.9468	35.1367	52	110	0.2	-0.2
Tasucu	3.5	33.8327	36.2664	52	149	0.2	-0.2
Erdemli	2.9	34.2629	36.57	62	94	0.2	-0.2
Canakkale	2.5	26.3772	40.1043	209	219	0.0	0.0
Aliaga	3.9	26.9423	38.8421	157	165	0.0	0.0
Alsancak P.	6.8	27.1387	38.4464	217	237	0.0	0.0
Cesme	10	26.2879	38.3288	113	225	0.1	-0.1
Kusadasi	3.5	27.2588	37.8668	111	211	0.1	-0.1
Didim	3.7	27.2615	37.3329	80	170	0.1	-0.2
Bodrum	6.7	27.4242	37.0228	38	238	0.7	-0.7
Marmaris	1.9	28.3271	36.8107	11	130	0.7	-0.9
Fethiye	11.7	28.9502	36.7235	0	89	0.5	-0.5
Fethiye Bay	4.2	29.0546	36.6537	0	140	0.5	-0.5
Kas	10.8	29.6436	36.1965	0	91	0.8	-0.8
Finike	5.3	30.1554	36.3	0	60	0.6	-0.8
Kemer	0	30.5728	36.6052	0	0	0.0	0.0
Antalya B.	10.8	30.6123	36.8362	9	44	0.3	-0.2
Alanya	10	31.9911	36.5243	13	43	0.2	-0.2
Karatas	2.1	35.3872	36.5604	97	212	0.4	-0.3
Anamur	7.2	32.8582	36.0565	24	234	0.2	-0.2
Iskenderun B.	2.5	36.1898	36.6046	123	146	0.1	-0.1
Arsuz	3.2	35.8965	36.4272	97	209	0.3	-0.1
Samandag	7.9	35.9564	36.0549	76	102	0.2	-0.1

A.3.27. Simulation of Source s28-Z29-2

Table A.3.53: Rupture Parameters of Tsunami Source 28-Z29-2

Rupture Parameters			
Epicenter of fault axis	28.48E 35.16N	Dip angle (deg.)	45
Length of fault (km)	121.6	Slip angle (deg.)	45
Strike angle (deg. CW)	60	Fdisplacement (m)	6
Focal depth (km)	40	Maximum (+)ve amp. (m)	1.0
Width of fault (km)	40	Minimum (-)ve amp. (m)	-0.1

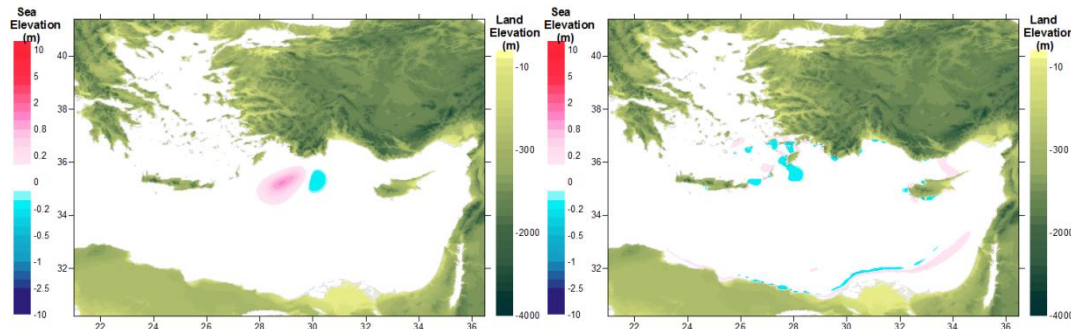


Figure A.3.53: The location of tsunami source 28-Z29-2 (left) and the distribution wave at t=1hr(right) in the study domain (Eastern Mediterranean) in the duration of simulation (4 hours) for the tsunami source 28-Z29-2

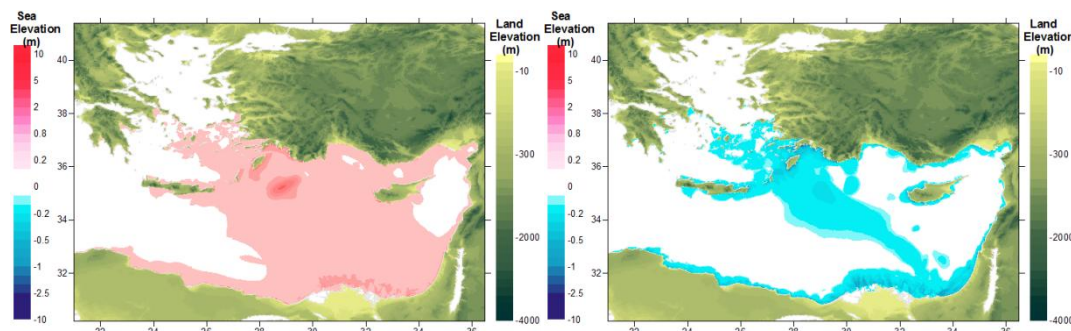


Figure A.3.54: The distributions of maximum positive of the water elevations(left) and negative water elevations(right) in the in the study domain (Eastern Mediterranean) in the duration of simulation (4 hours) for the tsunami source 28-Z29-2

Table A.3.54: Summary Results of tsunami impact at forecast points for source 28-Z29-2

Name of gauge pt.	Depth of gauge pt.(m)	Longitude	Latitude	Arrival time of initial wave (min)	Arrival time of max.wave (min)	Maximum (+)ve amp.(m)	Maximum (-)ve amp.(m)
Gokceada	0.4	25.9006	40.2379	191	191	0.0	0.0
Mentes	7.4	26.7374	38.434	170	185	0.0	0.0
Bodrum	8.4	27.4171	37.0193	29	196	0.8	-0.5
Aksaz	4.7	28.4313	36.8453	0	66	2.5	-2.1
Girne	1.1	33.3276	35.3493	22	46	0.2	-0.1
Gazimagusa	7.1	33.9468	35.1367	51	148	0.2	-0.2
Tasucu	3.5	33.8327	36.2664	46	157	0.4	-0.3
Erdemli	2.9	34.2629	36.57	55	88	0.3	-0.2
Canakkale	2.5	26.3772	40.1043	207	228	0.0	0.0
Aliaga	3.9	26.9423	38.8421	154	175	0.0	0.0
Alsancak P.	6.8	27.1387	38.4464	216	233	0.0	0.0
Cesme	10	26.2879	38.3288	109	225	0.1	-0.1
Kusadasi	3.5	27.2588	37.8668	106	208	0.2	-0.1
Didim	3.7	27.2615	37.3329	82	197	0.1	-0.2
Bodrum	6.7	27.4242	37.0228	30	195	0.8	-0.7
Marmaris	1.9	28.3271	36.8107	0	102	1.7	-1.7
Fethiye	11.7	28.9502	36.7235	0	23	1.0	-1.1
Fethiye Bay	4.2	29.0546	36.6537	0	75	0.9	-0.9
Kas	10.8	29.6436	36.1965	0	86	1.5	-1.6
Finike	5.3	30.1554	36.3	0	89	0.8	-1.1
Kemer	0	30.5728	36.6052	0	129	0.4	0.0
Antalya B.	10.8	30.6123	36.8362	0	33	0.3	-0.2
Alanya	10	31.9911	36.5243	5	34	0.3	-0.2
Karatas	2.1	35.3872	36.5604	91	211	0.4	-0.3
Anamur	7.2	32.8582	36.0565	18	44	0.3	-0.3
Iskenderun B.	2.5	36.1898	36.6046	117	141	0.2	-0.2
Arsuz	3.2	35.8965	36.4272	91	193	0.2	-0.2
Samandag	7.9	35.9564	36.0549	71	97	0.2	-0.1

A.3.28. Simulation of Source s29-Z30

Table A.3.55: Rupture Parameters of Tsunami Source 29-Z30

Rupture Parameters			
Epicenter of fault axis	32.98E 33.83N	Dip angle (deg.)	45
Length of fault (km)	149.3	Slip angle (deg.)	45
Strike angle (deg. CW)	330	Fdisplacement (m)	6
Focal depth (km)	40	Maximum (+)ve amp. (m)	1.1
Width of fault (km)	40	Minimum (-)ve amp. (m)	-0.1

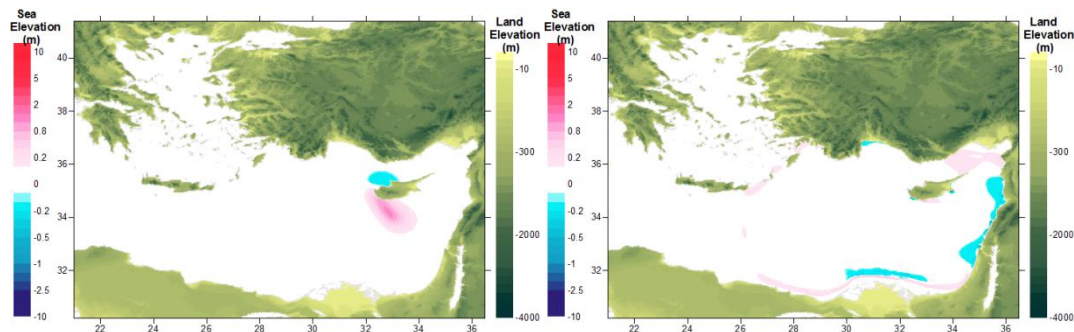


Figure A.3.55: The location of tsunami source 29-Z30 (left) and the distribution wave at $t=1\text{hr}$ (right) in the study domain (Eastern Mediterranean) in the duration of simulation (4 hours) for the tsunami source 29-Z30

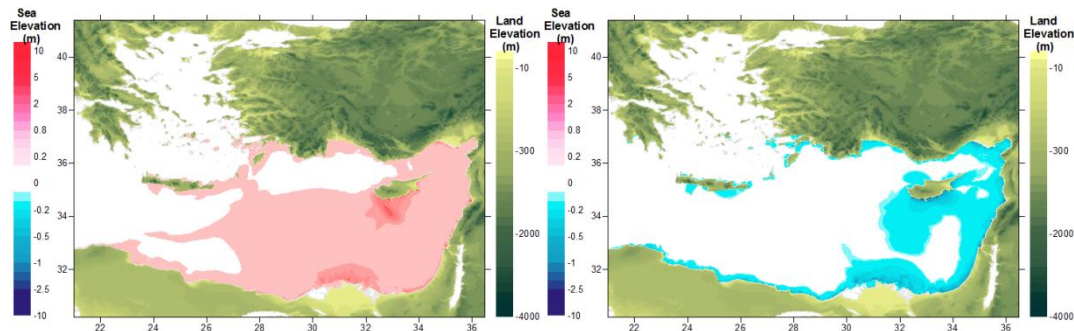


Figure A.3.56: The distributions of maximum positive of the water elevations(left) and negative water elevations(right) in the in the study domain (Eastern Mediterranean) in the duration of simulation (4 hours) for the tsunami source 29-Z30

Table A.3.56: Summary Results of tsunami impact at forecast points for source 29-Z30

Name of gauge pt.	Depth of gauge pt.(m)	Longitude	Latitude	Arrival time of initial wave (min)	Arrival time of max.wave (min)	Maximum (+)ve amp.(m)	Maximum (-)ve amp.(m)
Gokceada	0.4	25.9006	40.2379	0	0	0.0	0.0
Mentes	7.4	26.7374	38.434	219	219	0.0	0.0
Bodrum	8.4	27.4171	37.0193	66	135	0.3	-0.2
Aksaz	4.7	28.4313	36.8453	28	174	0.9	-0.9
Girne	1.1	33.3276	35.3493	0	84	0.2	-0.1
Gazimagusa	7.1	33.9468	35.1367	0	111	0.8	-0.6
Tasucu	3.5	33.8327	36.2664	0	72	0.3	-0.2
Erdemli	2.9	34.2629	36.57	20	68	0.4	-0.2
Canakkale	2.5	26.3772	40.1043	0	0	0.0	0.0
Aliaga	3.9	26.9423	38.8421	202	217	0.0	0.0
Alsancak P.	6.8	27.1387	38.4464	0	0	0.0	0.0
Cesme	10	26.2879	38.3288	142	237	0.0	0.0
Kusadasi	3.5	27.2588	37.8668	154	165	0.0	0.0
Didim	3.7	27.2615	37.3329	112	173	0.1	0.0
Bodrum	6.7	27.4242	37.0228	67	135	0.3	-0.3
Marmaris	1.9	28.3271	36.8107	26	236	0.5	-0.5
Fethiye	11.7	28.9502	36.7235	22	237	0.3	-0.3
Fethiye Bay	4.2	29.0546	36.6537	20	108	0.3	-0.3
Kas	10.8	29.6436	36.1965	5	109	0.4	-0.3
Finike	5.3	30.1554	36.3	0	168	0.5	-0.8
Kemer	0	30.5728	36.6052	0	191	0.4	0.0
Antalya B.	10.8	30.6123	36.8362	4	45	0.3	-0.4
Alanya	10	31.9911	36.5243	0	93	0.1	-0.1
Karatas	2.1	35.3872	36.5604	51	130	0.9	-0.7
Anamur	7.2	32.8582	36.0565	0	227	0.2	-0.2
Iskenderun B.	2.5	36.1898	36.6046	75	101	0.3	-0.3
Arsuz	3.2	35.8965	36.4272	50	77	0.4	-0.5
Samandag	7.9	35.9564	36.0549	29	56	0.4	-0.5

A.3.29. Simulation of Source s30-Z31-1

Table A.3.57: Rupture Parameters of Tsunami Source 30-Z31-1

Rupture Parameters			
Epicenter of fault axis	32.79E 34.68N	Dip angle (deg.)	45
Length of fault (km)	137	Slip angle (deg.)	45
Strike angle (deg. CW)	60	Fdisplacement (m)	6
Focal depth (km)	40	Maximum (+)ve amp. (m)	1.0
Width of fault (km)	40	Minimum (-)ve amp. (m)	-0.1

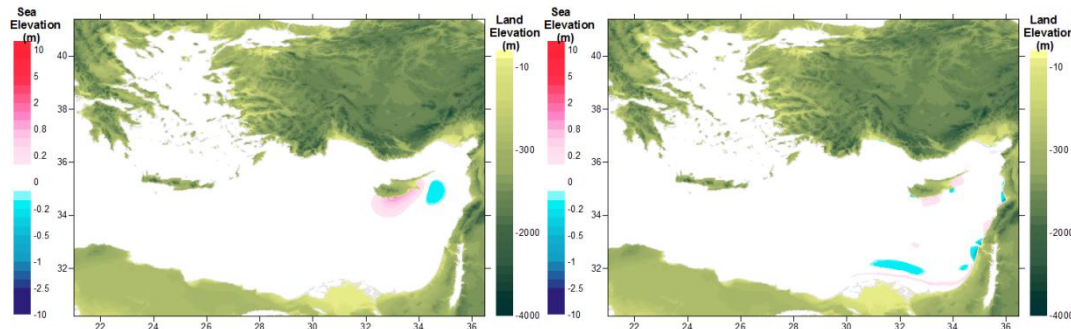


Figure A.3.57: The location of tsunami source 30-Z31-1 (left) and the distribution wave at t=1hr(right) in the study domain (Eastern Mediterranean) in the duration of simulation (4 hours) for the tsunami source 30-Z31-1

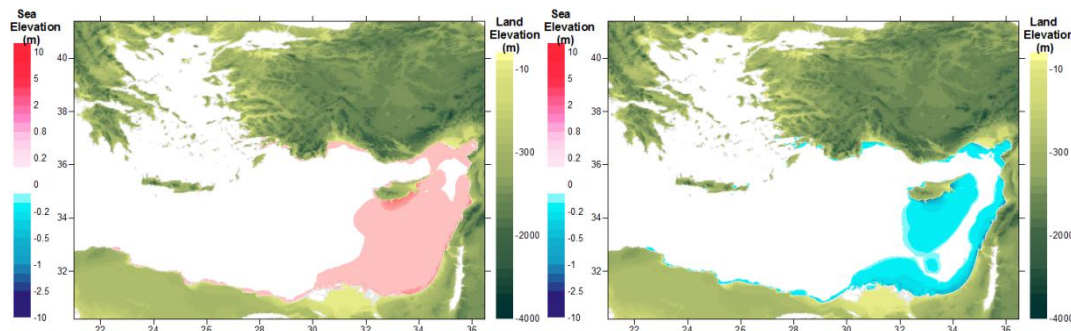


Figure A.3.58: The distributions of maximum positive of the water elevations(left) and negative water elevations(right) in the in the study domain (Eastern Mediterranean) in the duration of simulation (4 hours) for the tsunami source 30-Z31-1

Table A.3.58: Summary Results of tsunami impact at forecast points for source 30-Z31-1

Name of gauge pt.	Depth of gauge pt.(m)	Longitude	Latitude	Arrival time of initial wave (min)	Arrival time of max.wave (min)	Maximum (+)ve amp.(m)	Maximum (-)ve amp.(m)
Gokceada	0.4	25.9006	40.2379	0	0	0.0	0.0
Mentes	7.4	26.7374	38.434	223	223	0.0	0.0
Bodrum	8.4	27.4171	37.0193	90	234	0.2	-0.2
Aksaz	4.7	28.4313	36.8453	51	237	0.6	-0.5
Girne	1.1	33.3276	35.3493	0	224	0.1	-0.1
Gazimagusa	7.1	33.9468	35.1367	0	96	0.8	-0.8
Tasucu	3.5	33.8327	36.2664	0	62	0.2	-0.2
Erdemli	2.9	34.2629	36.57	0	214	0.2	-0.2
Canakkale	2.5	26.3772	40.1043	0	0	0.0	0.0
Aliaga	3.9	26.9423	38.8421	205	205	0.0	0.0
Alsancak P.	6.8	27.1387	38.4464	0	0	0.0	0.0
Cesme	10	26.2879	38.3288	155	155	0.0	0.0
Kusadasi	3.5	27.2588	37.8668	154	164	0.0	0.0
Didim	3.7	27.2615	37.3329	128	135	0.0	0.0
Bodrum	6.7	27.4242	37.0228	91	234	0.3	-0.2
Marmaris	1.9	28.3271	36.8107	49	155	0.2	-0.2
Fethiye	11.7	28.9502	36.7235	46	239	0.2	-0.2
Fethiye Bay	4.2	29.0546	36.6537	45	234	0.2	-0.2
Kas	10.8	29.6436	36.1965	29	106	0.2	-0.2
Finike	5.3	30.1554	36.3	24	130	0.3	-0.3
Kemer	0	30.5728	36.6052	0	0	0.0	0.0
Antalya B.	10.8	30.6123	36.8362	23	145	0.2	-0.2
Alanya	10	31.9911	36.5243	7	96	0.1	-0.1
Karatas	2.1	35.3872	36.5604	0	208	0.4	-0.5
Anamur	7.2	32.8582	36.0565	0	220	0.2	-0.1
Iskenderun B.	2.5	36.1898	36.6046	7	141	0.2	-0.2
Arsuz	3.2	35.8965	36.4272	0	151	0.4	-0.2
Samandag	7.9	35.9564	36.0549	0	45	0.2	-0.3

A.3.30. Simulation of Source s31-Z31-2

Table A.3.59: Rupture Parameters of Tsunami Source 31-Z31-2

Rupture Parameters			
Epicenter of fault axis	33.09E 34.33N	Dip angle (deg.)	45
Length of fault (km)	72.5	Slip angle (deg.)	45
Strike angle (deg. CW)	60	Fdisplacement (m)	6
Focal depth (km)	40	Maximum (+)ve amp. (m)	0.9
Width of fault (km)	40	Minimum (-)ve amp. (m)	-0.1

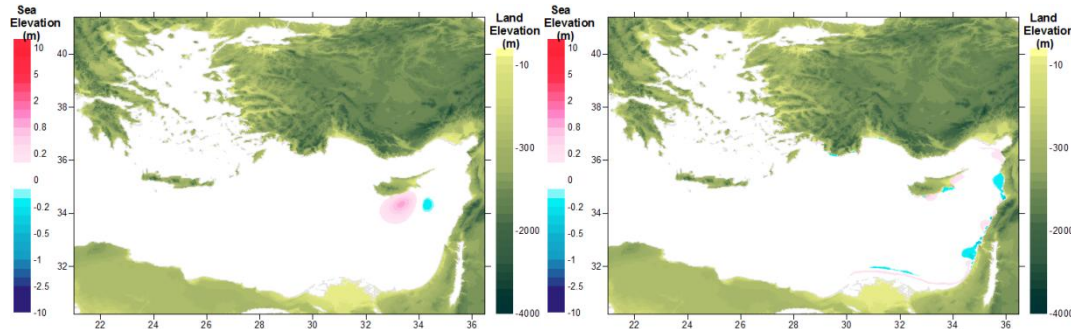


Figure A.3.59: The location of tsunami source 31-Z31-2 (left) and the distribution wave at $t=1\text{hr}$ (right) in the study domain (Eastern Mediterranean) in the duration of simulation (4 hours) for the tsunami source 31-Z31-2

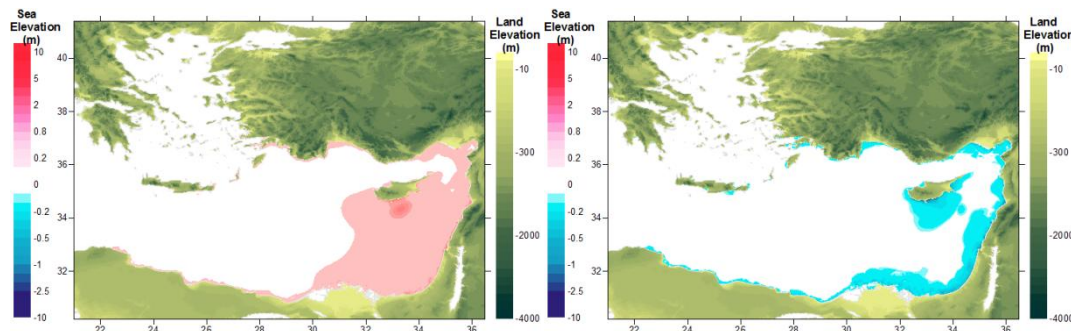


Figure A.3.60: The distributions of maximum positive of the water elevations(left) and negative water elevations(right) in the in the study domain (Eastern Mediterranean) in the duration of simulation (4 hours) for the tsunami source 31-Z31-2

Table A.3.60: Summary Results of tsunami impact at forecast points for source 31-Z31-2

Name of gauge pt.	Depth of gauge pt.(m)	Longitude	Latitude	Arrival time of initial wave (min)	Arrival time of max.wave (min)	Maximum (+)ve amp.(m)	Maximum (-)ve amp.(m)
Gokceada	0.4	25.9006	40.2379	0	0	0.0	0.0
Mentes	7.4	26.7374	38.434	224	224	0.0	0.0
Bodrum	8.4	27.4171	37.0193	94	237	0.2	-0.2
Aksaz	4.7	28.4313	36.8453	56	108	0.6	-0.6
Girne	1.1	33.3276	35.3493	0	227	0.1	-0.1
Gazimagusa	7.1	33.9468	35.1367	0	106	0.6	-0.6
Tasucu	3.5	33.8327	36.2664	18	221	0.2	-0.2
Erdemli	2.9	34.2629	36.57	22	82	0.2	-0.2
Canakkale	2.5	26.3772	40.1043	0	0	0.0	0.0
Aliaga	3.9	26.9423	38.8421	207	207	0.0	0.0
Alsancak P.	6.8	27.1387	38.4464	0	0	0.0	0.0
Cesme	10	26.2879	38.3288	157	212	0.0	0.0
Kusadasi	3.5	27.2588	37.8668	156	165	0.0	0.0
Didim	3.7	27.2615	37.3329	131	140	0.0	0.0
Bodrum	6.7	27.4242	37.0228	94	236	0.3	-0.2
Marmaris	1.9	28.3271	36.8107	54	193	0.3	-0.4
Fethiye	11.7	28.9502	36.7235	54	236	0.2	-0.2
Fethiye Bay	4.2	29.0546	36.6537	53	235	0.2	-0.2
Kas	10.8	29.6436	36.1965	35	68	0.3	-0.3
Finike	5.3	30.1554	36.3	30	69	0.4	-0.4
Kemer	0	30.5728	36.6052	94	146	0.4	0.0
Antalya B.	10.8	30.6123	36.8362	29	48	0.2	-0.2
Alanya	10	31.9911	36.5243	15	37	0.1	-0.1
Karatas	2.1	35.3872	36.5604	43	127	0.5	-0.5
Anamur	7.2	32.8582	36.0565	7	228	0.1	-0.1
Iskenderun B.	2.5	36.1898	36.6046	66	97	0.2	-0.2
Arsuz	3.2	35.8965	36.4272	40	70	0.3	-0.4
Samandag	7.9	35.9564	36.0549	19	52	0.3	-0.2

A.3.31. Simulation of Source s32-Z32

Table A.3.61: Rupture Parameters of Tsunami Source s32-Z32

Rupture Parameters			
Epicenter of fault axis	32.1E 35.4N	Dip angle (deg.)	45
Length of fault (km)	156	Slip angle (deg.)	45
Strike angle (deg. CW)	305	Fdisplacement (m)	6
Focal depth (km)	20	Maximum (+)ve amp. (m)	1.6
Width of fault (km)	40	Minimum (-)ve amp. (m)	-0.2

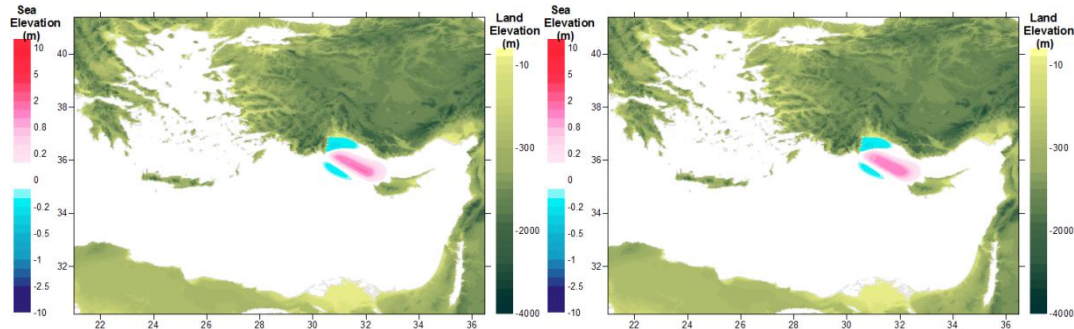


Figure A.3.61: The location of tsunami source s32-Z32 (left) and the distribution wave at t=1hr(right) in the study domain (Eastern Mediterranean) in the duration of simulation (4 hours) for the tsunami source s32-Z32

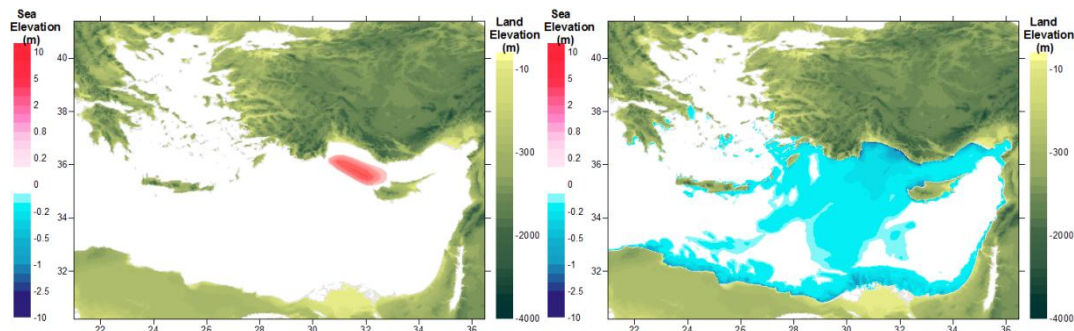


Figure A.3.62: The distributions of maximum positive of the water elevations(left) and negative water elevations(right) in the in the study domain (Eastern Mediterranean) in the duration of simulation (4 hours) for the tsunami source s32-Z32

Table A.3.62: Summary Results of tsunami impact at forecast points for source s32-Z32

Name of gauge pt.	Depth of gauge pt.(m)	Longitude	Latitude	Arrival time of initial wave (min)	Arrival time of max.wave (min)	Maximum (+)ve amp.(m)	Maximum (-)ve amp.(m)
Gokceada	0.4	25.9006	40.2379	220	220	0.0	0.0
Mentes	7.4	26.7374	38.4340	207	208	0.0	0.0
Bodrum	8.4	27.4171	37.0193	13	228	0.3	-0.2
Aksaz	4.7	28.4313	36.8453	0	194	0.6	-0.6
Girne	1.1	33.3276	35.3493	9	19	0.6	-0.4
Gazimagusa	7.1	33.9468	35.1367	0	137	0.2	-0.2
Tasucu	3.5	33.8327	36.2664	0	199	0.6	-0.6
Erdemli	2.9	34.2629	36.5700	0	143	0.5	-0.6
Canakkale	2.5	26.3772	40.1043	0	0	0.0	0.0
Aliaga	3.9	26.9423	38.8421	190	205	0.0	0.0
Alsancak P.	6.8	27.1387	38.4464	0	0	0.0	0.0
Cesme	10.0	26.2879	38.3288	141	151	0.0	0.0
Kusadasi	3.5	27.2588	37.8668	139	238	0.1	-0.1
Didim	3.7	27.2615	37.3329	112	127	0.1	-0.1
Bodrum	6.7	27.4242	37.0228	13	229	0.3	-0.2
Marmaris	1.9	28.3271	36.8107	0	47	0.5	-0.5
Fethiye	11.7	28.9502	36.7235	0	93	0.3	-0.4
Fethiye Bay	4.2	29.0546	36.6537	0	191	0.4	-0.5
Kas	10.8	29.6436	36.1965	0	215	0.8	-1.1
Finike	5.3	30.1554	36.3000	0	130	1.1	-1.7
Kemer	0.0	30.5728	36.6052	0	29	1.2	-0.2
Antalya B.	10.8	30.6123	36.8362	0	18	1.2	-1.3
Alanya	10.0	31.9911	36.5243	0	12	2.1	-1.6
Karatas	2.1	35.3872	36.5604	41	174	0.5	-0.5
Anamur	7.2	32.8582	36.0565	4	16	0.9	-1.2
Iskenderun B.	2.5	36.1898	36.6046	68	110	0.2	-0.2
Arsuz	3.2	35.8965	36.4272	40	167	0.3	-0.3
Samandag	7.9	35.9564	36.0549	19	64	0.2	-0.2

A.3.32. Simulation of Source s33-Z38

Table A.3.63: Rupture Parameters of Tsunami Source s33-Z38

Rupture Parameters			
Epicenter of fault axis	34.41E 36.13N	Dip angle (deg.)	45
Length of fault (km)	106	Slip angle (deg.)	45
Strike angle (deg. CW)	45	Fdisplacement (m)	6
Focal depth (km)	40	Maximum (+)ve amp. (m)	1.0
Width of fault (km)	40	Minimum (-)ve amp. (m)	-0.1

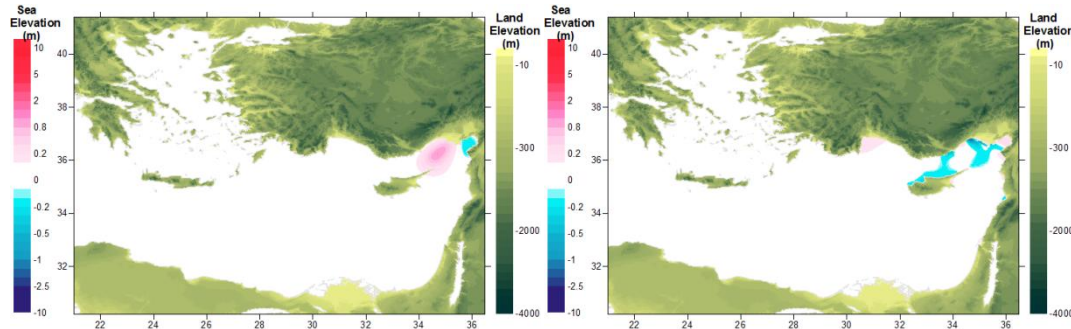


Figure A.3.63: The location of tsunami source s33-Z38 (left) and the distribution wave at t=1hr(right) in the study domain (Eastern Mediterranean) in the duration of simulation (4 hours) for the tsunami source s33-Z38

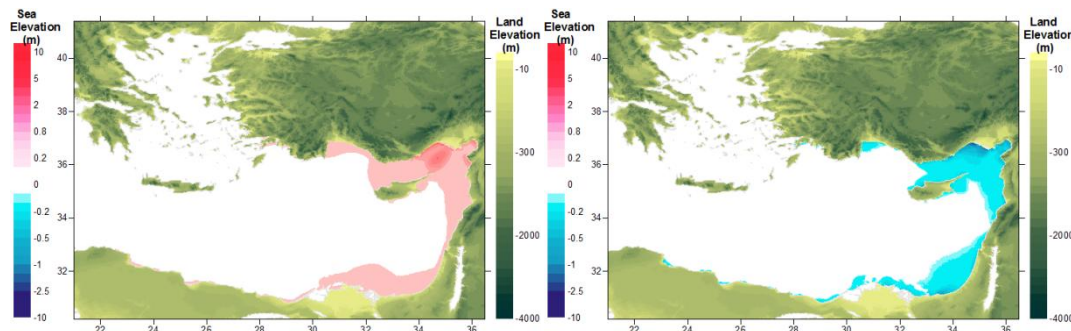


Figure A.3.64: The distributions of maximum positive of the water elevations(left) and negative water elevations(right) in the in the study domain (Eastern Mediterranean) in the duration of simulation (4 hours) for the tsunami source s33-Z38

Table A.3.64: Summary Results of tsunami impact at forecast points for source s33-Z38

Name of gauge pt.	Depth of gauge pt.(m)	Longitude	Latitude	Arrival time of initial wave (min)	Arrival time of max.wave (min)	Maximum (+)ve amp.(m)	Maximum (-)ve amp.(m)
Gokceada	0.4	25.9006	40.2379	0	0	0.0	0.0
Mentes	7.4	26.7374	38.434	0	0	0.0	0.0
Bodrum	8.4	27.4171	37.0193	113	202	0.1	-0.1
Aksaz	4.7	28.4313	36.8453	74	170	0.3	-0.3
Girne	1.1	33.3276	35.3493	4	26	0.3	-0.2
Gazimagusa	7.1	33.9468	35.1367	0	50	0.2	-0.3
Tasucu	3.5	33.8327	36.2664	0	33	0.7	-0.6
Erdemli	2.9	34.2629	36.57	0	18	1.2	-0.8
Canakkale	2.5	26.3772	40.1043	0	0	0.0	0.0
Aliaga	3.9	26.9423	38.8421	232	232	0.0	0.0
Alsancak P.	6.8	27.1387	38.4464	0	0	0.0	0.0
Cesme	10	26.2879	38.3288	182	238	0.0	0.0
Kusadasi	3.5	27.2588	37.8668	181	208	0.1	0.0
Didim	3.7	27.2615	37.3329	154	205	0.0	0.0
Bodrum	6.7	27.4242	37.0228	113	204	0.1	-0.1
Marmaris	1.9	28.3271	36.8107	72	91	0.1	-0.1
Fethiye	11.7	28.9502	36.7235	70	90	0.1	-0.1
Fethiye Bay	4.2	29.0546	36.6537	68	229	0.1	-0.1
Kas	10.8	29.6436	36.1965	51	68	0.1	0.0
Finike	5.3	30.1554	36.3	47	66	0.1	-0.1
Kemer	0	30.5728	36.6052	0	0	0.0	0.0
Antalya B.	10.8	30.6123	36.8362	44	65	0.2	-0.3
Alanya	10	31.9911	36.5243	30	48	0.1	-0.1
Karatas	2.1	35.3872	36.5604	0	64	0.7	-1.0
Anamur	7.2	32.8582	36.0565	14	177	0.4	-0.4
Iskenderun B.	2.5	36.1898	36.6046	0	68	0.6	-0.6
Arsuz	3.2	35.8965	36.4272	0	39	0.4	-0.5
Samandag	7.9	35.9564	36.0549	0	25	0.7	-0.5

A.3.33. Simulation of Source s34-Z41

Table A.3.65: Rupture Parameters of Tsunami Source 34-Z41

Rupture Parameters			
Epicenter of fault axis	35.7E 35.07N	Dip angle (deg.)	45
Length of fault (km)	175.5	Slip angle (deg.)	45
Strike angle (deg. CW)	5	Fdisplacement (m)	6
Focal depth (km)	40	Maximum (+)ve amp. (m)	1.0
Width of fault (km)	40	Minimum (-)ve amp. (m)	-0.1

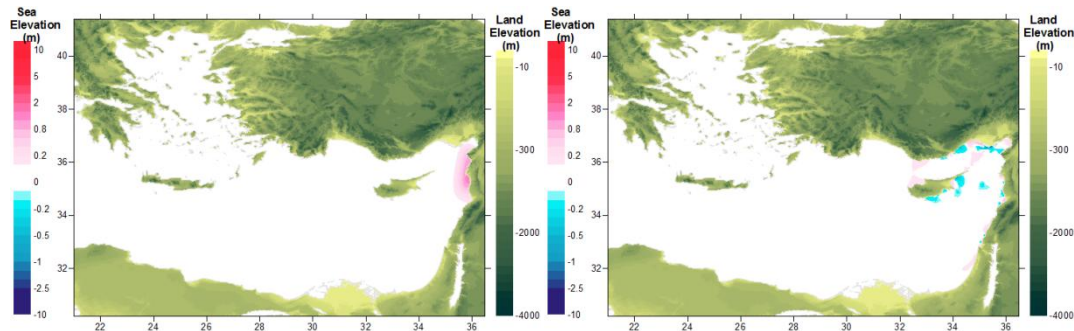


Figure A.3.65: The location of tsunami source 34-Z41 (left) and the distribution wave at $t=1\text{hr}$ (right) in the study domain (Eastern Mediterranean) in the duration of simulation (4 hours) for the tsunami source 34-Z41

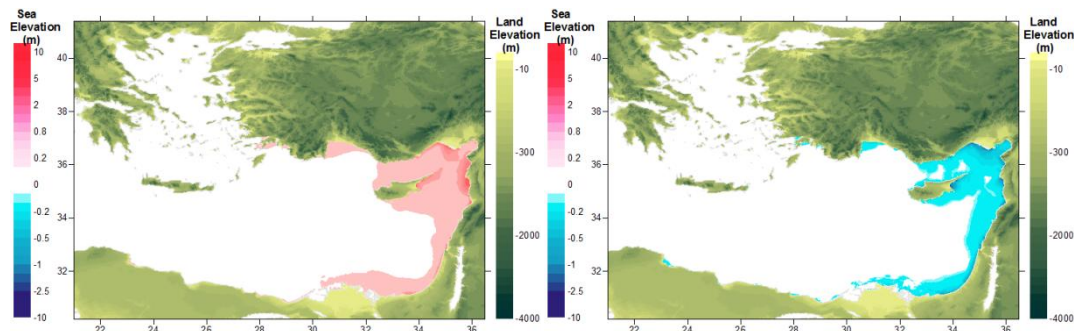


Figure A.3.66: The distributions of maximum positive of the water elevations(left) and negative water elevations(right) in the in the study domain (Eastern Mediterranean) in the duration of simulation (4 hours) for the tsunami source 34-Z41

Table A.3.66: Summary Results of tsunami impact at forecast points for source 34-Z41

Name of gauge pt.	Depth of gauge pt.(m)	Longitude	Latitude	Arrival time of initial wave (min)	Arrival time of max.wave (min)	Maximum (+)ve amp.(m)	Maximum (-)ve amp.(m)
Gokceada	0.4	25.9006	40.2379	0	0	0.0	0.0
Mentes	7.4	26.7374	38.434	0	0	0.0	0.0
Bodrum	8.4	27.4171	37.0193	133	221	0.1	-0.1
Aksaz	4.7	28.4313	36.8453	82	189	0.5	-0.5
Girne	1.1	33.3276	35.3493	11	45	0.3	-0.2
Gazimagusa	7.1	33.9468	35.1367	0	32	1.0	-1.6
Tasucu	3.5	33.8327	36.2664	0	47	0.6	-0.4
Erdemli	2.9	34.2629	36.57	0	41	0.7	-0.6
Canakkale	2.5	26.3772	40.1043	0	0	0.0	0.0
Aliaga	3.9	26.9423	38.8421	0	0	0.0	0.0
Alsancak P.	6.8	27.1387	38.4464	0	0	0.0	0.0
Cesme	10	26.2879	38.3288	199	199	0.0	0.0
Kusadasi	3.5	27.2588	37.8668	197	222	0.1	0.0
Didim	3.7	27.2615	37.3329	171	220	0.0	0.0
Bodrum	6.7	27.4242	37.0228	125	222	0.1	-0.1
Marmaris	1.9	28.3271	36.8107	80	107	0.2	-0.2
Fethiye	11.7	28.9502	36.7235	78	108	0.1	-0.1
Fethiye Bay	4.2	29.0546	36.6537	80	107	0.1	-0.1
Kas	10.8	29.6436	36.1965	58	83	0.1	-0.1
Finike	5.3	30.1554	36.3	53	87	0.2	-0.1
Kemer	0	30.5728	36.6052	0	0	0.0	0.0
Antalya B.	10.8	30.6123	36.8362	50	87	0.2	-0.2
Alanya	10	31.9911	36.5243	37	71	0.1	-0.1
Karatas	2.1	35.3872	36.5604	0	191	1.0	-1.1
Anamur	7.2	32.8582	36.0565	17	122	0.3	-0.3
Iskenderun B.	2.5	36.1898	36.6046	0	58	0.4	-0.4
Arsuz	3.2	35.8965	36.4272	0	0	0.6	-0.6
Samandag	7.9	35.9564	36.0549	0	3	0.9	-0.8

A.3.34. Simulation of Source s35

Table A.3.67: Rupture Parameters of Tsunami Source s35

Rupture Parameters			
Epicenter of fault axis	28.46E 36.45N	Dip angle (deg.)	27
Length of fault (km)	126	Slip angle (deg.)	99
Strike angle (deg. CW)	294	Fdisplacement (m)	3.65
Focal depth (km)	7.5	Maximum (+)ve amp. (m)	1.8
Width of fault (km)	63	Minimum (-)ve amp. (m)	-0.2

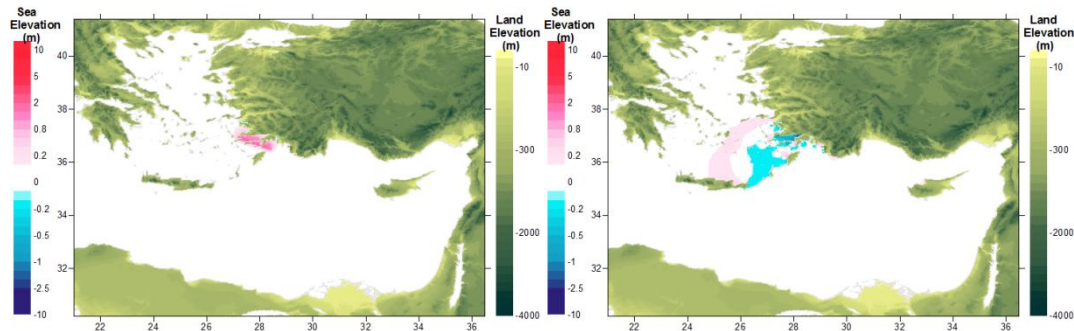


Figure A.3.67: The location of tsunami source s35 (left) and the distribution wave at $t=1\text{hr}$ (right) in the study domain (Eastern Mediterranean) in the duration of simulation (4 hours) for the tsunami source s35

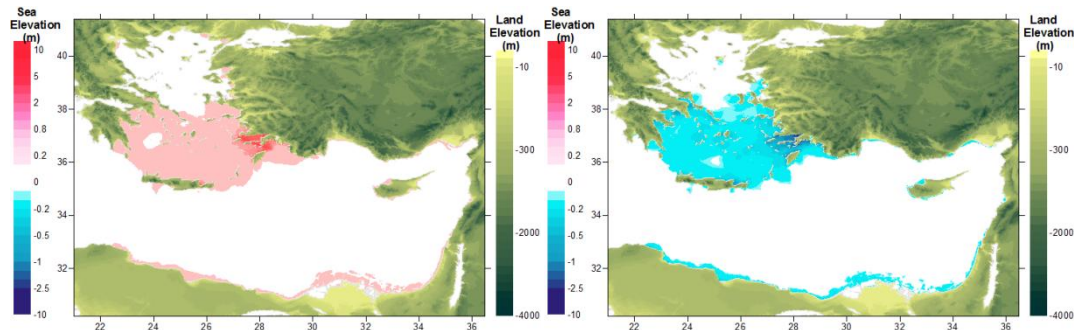


Figure A.3.68: The distributions of maximum positive of the water elevations(left) and negative water elevations(right) in the in the study domain (Eastern Mediterranean) in the duration of simulation (4 hours) for the tsunami source s35

Table A.3.68: Summary Results of tsunami impact at forecast points for source s35

Name of gauge pt.	Depth of gauge pt.(m)	Longitude	Latitude	Arrival time of initial wave (min)	Arrival time of max.wave (min)	Maximum (+)ve amp.(m)	Maximum (-)ve amp.(m)
Gokceada	0.4	25.9006	40.2379	113	198	0.1	0.0
Mentes	7.4	26.7374	38.434	0	172	0.1	0.0
Bodrum	8.4	27.4171	37.0193	0	10	1.8	-2.0
Aksaz	4.7	28.4313	36.8453	0	47	2.3	-2.4
Girne	1.1	33.3276	35.3493	33	158	0.1	-0.1
Gazimagusa	7.1	33.9468	35.1367	70	166	0.1	-0.1
Tasucu	3.5	33.8327	36.2664	58	157	0.2	-0.2
Erdemli	2.9	34.2629	36.57	70	100	0.1	-0.1
Canakkale	2.5	26.3772	40.1043	123	201	0.1	-0.1
Aliaga	3.9	26.9423	38.8421	44	157	0.1	-0.1
Alsancak P.	6.8	27.1387	38.4464	0	221	0.2	0.0
Cesme	10	26.2879	38.3288	0	111	0.1	-0.1
Kusadasi	3.5	27.2588	37.8668	0	105	0.2	-0.3
Didim	3.7	27.2615	37.3329	0	190	0.5	-0.3
Bodrum	6.7	27.4242	37.0228	0	10	1.7	-2.0
Marmaris	1.9	28.3271	36.8107	0	29	1.9	-2.5
Fethiye	11.7	28.9502	36.7235	0	186	0.8	-0.9
Fethiye Bay	4.2	29.0546	36.6537	0	101	0.9	-0.9
Kas	10.8	29.6436	36.1965	0	59	0.7	-0.6
Finike	5.3	30.1554	36.3	0	120	0.4	-0.5
Kemer	0	30.5728	36.6052	0	0	0.0	0.0
Antalya B.	10.8	30.6123	36.8362	0	134	0.1	-0.1
Alanya	10	31.9911	36.5243	15	47	0.1	-0.1
Karatas	2.1	35.3872	36.5604	107	228	0.2	-0.1
Anamur	7.2	32.8582	36.0565	29	151	0.1	-0.1
Iskenderun B.	2.5	36.1898	36.6046	137	160	0.1	0.0
Arsuz	3.2	35.8965	36.4272	108	221	0.1	-0.1
Samandag	7.9	35.9564	36.0549	87	114	0.1	-0.1

A.3.35. Simulation of Source s36

Table A.3.69: Rupture Parameters of Tsunami Source s36

Rupture Parameters			
Epicenter of fault axis	28.43E 36.07N	Dip angle (deg.)	47
Length of fault (km)	184	Slip angle (deg.)	262
Strike angle (deg. CW)	184	Fdisplacement (m)	2.9
Focal depth (km)	7.5	Maximum (+)ve amp. (m)	0.2
Width of fault (km)	50	Minimum (-)ve amp. (m)	-1.5

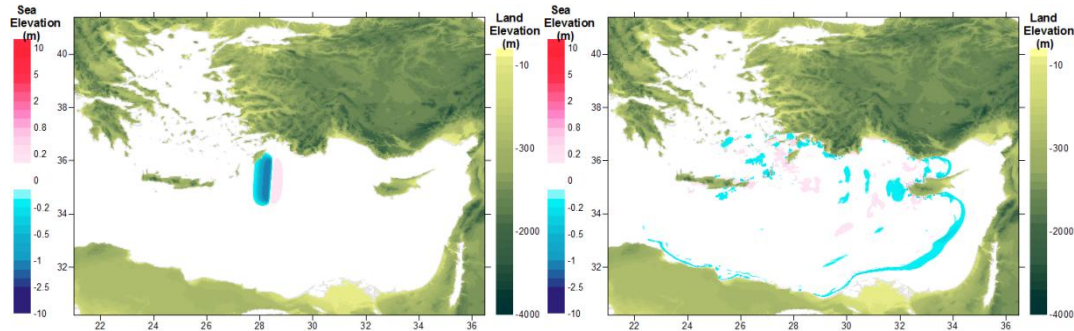


Figure A.3.69: The location of tsunami source s36 (left) and the distribution wave at t=1hr(right) in the study domain (Eastern Mediterranean) in the duration of simulation (4 hours) for the tsunami source s36

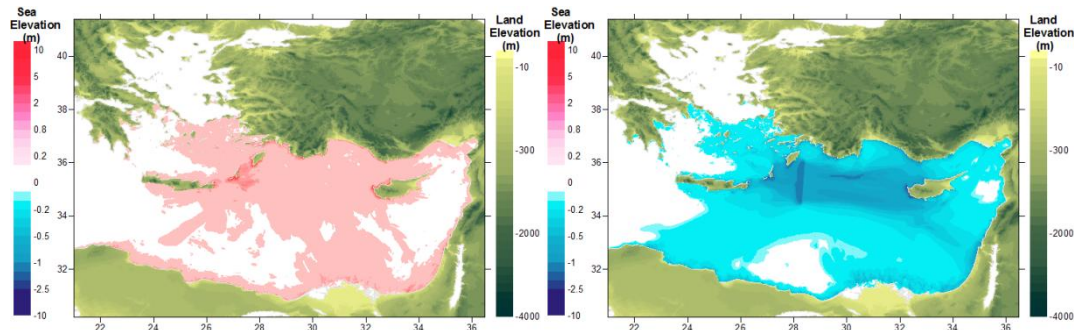


Figure A.3.70: The distributions of maximum positive of the water elevations(left) and negative water elevations(right) in the in the study domain (Eastern Mediterranean) in the duration of simulation (4 hours) for the tsunami source s36

Table A.3.70: Summary Results of tsunami impact at forecast points for source s36

Name of gauge pt.	Depth of gauge pt.(m)	Longitude	Latitude	Arrival time of initial wave (min)	Arrival time of max.wave (min)	Maximum (+)ve amp.(m)	Maximum (-)ve amp.(m)
Gokceada	0.4	25.9006	40.2379	192	0	0.0	0.0
Mentes	7.4	26.7374	38.434	168	0	0.0	0.0
Bodrum	8.4	27.4171	37.0193	0	211	0.5	-0.6
Aksaz	4.7	28.4313	36.8453	0	41	1.4	-1.7
Girne	1.1	33.3276	35.3493	46	122	0.9	-0.9
Gazimagusa	7.1	33.9468	35.1367	67	131	0.4	-0.4
Tasucu	3.5	33.8327	36.2664	68	184	0.7	-0.6
Erdemli	2.9	34.2629	36.57	78	113	0.4	-0.5
Canakkale	2.5	26.3772	40.1043	206	0	0.0	0.0
Aliaga	3.9	26.9423	38.8421	153	207	0.0	0.0
Alsancak P.	6.8	27.1387	38.4464	214	0	0.0	0.0
Cesme	10	26.2879	38.3288	103	207	0.1	-0.1
Kusadasi	3.5	27.2588	37.8668	83	166	0.1	-0.2
Didim	3.7	27.2615	37.3329	0	183	0.2	-0.2
Bodrum	6.7	27.4242	37.0228	0	141	0.5	-0.6
Marmaris	1.9	28.3271	36.8107	0	38	1.5	-1.0
Fethiye	11.7	28.9502	36.7235	0	88	0.8	-0.8
Fethiye Bay	4.2	29.0546	36.6537	0	36	0.8	-1.1
Kas	10.8	29.6436	36.1965	5	29	2.6	-2.3
Finike	5.3	30.1554	36.3	15	60	1.6	-2.2
Kemer	0	30.5728	36.6052	76	78	0.6	0.0
Antalya B.	10.8	30.6123	36.8362	28	101	0.6	-0.4
Alanya	10	31.9911	36.5243	29	53	1.0	-0.9
Karatas	2.1	35.3872	36.5604	112	167	0.6	-0.5
Anamur	7.2	32.8582	36.0565	42	169	0.7	-0.9
Iskenderun B.	2.5	36.1898	36.6046	140	220	0.2	-0.2
Arsuz	3.2	35.8965	36.4272	111	235	0.3	-0.3
Samandag	7.9	35.9564	36.0549	91	124	0.3	-0.3

A.3.36. Simulation of Source s37

Table A.3.71: Rupture Parameters of Tsunami Source s37

Rupture Parameters			
Epicenter of fault axis	28.39E 35.82N	Dip angle (deg.)	25
Length of fault (km)	91	Slip angle (deg.)	90
Strike angle (deg. CW)	303	Fdisplacement (m)	2.7
Focal depth (km)	7.5	Maximum (+)ve amp. (m)	1.3
Width of fault (km)	45	Minimum (-)ve amp. (m)	-0.3

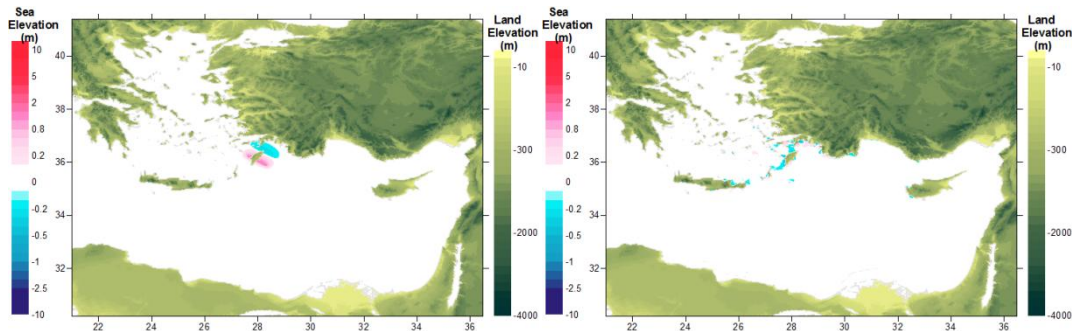


Figure A.3.71: The location of tsunami source s37 (left) and the distribution wave at t=1hr(right) in the study domain (Eastern Mediterranean) in the duration of simulation (4 hours) for the tsunami source s37

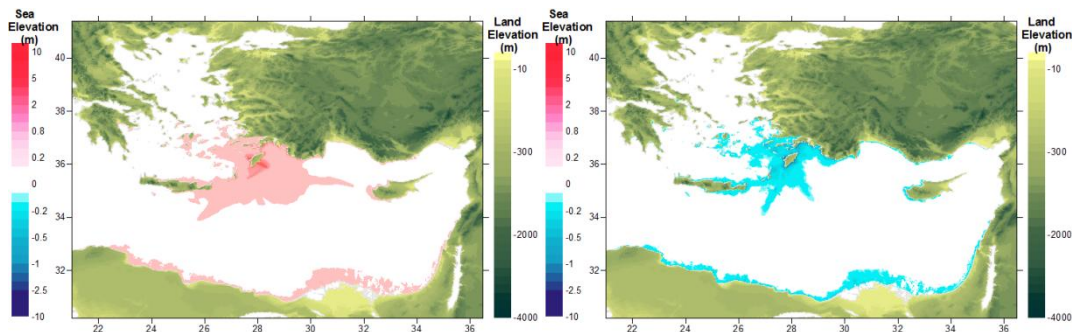


Figure A.3.72: The distributions of maximum positive of the water elevations(left) and negative water elevations(right) in the in the study domain (Eastern Mediterranean) in the duration of simulation (4 hours) for the tsunami source s37

Table A.3.72: Summary Results of tsunami impact at forecast points for source s37

Name of gauge pt.	Depth of gauge pt.(m)	Longitude	Latitude	Arrival time of initial wave (min)	Arrival time of max.wave (min)	Maximum (+)ve amp.(m)	Maximum (-)ve amp.(m)
Gokceada	0.4	25.9006	40.2379	212	212	0.0	0.0
Mentes	7.4	26.7374	38.434	154	154	0.0	0.0
Bodrum	8.4	27.4171	37.0193	0	66	0.4	-0.5
Aksaz	4.7	28.4313	36.8453	0	58	1.4	-1.4
Girne	1.1	33.3276	35.3493	45	178	0.1	-0.1
Gazimagusa	7.1	33.9468	35.1367	79	146	0.1	-0.1
Tasucu	3.5	33.8327	36.2664	70	173	0.1	-0.1
Erdemli	2.9	34.2629	36.57	84	178	0.1	-0.1
Canakkale	2.5	26.3772	40.1043	192	192	0.0	0.0
Aliaga	3.9	26.9423	38.8421	137	137	0.0	0.0
Alsancak P.	6.8	27.1387	38.4464	202	202	0.0	0.0
Cesme	10	26.2879	38.3288	73	197	0.0	0.0
Kusadasi	3.5	27.2588	37.8668	72	203	0.1	-0.1
Didim	3.7	27.2615	37.3329	3	225	0.1	-0.2
Bodrum	6.7	27.4242	37.0228	0	66	0.5	-0.4
Marmaris	1.9	28.3271	36.8107	0	93	1.7	-1.7
Fethiye	11.7	28.9502	36.7235	0	18	0.6	-0.9
Fethiye Bay	4.2	29.0546	36.6537	0	121	0.7	-0.6
Kas	10.8	29.6436	36.1965	1	34	1.2	-1.2
Finike	5.3	30.1554	36.3	14	75	0.7	-1.0
Kemer	0	30.5728	36.6052	0	0	0.0	0.0
Antalya B.	10.8	30.6123	36.8362	27	64	0.1	-0.1
Alanya	10	31.9911	36.5243	28	88	0.1	-0.1
Karatas	2.1	35.3872	36.5604	118	147	0.1	-0.1
Anamur	7.2	32.8582	36.0565	41	175	0.1	-0.1
Iskenderun B.	2.5	36.1898	36.6046	145	147	0.0	0.0
Arsuz	3.2	35.8965	36.4272	118	203	0.1	-0.1
Samandag	7.9	35.9564	36.0549	100	106	0.1	0.0

A.3.37. Simulation of Source s38

Table A.3.73: Rupture Parameters of Tsunami Source s38

Rupture Parameters			
Epicenter of fault axis	28.4E 35.5N	Dip angle (deg.)	20
Length of fault (km)	190	Slip angle (deg.)	90
Strike angle (deg. CW)	55	Fdisplacement (m)	5
Focal depth (km)	7.5	Maximum (+)ve amp. (m)	2.4
Width of fault (km)	90	Minimum (-)ve amp. (m)	-0.7

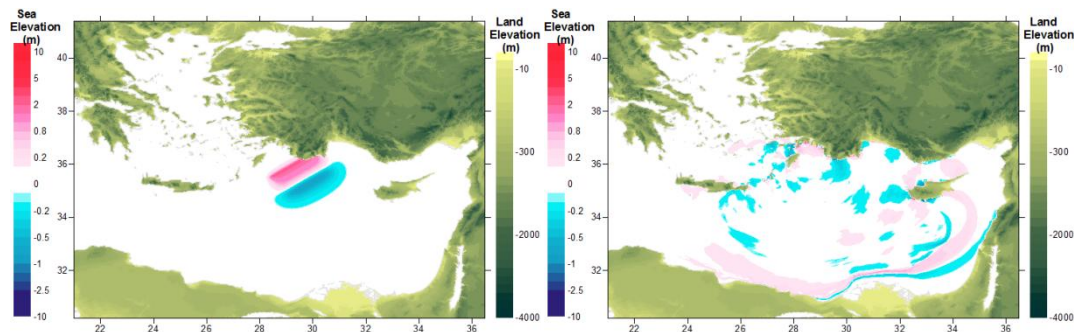


Figure A.3.73: The location of tsunami source s38 (left) and the distribution wave at $t=1\text{hr}$ (right) in the study domain (Eastern Mediterranean) in the duration of simulation (4 hours) for the tsunami source s38

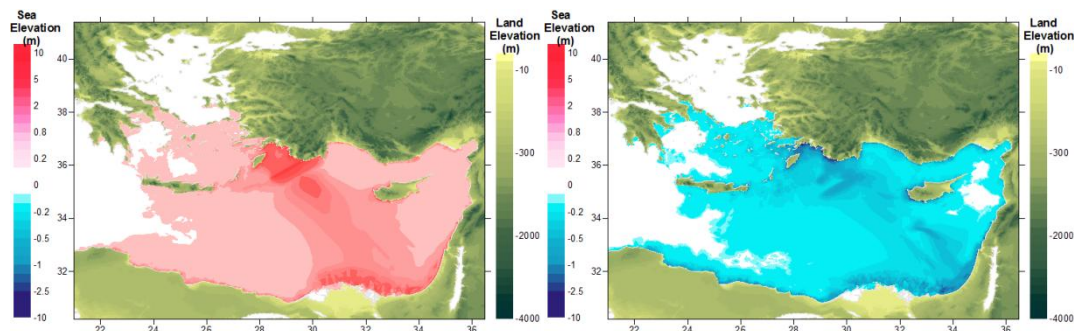


Figure A.3.74: The distributions of maximum positive of the water elevations(left) and negative water elevations(right) in the in the study domain (Eastern Mediterranean) in the duration of simulation (4 hours) for the tsunami source s38

Table A.3.74: Summary Results of tsunami impact at forecast points for source s38

Name of gauge pt.	Depth of gauge pt.(m)	Longitude	Latitude	Arrival time of initial wave (min)	Arrival time of max.wave (min)	Maximum (+)ve amp.(m)	Maximum (-)ve amp.(m)
Gokceada	0.4	25.9006	40.2379	190	208	0.0	0.0
Mentes	7.4	26.7374	38.434	169	185	0.0	0.0
Bodrum	8.4	27.4171	37.0193	0	193	1.1	-1.0
Aksaz	4.7	28.4313	36.8453	0	62	4.7	-4.6
Girne	1.1	33.3276	35.3493	11	141	0.4	-0.5
Gazimagusa	7.1	33.9468	35.1367	50	152	0.7	-0.8
Tasucu	3.5	33.8327	36.2664	28	148	0.7	-0.7
Erdemli	2.9	34.2629	36.57	40	168	0.5	-0.6
Canakkale	2.5	26.3772	40.1043	206	222	0.0	0.0
Aliaga	3.9	26.9423	38.8421	153	180	0.1	0.0
Alsancak P.	6.8	27.1387	38.4464	213	234	0.1	0.0
Cesme	10	26.2879	38.3288	101	239	0.1	-0.1
Kusadasi	3.5	27.2588	37.8668	0	206	0.4	-0.2
Didim	3.7	27.2615	37.3329	0	207	0.2	-0.1
Bodrum	6.7	27.4242	37.0228	0	192	1.2	-1.1
Marmaris	1.9	28.3271	36.8107	0	22	4.0	-2.3
Fethiye	11.7	28.9502	36.7235	0	20	2.7	-3.1
Fethiye Bay	4.2	29.0546	36.6537	0	65	2.0	-2.5
Kas	10.8	29.6436	36.1965	0	48	4.5	-5.0
Finike	5.3	30.1554	36.3	0	81	2.2	-3.3
Kemer	0	30.5728	36.6052	0	105	0.8	0.0
Antalya B.	10.8	30.6123	36.8362	0	101	0.7	-0.8
Alanya	10	31.9911	36.5243	0	76	0.6	-0.7
Karatas	2.1	35.3872	36.5604	78	210	0.8	-0.8
Anamur	7.2	32.8582	36.0565	0	167	0.6	-0.7
Iskenderun B.	2.5	36.1898	36.6046	107	143	0.3	-0.3
Arsuz	3.2	35.8965	36.4272	79	195	0.4	-0.4
Samandag	7.9	35.9564	36.0549	57	97	0.5	-0.3